

ATMOSPHERIC EFFECTS ASSOCIATED WITH HIGHWAY NOISE PROPAGATION

Final Report 555

Prepared By:

Hugh Saurenman, ATS Consulting, LLC
Jim Chambers, National Center for Physical Acoustics,
The University of Mississippi
Louis C. Sutherland, Consultant in Acoustics
Robert L. Bronsdon, Consultant in Acoustics
Hans Forscher, Navcon Engineering Network

October 2005

Prepared for:

Arizona Department of Transportation
206 South 17th Avenue
Phoenix, Arizona 85007
in cooperation with
U.S. Department of Transportation
Federal Highway Administration

The contents of the report reflect the views of the authors who are responsible for the facts and the accuracy of the data presented herein. The contents do not necessarily reflect the official views or policies of the Arizona Department of Transportation or the Federal Highway Administration. This report does not constitute a standard, specification, or regulation. Trade or manufacturers' names that may appear herein are cited only because they are considered essential to the objectives of the report. The U.S. government and The State of Arizona do not endorse products or manufacturers.

Technical Report Documentation Page

1. Report No. FHWA-AZ-05-555		2. Government Accession No.		3. Recipient's Catalog No.	
4. Title and Subtitle Atmospheric Effects Associated with Highway Noise Propagation				5. Report Date October 2005	
				6. Performing Organization Code	
7. Author Hugh Saurenman, Jim Chambers, Louis C. Sutherland, Robert L. Bronsdon, Hans Forscher				8. Performing Organization Report No.	
9. Performing Organization Name and Address ATS Consulting, LLC 725 S. Figueroa Street, Suite 1580 Los Angeles, CA 90017				10. Work Unit No.	
				11. Contract or Grant No. T04-58-A0001	
12. Sponsoring Agency Name and Address ARIZONA DEPARTMENT OF TRANSPORTATION 206 S. 17TH AVENUE PHOENIX, ARIZONA 85007 ADOT Project Manager: Estomih Kombe				13. Type of Report & Period Covered Final Report September 2003, August 2005	
				14. Sponsoring Agency Code	
15. Supplementary Notes Prepared in cooperation with the U.S. Department of Transportation, Federal Highway Administration					
16. Abstract The primary questions investigated in this project were: What are the atmospheric conditions in the Phoenix valley that contribute to higher than normal sound levels? Are the conditions unique to the Phoenix valley? Can the atmospheric effects be anticipated? The main components of the project were: (1) a review of literature relevant to sound propagation, (2) detailed noise measurements in a Scottsdale neighborhood along the East Loop 101 Freeway, (3) computer modeling of sound propagation under various measured and inferred atmospheric conditions, (4) noise measurements before and after installation of an asphalt rubber friction course (ARFC) on the Pima Freeway by the ADOT Quiet Pavement Pilot Program, and (5) a pilot study investigating parametric models of tire/pavement noise. Some key conclusions are: nighttime thermal inversion conditions that are common in the Phoenix valley from October through March cause sound level increases of 5 to 8 dB at distances greater than 1/4 mile from freeways, nighttime down-slope drainage flows off the mountain ranges surrounding the Phoenix valley cause localized focusing and de-focusing of sound levels, sound level variations under inversion conditions appear to be greatest at locations that are upwind relative to the down-slope flows, the highest sound levels during the October to March period will usually occur right around sunrise when high traffic volumes coincide with strong inversion conditions, and installation of the ARFC reduces sound levels by 8 to 10 dBA both close to the roadway and at distances of 1/4 mile and greater. A final tentative conclusion is that, based on the computer modeling, there may be a rapid onset of refraction effects between about 200 and 300 m (650 to 1000 ft) from Phoenix valley roadways,					
17. Key Words Acoustics, sound propagation, highway noise, atmospheric effects, quiet pavement,			18. Distribution Statement Document is available to the U.S. public through the National Technical Information Service, Springfield, Virginia 22161		23. Registrant's Seal
19. Security Classification Unclassified	20. Security Classification Unclassified	21. No. of Pages 174	22. Price		

SI* (MODERN METRIC) CONVERSION FACTORS

APPROXIMATE CONVERSIONS TO SI UNITS					APPROXIMATE CONVERSIONS FROM SI UNITS				
Symbol	When You Know	Multiply By	To Find	Symbol	Symbol	When You Know	Multiply By	To Find	Symbol
<u>LENGTH</u>					<u>LENGTH</u>				
in	inches	25.4	millimeters	mm	mm	millimeters	0.039	inches	in
ft	feet	0.305	meters	m	m	meters	3.28	feet	ft
yd	yards	0.914	meters	m	m	meters	1.09	yards	yd
mi	miles	1.61	kilometers	km	km	kilometers	0.621	miles	mi
<u>AREA</u>					<u>AREA</u>				
in ²	square inches	645.2	square millimeters	mm ²	mm ²	Square millimeters	0.0016	square inches	in ²
ft ²	square feet	0.093	square meters	m ²	m ²	Square meters	10.764	square feet	ft ²
yd ²	square yards	0.836	square meters	m ²	m ²	Square meters	1.195	square yards	yd ²
ac	acres	0.405	hectares	ha	ha	hectares	2.47	acres	ac
mi ²	square miles	2.59	square kilometers	km ²	km ²	Square kilometers	0.386	square miles	mi ²
<u>VOLUME</u>					<u>VOLUME</u>				
fl oz	fluid ounces	29.57	milliliters	mL	mL	milliliters	0.034	fluid ounces	fl oz
gal	gallons	3.785	liters	L	L	liters	0.264	gallons	gal
ft ³	cubic feet	0.028	cubic meters	m ³	m ³	Cubic meters	35.315	cubic feet	ft ³
yd ³	cubic yards	0.765	cubic meters	m ³	m ³	Cubic meters	1.308	cubic yards	yd ³
NOTE: Volumes greater than 1000L shall be shown in m ³ .									
<u>MASS</u>					<u>MASS</u>				
oz	ounces	28.35	grams	g	g	grams	0.035	ounces	oz
lb	pounds	0.454	kilograms	kg	kg	kilograms	2.205	pounds	lb
T	short tons (2000lb)	0.907	megagrams (or "metric ton")	mg (or "t")	Mg	megagrams (or "metric ton")	1.102	short tons (2000lb)	T
<u>TEMPERATURE (exact)</u>					<u>TEMPERATURE (exact)</u>				
°F	Fahrenheit temperature	5(F-32)/9 or (F-32)/1.8	Celsius temperature	°C	°C	Celsius temperature	1.8C + 32	Fahrenheit temperature	°F
<u>ILLUMINATION</u>					<u>ILLUMINATION</u>				
fc	foot candles	10.76	lux	lx	lx	lux	0.0929	foot-candles	fc
fl	foot-Lamberts	3.426	candela/m ²	cd/m ²	cd/m ²	candela/m ²	0.2919	foot-Lamberts	fl
<u>FORCE AND PRESSURE OR STRESS</u>					<u>FORCE AND PRESSURE OR STRESS</u>				
lbf	poundforce	4.45	newtons	N	N	newtons	0.225	poundforce	lbf
lbf/in ²	poundforce per square inch	6.89	kilopascals	kPa	kPa	kilopascals	0.145	poundforce per square inch	lbf/in ²

Table of Contents

Executive Summary	1
Background	1
Atmospheric Parameters	1
Conditions in the Phoenix Valley	2
Diurnal Sound Level Patterns in the Phoenix Valley.....	4
Study Conclusions.....	6
1. Introduction.....	9
1.1 Basic Acoustical Concepts	10
1.2 Bending of Sound Waves by Diffraction and Refraction	13
2. Background on Sound Propagation.....	15
2.1 Neutral Atmospheric Conditions	15
2.1.1 Geometric Spreading	15
2.1.2 Atmospheric Absorption.....	16
2.1.3 Ground Effects.....	18
2.1.4 Diffraction by Barriers and Other Obstructions	19
2.2 Atmospheric Effects	20
2.2.1 Refraction	20
2.2.2 Turbulence	22
2.2.3 Computer Modeling of Refraction Effects	23
3. Conditions in the Phoenix Valley	29
3.1 General Meteorological Conditions.....	29
3.2 Wind Speed and Direction.....	31
4. Noise Measurements	35
4.1 Measurement Locations and Procedures	35
4.1.1 Measurement Sites.....	35
4.1.2 Measurement Equipment and Procedures	39
4.2 Analysis of A-Weighted Measurement	40
4.2.1 Noise Data	40
4.2.2 Traffic Counts.....	50
4.2.3 Meteorological Data	54
4.2.4 Normalized Noise Data	62
4.3 Short Term Noise Measurement Results	65
4.4 Acoustic Benefits of ARFC Installation	72
5. Computer Modeling	77
5.1 Outdoor Sound Propagation	77
5.2 Meteorological Modeling	78
5.3 Modeling Results	80
5.4 Line Source Model	88
6. Conclusions.....	91
6.1 Atmospheric Effects on Sound Propagation.....	91
6.2 Pavement Parameters Affecting Noise	92
6.3 Measured Effects of ARFC Pavement.....	93
Appendix A. Photographs of Noise Measurement Sites	95

Appendix B. Noise Measurement Results.....	101
B.1 One-Minute Leq Values	101
B.2 15-Minute Leq Values.....	104
B.3 1/3 Octave Band Spectra, 6 AM to 12 PM.....	107
B.4 SPECTROGRAMS, Weekdays, 5 AM to 11 AM.....	114
B.5 Meteorological Data.....	119
B.6 Traffic Counts.....	123
Appendix C. Detailed Results of PE Models	127
Appendix D. Tire Noise Parametric Studies	137
D.1 Overview of Tire Noise Study	137
Introduction	137
Noise Generating Mechanisms	137
Pavement Parameters.....	139
Summary of Conclusions from Structural-Acoustic Modeling	141
D.2 Tire Noise Ramifications of Pavement Characteristics.....	142
References	165

List of Figures

Figure 1. Sketch of Sound Refraction Effects	3
Figure 2. Illustration of Factors Driving Diurnal Variations in Sound Levels.....	6
Figure 3. Sound Wave with Just One Frequency (a Pure Tone)	12
Figure 4. Sound Wave from Highway Noise with many Frequencies	13
Figure 5. Conceptual Illustration of Sound Refracted By Atmospheric Profiles “Skipping” Over a Sound Barrier.....	14
Figure 6. Attenuation Curves for Line and Point Sources.....	16
Figure 7. Atmospheric Absorption Early Morning and Mid-Day for a Representative Day in March 2004.....	17
Figure 8. Difference in Atmospheric Absorption in Figure 7	17
Figure 9. Combined Geometric Attenuation and Excess Ground Attenuation, Automobile Traffic on Pima Freeway	18
Figure 10. Representative Values for the Barrier Insertion Loss as a Function of Barrier Height and Distance to Receiver	20
Figure 11. Sound Ray Paths for Different Patterns for Sound Velocity Gradients	21
Figure 12. Vertical Temperature Profiles for Four Days During Phase 1 Measurements.....	22
Figure 13. Example of Upward Refraction without Turbulence.....	26
Figure 14. Nighttime or Downward Refraction without Turbulence	26
Figure 15. PE Code Calculation of Sound Propagation with Turbulence.....	27
Figure 16. Drainage Flows in Complex Terrain Surrounding Phoenix.....	31
Figure 17. Example of Wind Speed Profile from DEQ Data at 43rd Avenue.....	33
Figure 18. Aerial Photograph of Noise Measurement Sites	37
Figure 19. Aerial Photograph of Sites 2 and 3	38
Figure 20. Aerial Photograph of Site 4 and 4B	38
Figure 21. Sketch of Field Set Up and Measurement Equipment, Phase 1	40
Figure 22. Variation of Daily Sound Levels, Phase 1, Sites 2 and 3 (Phase 1, March 2004)	45
Figure 23. 15-Minute Leq vs. Time of Day, March 8-22, 2004.....	47
Figure 24. 15-Minute Leq vs. Time of Day, October 17-23, 2004.....	48
Figure 25. First and Second Week Sound Levels, March, 2004	49

Figure 26. Average Sound Levels, First and Second Week of March, 2004 Measurements	50
Figure 27. Average Traffic Speeds.....	52
Figure 28. Average Traffic Volumes.....	53
Figure 29. Diurnal Temperature Variation, March 2004 Measurements	56
Figure 30. Diurnal Variation of Relative Humidity, March 2004 Measurements.....	57
Figure 31. Examples of TNM Predicted 1/3 Octave Band Sound Levels at Site 2.....	58
Figure 32. Temperature Gradients, March 2004 Measurements.....	59
Figure 33. Two Methods of Measuring Ground Level Temperature Gradient, March 8-10, 2004	60
Figure 34. Two Methods of Measuring Ground Level Temperature Gradient, March 17-23, 2004	61
Figure 35. TNM Projections over a 24-Hour Period.....	64
Figure 36. Average Sound Levels Normalized Using TNM Projections	65
Figure 37. 1-Minute and 5-Minute Leqs, Monday October 18, 2004	67
Figure 38. Change in 1/3 Octave Band Levels at Site 4B over 30-Minute Period on Oct. 18, 2004	67
Figure 39. Short-Term Noise Measurement on October 19, 2004	68
Figure 40. Short-Term Noise Measurement on October 23, 2004	69
Figure 41. Time History, March 18, 2004, 5:30 to 9:30 AM	71
Figure 42. Spectrogram, March 18, 2004, 5:30 to 9:15 AM	71
Figure 43. Comparison of Sound Levels Before and After Installation of ARFC	74
Figure 44. 1/3 Octave Band Spectra at Sites 1 and 2 Before and After Installation of ARFC.....	75
Figure 45. Influence of Wind Speed Gradients on Sound Propagation.....	77
Figure 46. Influence of Temperature Gradients on Sound Propagation.....	78
Figure 47. Sample PE Output, Temperature Effects Only, 1000 Hz.....	82
Figure 48. Sample PE Output, Temp and Downwind Condition, 1000 Hz.....	83
Figure 49. Sample PE Output, Wind Only, Upwind Condition, 1000 Hz.....	84
Figure 50. Measured vs. Predicted Levels, March 18, 7:15 and 9:15 AM.....	86
Figure 51. Measured and Predicted Octave Band Levels, March 18, 7:15 and 9:15 AM.....	87
Figure 52. Partial Line Source Model Constructed from 2-D PE Model.....	90
Figure 53. Results of Partial Line Source Model, March 18, 2004 Conditions	90
Figure 54. Site 1 Looking East Toward Freeway.....	95
Figure 55. Site 1 Looking Northeast	95
Figure 56. Meteorological Tower at Site 2 (8701 W. Highland Ave.), Looking Southwest.....	96
Figure 57. Site 2 (8701 E. Highland Avenue) Looking West	97
Figure 58. Short-Term Measurement in Front of Site 2 (8701 E. Highland Avenue) Looking East	97
Figure 59. Site 3 (8547 E. Highland Avenue) Looking East Toward Pima Freeway	98
Figure 60. Site 3 (8547 E. Highland Avenue) Looking Southwest.....	98
Figure 61. Short-Term Measurement in Front of Site 3 Looking East.....	99
Figure 62. Site 4 (Tribal land off 92nd Street), Looking West Toward Pima Freeway	99
Figure 63. Site 4, Looking Southwest Toward Indian School Road Overpass	100
Figure 64. One-Minute Leq Data, March 8-14, 2004.....	101
Figure 65. One-Minute Leq Data, March 17-22, 2004.....	102
Figure 66. One-Minute Leq Data, October 17-22, 2004	103
Figure 67. 15-Minute Leq Data, March 8-14, 2004	104
Figure 68. 15-Minute Leq Data, March 17-22, 2004	105
Figure 69. 15-Minute Leq Data, October 17-23, 2004.....	106
Figure 70. 1/3 Octave Band Spectra, Site 1, March 8-14, 2004.....	107
Figure 71. 1/3 Octave Band Spectra, Site 1, March 16-22, 2004.....	108
Figure 72. 1/3 Octave Band Spectra, Site 2, March 8-14, 2004.....	109
Figure 73. 1/3 Octave Band Spectra, Site 2, March 16-22, 2004.....	110

Figure 74. 1/3 Octave Band Spectra, Site 3, March 8-11, 2004.....	111
Figure 75. 1/3 Octave Band Spectra, Site 3, March 15-20, 2004.....	111
Figure 76. 1/3 Octave Band Spectra (15-min Leq), Site 4, March 2004.....	112
Figure 77. 1/3 Octave Band Spectra (15-min Leq), Site 1, October 2004.....	113
Figure 78. 1/3 Octave Band Spectra (15-min Leq), Site 2, October 2004.....	113
Figure 79. Spectrogram, Monday, March 8, 2004.....	114
Figure 80. Spectrogram, Tuesday, March 9, 2004.....	114
Figure 81. Spectrogram, Wednesday, March 10, 2004.....	115
Figure 82. Spectrogram, Thursday, March 11, 2004.....	115
Figure 83. Spectrogram, Monday, March 15, 2004.....	116
Figure 84. Spectrogram, Tuesday, March 16, 2004.....	116
Figure 85. Spectrogram, Wednesday, March 17, 2004.....	117
Figure 86. Spectrogram, Thursday, March 18, 2004.....	117
Figure 87. Spectrogram, Friday, March 19, 2004.....	118
Figure 88. Spectrogram, Saturday, March 20, 2004.....	118
Figure 89. Temperature and Humidity, Site 3, March 8-14, 2004.....	119
Figure 90. Temperature and Humidity, Site 3, March 8-14, 2004.....	120
Figure 91. Temperature and Humidity, October 17-23, 2004.....	121
Figure 92. Wind Speed at 43.5 ft, Site 2, March 17-23, 2004.....	122
Figure 93. Summary of Traffic Counts, March 16-22, 2004.....	123
Figure 94. Summary of Traffic Counts, March 23-26, 2004.....	124
Figure 95. Summary of Traffic Counts, October 17-22, 2004.....	125
Figure 96. PE Model Output, March 18, 6:00 AM.....	127
Figure 97. PE Model Output, March 18, 7:15 AM.....	128
Figure 98. PE Model Output, March 18, 8:15 AM.....	129
Figure 99. PE Model Output, March 18, 9:15 AM.....	130
Figure 100. PE Model Output, March 18, 3:00 PM.....	131
Figure 101. PE Model Output, March 19, 6:00 AM.....	132
Figure 102. PE Model Output, March 19, 7:15 AM.....	133
Figure 103. PE Model Output, March 19, 8:15 AM.....	134
Figure 104. PE Model Output, March 19, 9:15 AM.....	135
Figure 105. PE Model Output, March 18, 3:00 PM.....	136

List of Tables

Table 1. Effects of Ground Impedance on Leq as a Function of Distance from Highway.....	19
Table 2. Distance of Measurement Sites from Near Lane of Pima Freeway.....	36
Table 3. Daily Results, Site 2 (8701 E. Highland).....	42
Table 4. Daily Results, Site 3 (8547 E. Highland).....	43
Table 5. Daily Results, Site 4 (Tribal Land East of Freeway), Phase 1.....	44
Table 6. Average Weekday Truck Volumes During October 2004 Measurements.....	51
Table 7. Comparison of Average Sound Levels Before and After ARFC Installation.....	73
Table 8. Measured and Predicted Octave Band Levels for 7:15 AM March 18.....	85
Table 9. Measured and Predicted Octave Band Levels for 9:15 AM March 18.....	86
Table 10. Noise Generating Mechanisms.....	138
Table 11. Effect of Pavement Parameters on Tire/Pavement Noise.....	140

Acknowledgement

We want to recognize the contributions of all the individuals and firms who contributed to this project. They are:

Hugh Saurenman, ATS Consulting, LLC: Principal Investigator.

Estomih (Tom) Kombe: ATRC Project Manager.

Technical Advisory Committee: Fred Garcia, Arizona Department of Transportation, Environmental Planning Group; Kelly McMullen, Maricopa County Department of Transportation; Robert Pikora, City of Phoenix; Steve Thomas, Federal Highway Administration, Arizona Division; Jerri Horst, S. R. Beard & Associates.

Jim Chambers, University of Mississippi, National Center for Physical Acoustics: Jim performed all of the computer modeling, contributed to the field studies, and prepared the modeling sections of the final report.

Hans Forscher, Navcon Engineering Network: Hans was responsible for analysis of the large quantity of short-interval measurement data from the Phase 1 tests. His work included generating 1-minute and 15-minute averages from the 1-second data, producing spectrograms like the ones in Appendix B.4, and preparing the initial plots of the A-weighted noise, frequency spectrum, and weather results. He also processed the WAV files to generate 15-second 1/3 octave band spectra.

Lou Sutherland, Consultant in Acoustics: Lou's vast experience with previous sound propagation studies gave us an enormous leg up in the initial phases of the project. He did most of the work on the literature review and prepared the first draft of the background sections of the final report. His insights were a valuable resource throughout the project.

Robert Bronsdon, Consultant in Acoustics: Bob's role in the project was as a technical advisor, something he is very qualified for through his work on sound propagation for Disney Imagineering. His experience and insights on how atmospheric conditions affect sound propagation and his untiring energy in identifying interesting events in the data were valuable assets to the project.

Joel Garrelick, Applied Physical Sciences, Inc.: Joel was responsible for the pilot study of how different pavement parameters affect noise generation. The study demonstrated that valuable information could be gleaned through the application of straightforward mathematical models.

Gonzalo Sanchez, Sanchez Industrial Design: Sanchez Industrial Design supplied most of the equipment used in the field measurements. This included noise monitors, the 13 m meteorological tower with temperature sensors and anemometers, the data logging equipment, and the digital recorder used to make continuous audio recordings.

Jennifer Love, Parsons Brinckerhoff: The budget on this project was somewhat tight, which meant that none of the principals could be on site for the Phase 1 measurements. Jennifer took responsibility for the monitoring equipment during Phase 1, including placing the equipment at two sites early each morning and then picking them up late that night, downloading the data from the monitors, and generally checking that the equipment was operating properly.

Peter Hyde, Mark Fitch, and Randy Redman, Arizona Department of Environmental Quality: These three people and their understanding of meteorological conditions and air flows in the Phoenix valley turned out to be an important resource for this project. We are grateful for the time that they spent with us talking about meteorology.

EXECUTIVE SUMMARY

BACKGROUND

This report presents the final results of Arizona Transportation Research Center project SPR 555, "Evaluate the Atmospheric Effects Associated with Highway Noise Propagation." The prime motivator for this project was the observation that traffic noise from freeways in the Phoenix area was sometimes substantially higher than expected at distances of 1/4 mile or farther from the roadway. It is evident that these higher than normal sound levels are caused by atmospheric conditions. The primary questions investigated in this project were: What are the atmospheric conditions in the Phoenix valley that contribute to higher than normal sound levels? Are the conditions unique to the Phoenix valley? Can the atmospheric effects be anticipated?

The main components of the project are:

- A review of the literature relevant to how atmospheric conditions affect sound propagation.
- Detailed noise measurements in a Scottsdale neighborhood along the East Loop 101 Freeway (Pima Freeway) where there had been complaints about freeway noise from residents living more than 400 m (1/4 mile) west of the freeway. Measurements were performed over a two-week period in March 2004 and a one-week period in October 2004 out to distances of approximately 800 m (1/2 mile) west and 400 m (1/4 mile) east of the freeway.
- Computer modeling of sound propagation under various measured and inferred atmospheric conditions.
- Noise measurements before and after installation of an asphalt rubber friction course (ARFC) on the Pima Freeway. The ARFC installation was part of the ADOT Quiet Pavement Pilot Program. The scope of this project was adjusted to coincide with the Quiet Pavement Program and to collect valuable information on the benefits of ARFC pavements in residential areas that are more than 400 m from the freeway.
- A pilot study investigating parametric models of tire/pavement noise.

The results of each of these tasks are summarized here and discussed in detail in the body of the report.

ATMOSPHERIC PARAMETERS

The atmospheric parameters that affect sound propagation are:

- **Atmospheric absorption:** As sound propagates through a uniform atmosphere, some of the sound energy is absorbed by temperature and humidity-dependent processes. The sound energy absorbed increases dramatically at frequencies greater than 1,000 Hz. As a result, high frequencies tend to disappear at distances greater than 400 m from the source. Atmospheric absorption is greatest under high temperature, low humidity conditions. However, for highway noise, changes in temperature and humidity generally result in relatively small changes (1 to 3 dB) in the overall A-weighted sound level.
- **Thermal and wind gradients:** The effective speed of sound in air is a function of air temperature and wind speed. Similar to the way that light is bent at an air/water interface because of the different speeds of light in the two media, sound waves are refracted, or bent, when sound speed varies because of wind and thermal gradients.
- **Turbulence:** Turbulence causes scattering of sound and will result in short-term temporal variations in sound levels. This means that when sound propagates through turbulent air,

sound levels will fluctuate by several decibels even when there is no change in the noise source and other atmospheric conditions are stable. Since atmospheric conditions are never completely stable, the combination of turbulence and wind fluctuations causes highway sound levels at distances of 400 m or greater from a sound source to constantly fluctuate, the greater the distance, the greater the fluctuation. The maximum fluctuation is about ± 6 dB, although with the relatively stable conditions and low wind speeds typical in the Phoenix area, we believe the typical fluctuations from turbulence in the study area are closer to ± 2 dB.

CONDITIONS IN THE PHOENIX VALLEY

The Phoenix valley is characterized by light winds, clear skies, and, for approximately 70% of the time, relatively weak synoptic flow* conditions. On a typical clear sunny day, solar radiation heats the ground, which in turn heats the air in contact with the ground. The result is that the warmest air is at ground level and air temperature tends to decrease with elevation. This is referred to as a temperature *lapse*. After sunset, the ground cools faster than the air causing air temperature to increase with elevation. Air temperature increasing with elevation is referred to as a temperature *inversion*. Temperature lapse during the daytime and inversion at night is the typical pattern for the Phoenix valley. As illustrated in Figure 1B and Figure 1C, a temperature lapse causes sound waves to bend up creating a sound shadow and a temperature inversion causes sound waves to bend down and increase the sound at the ground level.

The other effect of the clear skies and weak synoptic flow conditions is that warming of the air during the daytime causes air to flow up the slopes of the local mountain ranges and cooling at night causes air to flow back down the slopes. Figure 1D illustrates the effects on sound waves when wind speed monotonically increases with elevation. There is a shadow zone upwind from the noise source and amplified sound levels downwind. During the nighttime inversion conditions, down-slope winds in the Phoenix valley tend to be characterized by calm, or nearly calm, conditions at the ground surface and low-speed jets (3 to 5 m/sec, 6 to 10 mph) at elevations of 15 to 100 m (50 to 330 ft). Thus, the wind speed profile can be quite complex with wind speed increasing and decreasing with elevation and wind direction changing with elevation. The wind conditions are apt to be particularly complex and unstable around sunrise as the inversion conditions start to break up and wind directions start to change.

Based on our literature review and discussions with meteorologists at the Arizona Department of Environmental Quality, we understand that the down-slope flow tends to be east to west in the Scottsdale area where we performed the noise measurements. Figure 1E illustrates the sound focusing and de-focusing that can be created with combination of the down-slope winds and the temperature inversions.

We can generalize the sound fields that are created by atmospheric conditions into five categories:

1. **Neutral Conditions** (Figure 1A): Sound propagates equally in all directions. Completely neutral conditions almost never exist although it is a reasonable assumption within several hundred feet of a noise source.
2. **Temperature Lapse Shadow Zone** (Figure 1B): The normal mid-day temperature lapse on clear, sunny days in the Phoenix valley creates a shadow zone around noise sources.
3. **Temperature Inversion** (Figure 1C): The temperature inversion conditions that form in the Phoenix valley on most clear nights cause sound waves to curve downward and increase sound levels. The result is that sound levels near Phoenix area freeways tend to be relatively high between sunset and about one hour after sunrise.

* *Synoptic* flow is defined as large scale meteorological patterns on a scale of 1000 km or greater.

4. **Uniform Wind Gradient** (Figure 1D): The Phoenix valley is characterized by light winds except for a few events per year. As such, sound levels are rarely controlled by upwind shadow zones and downwind sound amplification.
5. **Complex Sound Fields** (Figure 1E): The combination of nighttime temperature inversions and the down-slope drainage air flow creates complex sound fields. The average sound levels are caused by the temperature inversion conditions. Layered on top of the increased sound levels from the inversion will be both hot spots from sound focusing and cool spots from sound de-focusing. The hot spots tend to be in the downwind direction from the noise source and the cool spots in the upwind direction. Focusing/de-focusing effects can occur intermittently over 30- to 60-minute periods or can be a fairly consistent occurrence over several days. An example of consistent focusing was observed at one of the noise measurement locations during the second week of the March 2004 measurements. A dramatic example of de-focusing was observed in October 2004 at a site east of the Pima Freeway. Sound levels dropped about 10 dB from about 7:45 AM to 8:00 AM and then returned close to the original levels by 8:15 AM. At the lowest point, the traffic noise had almost completely disappeared into the background noise even though traffic volumes and speeds were relatively constant.

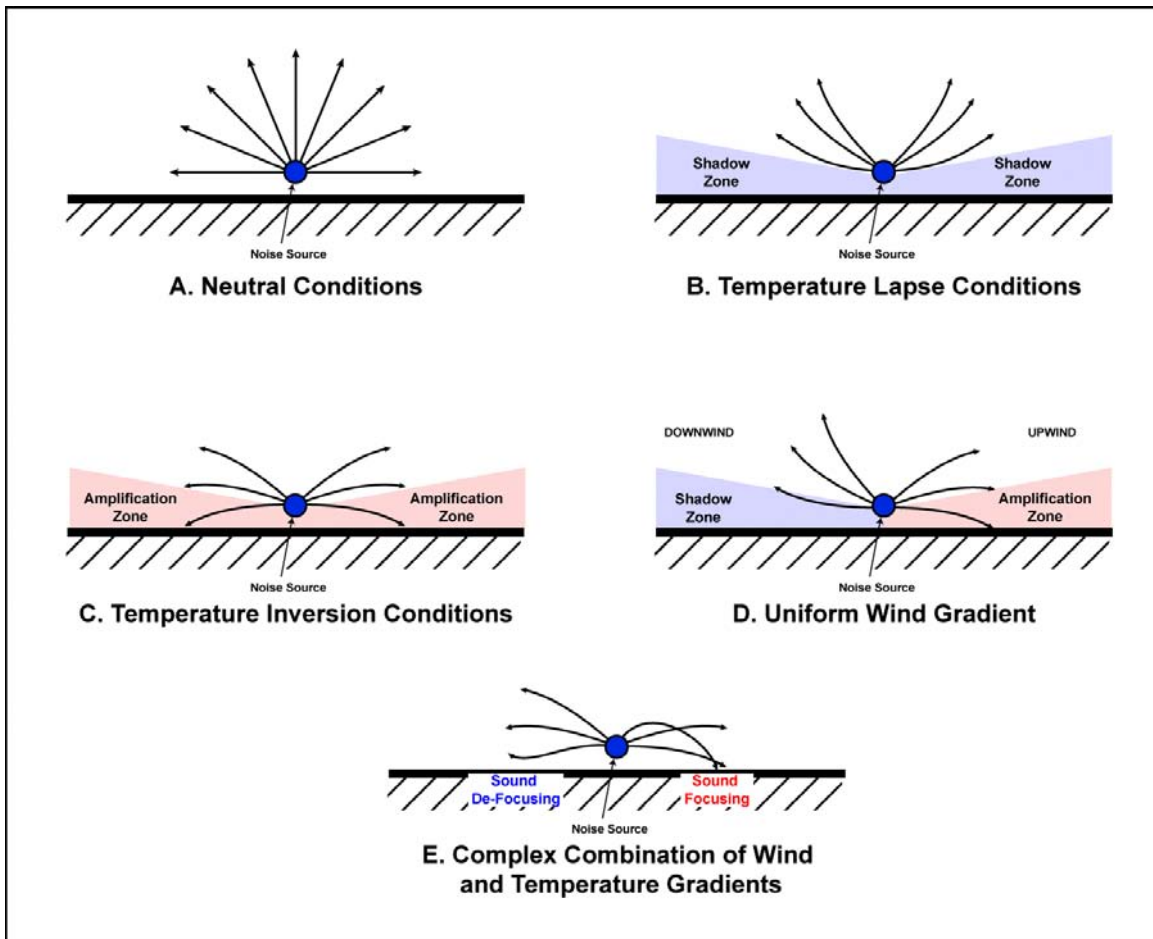


Figure 1. Sketch of Sound Refraction Effects

DIURNAL SOUND LEVEL PATTERNS IN THE PHOENIX VALLEY

In Figure 2 we have consolidated the factors that contribute to diurnal variations of traffic noise in the Phoenix valley into idealized curves. These idealized curves apply to locations more than about 300 m (1000 ft) from major freeways and are based on the measurements and modeling performed for this project. Figure 2A shows the effects for sites that are downwind relative to the early morning down-slope air flows and Figure 2B shows the effects for sites that are upwind. The plots on the left show the approximate effects of the thermal and wind gradients and the plots on the right show both the sound levels that would exist under neutral atmospheric conditions and the range of sound levels expected when atmospheric effects are included.

The hourly Leqs for the neutral atmospheric case are based on average hourly traffic counts at the Scottsdale test site in October 2004. The neutral case sound levels are lowest between 3 and 4 AM when traffic volumes are lowest. By 6 AM traffic volumes have reached their typical daytime levels and sound levels are relatively constant until 8 PM. The exceptions are a small dip at 8 AM, and a larger dip between 4 to 7 PM when traffic speeds drop because of rush hour congestion. After 8 PM traffic volumes and sound levels drop each hour until 4 AM when the morning commute period starts again.

Next the effects of refraction by temperature and wind gradients are added in. The effects of temperature inversion at night and temperature lapse during the day are an approximately 8 dB increase in sound levels between sunset and sunrise relative to neutral atmospheric conditions and an approximately 6 dB reduction in sound levels during the daytime. The transitions from inversion to lapse in the morning and lapse to inversion in the evening take 2 to 3 hours. The more rapidly the temperature increases at sunrise and decreases at sunset, the shorter the transition periods.

The final effect is the wind gradient, which, under inversion conditions, often consists of low speed jets at elevations of 15 to 100 m (50 to 330 ft). We expect that although there is a complex pattern for the inversion condition wind gradients over the Phoenix valley, the pattern is fairly consistent. This means that there may be locations that are consistently acoustic “hot spots” and others that may be only a few blocks away that are consistently acoustic “cool spots.” Without the ability to characterize the wind gradients at specific locations, it does not appear that it will be feasible to predict where acoustic hot spots will occur without extensive noise measurements.

The sound level variation for different wind gradient conditions shown in Figure 2 are:

- Inversion, downwind (Figure 2A, nighttime and early morning): In this case the wind tends to strengthen the downward refraction of the inversion conditions. The result is a small increase in the sound levels shown as 2 ± 3 dB in Figure 2A. This 2 ± 3 dB is added to the approximately 8 dB caused by the inversion giving a range of 7 to 13 dB.
- Lapse, upwind (Figure 2A, daytime): Wind directions in the Phoenix valley tend to shift 180° between inversion and lapse conditions, which means that where nighttime conditions are an inversion and downwind, the daytime condition will tend to be a lapse and upwind. Because both the wind and the temperature gradient tend to create a sound shadow, we expect the wind gradient to slightly reduce sound levels. This is shown as 1 ± 2 dB in Figure 2A added to the -6 dB due to the lapse conditions giving a range of -9 to -5 dB.
- Inversion, upwind (Figure 2B, nighttime and early morning): Now the wind gradient tends to counteract the temperature gradient. The result appears to be that sound levels fluctuate over a wider range than for the downwind case. Sometimes the wind will act to increase sound levels and other times it will act to decrease sound levels to be approximately equal to the neutral atmospheric condition case. The wind-effect range

shown in Figure 2B is ± 5 dB, which, again, is added to the approximately 8 dB caused by the inversion. The final range is 3 to 13 dB.

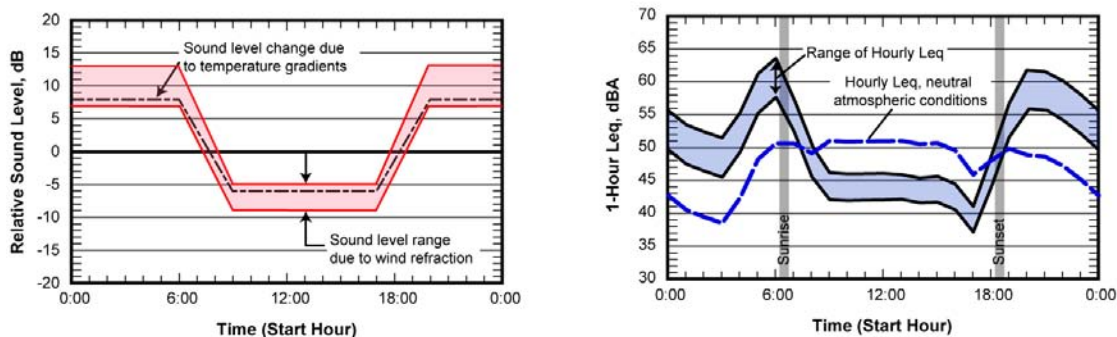
- Lapse, downwind (Figure 2B, daytime): Now the wind tends to counteract the sound shadow created by the lapse conditions. The result is expected to range from no effect to almost completely counteracting the effect of the temperature lapse. This is shown in Figure 2B as a 0 to 5 dB increase that is added to the -6 dB caused by the lapse conditions. The combined range is -6 to -1 dB.

The combined effect of traffic speed and volume variations, temperature gradients, and wind gradients is shown in the graphs on the right in Figure 2. This figure illustrates that at locations where atmospheric effects are important, the actual levels can be expected to range approximately ± 10 dB relative to neutral atmospheric conditions. Indeed, the only time the two coincide is when the lines cross during the morning and evening transition periods.

The curves in Figure 2 are based on sunset and sunrise times in March and October. In January when days are shorter, the higher noise levels will extend longer in the morning and will start earlier in the afternoon. Correspondingly, the longer days in the mid-summer will mean that inversion conditions generally will dissipate by the morning commute period and will not form until after the evening commute period. As a result, the noise increases due to inversions are probably most noticeable in cool months because the increased noise levels coincide with periods with high traffic volumes and when people tend to spend more time outside.

Another important factor is that since the range for the expected levels can be up to 20 dB, it is difficult to extrapolate from a limited number of noise measurements. However, the patterns of sound level variation observed in this project are believed to be reasonably representative of conditions in the Phoenix valley and in other locations in Arizona with similar topography and weather.

**A. Downwind Location Under Late Night/Early Morning Down-Slope Flow,
Upwind Under Daytime Up-Slope Flow**



**B. Upwind Location Under Late Night/Early Morning Down-Slope Flow,
Downwind Under Daytime Up-Slope Flow**

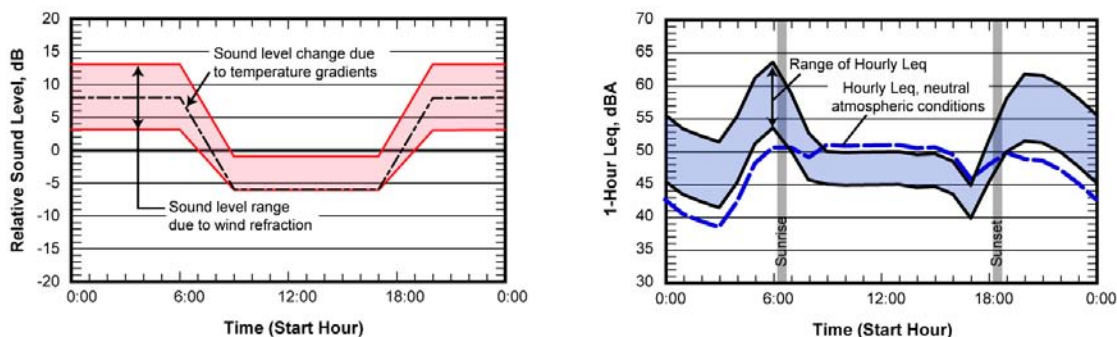


Figure 2. Illustration of Factors Driving Diurnal Variations in Sound Levels

STUDY CONCLUSIONS

The key overall conclusions of this study on how atmospheric conditions affect long distance sound propagation in the Phoenix valley are:

1. **Nighttime Inversion:** The nighttime inversion condition that is common from October through March results in sound level increases averaging from 5 to 8 dB at distances greater than 400 m (1/4 mile) from freeways. This is probably a year-round phenomenon since nighttime inversions occur in the warm weather months as well.
2. **Drainage Flow:** The nighttime down-slope drainage flows off the mountain ranges surrounding the Phoenix valley cause localized focusing and de-focusing of sound levels. These can be consistent patterns over several days or can be isolated events occurring over periods of 15 to 20 minutes. Focusing/de-focusing effects on the order of +4 to -10 dB were observed during the measurements. The Parabolic Equation computer model, a valuable tool for investigating refraction effects, could be used to investigate specific focusing effects if it were possible to obtain instantaneous wind speed and direction profiles up to elevations of 60 to 90 m (200 to 300 ft).
3. **Sound Level Variations:** Sound level variations under inversion conditions appear to be greatest at locations that are upwind relative to the down-slope flows.
4. **Seasonal Effects:** The highest sound levels during the October to March period will usually occur around sunrise when high traffic volumes coincide with strong inversion conditions.

The loudest hour during the March and October measurements was consistently 6 AM. The loudest hour is likely to shift with seasonal changes in sunrise and sunset.

5. **Onset of Refraction Effects:** The computer modeling indicates that there is a rapid onset of refraction effects between about 200 and 300 m (650 to 1000 ft) from Phoenix valley roadways. Closer than 150 to 200 m (500 to 650 ft) from a roadway the atmospheric refraction effects are generally less than ± 5 dB. At greater than 300 m (1000 ft) the refraction effects are often on the order of ± 10 dB. This is a tentative conclusion based on the computer modeling.
6. **Quiet Pavement Pilot Program:** The noise measurements before and after resurfacing the Pima Freeway with ARFC showed that sound levels were consistently reduced by 8 to 10 dB at the close-in and community measurement sites. The effects were almost entirely at frequencies of 500 Hz and higher. Before the ARFC, the sound level spectrum was dominated by sound in the 630 to 3000 Hz 1/3 octave bands. The spectrum was much more evenly balanced after the ARFC surfacing. The reduced sound levels were very evident at all of the measurement sites and a number of residents commented to us how pleased they were with the lower community sound levels. The more balanced spectrum also improved the sound "quality" and reduced the annoyance characteristic of the noise. This improved sound quality was evident at the freeway shoulder, but was less evident at the community sites because, with the reduced sound levels, the traffic noise often was no longer the dominant noise source.

1. INTRODUCTION

This report presents the final results of Arizona Transportation Research Center Project SPR 555, "Evaluate the Atmospheric Effects Associated with Highway Noise Propagation." The primary atmospheric parameters that affect sound propagation are: (1) the absolute temperature and humidity that affect the amount of atmospheric absorption, (2) temperature and wind speed gradients that cause refraction of sound, and (3) turbulence that causes scattering of the sound and short-term temporal variations in the sound levels. These atmospheric parameters can result in large fluctuations in sound level. The results of this study confirm previous measurements and anecdotal information that the Phoenix area is particularly prone to high sound levels because of strong temperature inversion conditions that occur on clear, calm nights.

Highway noise levels can vary widely with atmospheric conditions, a factor which most highway noise prediction models do not incorporate. The implicit assumption of the current version of the Federal Highway Administration (FHWA) Traffic Noise Model (TNM) Version 2.5 is a uniform (isothermal) atmosphere with no wind; conditions far from the real world of ever changing weather. However, it is a reasonable assumption within a few hundred feet of a highway and generally representative of typical or average conditions. It has long been understood that wind and thermal gradients cause refractions (bending) of sound waves that can result in substantially higher or lower sound levels than under low-wind, isothermal conditions. The primary goals of this study have been to develop insights on how and when atmospheric conditions in the Phoenix valley cause higher than normal levels of highway noise and to provide ADOT with guidelines that can be used to anticipate these conditions.

The physics behind wind and thermal gradients causing higher than normal sound levels are well understood. However, the differential equations that describe sound propagation under realistic atmospheric conditions must be solved numerically and it is difficult to obtain the detailed atmospheric data required for accurate predictions. It is only recently that researchers have been successful in developing accurate projections of some common sound focusing effects. With modern computing power and numerical methods of solving the differential equations plus new equipment that facilitates detailed atmospheric measurements, it is becoming more and more feasible to develop realistic projections based on measured atmospheric conditions.

The primary components of this study have been:

- A review of the literature relevant to how atmospheric conditions affect sound propagation. The general discussion of sound propagation in Section 2 and the discussion of atmospheric conditions in the Phoenix valley in Section 3 incorporate key elements of the literature review. In addition, a comprehensive list of references can be found at the end of the report.
- Detailed noise measurements in a Scottsdale neighborhood along the East Loop 101 Freeway (Pima Freeway). This is an area where there had been complaints about freeway noise from residents living more than 400 m (1/4 mile) west of the freeway. Measurements were performed over a two-week period in March 2004 and a one-week period in October 2004. The measurements in March included continuous noise monitoring at four sites plus meteorological measurements at elevations from 1.5 to 13.5 m (5 to 43.5 ft).
- Computer modeling of sound propagation under various measured and inferred atmospheric conditions. One of the problems with applying the computer modeling was developing representative meteorological data. We believe that the meteorological measurements performed in this study provided sufficient information to estimate the temperature gradients. However, the 13.5 m tower was not sufficiently high enough to obtain useful data on wind speed and direction at the elevations significant for refraction.

- Noise measurements before and after installation of an asphalt rubber friction course (ARFC) on the Pima Freeway. The ARFC installation was part of the ADOT Quiet Pavement Pilot Program. The scope of this project was adjusted so that the first set of measurements in March 2004 were made before ARFC was installed in the test area and the October 2004 measurements were made after the ARFC had been in place for several months. These measurements provided valuable information on the benefits of ARFC pavements in residential areas that are more than 400 m (1/4 mile) from the freeway and demonstrated that ARFC can be very effective at reducing noise at distances well beyond where sound walls are effective.
- A pilot study investigating parametric models of tire/pavement noise. Our goal for this task was to determine whether relatively simple mathematical models of tire/pavement noise that are based on fundamental acoustical principles can predict how some key parameters, such as texture and smoothness, affect levels of tire/pavement noise. The ultimate goal is to have tools that provide insights about how variations in different pavement parameters will affect noise and that can be applied in developing pavements that are optimized for low noise levels.

The remainder of this introduction presents some key acoustical concepts. The other sections in the report are:

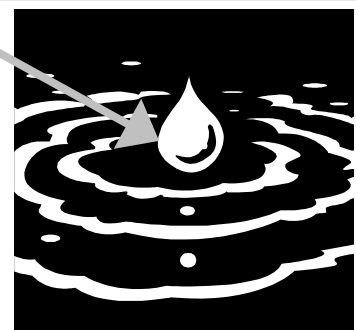
- Section 2: Background on sound propagation incorporating the most relevant information obtained during the literature review.
- Section 3: Summary of general meteorological patterns of the Phoenix valley.
- Section 4: Results of the noise measurement program.
- Section 5: Presentation of the computer modeling efforts.
- Section 6: Consolidation of the primary conclusions and important observations of this study.

In addition, photographs of the noise measurement sites are given in Appendix A, measurement details are presented in Appendix B, detailed results of the computer models are given in Appendix C, and the results of the pilot study on tire/pavement noise are given in Appendix D. A list of relevant references is located at the end of the report.

1.1 BASIC ACOUSTICAL CONCEPTS

The following opening sentence in a classic book on the history of acoustics^{11*} is a fitting point of departure for this discussion of acoustical concepts: “Man lives in an uneasy ocean of air continually agitated by the disturbances called sound waves.” Sound can be pictured as similar to the sketch on the right of an expanding circular pattern of ripples on the surface of a lake when a stone is thrown into the water. However, sound waves in the three-dimensional “ocean of air” are minute condensations and rarefactions or, simply, fluctuations of the atmospheric pressure which our ears perceive as sound. The height of the wave on the water is analogous to the magnitude of the sound pressure

A rock thrown into a lake causes ripples on the surface that are like a 2-dimensional model for sound waves in 3-dimensional space.



* See reference list at end of report.

wave. The sound of highway traffic is normally an unwanted sound and is thus, by definition, *noise*.

The basic parameters that define a sound wave are:

- the sound **pressure** or sound **level** of the sound wave,
- the **speed** of the sound wave,
- the **frequency** or **frequency spectrum** of the sound wave, and
- the **wavelength** of the sound wave.

Each of these parameters is discussed briefly below:

Sound Pressure or Sound Pressure Level: Sound waves are very small alternating perturbations in the atmospheric pressure. The sound we hear from traffic can vary in sound pressure amplitude by over 10,000 to 1 from the quietest, barely audible highway noise to the loud noise of a nearby freeway. This wide range in the magnitude of sound is compressed using the logarithmic scale for sound pressure level, in decibels (abbreviated by the symbol dB). Sound level decibels are defined by the following formula:

$$L_p = 20 \times \log_{10} \left(\frac{P}{P_{ref}} \right)$$

where P is the root-mean-square (rms) pressure in pascals and P_{ref} is the reference pressure equal to 20 micro-pascals (μPa). The decibel is abbreviated by the symbol dB.* With this scale, the sound pressure level corresponding to the lowest sound most people can hear is about 0 dB ($20\mu\text{Pa}$) and the loudest sounds from highways are around 94 dB (1 Pa).

Another detail is that environmental noise is almost always characterized in terms of the A-weighted sound level. At average listening levels, sounds of lower frequency do not sound as loud to humans as higher frequency sounds with the same sound pressure. *A-weighting* approximates this characteristic of human hearing by reducing the level of lower frequency and very high frequency sounds. Environmental sounds are almost always identified by their A-weighted sound level. The units are still decibels (dB) but are usually signified by the symbol *dBA* or *dB(A)*.

A few benchmarks about decibel scales for sound levels are useful:

- Adding one sound to another identical sound increases the sound level by 3 dB. For example, adding a sound with a level of 50 dBA to another sound with the same sound level produces a sound level of 53 dBA, not 100 dBA.
- In a still atmosphere, doubling the distance between a single sound source (e.g., the exhaust of a stationary truck) and a receiver decreases the sound level at the receiver by 6 dB in the absence of any other propagation effects. (This is called the inverse square law for the basic spreading loss in the outdoor propagation of sound.)
- If the intensity of a sound is increased by a factor of 10, the sound level is increased by 10 dB. For such a 10 dB increase in a sound level, the subjective response is that the loudness has doubled. This is a common rule of thumb that seems to be reasonably accurate, although it must be recognized that every human perceives sound differently and what sounds twice as loud to one person may sound only 50% louder to another

* An interesting historical footnote, the decibel is one tenth of a Bel, a unit named after Alexander Graham Bell, the inventor of the telephone and a pioneering advocate for the hearing impaired.

person. As discussed later, we found in the Phase 1 measurements that atmospheric conditions at some locations caused sound levels in the early morning hours to be consistently 10 to 20 decibels higher than in the mid-day period. The subjective impression was that traffic noise was two to three times louder in the early morning hours than at mid-day.

- Although A-weighting is almost universally recognized as an appropriate measure of community noise, it has also long been recognized that different sounds with the same A-weighted sound level will not always be perceived as equally loud and particularly not as equally annoying. A good example of this is tire/pavement noise. Some pavements result in a 2 to 3 reduction in the A-weighted sound level, which would be generally considered an insignificant improvement. However, as we observed in this study, most of the reduction is in the high frequencies which changes the character of the sound such that many people find it to be less annoying. The result is that the perceived improvement may be substantially more than suggested by the change in A-weighted sound level.

The Effective Speed of Sound: The speed of sound is a particularly important parameter for this study. Sound speed is nominally 345 m/sec (1,132 ft/sec or 772 mph) at the average annual outdoor temperature in Phoenix, Arizona of 73° F (22.8° C). The speed of sound in a still atmosphere increases as the temperature of the air increases. The effective speed of sound waves in a real atmosphere also changes due to wind. Similar to the way that light waves are bent when they pass from the air through another substance, sound waves will bend when they pass through an atmosphere where the sound speed varies. This effect is called refraction. Refraction of sound waves caused by sound speed gradients is the primary focus of this study and is discussed in considerably more detail in the next section.

Frequency of Sound: The frequency is the rate at which sound pressure varies with time. Pure tones, or sounds that consist of a single frequency, have a sinusoidal pattern as shown in Figure 3. The unit of frequency is “cycles per second.” It is customary to shorten the long name for the units of frequency from “cycles per second” to “Hertz” the name of a prominent German acoustician of the 1800’s and abbreviated “Hz.” Our ears can hear sounds that vary at rates from about 20 Hz up to 20,000 Hz (for people with very good hearing who haven’t been at too many rock concerts). Highway noise is made up of sounds of many frequencies and is called a broadband sound. It is characterized by the simultaneous variation of sound pressures at many different frequencies as illustrated in Figure 4.

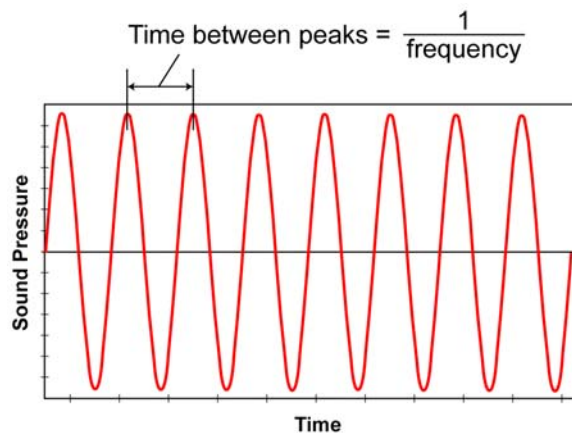


Figure 3. Sound Wave with Just One Frequency (a Pure Tone)

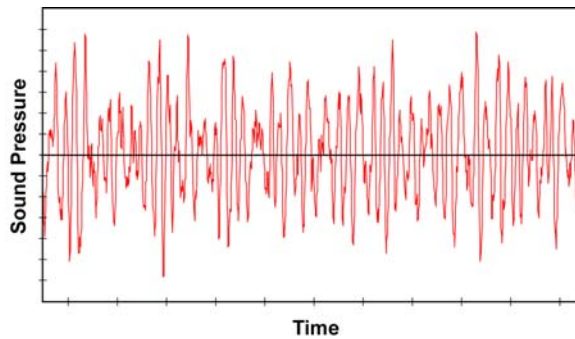


Figure 4. Sound Wave from Highway Noise with Many Frequencies

Wavelength of a sound: The wavelength, λ , of a sound is the distance between the peak values of succeeding cycles of a sinusoidal sound wave. This is just like the distance between the ripples of the waves on the pond. The wavelength is equal to the speed of sound times the time period (e.g., $1/\text{frequency}$) between two peaks of the sinusoidal signal or:

$$\lambda = \frac{c}{f}$$

where c is the speed of the sound wave and f is the frequency of the sound wave. Thus, sounds of high frequency have short wavelengths and *visa versa*. For a sound speed of 345 m/sec, the wavelength is 1.7 m (5.7 ft) at 200 Hz and 0.12 m (4.5 inches) at 3000 Hz.

Wavelength is an important parameter when looking at how obstructions such as highway sound barriers and buildings affect propagation of sound. Again, picture the ripples on the lake. It is easy to see that placing an obstacle (e.g., a barrier) at right angles to the ripples that is much larger than the wavelength of these ripples would be very effective in blocking the ripples from getting to the space behind the barrier. Conversely, placing a small post in the way of the ripples with a diameter much less than the wavelength of these ripples will have little effect and the waves will move around the post with little or no hindrance. Translating this to sound, barriers are better able to block high-frequency, short-wavelength sound than low-frequency sound with its longer wavelengths.

1.2 BENDING OF SOUND WAVES BY DIFFRACTION AND REFRACTION

Two other key characteristics of sound important for this study are *diffraction* and *refraction*, both of which represent ways in which sound waves can be bent. The concepts of diffraction and refraction are shown in the sketch of Figure 5. Diffraction is what causes sound waves to bend into the shadow zone of barriers. As discussed above, longer wavelength sounds will bend into the shadow zone easier than higher frequency sound. Refraction, which is the key characteristic of sound waves pertinent to this study, is the bending of sound waves caused by changes in the sound speed. This is the same basic phenomenon that causes a prism to split white light into different colors and causes rainbows to form when the sun shines through water droplets in the air.

Refraction of sound is caused by variations in wind speed and air temperature, which translate into variations in the effective sound speed along the sound path and corresponding variations in the direction of the sound wave. As shown conceptually in Figure 5, refraction will limit and sometimes completely negate the effectiveness of highway noise barriers, particularly at relatively large distances from the highway. When there is downward refraction, sound which would normally travel in a direction into the sky above the barrier and not be heard, can be bent back down to the ground (i.e., refracted) into the normal shadow zone of the barrier.

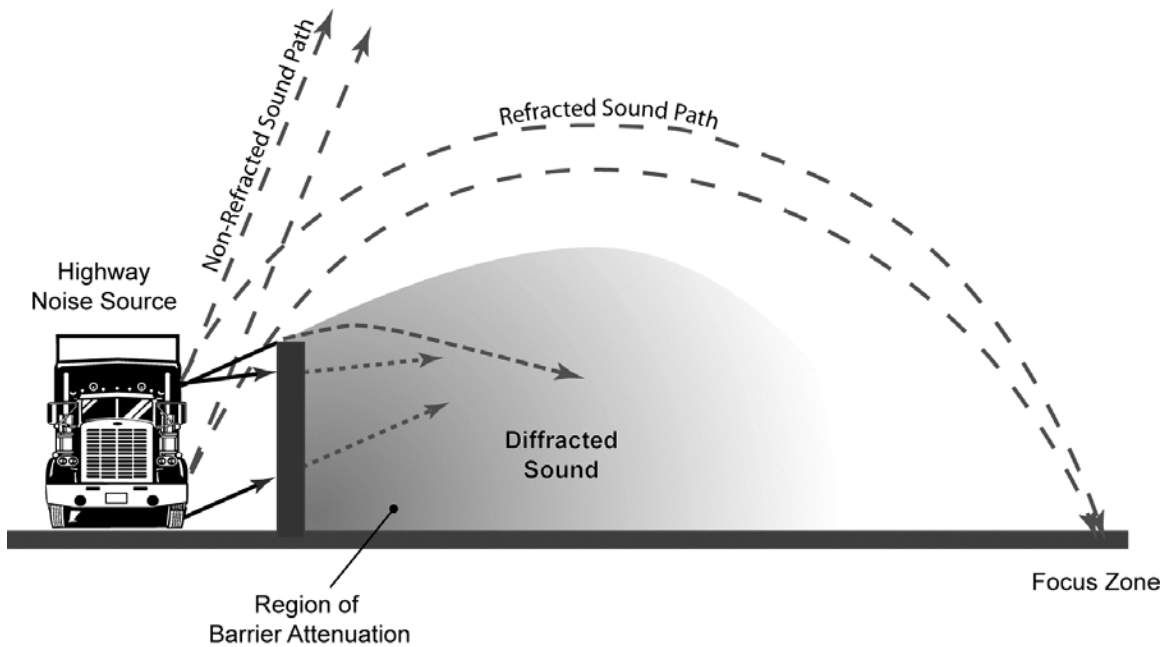


Figure 5. Conceptual Illustration of Sound Refracted By Atmospheric Profiles “Skipping” Over a Sound Barrier

The FHWA highway noise prediction computer program TNM 2.5 does not include any method to account for the effects of refraction and always assumes “neutral atmospheric conditions.” This approach is reasonably accurate at locations relatively close to a highway (perhaps 150 m, 500 ft, or less), but becomes less accurate with increasing distance from the highway. More typically, the atmosphere is not neutral and there are wind and temperature gradients which refract highway noise.

A temperature lapse is the condition for which air temperature decreases with elevation; this is the normal daytime condition in the Phoenix valley. Under lapse conditions, sound waves tend to bend up causing sound levels to be lower than under neutral atmospheric conditions. Inversion conditions are the opposite. Air temperature increases with elevation up to an inversion cap and then decreases at elevations above the cap. The result is that, below the inversion cap, sound speed increases with elevation and sound waves will tend to bend down and cause higher sound levels than under neutral atmospheric conditions. Under real world conditions, the sound speed gradient will be caused by a combination of wind and temperature gradients, which can result in very complex sound propagation patterns. Under both lapse and inversion conditions, sound levels may vary widely over relatively short distances and there can be focusing effects that cause sound levels to be substantially higher than normal.

A large part of this study has been to identify when downward refraction and focusing occurs in the Phoenix valley and to measure and predict how highway noise is affected by these phenomena.

2. BACKGROUND ON SOUND PROPAGATION

The primary purpose of this study was to increase the understanding of how atmospheric conditions in the Phoenix valley affect propagation of highway noise. Our focus has been on propagation at distances of 400 m (1/4 mile) or more where, under neutral atmospheric conditions, highway noise is almost always well below the FHWA Noise Abatement Criterion (NAC). The FHWA guidelines are that noise abatement should be considered when the maximum hourly Leq from traffic approaches or exceeds 67 dBA. ADOT defines an Leq of 64 dBA as the point where Leq “approaches” 67 dBA.

This section discusses the different mechanisms by which traffic noise changes as it propagates away from the highway. Section 2.1 discusses the primary factors that cause traffic noise to be attenuated under neutral atmospheric conditions. This includes geometric spreading, ground effects, diffraction by barriers, and atmospheric absorption. Note that TNM incorporates algorithms to account for all of these effects.

Section 2.2 discusses atmospheric conditions that affect sound propagation including refraction and air turbulence. Refraction is discussed in Section 2.2.1, turbulence in Section 2.2.2, and Section 2.2.3 is an introduction to computer models that are used to predict refraction effects. In this study, we have used the Parabolic Equation (PE) Method to predict how refraction caused by different temperature and wind gradients will affect sound levels.

2.1 NEUTRAL ATMOSPHERIC CONDITIONS

2.1.1 Geometric Spreading

Recalling the sketch earlier in Section 1.1 (page 10), as a sound wave travels out from a source with an ever-increasing radius of the wave front, the sound intensity decays as the surface of this wave front increases. A point sound source creates a spherical wave with geometric spreading loss that obeys an “inverse square” law. This causes the sound level to decay by 6 dB for every doubling of the distance from the source in the absence of any other propagation effects. This is the pattern for the decay of sound from a single, stationary vehicle.

However, highway noise analysis is typically based on Leq, the energy average or equivalent sound level over a period of time. This means that we are really concerned with the integrated time average of sound as vehicles move along the highway. Thus, the time average level from a line of traffic decreases with distance (in a loss-less, neutral atmosphere) as if the sound source is an infinite cylinder, not a single point. In terms of Leq, even a single moving vehicle acts like a line source. For a very long, straight roadway, traffic noise can thus be modeled as a cylindrical source and the area of the expanding cylindrical wave front increases with just the radius, not the square of the radius as for spherical spreading. In this case, the spreading loss causes a 3 dB reduction in sound level for every doubling of the distance from the source.

The idealized attenuations for point and line sources are shown in Figure 6. The three lines in Figure 6 are all based on a sound level of approximately 80 dB at 50 feet from the source. As can be seen, the difference between line and point sources at a distance of 1,000 feet is 13 dB. Also shown in Figure 6 is the commonly assumed attenuation curve for highway noise propagation over soft ground, an attenuation rate of 4.5 dB per distance doubling. At 1,000 ft, the difference between propagation over very hard ground and over soft ground is 6.5 dB.

For a finite segment, the road will act like a line source when the distance to the receiver is much less than the length of the segment. Conversely, it will act as a point source when the distance to the receiver is much greater than the length of the roadway. The general approach used by TNM to accurately model geometric spreading is to divide all roadways in to relatively small segments and consider the propagation from each segment independently. The

contributions from all the segments are combined to get the projected sound level at each receiver.

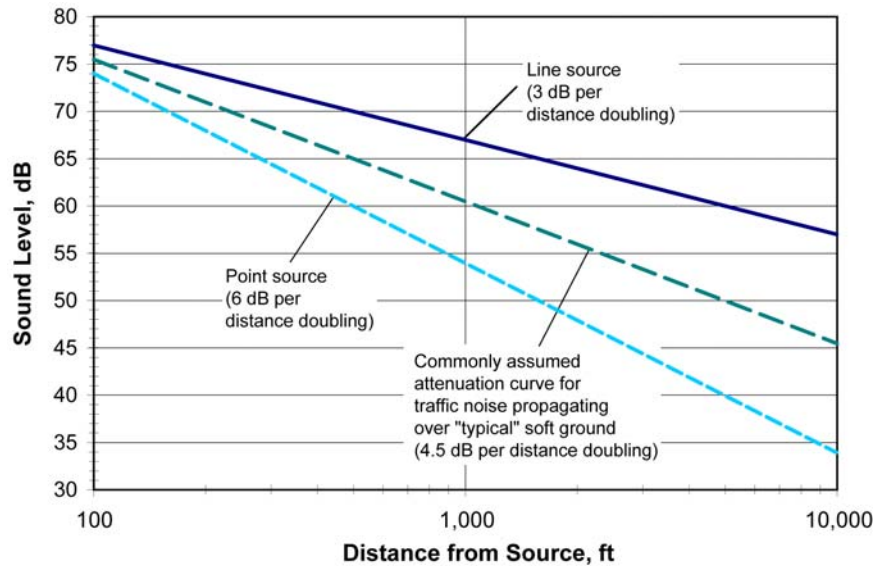


Figure 6. Attenuation Curves for Line and Point Sources

2.1.2 Atmospheric Absorption

Spreading losses do not represent a loss of sound power from a noise source, only a reduction in the sound power per unit area as the radius of an expanding wave front increases. However, there is a true loss in the total sound power as the sound propagates through the atmosphere. This loss occurs as a result of small amounts of heating and viscous losses and energy exchange between air molecules as a sound wave passes. This is called *atmospheric absorption*. Atmospheric absorption varies strongly with the frequency of the sound wave and the temperature, humidity, and, to a minor extent, the atmospheric pressure in the air. This loss is greatest at high frequencies and in hot, dry air.

Figure 7 shows atmospheric absorption as a function of frequency over a distance of 500 m (1640 ft) for the early morning and mid-day conditions of one day in March 2004. The atmospheric absorption at 1000 Hz is about 2 dB in the early morning and about 3 dB mid-day. However, by 5000 Hz, the attenuation for both times of day is over 20 dB. This is the reason that sounds lose their high-frequency content as they propagate over long distances. In fact, we judge how close a noise source is not only by the loudness but also by the high frequency content of the sound. The less high frequency, the farther away a source seems to be.

Figure 8 shows the difference between the two curves shown in Figure 7. Although there is a substantial difference at the higher frequencies, referring back to Figure 7, it is seen that these frequencies are severely attenuated in both cases so that the difference in A-weighted sound level is small.

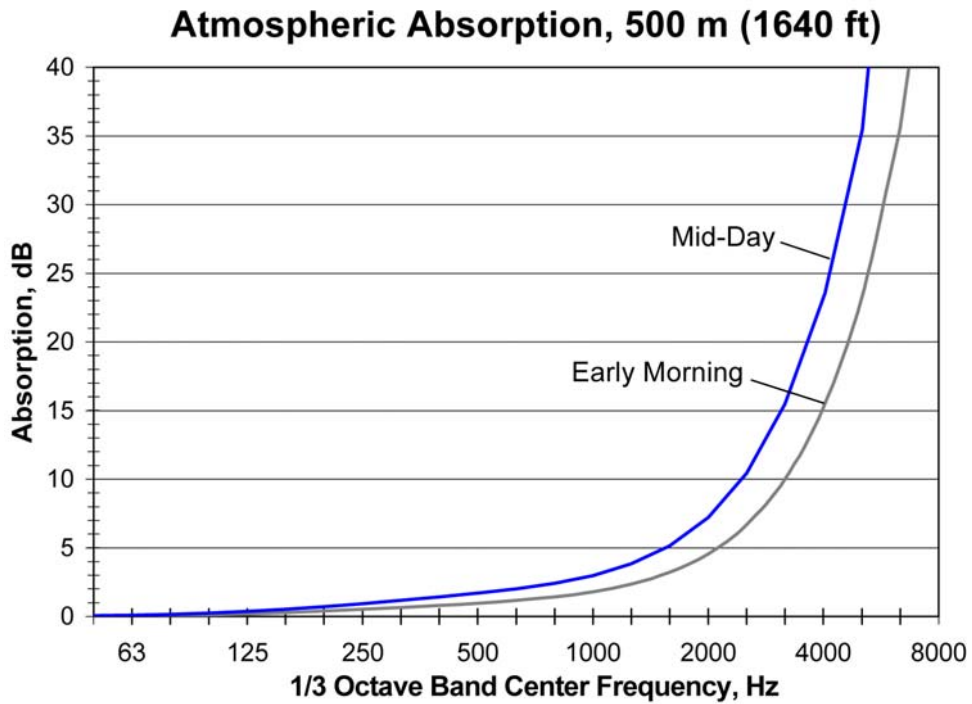


Figure 7. Atmospheric Absorption Early Morning and Mid-Day for a Representative Day in March 2004

Early morning conditions: 50°F, 75% Relative Humidity
 Mid-day conditions: 86°F, 20% Relative Humidity

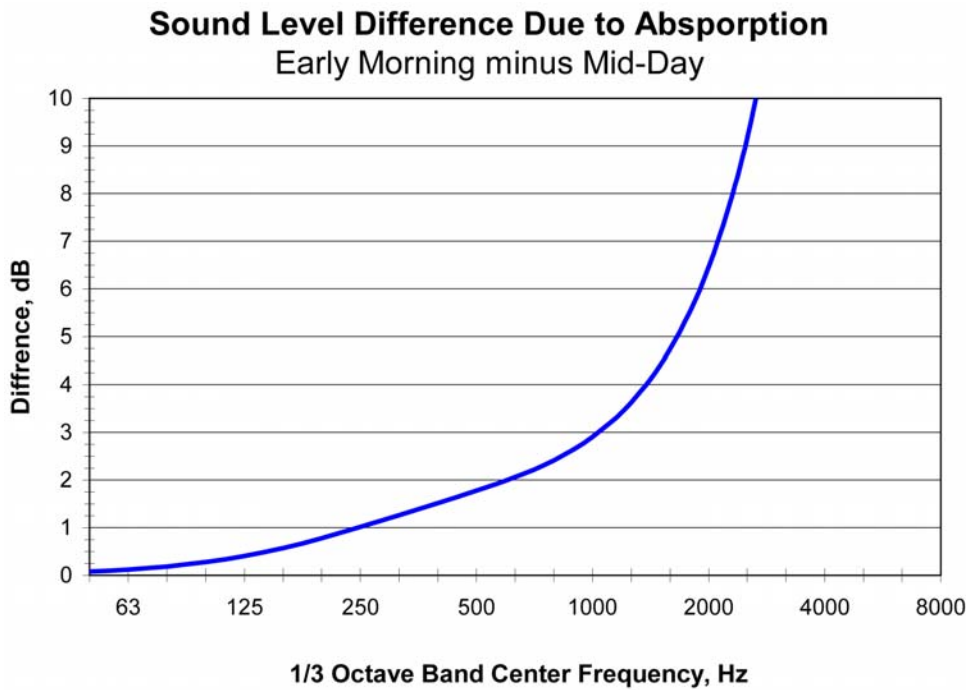


Figure 8. Difference in Atmospheric Absorption in Figure 7

2.1.3 Ground Effects

Sound propagation primarily parallel to the ground is affected by the complex interaction of the sound waves and the ground surface, which can both increase and decrease the propagation loss in excess of that provided by geometrical spreading and atmospheric absorption. The amount of ground attenuation depends on the nature of the ground, the frequency of the sound, the distance over the ground, and the source and receiver heights. TNM includes an algorithm to approximate the ground effect attenuation based on the acoustic impedance of the ground. This is illustrated in Figure 9. TNM Version 2.5 characterizes the ground impedance in terms of cgs Rayls* and allows default values ranging from 20,000 cgs Rayls (pavement) to 10 cgs Rayls (powder snow). The difference in predicted A-weighted Leq values between pavement and lower impedance ground types at several distances are tabulated in Table 1. At 305 m (1,000 ft), the difference between very high impedance (pavement) and high impedance (hard soil) results in about a 3 dB difference in the A-weighted sound level. Going from hard soil to loose soil results in an additional 8 dB difference. However, going from loose soil to the lowest default impedance in TNM (powder snow, an uncommon occurrence in Phoenix) results in an additional attenuation of only 4 dB.

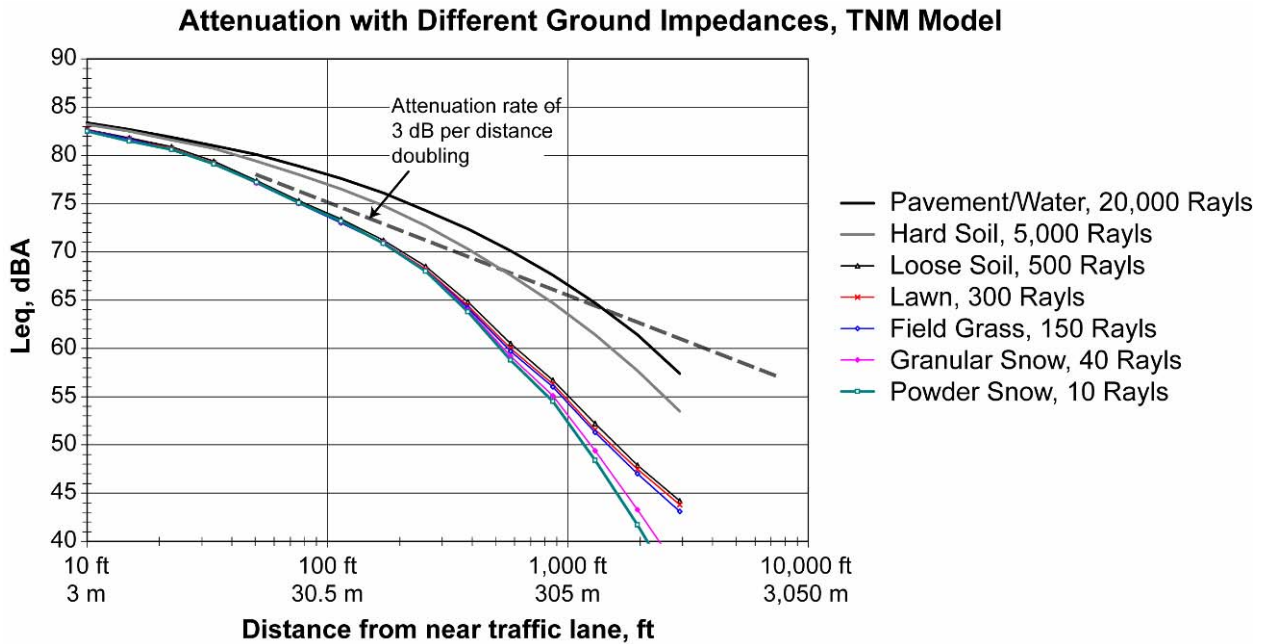


Figure 9. Combined Geometric Attenuation and Excess Ground Attenuation, Automobile Traffic on Pima Freeway
(Ground impedance in terms of cgs Rayls, receiver height = 5 ft, 1.5 m)

* Acoustic impedance is the complex ratio of the dynamic pressure to acoustic particle velocity, 1 cgs Rayl = 1 dyne·sec/cm³.

Table 1. Effects of Ground Impedance on Leq as a Function of Distance from Highway (calculations performed using TNM version 2.5)						
Distance	Difference in Average A-weighted Sound Levels Compared to Pavement^(a), dB					
	Hard Soil (5000 Rayls)	Loose Soil (500 Rayls)	Lawn (300 Rayls)	Field Grass (150 Rayls)	Granular Snow (40 Rayls)	Powder Snow (10 Rayls)
152 m (500 ft)	-2	-8	-9	-9	-10	-10
305 m (1000 ft)	-3	-11	-11	-12	-14	-15
610 m (2000 ft)	-4	-13	-14	-14	-18	-20
914 m (3000 ft)	-4	-14	-15	-16	-21	-23

Notes:
(a) Ground impedance is in terms of cgs Rayls. Pavement is assumed to have an impedance of 20,000 cgs Rayls.

2.1.4 Diffraction by Barriers and Other Obstructions

Barriers have been extensively employed along highways to help reduce the impact of highway noise at nearby residences. They are most effective at relatively short distances, typically within the first block or two from a highway. At larger distances from sound barriers, downward refraction of sound initially headed skyward can short-circuit the sound attenuation by a barrier.

In the absence of these atmospheric effects, the attenuation of barriers can be accurately predicted by well-known methods already incorporated into highway noise prediction models. For example, TNM includes provisions for evaluating attenuation from single or dual parallel noise barriers and attenuation over/through rows of buildings and dense vegetation.

The basic design and performance parameters for highway noise barriers can be summarized in a simplified form as follows:

- The barrier must block the straight-line direct path from the noise source to the receiver.
- Barrier attenuation increases as the barrier height increases.
- For structural reasons, barrier heights are generally limited to heights of no more than 30 feet.
- Barrier attenuation is greater when the distance between the barrier and the noise source or between the barrier and the listener is relatively small. That is, to be effective a barrier should be close to the noise source or close to the receiver; the farther the receiver is from the barrier, the less benefit there will be from the barrier.

A few of the trends in barrier insertion loss as a function of barrier height and distance from the source are shown in Figure 10. This example is based on the geometry at the Scottsdale test site along the Pima Freeway with a 2.4 to 8.5 m (8 to 28 ft) high sound wall located parallel to the west side of the freeway, 4.6 m (15 ft) from the edge of the pavement. The model used a default ground impedance of 500 cgs Rayls (loose soil). Figure 10 illustrates how barrier effectiveness increases with barrier height and decreases with distance from the noise source. The noise source heights are as assumed in TNM and the receiver height is 1.5 m (5 ft).

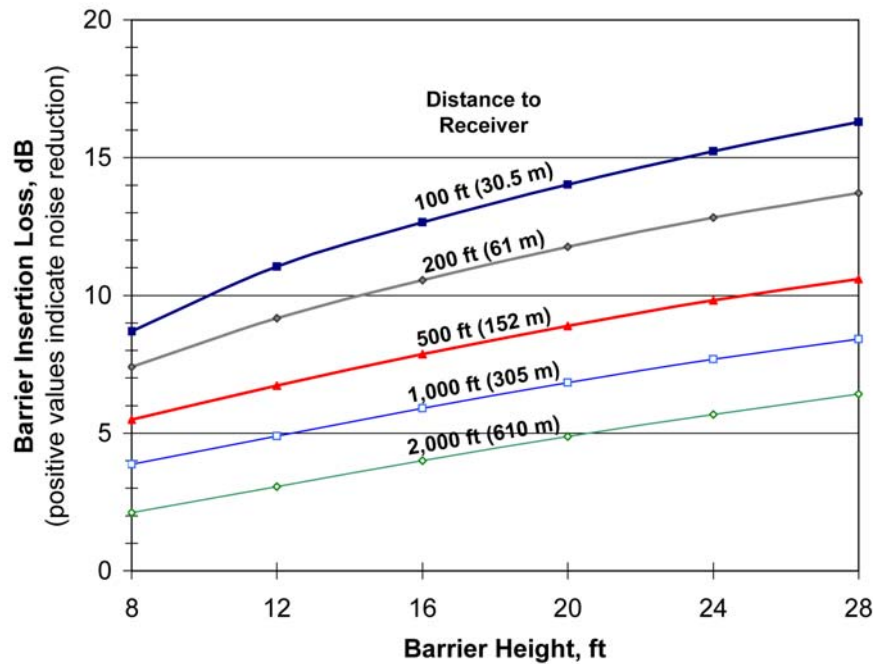


Figure 10. Representative Values for the Barrier Insertion Loss as a Function of Barrier Height and Distance to Receiver

Atmospheric effects on the propagation of sound over buildings acting as barriers in urban areas can be expected to have some similarities to those for thin barriers discussed above. However, the buildings can partially obstruct the flow of air causing the viscous and thermal boundary layer to approach the height of buildings. Thus, weather-induced refraction effects could be more limited in areas with buildings. The same influence on the surface boundary layer is also true for propagation through forests.

The ground attenuation effect in urban areas is generally much smaller than in suburban or rural areas because of more paving. The interference or sound reflection pattern of buildings is much different from that encountered over flat terrain. Prediction of sound propagation of noise from highways in suburban areas is based largely on empirical methods.^{17, 19}

2.2 ATMOSPHERIC EFFECTS

2.2.1 Refraction

Refraction of highway noise is the key factor for this study. As sound travels through still air with a uniform temperature at all altitudes, sound rays emanating in all directions from a source on the ground will travel in straight lines as illustrated in Figure 11A below. During the day, solar radiation heats the earth surface resulting in warmer air near the ground. This condition, called a temperature lapse (Figure 11B), is pronounced on sunny days but can also exist under overcast skies. A temperature lapse is the common daytime condition during most of the year and causes ray paths to curve upward. After sunset, there is often radiation cooling of the ground, which produces cooler air near the ground surface and forms a temperature inversion. Within the temperature inversion, the temperature increases with height and ray paths curve downward. (Figure 11C). Finally, when the temperature change with elevation is initially negative, close to the ground (like in Figure 11A), and then begins to increase at higher altitudes, and/or the wind is initially opposite to the propagation direction close to the ground and then reverses direction at a higher altitude, a more complex pattern such as in Figure 11D can occur. These four patterns may be categorized by their sound propagation character as:

- (A) Uniform geometric spreading without any excess attenuation or amplification from refraction effects.
- (B) Upward refraction creating an acoustic shadow zone with lower than normal sound levels. Sound levels with this condition will often be about 5 dB lower than for condition (A).
- (C) Downward refraction creating an enhanced sound fields and higher than normal sound levels. Sound levels with this condition can be 5 to 10 dB higher than for condition (A).
- (D) Sound focusing in localized regions. Depending on the amount of focusing, sound levels for this condition could be 15 to 20 dB higher than for condition (A) and more than 20 dB higher than for condition (B).

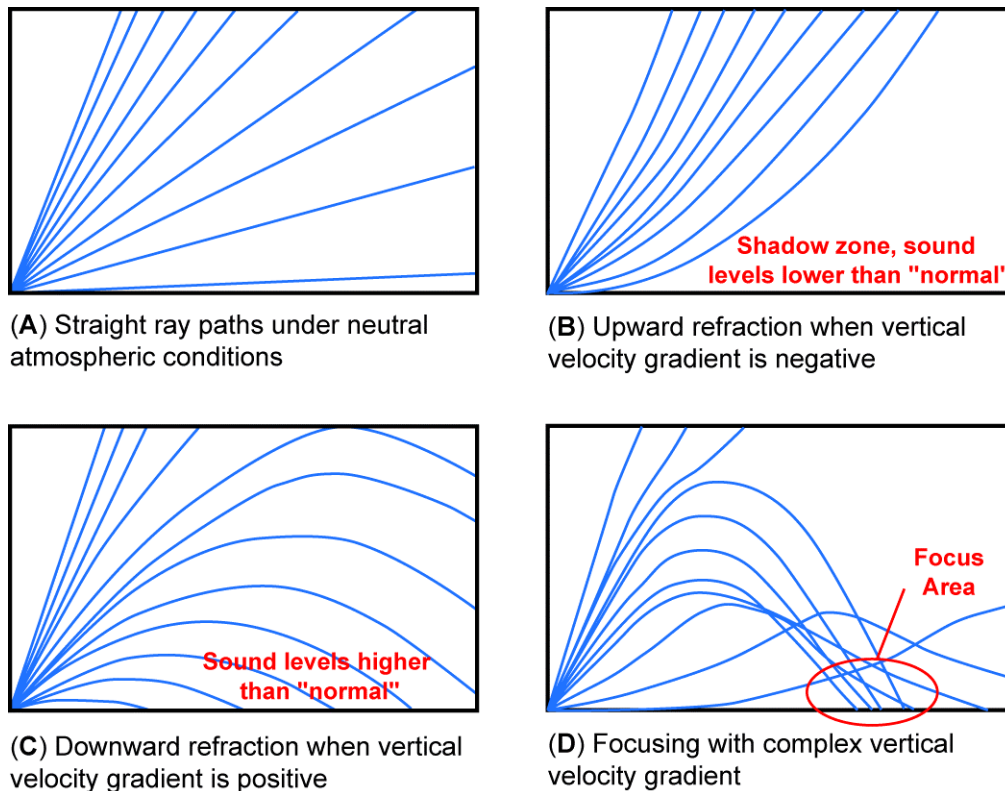


Figure 11. Sound Ray Paths for Different Patterns for Sound Velocity Gradients
(Figure after reference 20)

Representative temperature profiles measured during the Phase 1 measurements in March 2004 are shown in Figure 12. Shown are the vertical temperature profiles on the hour for 4 days. The first curve on the left is the temperature profile at midnight and the last curve on the right is the temperature profile the following night at 23:00 (11 PM). As can be seen, the vertical profile varies significantly through the day. Starting at midnight, the profile was slightly positive on March 8 and strongly positive on the other 3 days. Around 8:00, the transition from inversion to lapse starts and by 9:00 the profile is almost straight on all 4 days. This represents neutral atmospheric conditions as is assumed by the highway noise prediction programs. At around 18:00 (6 PM), the profiles are once again vertical. This means that between 9:00 and 18:00 we would expect levels of freeway noise to be equal to or lower than projected by TNM and between about 18:00 and 8:00 the following day, we would expect freeway noise to be higher than projected by TNM.

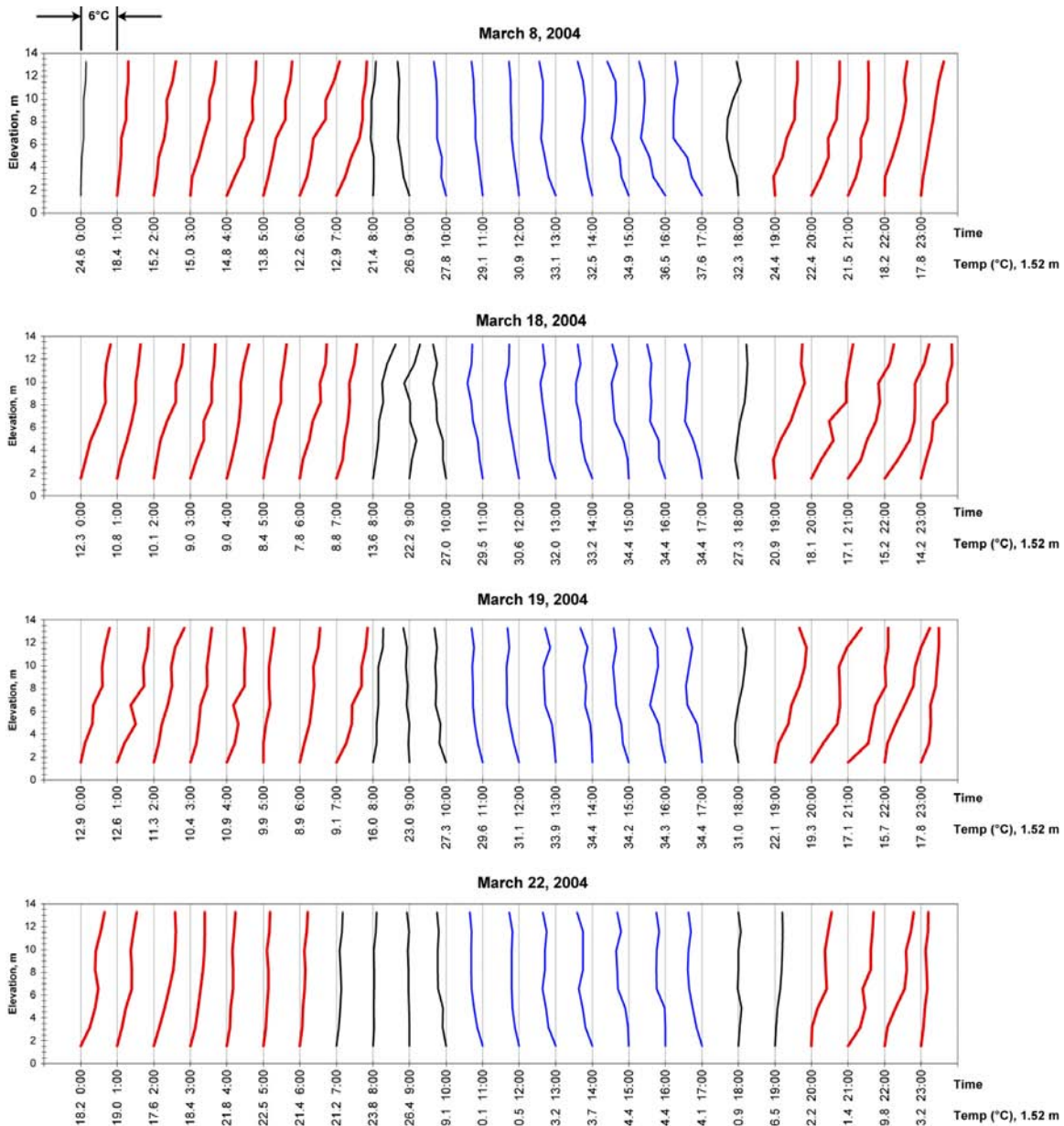


Figure 12. Vertical Temperature Profiles for 4 Days During Phase 1 Measurements

Slope to the left indicates a temperature lapse and slope to the right indicates an inversion (temperature increases with elevation)

As discussed above, downwind sound refraction can cause the initially skyward-bound sound to be refracted over buildings, trees, and other obstructions, and thus negate any benefits from obstructions partially blocking the direct path. This concept is included in ISO Standard 9613-2 where it is assumed that the refracted path, such as illustrated in Figure 5 (page 14), has a radius of 5 km (3.1 mi). However, based on a brief analysis, it appears that use of the ISO model to evaluate sound propagation from Phoenix area freeways is impractical.

2.2.2 Turbulence

Sound from a directive sound source loses energy from the primary beam of radiation by scattering or diffraction from atmospheric turbulence in addition to spreading loss, atmospheric absorption, and refraction. Theoretical predictions by Brown and Clifford⁴ indicate that this

scattering attenuation should vary substantially with the elevation of the source, the scattering attenuation decreases as the source elevation increases. This mechanism for sound attenuation is generally not included in engineering prediction models for outdoor sound propagation.

Another, more important effect of scattering by turbulence is to limit the maximum attenuation achieved in a sound shadow zone created by a negative sound speed gradient (see Figure 11B) or behind a solid body or barrier. The ray theory of sound propagation predicts that this shadow zone has sharply defined boundaries. Thus, in principle, on one side of the boundary there is a finite sound field and close by on the other side of the boundary there would be no sound. This does not really happen in practice. As sound waves propagate along the boundary of a shadow, sound is scattered (diffracted or “leaked”) by turbulence across this sharp boundary into the shadow zone. A more complete discussion of diffraction of sound can be found in Reference 23. For engineering prediction models of attenuation into a shadow zone, it is reasonable to limit the maximum attenuation to somewhere between 15 to 30 dB depending on the intensity of the turbulence in the air.^{12,24}

One final detail about the effect of turbulence on sound propagation deserves mentioning: the temporal fluctuation in sound levels caused by passage of a sound wave through the turbulent structure of the atmosphere.^{5,8} These fluctuations are normally averaged-out, even in measurements conducted over relatively short time intervals. However, the presence of these fluctuations should be recognized when acquiring any valid outdoor noise measurements and in presenting a story about outdoor sounds to the public. Their rate of fluctuation can vary from seconds to many minutes reflecting the wide range scale of turbulent patches in the air, often called “turbules.” These fluctuations of sound, when rapid, can be considered as acoustic “twinkle” like the optical twinkle in starlight or, when very slow, as like the slowly changing brightness of the moon as a patch of clouds passes though its image.

Although scattering by turbulence must be recognized as one of reasons that sound level fluctuate, turbulence will not typically cause sound levels to increase significantly compared to the non-turbulence condition. As such, turbulence is unlikely to have an important role in the relatively high noise levels observed at distances greater than 400 m (1/4 mi) from Phoenix area freeways.

2.2.3 Computer Modeling of Refraction Effects

For years, theoretical methods that used ray-tracing of sound propagation paths in the atmosphere, such as those illustrated in Figure 11, have been capable of predicting sound refraction effects. See References 18 and 20 for an introduction to these methods and Reference 21 for an updated treatment of the subject. At low frequencies, due to diffraction by turbulence, ray tracing leads to unreliable predictions of long-range sound propagation. When the effects of terrain and scattering by turbulence are included, numerical solutions to the wave equation become necessary. Until recently, the costly computation time tended to make this approach impractical. Recent advances in computers and new computer codes have made it possible to efficiently and quickly evaluate actual sound propagation under realistic weather conditions. Nevertheless, it should be made clear that earlier, but slower, computational techniques (e.g., in the days of punch cards and mainframes) were successfully employed in many situations to evaluate the risk of sound focus conditions.

The following three basic numerical programs, some with variations, have been found to be valuable tools in studying refraction effects:

- Gaussian Beam Model
- Fast Field Program (FFP) Model
- Parabolic Equation (PE) Model

An extended benchmark evaluation of these models is reported by 16 authors in Reference 2. The paper compares results for each of the models using one ground impedance model with a flow resistivity about 50% more than for grass turf and four sound speed gradient conditions (zero, negative, positive, and mixed). For the cases studied, it was found that the FFP and PE algorithms agreed to within numerical accuracy and agreed with analytical closed-form solutions for the constant gradient cases for which solutions were available. The Gaussian beam model, which is effectively a more accurate ray tracing model, apparently agreed with the more accurate FFP and PE models for the cases not involving upward refraction. No attempt was made to validate the calculations with any measurements. Each of these models is discussed below.

Gaussian Beam Model

The Gaussian Beam method calculates the path of a Gaussian cross section sound beam, as opposed to a single ray, for an arbitrary set of temperature and wind conditions and an arbitrary source above an absorptive ground plane.⁷

The Gaussian beam approach solves the wave equation in the neighborhood of the conventional rays. The solution associates with each ray a beam having a Gaussian amplitude profile normal to the ray. The approximate overall solution for a given source is then constructed by a superposition of Gaussian beams along nearby rays. The solution removes ray-tracing artifacts such as perfect shadows and infinite energy at caustics without the computational difficulties of numerical solutions to the wave equation. The method results suggest that the augmented beam tracing can be applied to complex atmospheric sound propagation problems with advantages over conventional ray tracing and full-wave solutions.

In one application written for SoundPLAN (a commercial computer program for environmental noise mapping), the sound path transmission data from the Gaussian beam program is handed off to SoundPLAN, and SoundPLAN then computes the far-field sound contours.³ This approach, called Gausbeam, was developed by acousticians at the Applied Research Laboratory at Pennsylvania State University. Gausbeam calculates the beam paths for a given set of temperature and wind conditions for a full 180° around an arbitrary sound source of known height above an absorptive plane. This model has the benefit of preserving the concept of propagation path while enabling a path computation based on actual propagation conditions. After path and propagation loss are handed over to SoundPLAN, SoundPLAN calculates barrier insertion losses based on the Gausbeam curved paths.

Gausbeam applies the concept of similarity in meteorology to either two or three temperature and two wind data points to estimate what the average sound speed profile will be for each azimuth angle relative to the direction of the wind. Ray paths are constructed using these vertical profiles. SoundPLAN then employs these path calculations to generate noise estimates and noise contours.

Fast Field Program (FFP) Model

Fast field programs permit the prediction of sound pressure in a layered (horizontally-homogeneous) refracting atmosphere at an arbitrary receiver on or above a flat continuous ground from a point source above the ground. The sound speed can be computed from known temperature and wind profiles or specified as an arbitrary function of height above the ground. The FFP method works numerically from exact integral representations of the sound field within the layered atmosphere in terms of coefficients that may be determined from the ground impedance.^{14,15} The method gets its name from the discrete Fourier transform used to evaluate these integrals. Several variants of the FFP model (CERL FFP, CFFP, FFLAG FFP, and SAFARI FFP) were included in the benchmark evaluation.²

The solution for the integral equation is found and the total field at the desired frequency calculated at any range by carrying out an inverse transform. The mathematically-indefinite integral is replaced by a numerically-finite sum using discrete Fourier transforms.

At very long ranges, the FFP has an advantage in run time but can still be time consuming. The method has the ability to provide useful predictions for any arbitrary layered atmospheric profile that is the same at all points along the propagation path.

The FFP is capable of handling realistically complicated atmospheric profiles through the altitude dependant sound speed but it is limited to either flat topography or a single large-scale topographical feature, such as a large hill. As such, it is difficult to envision adopting the FFP for analysis of realistic topography and highway barrier effects without significant additional development.

Parabolic Equation (PE) Model

In contrast to the FFP model, the PE model is a marching solution that begins at the source and sequentially solves the governing wave equation, step by step, to the receiver position. As such, it is capable of being “perturbed” along its route to account for range-dependent changes in the atmospheric profile and for modifications to account for topography and barriers. Thus, it should be superior to the FFP for real-world predictions. This is the model that we have used to analyze the effects of atmospheric conditions on sound propagation in this study.

The PE has the capability of including the largest number of atmospheric effects. It assumes that the sound wave from a source is always directed outwards and solves a two-dimensional Helmholtz wave equation with this constraint. Two variants of the PE model (Finite-PE and Fast PE) were included in the benchmark evaluation.²

The current state-of-the-art in propagation modeling is the Parabolic Equation with Greens Functions, identified as the GE-PE^{10,16}. This technique makes a stepwise calculation of the sound field as it propagates outward from the source. It can use specific sound speed profiles at each range step. However, a sound speed profile is normally measured for average conditions at one location, and generally not within the sound propagation field. This average condition is then used for each range step.

It is not practical to evaluate the real propagation path between the source and the receiver without an accurate knowledge of the atmospheric conditions that exist at each range step between the two. It is, however, possible to infer complex propagation conditions in a sound field if the atmospheric conditions are, while being complex, relatively stable. In other words, if the received sound pressure level indicates that a stable, complex propagation path has been established, then a wind and temperature profile measured near the propagation field can be applied to the entire sound field calculation.

Some examples of the PE calculations for representative weather conditions in the Phoenix valley are shown in Figure 13, Figure 14, and Figure 15. Figure 13 is for typical daytime conditions with no wind and air temperature decreasing with altitude (temperature lapse). This causes the sound rays to bend up and creates a strong shadow zone at distances greater than about 300 m (1,000 ft) from the roadway. For this situation, traffic noise even in quiet suburban areas would probably be inaudible beyond about 400 m (1/4 mile) of the roadway.

Figure 14 shows the much more complex situation that occurs under nighttime or downwind conditions. Even without air turbulence, the sound rays bend down with the result that the sound levels at distances as far as about 5 miles from the highway are attenuated by only 10 to 15 dB. These sound levels would be clearly audible in many suburban areas.

Figure 15 shows the same conditions from Figure 13 and Figure 14 except that turbulence is added. As can be seen, the results are similar in form but the turbulence increases the complexity

of the sound field and tends to reduce the shadow effect and the focusing. As discussed above, including turbulence is necessary for a comprehensive accounting of atmospheric effects. At the time of this study, the available PE codes were not sufficiently sophisticated to deal with turbulence and detailed refraction effects. As such, the PE models presented in Section 5 do not account for turbulence and the results must be used with care. In general, the results tend to overstate the effects of sound shadows and have sharper peaks and dips than would be the case were some turbulence introduced into the models.

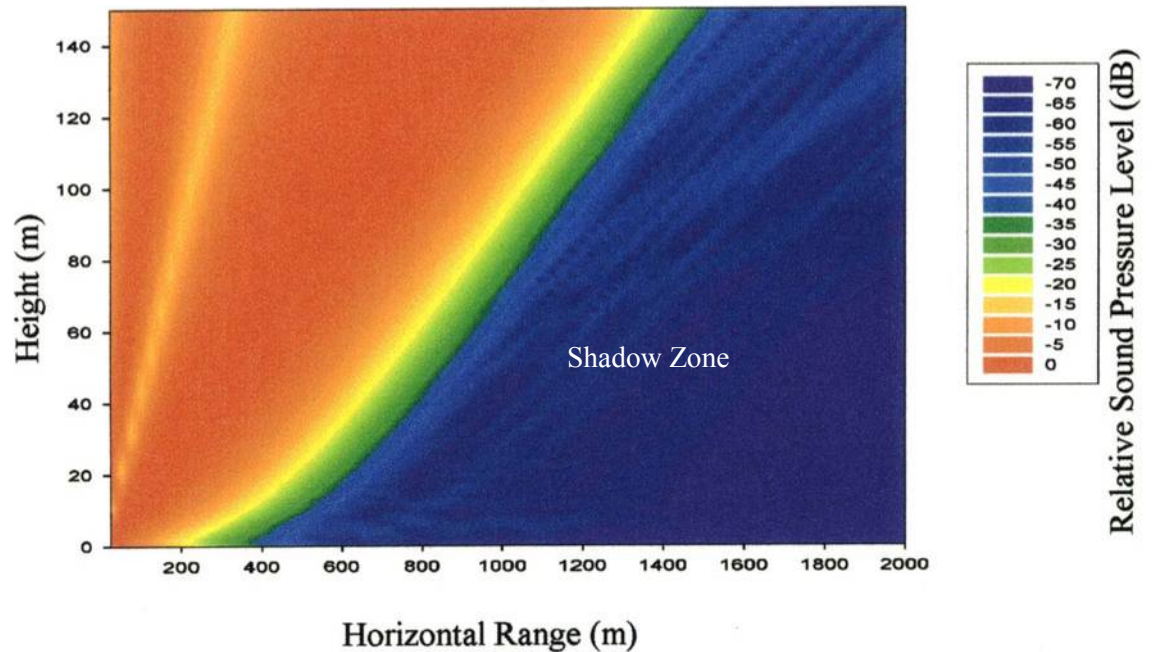


Figure 13. Example of Upward Refraction without Turbulence

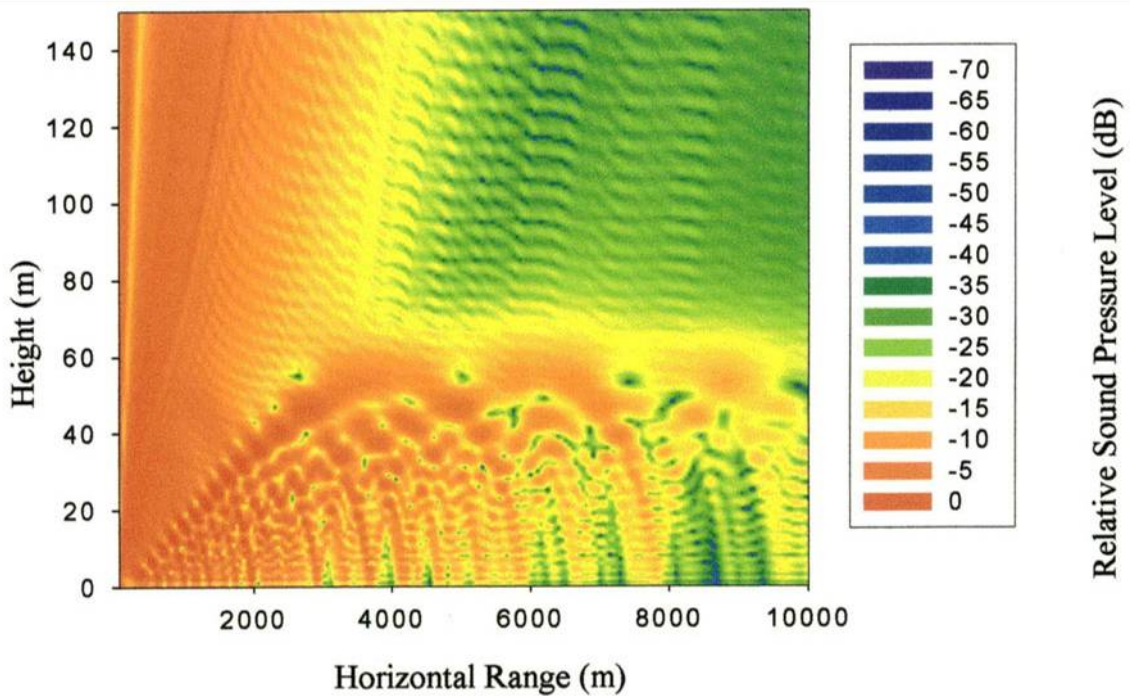
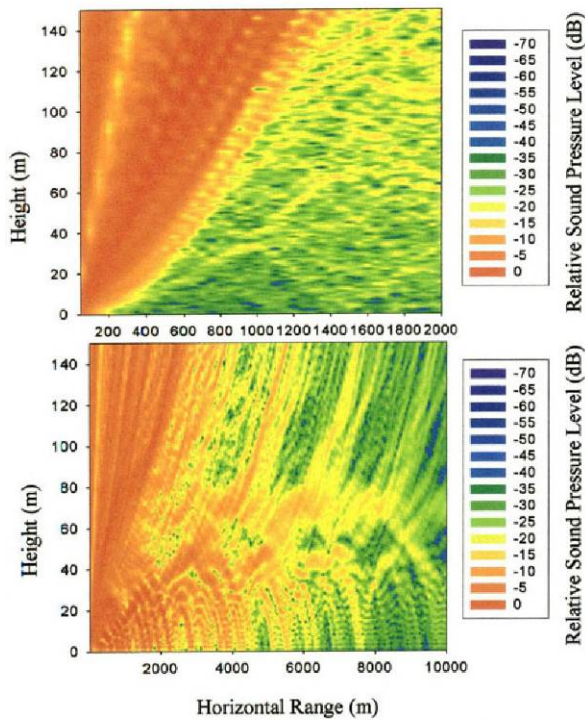


Figure 14. Nighttime or Downward Refraction without Turbulence



a. Upward refraction with no turbulence. Note reduced shadow zone.

b. Upward refraction with turbulence. Minimal global changes compared to turbulence.

Figure 15. PE Code Calculation of Sound Propagation with Turbulence

3. CONDITIONS IN THE PHOENIX VALLEY

3.1 GENERAL METEOROLOGICAL CONDITIONS

One of the questions we looked at in the literature review is whether weather conditions in the Phoenix valley are unusually conducive to higher than normal sound levels from refraction and whether focusing is likely to occur on a regular basis. The following overall summary of weather patterns in the Phoenix valley was taken from the web site of the National Climatic Data Center (www.ncdc.noaa.gov):

Phoenix is located in the Salt River Valley at an elevation of about 1,100 feet. The valley is oval shaped and flat except for scattered precipitous mountains rising a few hundred to as much as 1,500 feet above the valley floor. Sky Harbor Airport, where the weather observations are taken, is in the southern part of the city. Six miles to the south of the airport are the South Mountains rising to 2,500 feet. Eighteen miles southwest, the Estrella Mountains rise to 4,500 feet, and 30 miles to the west are the White Tank Mountains rising to 4,100 feet. The Superstition Mountains, over 30 miles to the east, rise to as much as 5,000 feet.

Temperatures range from very hot in summer to mild in winter. Many winter days reach over 70 degrees and typical high temperatures in the middle of the winter are in the 60s. The climate becomes less attractive in the summer. The normal high temperature is over 90 degrees from early May through early October, and over 100 degrees from early June through early September. Many days each summer will exceed 110 degrees in the afternoon and remain above 85 degrees all night. When temperatures are extremely high, the low humidity does not provide much comfort. Indeed, the climate is very dry. Annual precipitation is only about 7 inches, and afternoon humidities range from about 30 percent in winter to only about 10 percent in June. Rain comes mostly in two seasons. From about Thanksgiving to early April there are periodic rains from Pacific storms. Moisture from the south and southeast results in a summer thunderstorm peak in July and August. Usually the break from extreme dryness in June to the onset of thunderstorms in early July is very abrupt. Afternoon humidities suddenly double to about 20 percent, which with the great heat, gives a feeling of mugginess. Fog is rare, occurring about once per winter, and is unknown in the other seasons.

The valley is characterized by light winds. High winds associated with thunderstorms occur periodically in the summer. These occasionally create dust storms which move large distances across the deserts. Strong thunderstorm winds occur any month of the year, but are rare outside the summer months. Persistent strong winds of 30 mph or more are rare except for two or three events in an average spring due to Pacific storms. Winter storms rarely bring high winds due to the relatively stable air in the valley during that season.

Some of the key points from this discussion are:

1. The Phoenix valley is characterized by light winds. This means less air mixing and turbulence, particularly at night when inversion conditions form, which means that stronger inversion gradients form than would be the case with stronger winds.
2. Clear skies are common, which encourages formation of inversion conditions at night. Solar radiation heats the ground during the day more than the air, particularly when the air is dry as is normally the case in Phoenix. The warm ground heats the air in contact with it; this air then tends to rise. The result is that the air is warmest at the ground surface and air temperature decreases with elevation. This is a temperature lapse condition which tends to refract sound waves upward. When the sun sets, the ground surface temperature drops from radiational cooling and convection faster than the air temperature drops. This cools the air immediately above the ground surface and sets up a temperature inversion. The upper bound of the inversion condition will grow through the night. The air below the inversion cap will

be relatively stable because the air density decreases with increasing height. Overcast conditions will moderate the formation of temperature gradients.

Although we do not have access to detailed meteorological measurements in the Scottsdale neighborhoods, we can infer what the conditions are from some of the ongoing research on air quality in the Phoenix valley. One of the key air quality issues is how various air flows in the Phoenix valley mix and disperse pollutants. We derived considerable insights on air flows in southwestern cities in general, and the Phoenix valley in specific, from a paper by Fernando, et al.⁶ Some key quotes are:

“Many complex-terrain cities, particularly those in the ‘Sun Belt’ of the Southwestern U.S. (e.g., Phoenix, El Paso and Las Vegas), nevertheless, are located in areas characterized by high pressure and low synoptic winds* (Wang and Angell, 1999), and their microclimate is dominated by local thermal circulation.”

“Approximately 70% of the year, the synoptic flow in this area (Phoenix valley) is weak and local slope and valley winds are dominant.”

“The typical velocity structure that prevailed during the measurements is ... a well-defined low-level jet of which the wind speed is about 8 times that at the surface...”

“This elevated (~30 m) jet is the major mechanism for aerosol pollutant transport...”

Figure 16, taken from Fernando, et al, shows the complex terrain surrounding Phoenix and the local thermal circulation. During the day, warm air from the valley tends to rise and flow up the slopes. When the sun sets and the valley air cools, the flow changes to down slope (referred to as katabatic winds). As shown in the drawing, the adjacent slopes have a scale of 10 km and the drainage flow through the complex geometry of the more distant slopes is a scale of 100 km. We believe that a key factor of these flows for sound propagation is the low level jets that form at elevations of 20 to 50 m (66 to 165 ft). Not only will the wind speed of the jets be about eight times that at the surface, but the temperatures are likely to be lower. The other key factor is that katabatic winds with the formation of low level jets is a relatively stable phenomenon that occurs about 70% of the time.

* *Synoptic* flow is defined as large-scale meteorological patterns on a scale of 1000 km or greater.

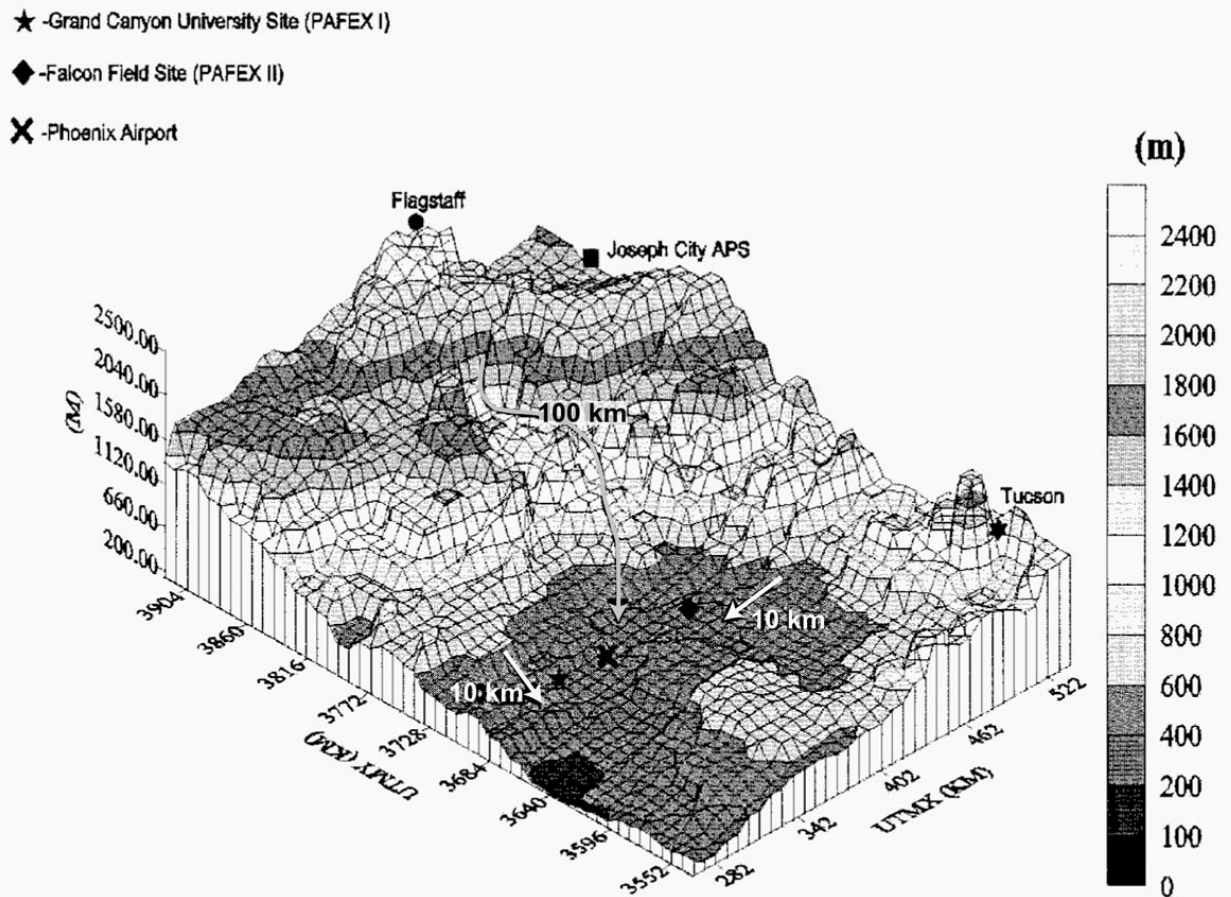


Figure 16. Drainage Flows in Complex Terrain Surrounding Phoenix

Figure 9b in Fernando, et al, Reference 6. Caption: The complex terrain surrounding Phoenix, Arizona. Some key cities, sites of PAFEX field experiments (Section 4), and the Phoenix Sky Harbor International Airport are indicated. Scales of katabatic winds induced by adjacent slopes (10 km) and drainage flow through the complex topography (100 km) are indicated.

3.2 WIND SPEED AND DIRECTION

From some discussions with meteorologists at the Arizona Department of Environmental Quality (ADEQ), we developed a general understanding of the normal air flows in the Phoenix valley. Since this is a key factor in how air pollutants are disbursed through the valley, it is a topic they are very familiar with. At the noise measurement locations in Scottsdale, the normal drainage flows off the mountain ranges in the nighttime hours is from the northeast, which means that in the early morning hours when sound levels are highest, these neighborhoods are downwind from the Pima Freeway at about a 45° angle. In addition, the ADEQ data from 43rd Avenue along with other air flow data for the Phoenix valley shows that the drainage flows often have low speed air jets at elevations of 20 to 50 m (66 to 165 ft) elevation. In combination with the typical early morning inversion conditions, this scenario could result in very localized focusing where noise levels are substantially higher than normal over a limited area.

Before the measurements, we expected to find that the wind was the primary cause of the reported higher than normal sound levels in the Scottsdale neighborhoods west of the Pima Freeway. As discussed later, after the measurements and additional computer modeling, we

believe that the main driver of the higher noise levels in the early morning hours is downward refraction caused by the inversion conditions with the drainage flow winds probably causing focusing and other localized effects.

An extended series of wind speed and direction measurements performed by ADEQ near the southern end of 43rd Avenue is the most extensive set of wind data that we were able to locate. We are very grateful for the help that ADEQ staff gave us in understanding and interpreting this data. During the March 2004 tests, we measured wind speed and direction at a height of 13.3 m (43.5 ft). Unfortunately, this was not sufficiently high enough to get out of the surface boundary layer and did not provide information on the low speed air jets. As a result, we used a selected set of the 43rd Avenue data as representative of wind conditions where the measurements were performed.

Figure 17 illustrates the 43rd Avenue data between midnight and 7 AM on January 2, 2003. Shown are the wind speeds up to an elevation of 200 m (656 ft). Except for the low-speed jet between 50 and 70 m (164 to 230 ft), wind speeds were relatively low, usually in the range of 0 to 2 m/sec (0 to 4.5 mph). The wind speeds in the 50 to 70 m jet were mostly in the range of 2 to 4 m/sec (4.5 to 8.9 mph). These wind speeds are all relatively low, even within the 50 to 70 m jet. As discussed later, our computer modeling of sound propagation indicates that the low-speed jet shown in Figure 17 causes sufficient refraction to create about a ± 5 dB fluctuation around the sound level that would occur with just the downward refraction caused by the inversion condition.

Wind Speed at 43rd Avenue, Phoenix, Morning of January 2, 2003

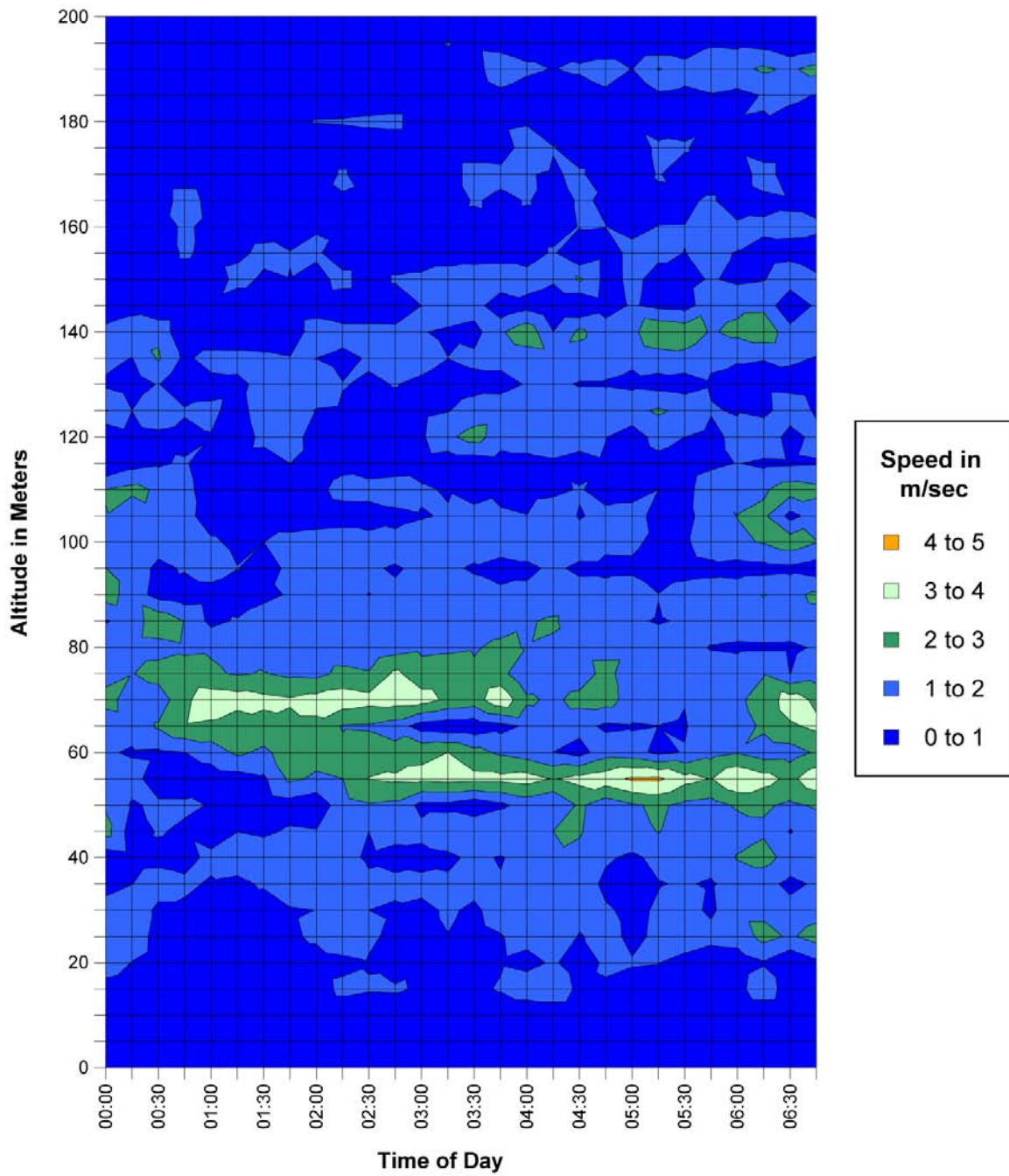


Figure 17. Example of Wind Speed Profile from ADEQ Data at 43rd Avenue

4. NOISE MEASUREMENTS

The noise measurement program consisted of measurements at four locations over a two week period in March 2004 (Phase 1) and less comprehensive follow-up measurements in October 2004 (Phase 2). The primary purpose of the measurements was to document diurnal sound level fluctuations and correlate the fluctuations to atmospheric conditions. A secondary purpose was to document the effects of the ARFC that was installed on the Pima Freeway in June 2004, 4 months prior to the Phase 2 measurements.

The Phase 1 measurements included continuous noise measurements at four sites, three west of the Pima Freeway and one east of the freeway, monitoring of temperature at intervals of 1.7 m (5.5 ft) from 1.5 m (5 ft) to 13.3 m (43.5 ft) above ground level, and wind speed and direction at 2.1 m (7 ft) and 13.7 m (45 ft) above ground level. Because of a vandalism incident at one site and concerns about vandalism at a second site, the noise monitors at these sites were picked up every night and put out again early the next morning. In all cases, the microphones were mounted at an elevation of 2 m (6.5 ft) above the ground.

The Phase 2 measurements in October 2004 were limited to noise monitoring at the three sites west of the Pima Freeway plus short-term (3 hour) measurements at selected sites on three mornings. Continuous traffic counts were performed by another consultant (Traffic Research & Analysis, Inc.) using an automated radar system for several days during the Phase 1 measurements and over the entire Phase 2 measurement period.

Details of the monitoring sites are given in the next section (Section 4.1) and photographs of the sites are given in Appendix A. The detailed measurement results are presented in Appendix B. Section 4.2 presents our analysis of the long term A-weighted noise data and Section 4.3 presents the results of the short term measurements. The Phase 1 and Phase 2 results are compared in Section 4.4 to estimate how much and over what frequency range the sound levels changed due to the ARFC.

4.1 MEASUREMENT LOCATIONS AND PROCEDURES

4.1.1 Measurement Sites

All of the noise measurements were performed in the Scottsdale area along the Pima Freeway between Indian School Road to the south and Chaparral Road to the north. Figure 18 is an aerial photograph showing the noise measurement locations. The area is quite flat with the overpasses at Indian School and Chaparral the only significant changes in roadway elevation. The open land is all part of the Salt River Pima-Maricopa Indian Community (SRPMIC). The fields were freshly plowed in March 2004 at the start of the measurements. By the Phase 2 measurements, the fields east of the freeway were full of mature Pima cotton plants. The Scottsdale residential area west of the freeway is single family houses, most of which are single story.

This area was selected for the noise testing because the flat terrain and straightforward geometry minimized the number of non-atmospheric parameters that might affect sound propagation, and, perhaps more importantly, because there had been complaints about high noise levels from the Scottsdale community west of the freeway. Previous spot-check noise measurements in response to the complaints had found sound levels between 6 AM to 7 AM to be 64 to 68 dBA (10-minute Leq). The previous noise measurements were performed in November 2000 and February 2001.

The measurement sites, distance from the freeway, and types of measurements performed at each site are summarized in Table 2. Brief descriptions of each site are given below:

4. NOISE MEASUREMENTS

The noise measurement program consisted of measurements at four locations over a two week period in March 2004 (Phase 1) and less comprehensive follow-up measurements in October 2004 (Phase 2). The primary purpose of the measurements was to document diurnal sound level fluctuations and correlate the fluctuations to atmospheric conditions. A secondary purpose was to document the effects of the ARFC that was installed on the Pima Freeway in June 2004, 4 months prior to the Phase 2 measurements.

The Phase 1 measurements included continuous noise measurements at four sites, three west of the Pima Freeway and one east of the freeway, monitoring of temperature at intervals of 1.7 m (5.5 ft) from 1.5 m (5 ft) to 13.3 m (43.5 ft) above ground level, and wind speed and direction at 2.1 m (7 ft) and 13.7 m (45 ft) above ground level. Because of a vandalism incident at one site and concerns about vandalism at a second site, the noise monitors at these sites were picked up every night and put out again early the next morning. In all cases, the microphones were mounted at an elevation of 2 m (6.5 ft) above the ground.

The Phase 2 measurements in October 2004 were limited to noise monitoring at the three sites west of the Pima Freeway plus short-term (3 hour) measurements at selected sites on three mornings. Continuous traffic counts were performed by another consultant (Traffic Research & Analysis, Inc.) using an automated radar system for several days during the Phase 1 measurements and over the entire Phase 2 measurement period.

Details of the monitoring sites are given in the next section (Section 4.1) and photographs of the sites are given in Appendix A. The detailed measurement results are presented in Appendix B. Section 4.2 presents our analysis of the long term A-weighted noise data and Section 4.3 presents the results of the short term measurements. The Phase 1 and Phase 2 results are compared in Section 4.4 to estimate how much and over what frequency range the sound levels changed due to the ARFC.

4.1 MEASUREMENT LOCATIONS AND PROCEDURES

4.1.1 Measurement Sites

All of the noise measurements were performed in the Scottsdale area along the Pima Freeway between Indian School Road to the south and Chaparral Road to the north. Figure 18 is an aerial photograph showing the noise measurement locations. The area is quite flat with the overpasses at Indian School and Chaparral the only significant changes in roadway elevation. The open land is all part of the Salt River Pima-Maricopa Indian Community (SRPMIC). The fields were freshly plowed in March 2004 at the start of the measurements. By the Phase 2 measurements, the fields east of the freeway were full of mature Pima cotton plants. The Scottsdale residential area west of the freeway is single family houses, most of which are single story.

This area was selected for the noise testing because the flat terrain and straightforward geometry minimized the number of non-atmospheric parameters that might affect sound propagation, and, perhaps more importantly, because there had been complaints about high noise levels from the Scottsdale community west of the freeway. Previous spot-check noise measurements in response to the complaints had found sound levels between 6 AM to 7 AM to be 64 to 68 dBA (10-minute Leq). The previous noise measurements were performed in November 2000 and February 2001.

The measurement sites, distance from the freeway, and types of measurements performed at each site are summarized in Table 2. Brief descriptions of each site are given below:

Long-Term Sites

- **Site 1**, Pima Freeway right-of-way 30.5 m (100 ft) west of centerline of southbound traffic lanes. This is the same location as Site 3E for the Quiet Pavement Pilot Program. The monitor was located just south of mile post 47 between Chaparral Road and Indian School Road.
- **Site 2**, Backyard of 8701 E. Highland Avenue: The monitor and a 13.7 m (45 ft) weather station tower were located in the middle of the east side of the backyard. For the Phase 2 measurements it was not possible to locate the monitor in the same yard, so the monitor location was shifted to the next yard to the east 12.2 m (40 ft) closer to the freeway. Figure 19 is a closer aerial view of Sites 2 and 3.
- **Site 3**, Backyard of 8547 E. Highland Avenue: The monitor was located in the backyard next to the garage. Measuring from the NE corner of the garage, the microphone was located 20 ft east and 15 feet north. Temperature and humidity at a height of 2.3 m (7.5 ft) was measured at 15 minute intervals during the Phase 1 measurements.
- **Site 4**, SRPMIC land east of freeway: This site was approximately 9 m (30 ft) west of 92nd Street (a dirt road between Indian School and Chaparral) and approximately 400 m (1/4 mile) north of Indian School Road. This site was used as a short-term site in the Phase 2 measurements. Figure 20 is a closer aerial view of Site 4.

Short-Term Sites

- **Site 2B**, on sidewalk in front of 8707 Camelback Road. Two 3-hour measurements were performed at this site during the Phase 2 measurements.
- **Site 2C**, on sidewalk in front of 8721 Sells Drive. Two 3-hour measurements were performed at this site during the Phase 2 measurements.
- **Site 3B**, on sidewalk of Camelback Road near the eastern edge the Navajo School playing fields.
- **Site 4B**, just west of 92nd Street, 400 m (1/4 mile) north of Site 4. Site 4B was the same distance from the Pima Freeway as Site 4 (see Figure 20).

Table 2. Distance of Measurement Sites from Near Lane of Pima Freeway

Site Description	Distance from Freeway		Measurement Type
	Meters ^(a)	Feet ^(b)	
Site 1: Freeway Right of Way	30.5	100	Continuous ^(c)
Site 2 (Phase 1): 8701 E. Highland Ave. (backyard)	525	1720	Continuous
Site 2 (Phase 2): 8711 E. Highland Ave. (backyard)	510	1680	Continuous
Site 2B: 8707 Camelback Rd. (sidewalk)	450	1475	Short-Term
Site 2C: 8721 Sells Dr.(sidewalk)	430	1415	Short-Term
Site 3: 8547 E. Highland Ave. (backyard)	800	2620	Continuous
Site 3B: Navajo School (sidewalk of Camelback Road)	755	2475	Short-Term
Site 4: 92nd Street 1/4 mile north of Indian School Road	450	1485	Continuous ^(c)
Site 4B: 92nd Street 1/2 mile north of Indian School Road	450	1485	Short-Term

Notes:
 (a) Except for Site 1, distances rounded to nearest 5 m.
 (b) Except for Site 1, distances rounded to nearest 5 ft.
 (c) Monitors were picked up in the evening and reinstalled in the morning because of vandalism potential.



Figure 18. Aerial Photograph of Noise Measurement Sites

Distances from center of near lane of Pima Freeway:

Site 1	Phase 1&2	30.5 m	100 ft	Long-Term
Site 2	Phase 1	524 m	1720 ft	Long-Term
Site 2	Phase 2	512 m	1680 ft	Long-Term
Site 2B	Phase 2	450 m	1475 ft	Short-Term
Site 2C	Phase 2	432 m	1415 ft	Short-Term
Site 3	Phase 1&2	798 m	2620 ft	Long-Term
Site 3B	Phase 2	755 m	2475 ft	Short-Term
Site 4	Phase 1&2	452 m	1485 ft	Long-Term (Short-Term for Phase 2)
Site 4B	Phase 2	452 m	1485 ft	Short-Term

(distances in feet rounded to nearest 5 ft)



Figure 19. Aerial Photograph of Sites 2 and 3

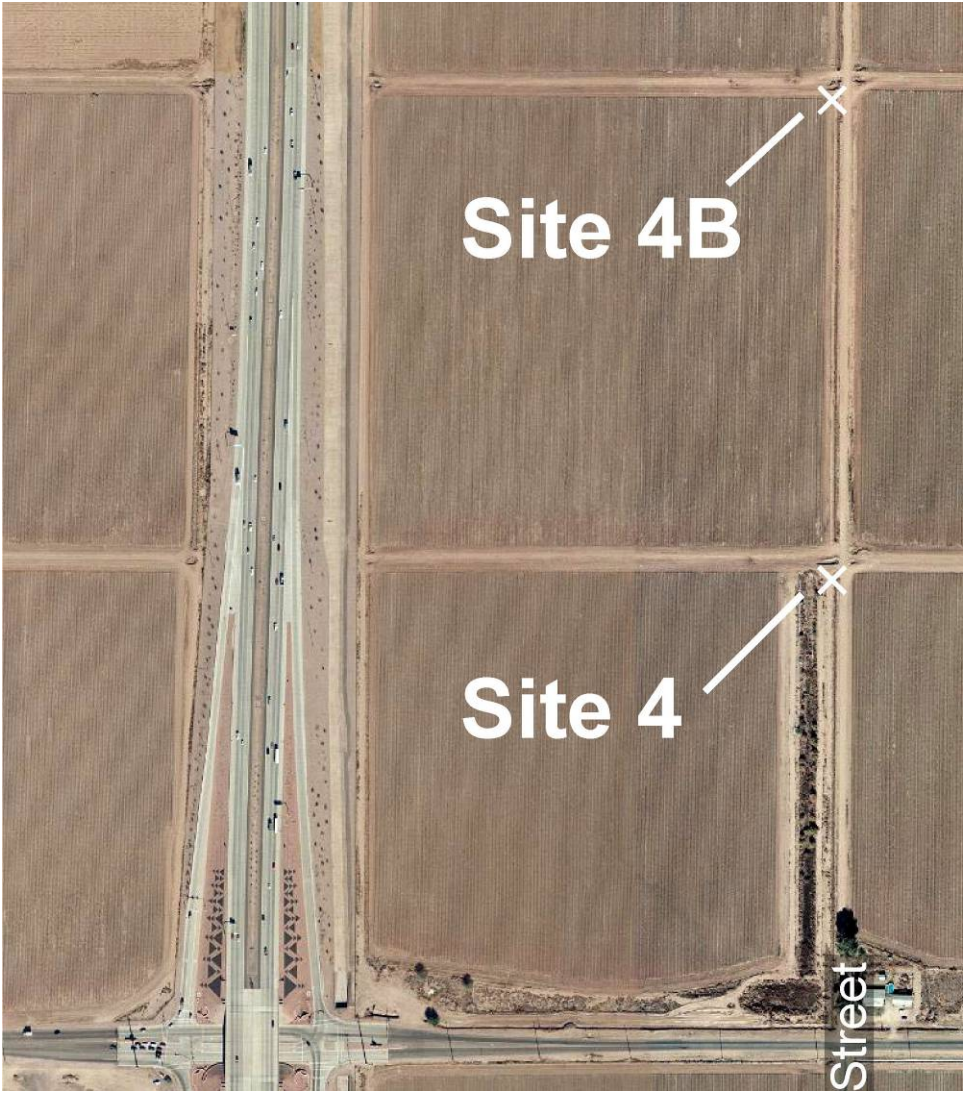


Figure 20. Aerial Photograph of Sites 4 and 4B

4.1.2 Measurement Equipment and Procedures

Figure 21 is a schematic of the field equipment used for the Phase 1 measurements. The configuration was:

- Continuous noise monitoring at all four sites. A-weighted and 1/3 octave band data were collected at 1-second intervals at Sites 2 and 3 and at 15-second intervals at Sites 1 and 4.
- Continuous audio recording at Site 3 to allow verification of whether specific periods were traffic noise or another noise source.
- Meteorological monitoring at Sites 2 and 3. The meteorological data collected at Site 2 included wind speed and direction at elevations of 13.3 m (43.5 ft) and 2.1 m (7 ft) plus air temperature at 1.7 m (5.5 ft) intervals from 1.5 m (5 ft) to 13.3 m (43.5 ft). The Site 2 meteorological data were collected at 15-second intervals. In addition, ground level temperature and humidity data were collected at Site 3 at 15-minute intervals.
- Continuous counts of traffic and measurements of speed on the Pima Freeway. This information was provided by another ADOT consultant (Traffic Research & Analysis, Inc.) using a radar system. The traffic count data consisted of volumes, average speed, and the traffic distribution between autos and heavy trucks at 15-minute intervals. The traffic counts did not start until the second week of the Phase 1 measurements.

All of the noise monitoring for Phase 1 was performed with Larson Davis Model 824 sound level meters equipped with the 1/3 octave band option. The monitors at Sites 1 and 4 were placed between 5 and 6 AM each morning and picked up around 8 PM each evening. The monitors at Sites 2 and 3 were located in the backyards of two residences on East Highland and were left in place for the entire measurement period. We were unable to leave the monitors at Sites 1 and 4 in place for extended periods of time because of problems with vandalism.

The original test plan was to do simultaneous measurements in March 2004 at two locations, the primary site in Scottsdale and a secondary site elsewhere in the Phoenix area. Because the Pima Freeway at the primary site in Scottsdale was scheduled to be resurfaced with ARFC shortly after the March measurements, the project team and the Technical Advisory Committee decided that it would be more valuable to ADOT to perform a second set of noise measurements at the Scottsdale site after the resurfacing had been completed. The resurfacing was completed in June 2004 and the second set of measurements was performed 4 months later in October 2004.

The goals of the Phase 2 measurements were to verify the observations and conclusions from Phase 1, determine whether there were consistent differences in the diurnal sound level variations in October compared to March, and document the effects of the Pima Freeway resurfacing on neighborhood noise levels. The Phase 2 measurements included:

1. Continuous monitoring at Sites 2 and 3 starting on Monday October 18 and ending around noon on Saturday October 23. The noise monitoring was suspended on October 21 and 22 when a strong storm front passed through the Phoenix area.
2. Measurements at Site 1 using a monitor that was placed in the early morning and picked up in the evening.
3. Supplementary short-term measurements using handheld sound level meters. The locations for the short-term measurements are shown in Figure 18 (page 37). The short-term measurements were from 6 AM to 9 AM. Short-term measurements were performed at Sites 4 and 4B on Monday, October 18; Sites 2B and 2C on Tuesday, October 19; and Sites 2B, 2C, and 3B on Saturday, October 23. There was an observer at each site during the short-term measurements taking notes about non-freeway noise sources, the apparent direction the noise was coming from, and wind conditions.

All of the monitors for the Phase 2 measurements were programmed to collect Leq and 1/3 octave band spectrum at 15-second intervals.

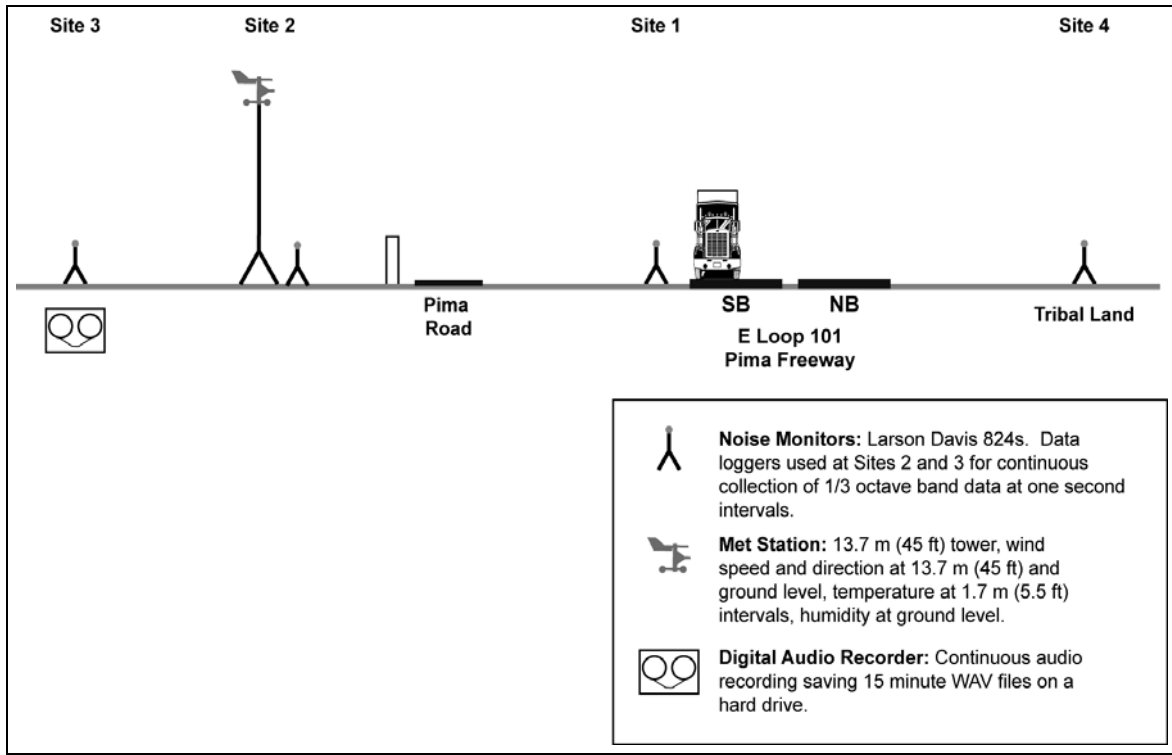


Figure 21. Sketch of Field Set Up and Measurement Equipment, Phase 1

4.2 ANALYSIS OF A-WEIGHTED MEASUREMENT

This section discusses the overall results of the noise measurements, atmospheric parameters, and traffic counts for 15-minute intervals. Although we collected noise data at intervals down to 1 second, we found that 15-minute intervals generally were sufficiently fine resolution to identify the effects of atmospheric conditions and traffic variations. Additional details on the measurement results are given in Appendix B. The graphs in Appendix B include the noise data at 1-minute and 15-minute intervals, along with additional details on the meteorological measurements and the 1/3 octave band spectra results. Along with plots of the 15-minute average 1/3 octave band spectra, Appendix B includes spectrograms of the weekday measurements in March 2004.

4.2.1 Noise Data

Daily Sound Levels

The daily sound level results for the noise measurements are given in Table 3, Table 4, and Table 5 for Sites 2 through 4 respectively. Shown for each day of testing are the number of hours during the daytime (7 AM to 10 PM) and nighttime (10 PM to 7 AM) periods that the monitors were operating, the Leq for the daytime and nighttime hours, the Day-Night Average Level (Ldn) for each day, the maximum hourly Leq, and the hour that the maximum hourly Leq occurred. The data for Sites 2 and 3 are shown graphically in Figure 22. The values shown are the most common descriptors used to characterize community noise exposure.

All of the monitors for the Phase 2 measurements were programmed to collect Leq and 1/3 octave band spectrum at 15-second intervals.

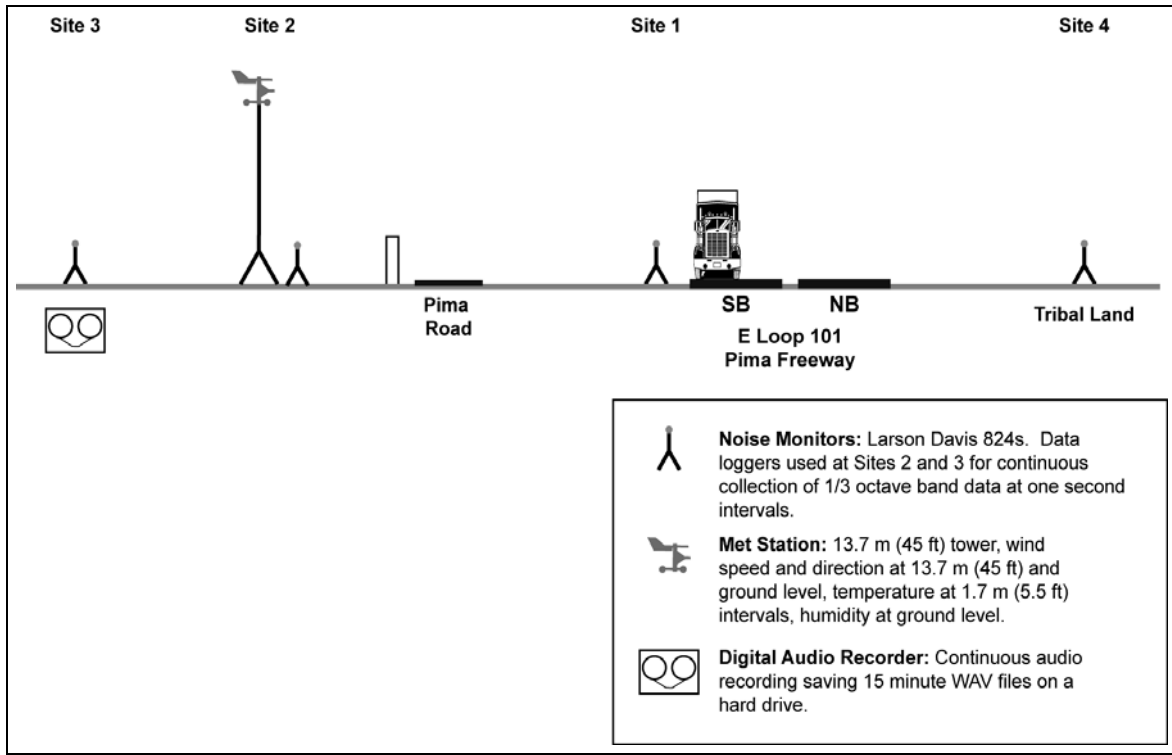


Figure 21. Sketch of Field Set Up and Measurement Equipment, Phase 1

4.2 ANALYSIS OF A-WEIGHTED MEASUREMENT

This section discusses the overall results of the noise measurements, atmospheric parameters, and traffic counts for 15-minute intervals. Although we collected noise data at intervals down to 1 second, we found that 15-minute intervals generally were sufficiently fine resolution to identify the effects of atmospheric conditions and traffic variations. Additional details on the measurement results are given in Appendix B. The graphs in Appendix B include the noise data at 1-minute and 15-minute intervals, along with additional details on the meteorological measurements and the 1/3 octave band spectra results. Along with plots of the 15-minute average 1/3 octave band spectra, Appendix B includes spectrograms of the weekday measurements in March 2004.

4.2.1 Noise Data

Daily Sound Levels

The daily sound level results for the noise measurements are given in Table 3, Table 4, and Table 5 for Sites 2 through 4 respectively. Shown for each day of testing are the number of hours during the daytime (7 AM to 10 PM) and nighttime (10 PM to 7 AM) periods that the monitors were operating, the Leq for the daytime and nighttime hours, the Day-Night Average Level (Ldn) for each day, the maximum hourly Leq, and the hour that the maximum hourly Leq occurred. The data for Sites 2 and 3 are shown graphically in Figure 22. The values shown are the most common descriptors used to characterize community noise exposure.

The Ldn is the 24-hour Leq with a 10 dB adjustment for noise during the nighttime hours of 10 PM to 7 AM. Ldn is used by agencies such as the Federal Transit Administration, the Federal Aviation Administration and HUD to characterize noise exposure. Highway noise analysis is typically based on the maximum hourly Leq. The ADOT Noise Abatement Criterion is a maximum hourly Leq of 64 dBA or greater.

Following is a summary of the key points deduced from the daily data:

- The maximum hourly Leq follows Ldn remarkably closely. This is at least partially attributable to the maximum hourly Leq usually occurring before 7 AM when a 10 dB adjustment is added in calculating Ldn. The result is that the maximum hourly Leq tends to drive Ldn.
- The Ldn values at Site 2 for the entire Phase 1 measurement period were fairly consistent. Except for March 17, which was not measured for a full 24 hours, the weekday Ldn ranges from 64 to 66 dBA.
- The Ldn values were much less consistent at Site 3. During the first week, Ldn ranged from 58 to 61 dBA. In the second week Ldn at Site 3 was consistently higher, around 64 dBA, except for March 17. During the first week, Site 3 was consistently around 4 dB lower than Site 2. During the second week, sound levels at Site 3 were about the same as at Site 2. This is discussed in more detail later, but the indication is that the early morning wind patterns during the second week of the March measurements resulted in about 4 dB of focusing at Site 3. This is 4 dB in addition to the increase caused by the normal early morning inversion conditions.
- The jump in Ldn at Site 3 during the second week of the March measurements is largely due to the higher levels in the early morning hours. The difference between the daytime Leq at Sites 2 and 3 is also lower the second week. However, the daytime levels do not drive the Ldn or maximum hourly Leq. Note that during the daytime hours, background noise at the community sites was often as high as, or higher, than the freeway noise. This was particularly true during the October measurements after the ARFC had been installed and the A-weighted levels of traffic noise were approximately 10 dB lower.
- The differences at Site 2 between the Phase 1 and Phase 2 measurements were 5 dB for the daytime Leq, 8 dB for the nighttime Leq, and 9 dB for the maximum hourly Leq. The differences at Site 3 were all between 7 and 8 dB. As discussed in Section 4.4, the acoustic benefits of the ARFC included both a substantial reduction in the loudness of the traffic noise as well as an improvement in the sound “quality” of the traffic noise.

Table 3. Daily Results, Site 2 (8701 E. Highland)							
Date	Number of Hours		Leq, dBA		Ldn, dBA	Maximum Hourly Leq	
	Day⁽¹⁾	Night⁽²⁾	Day⁽¹⁾	Night⁽²⁾		Max Leq	Hour
Phase 1							
Sun, Mar 07	7	2	59.3	59.2	65.7	63.6	20:00
Mon, Mar 08	15	9	57.9	59.4	65.6	65.3	6:00
Tue, Mar 09	15	9	59.4	59.7	66.1	64.8	6:00
Wed, Mar 10	13	9	54.1	59.0	65.0	64.2	5:00
Thu, Mar 11	15	9	56.3	58.7	64.9	63.5	6:00
Fri, Mar 12	15	9	55.3	59.4	65.4	63.7	5:00
Sat, Mar 13	15	9	57.3	55.3	62.1	61.9	19:00
Sun, Mar 14	15	9	56.6	57.1	63.5	62.8	21:00
Mon, Mar 15	15	9	55.6	57.7	63.9	62.1	6:00
Tue, Mar 16	2	7	56.8	58.7	64.9	64.1	6:00
Wed, Mar 17	13	2	53.4	54.9	61.1	58.4	20:00
Thu, Mar 18	15	9	53.6	59.8	65.7	66.2	6:00
Fri, Mar 19	15	9	55.7	58.0	64.2	64.2	6:00
Sat, Mar 20	15	9	55.1	57.8	63.9	62.3	6:00
Sun, Mar 21	15	9	59.0	56.0	63.0	62.1	19:00
Average Weekday, Phase 1			56.1	58.9	65.1	64.2	
Phase 2, After ARFC Installation (8711 E. Highland)							
Sun, Oct 17	6	2	48.9	43.3	51.1	53.3	17:00
Mon, Oct 18	15	9	50.3	47.0	54.1	52.3	21:00
Tue, Oct 19	15	9	50.2	51.5	57.7	55.6	5:00
Wed, Oct 20	11	7	51.9	53.8	60.0	58.5	5:00
Fri, Oct 22	7	2	50.7	51.4	57.7	52.9	17:00
Sat, Oct 23	4	7	52.8	52.3	58.8	55.9	5:00
Average Weekday (Mon through Wed), Phase 2			50.8	50.7	57.2	55.5	
Notes:							
⁽¹⁾ Daytime is defined as 7 AM to 10 PM (7:00 to 22:00).							
⁽²⁾ Nighttime is defined as 10 PM to 7 AM (22:00 to 7:00).							

Table 4. Daily Results, Site 3 (8547 E. Highland)

Date	Number of Hours		Leq, dBA		Ldn, dBA	Maximum Hourly Leq	
	Day ⁽¹⁾	Night ⁽²⁾	Day ⁽¹⁾	Night ⁽²⁾		Max Leq	Hour
Phase 1							
Sun, Mar 07	3	2	56.1	53.8	60.6	56.7	19:00
Mon, Mar 08	15	9	54.3	55.3	61.6	60.9	6:00
Tue, Mar 09	15	9	54.6	55.4	61.7	60.1	6:00
Wed, Mar 10	15	9	52.7	56.2	62.2	61.7	6:00
Thu, Mar 11	15	7	53.6	52.7	59.3	58.1	7:00
Fri, Mar 12	0	0					
Sat, Mar 13	0	0					
Sun, Mar 14	7	2	54.4	59.7	65.6	60.9	22:00
Mon, Mar 15	15	9	53.7	58.0	64.0	63.0	6:00
Tue, Mar 16	10	9	53.1	58.3	64.2	64.4	6:00
Wed, Mar 17	15	9	53.7	55.5	61.7	61.8	7:00
Thu, Mar 18	15	9	53.4	59.2	65.1	65.4	6:00
Fri, Mar 19	15	9	56.0	58.0	64.2	65.4	7:00
Sat, Mar 20	8	7	55.6	55.6	62.0	62.8	7:00
Average Weekday, Phase 1			54.1	56.4	62.6	62.4	
Phase 2, After ARFC Installation							
Sun, Oct 17	6	2	46.7	42.0	49.5	51.1	17:00
Mon, Oct 18	15	9	47.7	42.6	50.2	52.4	15:00
Tue, Oct 19	15	9	45.9	54.5	60.4	58.0	6:00
Wed, Oct 20	3	3	48.7	48.9	55.2	51.1	17:00
Fri, Oct 22	7	2	46.8	42.0	49.5	51.1	17:00
Sat, Oct 23	4	7	51.7	51.1	57.6	56.4	6:00
Average Weekday (Mon and Tues)			46.8	48.6	55.3	55.2	
Notes:							
⁽¹⁾ Daytime is defined as 7 AM to 10 PM (7:00 to 22:00).							
⁽²⁾ Nighttime is defined as 10 PM to 7 AM (22:00 to 7:00).							

Table 5. Daily Results, Site 4 (Tribal Land East of Freeway), Phase 1

Date	Number of Hours		Leq		Ldn	Maximum Hourly Leq	
	Day ⁽¹⁾	Night ⁽²⁾	Day ⁽¹⁾	Night ⁽²⁾	Ldn (S1)	Max Leq	Hour
Sun, Mar 07	9	2	56.1	53.3	60.2	59.9	19:00
Mon, Mar 08	10	7	54.4	54.9	61.3	60.8	7:00
Tue, Mar 09	0	0					
Wed, Mar 10	0	0					
Thu, Mar 11	0	0					
Fri, Mar 12	0	0					
Sat, Mar 13	0	0					
Sun, Mar 14	0	0					
Mon, Mar 15	0	0					
Tue, Mar 16	15	2	56.7	63.3	69.2	64.3	5:00
Wed, Mar 17	15	2	55.3	62.7	68.5	64.3	5:00
Thu, Mar 18	13	2	56.7	60.8	66.8	66.0	7:00
Fri, Mar 19	0	0					
Sat, Mar 20	12	0	57.6			61.8	10:00
Sun, Mar 21	13	2	52.5	53.3	59.6	56.1	21:00
Mon, Mar 22	14	7	58.2	51.6	59.8	63.3	13:00

Notes:

⁽¹⁾ Daytime is defined as 7 AM to 10 PM (7:00 to 22:00).

⁽²⁾ Nighttime is defined as 10 PM to 7 AM (22:00 to 7:00).

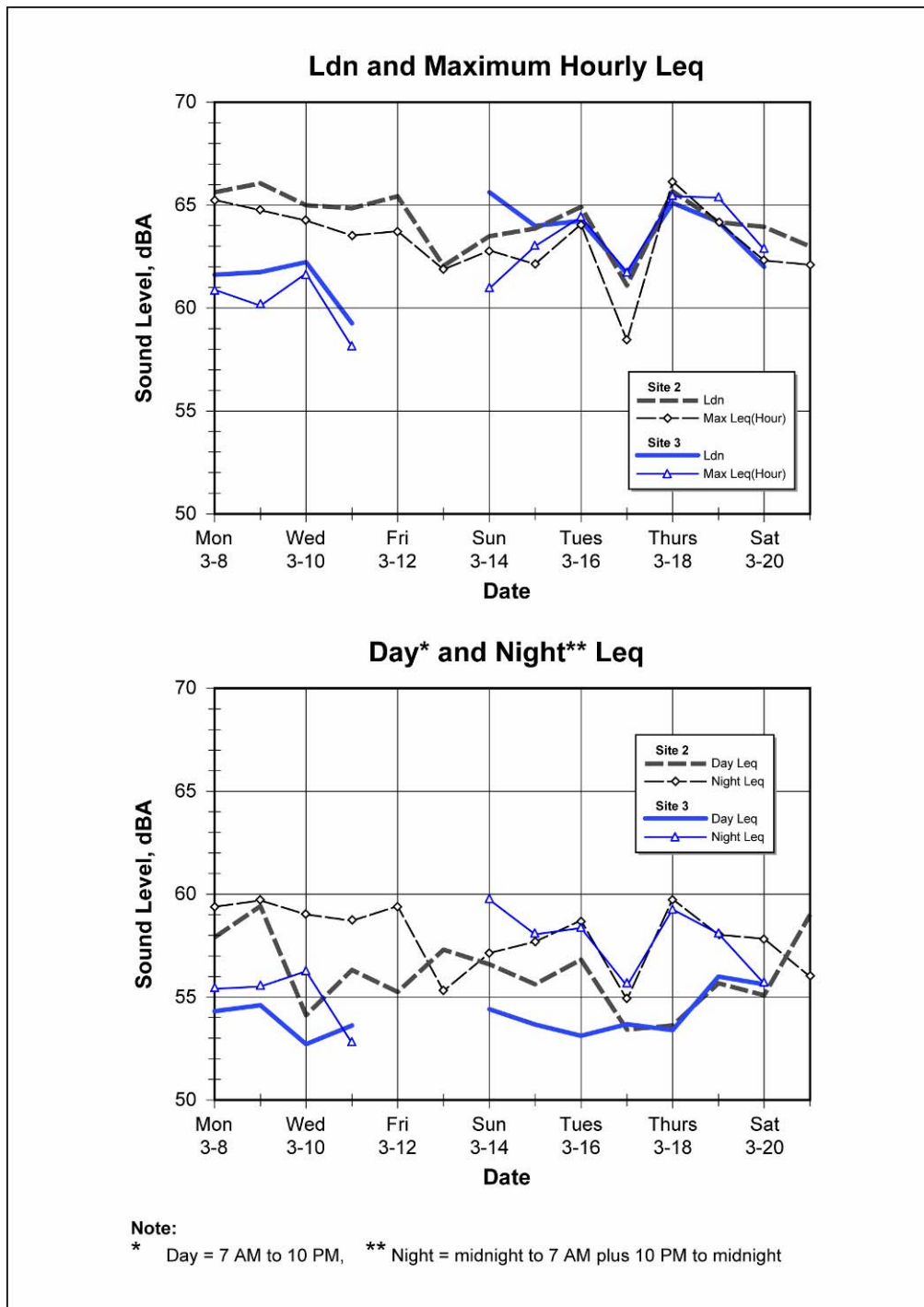


Figure 22. Variation of Daily Sound Levels, Phase 1, Sites 2 and 3 (Phase 1, March 2004)

15-Minute Interval Sound Levels

Figure 23 and Figure 24 show graphs of the 15-minute Leq values at each site as a function of time of day.* These figures illustrate the pattern of the sound level variations throughout the day at each site and show how the sound levels cluster around the average curve. Referring to Figure 23, the graphs on the left show the data for all days and the ones on the right are just for weekdays. Some important points about Figure 23 are:

- The data at Site 1, 30.5 m from the edge of the southbound lanes, is generally clustered within ± 2 dB or less about the average levels. The primary exception to this is during the afternoon commute period when there is a consistent drop in the sound levels. During this period, traffic often became stop-and-go with average speeds around 30 mph.
- With the Saturday and Sunday measurements for Site 1 excluded, the data clusters even more closely around the average. This also removes the apparently errant group of data points between 4 and 8 AM that were on weekend days. Morning traffic volume on weekends does not increase as rapidly as on weekdays. Removing the Saturday and Sunday data also reduces the scatter during the weekday afternoon commute period when there is usually traffic congestion and lower sound levels.
- Although the data at the distant measurement sites shows much more scatter than at Site 1, there are clear patterns with the highest sound levels during the early morning hours and the lowest sound levels during the afternoon hours. An effort was made to remove the non-freeway noise. However, the measurements at the community sites inevitably include noise from sources such as aircraft over flights, local traffic, and resident activities. There were even several periods at Site 4 where it appeared that the fields were being plowed.
- The patterns at Sites 2 and 3 are quite similar. The only notable exception is in the late afternoon period when sound levels drop more at Site 2 than at Site 3. We suspect that this is because the afternoon background noise at both sites was around 45 dBA, which limited how much sound levels at Site 3 could drop in the afternoon periods.
- Although Site 4 has a similar pattern to Sites 2 and 3 with the highest levels in the morning before, and for 1 to 2 hours after sunrise, the pattern is less distinct with more scatter than at the other two field sites. Part of the scatter is because, even though Site 4 was in the middle of a field, there was more activity near the microphone than we anticipated. The dirt road was often used by 5 to 10 vehicles per hour as a shortcut and there were farming activities such as plowing during the March measurements. Also, we were limited in the amount of data we could collect at Site 4 because of problems with vandalism.

The results from the October measurements shown in Figure 24 have somewhat similar patterns to what was seen in March. One difference between the Phase 1 and Phase 2 measurements is that the weather patterns were much less consistent for the Phase 2 measurements. The Phase 2 measurements were limited to 6 days (Monday to Saturday) and a large weather front complete with thunder showers and a dust storm passed through the region on Thursday. In spite of this, it is clear that all the Phase 2 A-weighted sound levels were 8 to 10 dB lower because of the ARFC. The sound levels at Site 1 are still tightly grouped around the average, although there is a wider spread around the averages at Sites 2 and 3. We believe that the increased scatter is because the traffic noise was substantially lower in October (because of the ARFC), which meant that it was more common for noise

* Curves of the 15-minute Leq values for each day are given in Appendix B.2.

levels to be dominated by other community noise sources. In fact we observed that during the Phase 2 measurements in October 2004, the afternoon traffic noise was often only barely audible at Site 3 and just slightly above the background noise at Site 2.

15-Minute Leq vs. Time of Day, March 8-22, 2004

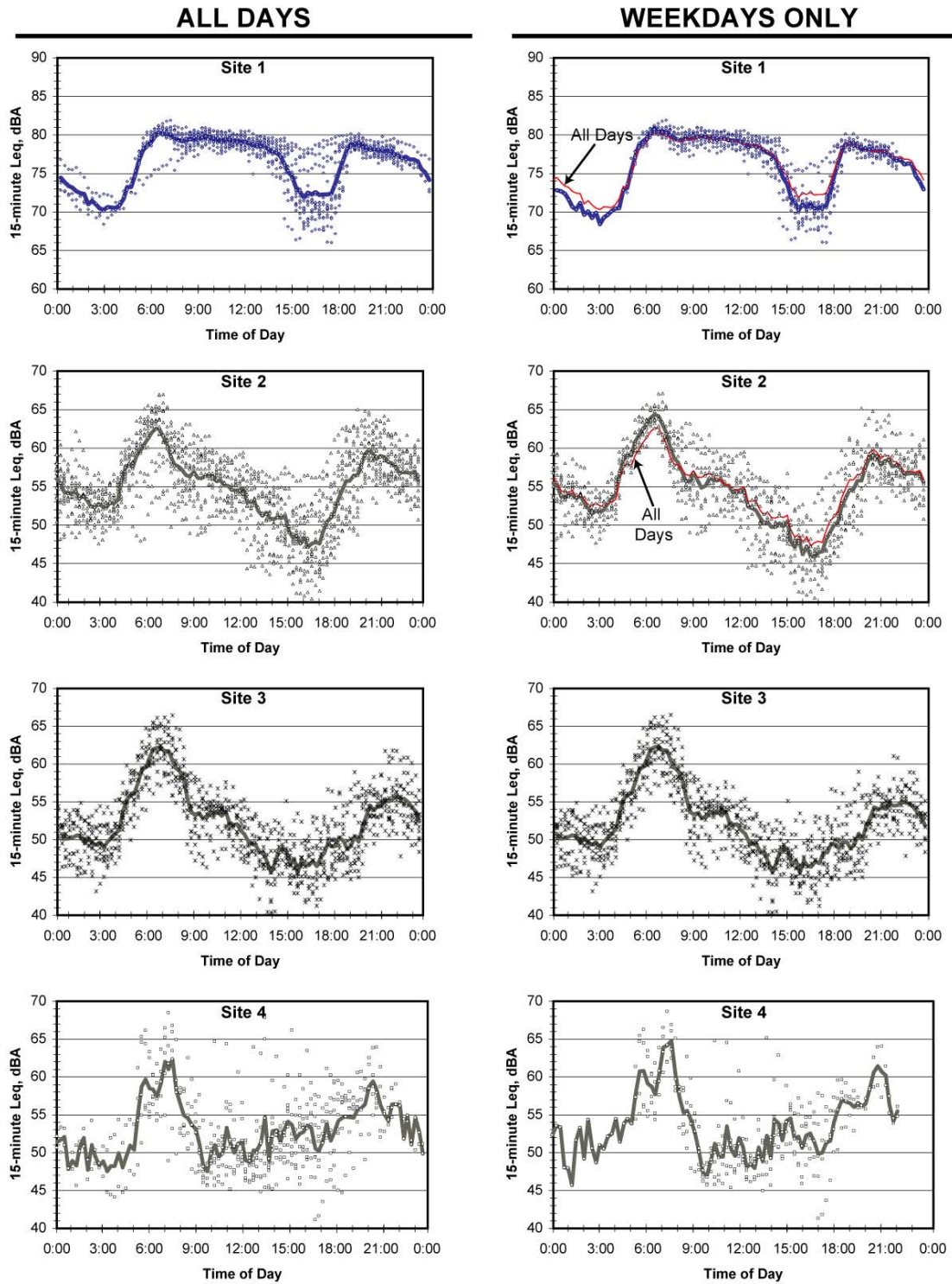


Figure 23. 15-Minute Leq vs. Time of Day, March 8-22, 2004

15-Minute Leq vs. Time of Day, October 17-23, 2004

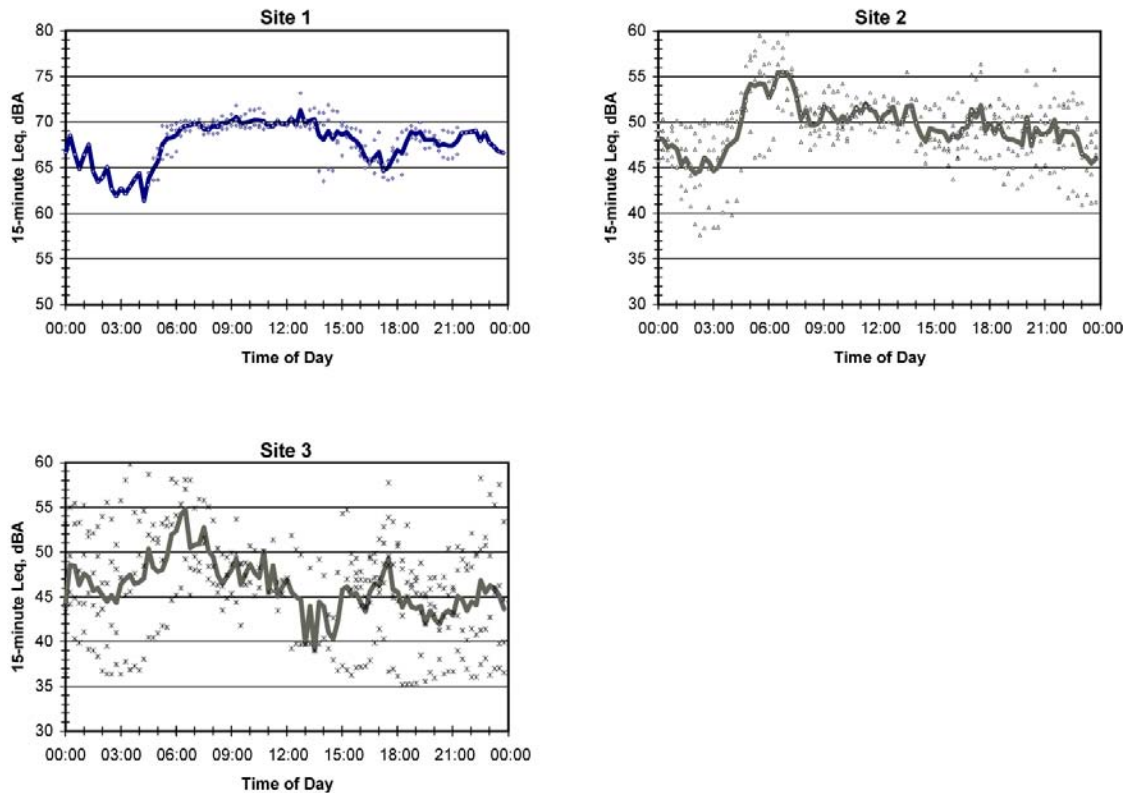


Figure 24. 15-Minute Leq vs. Time of Day, October 17-23, 2004

The basic diurnal patterns seen in Figure 23 are a combination of the sound level fluctuations due to the changes in atmospheric effects and due to variations in the traffic volume, mix, and speed. Inversion conditions lead to higher sound levels from approximately 1 hour after sunset to 1 hour after sunrise. Layered on top of this is the traffic pattern on the Pima Freeway that consists of low volumes during the late night hours and fairly consistent volumes during the daytime hours plus the effects of lower traffic speeds during an afternoon period of congestion.

The differences between the patterns for the 2 weeks of the March measurements are analyzed in Figure 25 and Figure 26. As seen in Figure 25, the sound levels at Site 1 close to the freeway are similar for the 2 weeks, but at Sites 2 and 3 the diurnal pattern is a bit enhanced during the second week. This is seen more clearly in Figure 26 where the average curves for week 1 and week 2 are compared. It is relevant that a weather pattern moved through the Phoenix valley towards the end of the first week and there was a pattern of clear sunny days and clear cool nights throughout most of the second week in Phase 1.

Interestingly, the average sound levels at Site 1 were somewhat lower the second week. It is not clear why this happened. We do not have traffic counts during the first week, but the available counts from both the Phase 1 and Phase 2 measurements indicate that day-to-day traffic volumes and speeds are quite consistent. The average curves at Site 2 suggest the increase in sound levels due to the nighttime/early morning inversion was similar for both week 1 and week 2 of the March 2004 measurements, but in week 2 there was a greater sound level reduction due to the daytime lapse conditions.

The Site 3 results are particularly interesting. The maximum sound levels occur during the early morning hours of both weeks. However, for week 2 there is a steeper increase in the morning, the maximum is about 4 dB higher, and a steeper decrease after sunrise. As discussed later, we believe that the higher morning sound levels during the second week are probably the result of sound level focusing between 5 AM to 8 AM. The most likely cause of focusing would be a wind jet similar to the one illustrated in Figure 17 (page 33), although perhaps at a lower elevation. Because the early morning air flow is typically controlled by drainage flow off the mountain ranges surrounding the Phoenix valley, even though the air flow patterns are very complex, they can be very similar from day to day. This means that if wind patterns cause focusing on one day, they are likely to cause similar focusing the next day.

15-Minute Leq vs. Time of Day, March 2004 Measurements

MARCH 8-12 (Mon-Fri)

MARCH 15-19 (Mon-Fri)

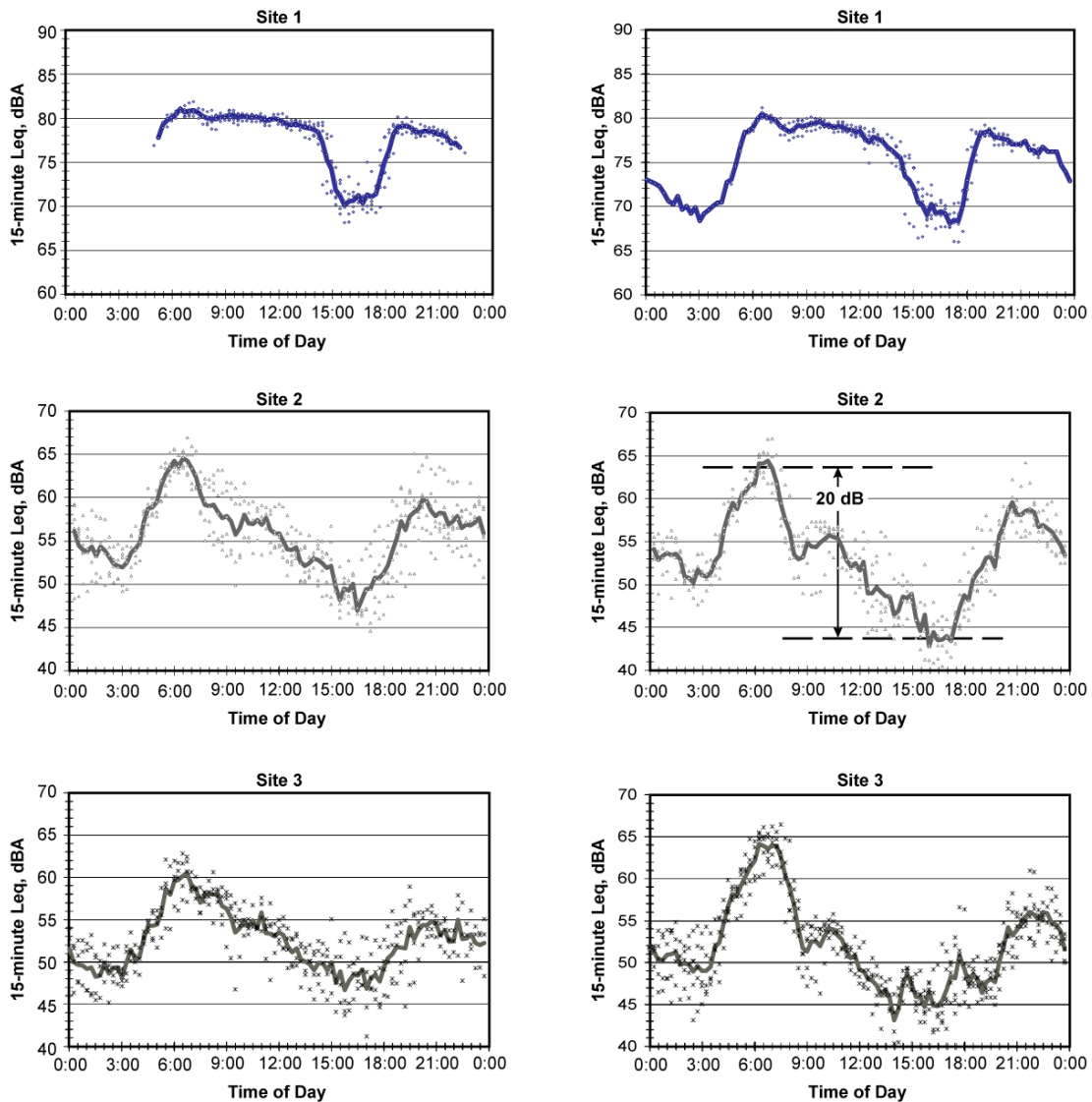


Figure 25. First and Second Week Sound Levels, March, 2004

Comparison of Average Sound Levels, Week 1 and Week 2 of March 2004 Measurements

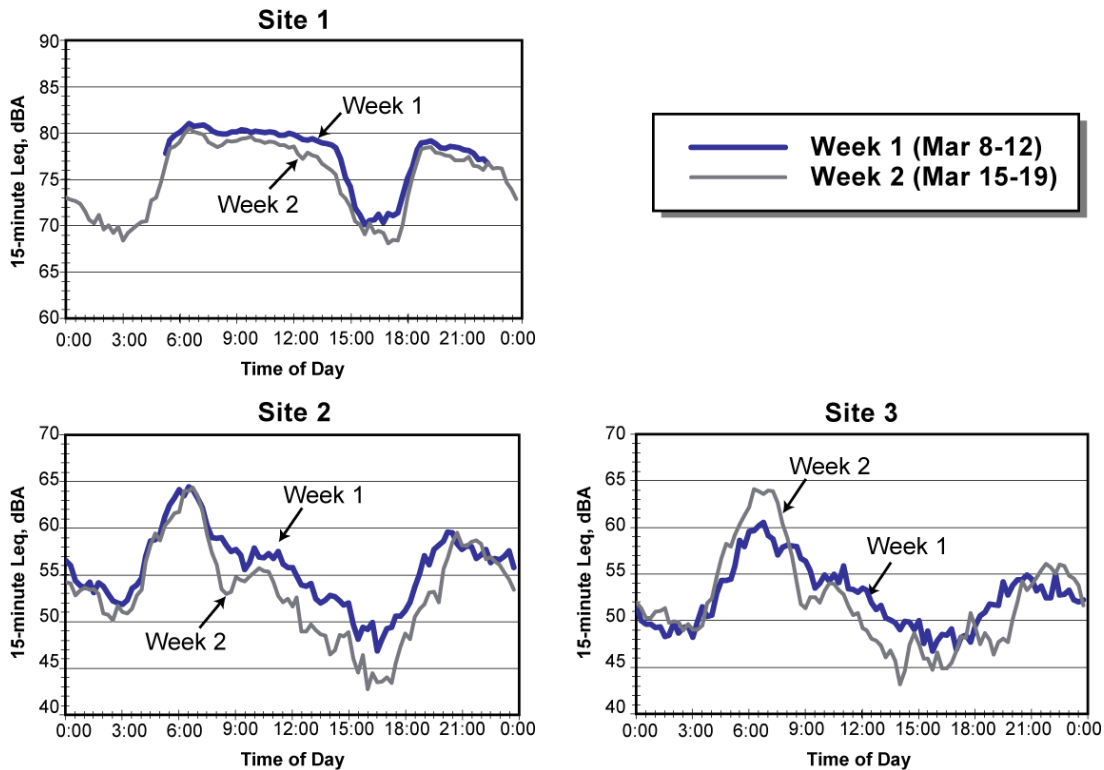


Figure 26. Average Sound Levels, First and Second Week of March, 2004 Measurements

4.2.2 Traffic Counts

Counts of traffic volume and speed were performed during the March and October measurements by Traffic Research & Analysis, Inc. on an independent contract from this research study. An automated radar system was used so that continuous counts could be obtained over 24-hour periods. The counts were reported on 15 minute intervals and included total volume and speed for each traffic lane plus a breakdown of the vehicle type based on vehicle length. The total volumes and speeds for all of the traffic counts are given in Appendix B.6. Because of problems with the equipment, there are traffic counts for only a few days during the March noise measurements. The traffic counts cover the full period of the Phase 2 measurements in October.

Figure 27 shows the average traffic speeds for both the March and October measurements and Figure 28 shows the average traffic volumes. Referring to Figure 27, the top graphs are the average, maximum, and minimum speeds from the March 2004 measurements, the middle graphs are the same data from the October 2004 measurement, and the bottom graphs compare the March and October speeds. Note that the maximum and minimum speeds are the highest and lowest average speeds over the 15-minute intervals, not the fastest and slowest individual vehicles.

The speed data in Figure 27 shows a consistent pattern of 80 mph during the late night hours dropping to 70 mph during the day. There are sharp drops in speed in both directions for several hours during the afternoon commute period that occurs in both directions. Also, the average speed drops for about 2 hours in the morning although only in the northbound direction. The

average speeds for the March and October periods are quite close with the October speeds tending to be somewhat higher. The speeds in the southbound direction were consistently about 4 mph higher during the October period. This would be expected to increase highway noise levels by less than 1 dB.

The average volumes shown in Figure 28 are even more consistent than the speeds. The volume is very low during the nighttime hours dropping to less than 100 vehicles every 15 minutes at 3 to 4 AM, rapidly increasing to a maximum of about 1600 vehicles/15 minutes at around 8 AM, staying around 1400 vehicle/15 minutes until 6 PM then steadily decreasing to the minimum at 3 AM.

In all of our models of traffic noise we have consolidated the traffic in each direction into a single lane and have ignored the truck traffic. The error caused by using a single lane of traffic was found to be only a fraction of a decibel based on tests with TNM version 2.5. The average weekday truck volumes during the October measurements are shown on an hourly basis in Table 6. As can be seen, the volume of heavy trucks is typically around 1% during daytime hours and is a maximum of 4 to 6% from 3 to 5 AM. The reason that the truck percent is higher between 3 and 5 AM is because the volume of automobiles is very low. Our conclusion was that we could safely ignore the truck volume without introducing significant error.

Hour	Northbound		Southbound	
	Volume*	Percent**	Volume*	Percent**
0:00	8	1.3%	12	1.7%
1:00	9	2.0%	11	2.7%
2:00	9	2.5%	17	5.4%
3:00	18	6.4%	15	5.2%
4:00	36	5.3%	21	3.7%
5:00	60	2.0%	39	2.2%
6:00	65	1.2%	58	1.6%
7:00	61	0.9%	57	0.9%
8:00	60	0.9%	76	1.3%
9:00	66	1.1%	97	1.9%
10:00	75	1.5%	89	1.8%
11:00	67	1.3%	96	1.9%
12:00	62	1.2%	99	1.9%
13:00	57	1.1%	95	1.7%
14:00	43	1.0%	88	2.1%
15:00	40	0.7%	95	1.8%
16:00	34	0.6%	114	2.3%
17:00	41	0.7%	118	2.3%
18:00	37	0.7%	84	1.7%
19:00	20	0.5%	41	1.1%
20:00	14	0.5%	28	0.9%
21:00	18	0.7%	22	0.8%
22:00	13	0.7%	24	1.1%
23:00	11	1.0%	16	1.2%

Notes:
* Volume is number of heavy trucks per hour.
** Percent of total traffic volume.

Average Speeds, Weekdays

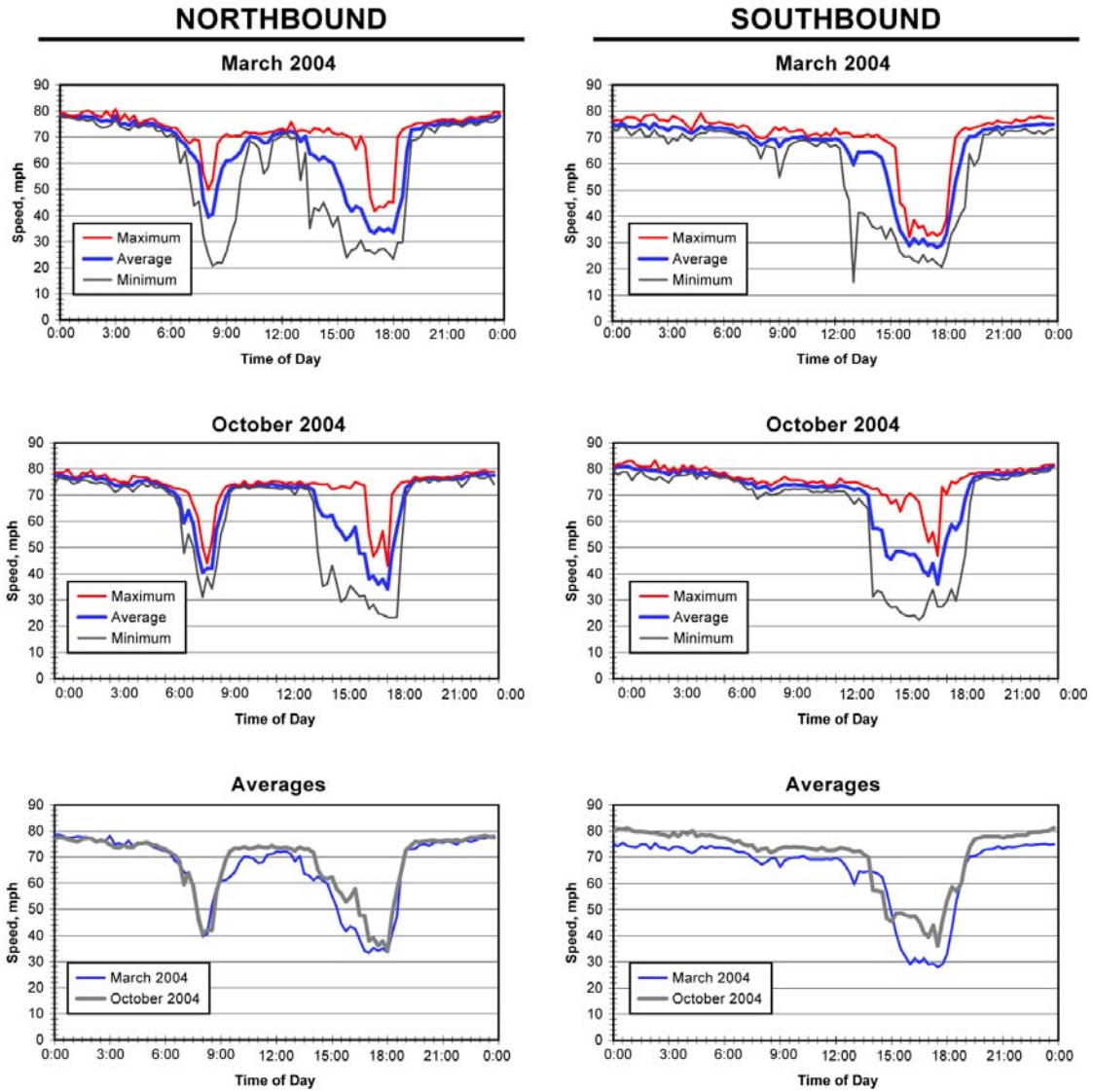


Figure 27. Average Traffic Speeds

Average Weekday Traffic Volumes

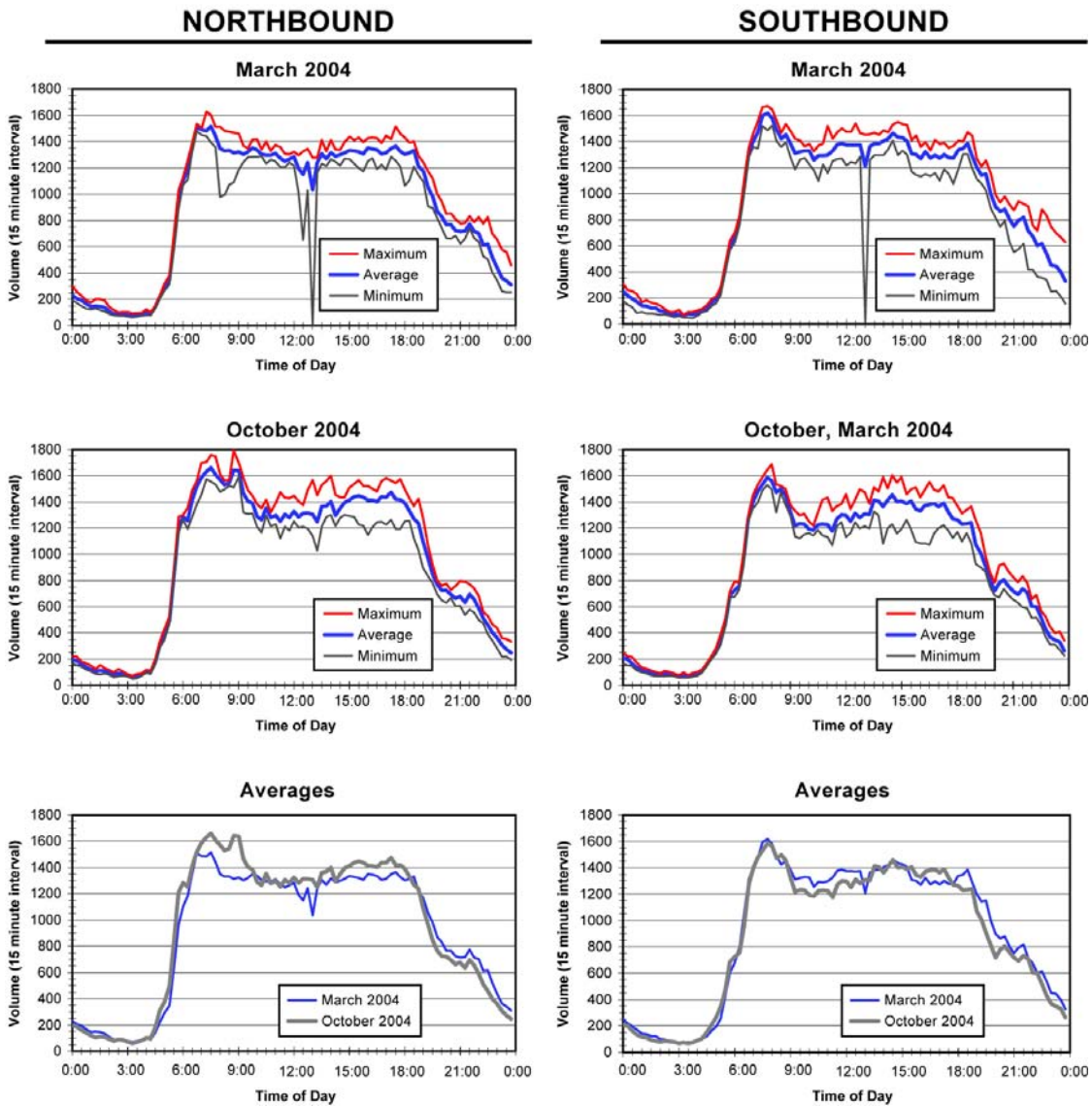


Figure 28. Average Traffic Volumes

4.2.3 Meteorological Data

The Phase 1 tests in March 2004 included continuous measurements of temperature, wind speed and direction, and humidity. This section summarizes the parameters that affected sound propagation. Graphs showing all of the meteorological data that were collected are given in Appendix B.5. Although wind speed and direction are critical factors in how atmospheric conditions affect sound propagation, we found that the wind data that we collected at 13.7 m (45 ft) was not well correlated with the noise levels. We believe that this is because the winds at higher altitudes were driving the sound level fluctuations. This conclusion was confirmed during the short-term measurements of Phase 2 when we observed significant sound level variations with no noticeable change in wind speed and direction either at the ground level or at the top of palm trees (approximately 15 m, 50 ft).

Temperature and Humidity

Although the wind data collected in Phase 1 was less useful than we had hoped for, the temperature data turns out to be quite valuable. The daily temperature variations for the period of March 8, 2004 through March 23, 2004 are shown in Figure 29. Perhaps the most notable factor in Figure 29 is the day-to-day consistency. Figure 29A shows the temperature for the first 8 days and Figure 29B shows the variation for the last 8 days. The normal pattern is that the temperature consistently drops through the night and then rapidly rises to the mid-day levels starting right after sunrise. The maximum temperature occurs about 2 hours before sunset, after which temperatures start to decline. The most rapid decline is right around sunset, followed by the steady decline until sunrise when the pattern starts over.

There are even more consistent patterns if the days are grouped as shown in Figure 29C and Figure 29D. Between March 8 and 11 (Figure 29C), the maximum temperature was about 30°C (86°F) and the minimum was about 12°C (54°F). The pattern started to breakup on March 11, perhaps an early indication of the weather front that passed through on March 13.

The pattern for March 16 through March 20 (Figure 29D) was even more consistent than for the March 8-11 period. The maximum temperature was typically 30°C (86°F) and the minimum was about 10°C (50°F). The average temperatures for the two periods are shown in Figure 29E. The patterns are very similar with a slightly greater difference between the nighttime and daytime temperatures for the March 16-20 period. We would expect that both of these periods would result in formation of strong inversion conditions at night and lapse conditions in the daytime. We would also expect the greater nighttime-daytime temperature differences for the March 16-20 period is an indication of stronger inversion and lapse conditions.

Graphs of relative humidity (RH) for the Phase 1 measurements are shown in Figure 30. The relative humidity closely tracks the inverse of the temperature. RH is a minimum in the afternoon when temperature is highest and is a maximum in the early morning hours when temperatures are lowest. As seen in Figure 30C and Figure 30D, the RH profiles for March 8-11 and March 16-20 are almost as closely grouped as the temperature profiles in Figure 29C and Figure 29D.

Atmospheric absorption will tend to be higher under high-temperature, low-humidity conditions. One question is whether the difference in atmospheric absorption is sufficient to make a noticeable difference in the sound levels. The effects of temperature and relative humidity are illustrated in Figure 31. Shown are the 1/3 octave band spectra at Site 2 for three TNM runs using mid-day traffic volumes and speeds. The top curve is for the average early morning conditions during the March 2004 measurements of 10.6°C (51°F) and a relative humidity of 73%; the representative conditions when sound levels were highest. The next curve is for typical mid-day conditions. The temperature has risen to 30°C (86°F) and relative humidity has fallen to 21%. The difference in the atmospheric absorption results in slightly less than 1 dB

difference in A-weighted sound levels. The third curve (30°C, 5% RH) is for the lowest relative humidity during the March 2004 measurements. Going from 21% to 5% relative humidity with no change in temperature causes a dramatic increase in the atmospheric absorption at frequencies of 1000 Hz and higher (e.g., there is a 35 dB increase in absorption at 2000 Hz). However, only the high frequencies are affected strongly and the change in the A-weighted level is less than 2 dB.

The results in Figure 31 show that very low relative humidity during the mid-day period can noticeably affect community noise levels. The primary effects are to reduce the A-weighted level by a small amount and to eliminate most of the higher frequency noise, both of which will tend to reduce the annoyance potential of the traffic noise. However, atmospheric absorption will not cause sound levels to be higher during any periods of the day.

Temperature Gradient

The temperature measurements at the eight positions on the meteorological tower at Site 2 were used to estimate the variation in temperature gradient as a function of time of day. The gradients were approximated as the slope of best-fit straight lines fit to the temperature readings. The temperature gradient results are shown in Figure 32. As expected, the temperature gradients are positive (inversion) until sunrise with a rapid transition to negative (lapse) 1 to 2 hours later. The transition from lapse to inversion starts about 2 hours before sunset.

As for the temperature profiles, the gradient profiles in the first week of the March measurements are closely grouped (Figure 32A) and the gradients in the second week are closely grouped (Figure 32B). There is a gap in the temperature profile data between March 10 and March 17 where data was lost because of equipment problems. The results for March 21 and 22 in Figure 32C are interesting in that the gradients are similar through most of the day except for a weaker inversion in the early morning hours of March 22 and a weaker lapse in the afternoon hours of March 21.

Having information on temperature gradient is required before it is possible to make any predictions of the refraction caused by atmospheric effects in the Phoenix valley. For the Phase 1 tests in March 2004, we obtained detailed temperature data up to an elevation of 13.3 m (43.5 ft), something that is not practical for the typical noise monitoring program. However, when atmospheric conditions are relatively calm, the temperature profile should also be relatively stable. This means that a simpler two point measurement of temperature gradient may provide useful information on whether there is downward refraction or upward refraction and perhaps provide an indication of how strong the refraction conditions are.

Comparisons of the temperature gradient calculated using all of the temperature data and just using the measurements at 3.2 and 4.9 m (10.5 and 16 ft) are shown in Figure 33 and Figure 34. There is considerably more variation in the gradient calculated with just two points. However, the basic diurnal patterns are similar and it is clear that useful information can be obtained from simply measuring temperature at two points relatively close to the ground. This is an important observation, although further investigation and refinement of the procedures are needed before temperature gradient measurements become a standard supplement to community noise measurements in the Phoenix area.

Temperature Variation, March 2004 Measurements

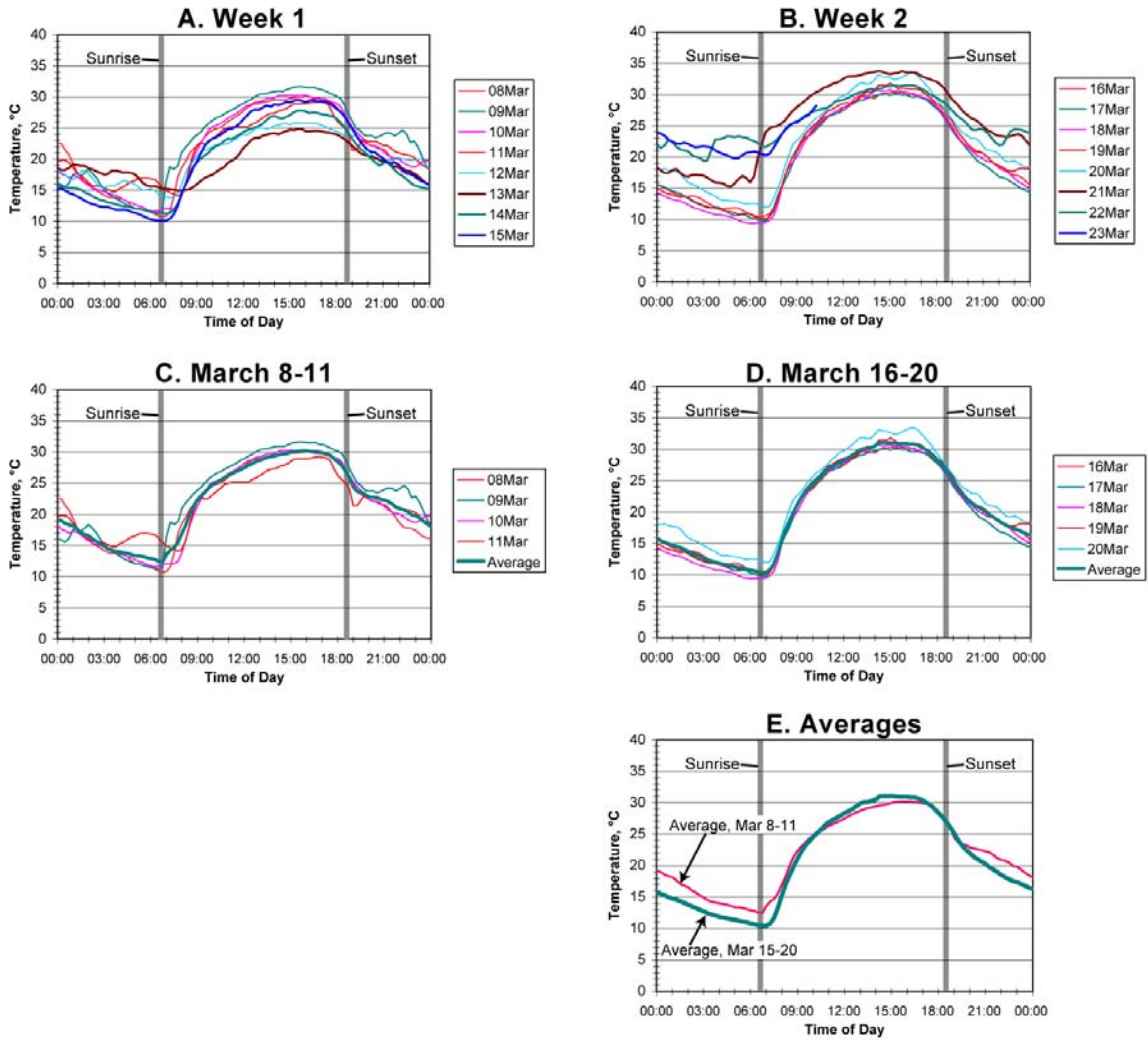


Figure 29. Diurnal Temperature Variation, March 2004 Measurements

Relative Humidity Variation, March 2004 Measurements

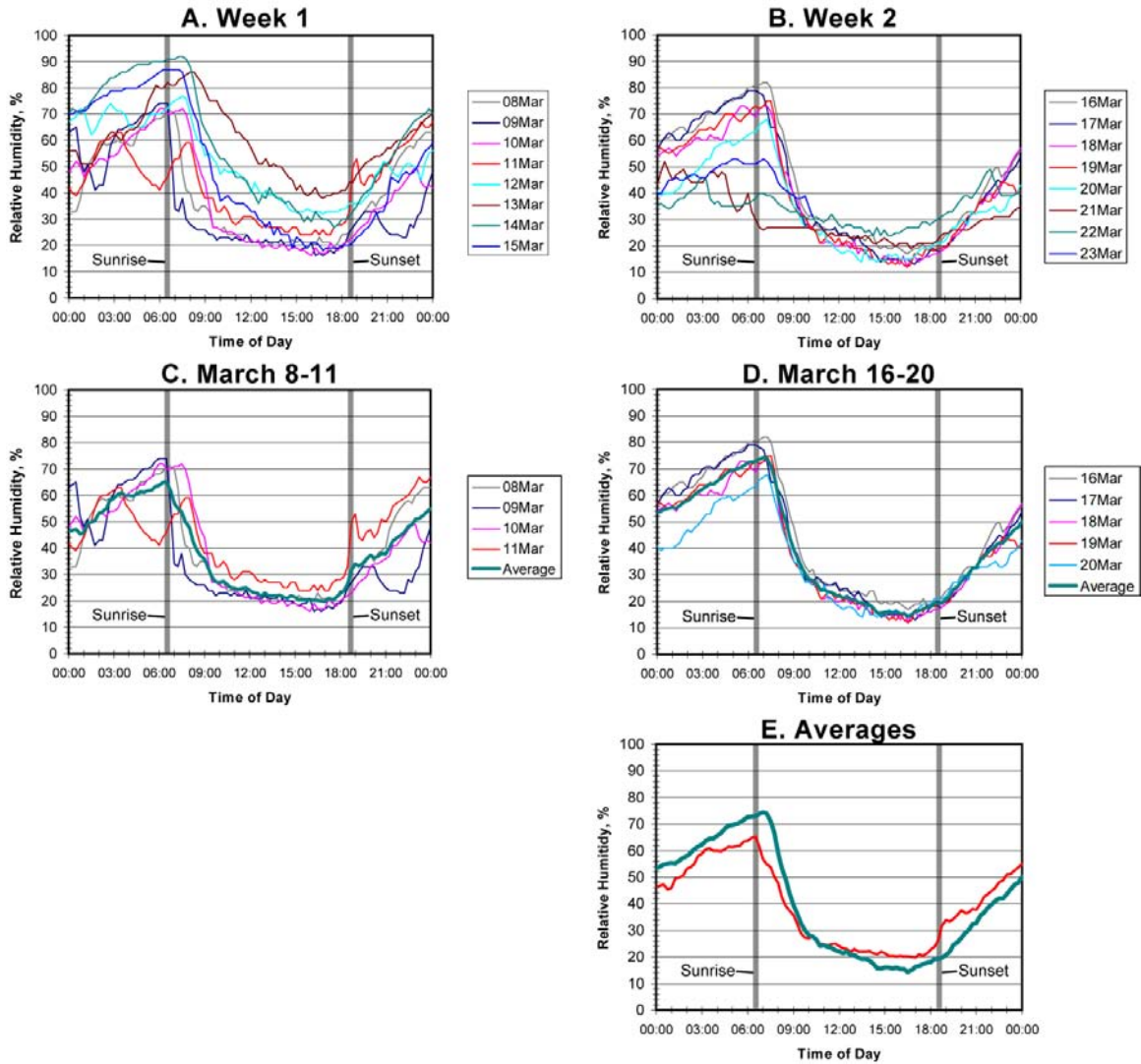


Figure 30. Diurnal Variation of Relative Humidity, March 2004 Measurements

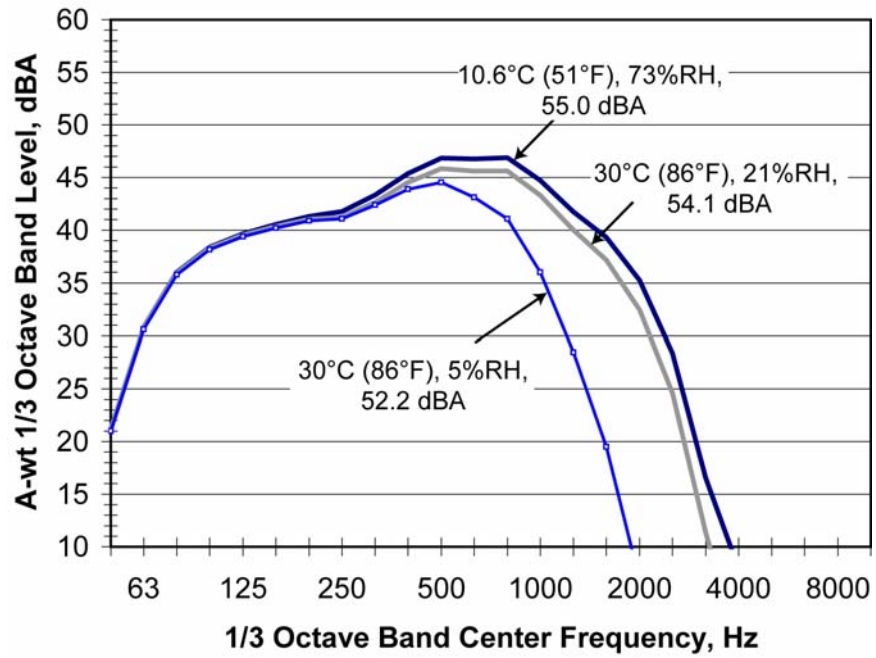


Figure 31. Examples of TNM Predicted 1/3 Octave Band Sound Levels at Site 2

Traffic Data Used for Figure 31:

Volume:

NB: 4143 vehicles/hr

SB: 4846 vehicles/hr

100% Automobiles

Average Speed:

NB: 68 mph

SB: 60 mph

Distance:

524 m (1,720 ft) from southbound lanes

Temperature Gradient, 15-Minute Moving Average

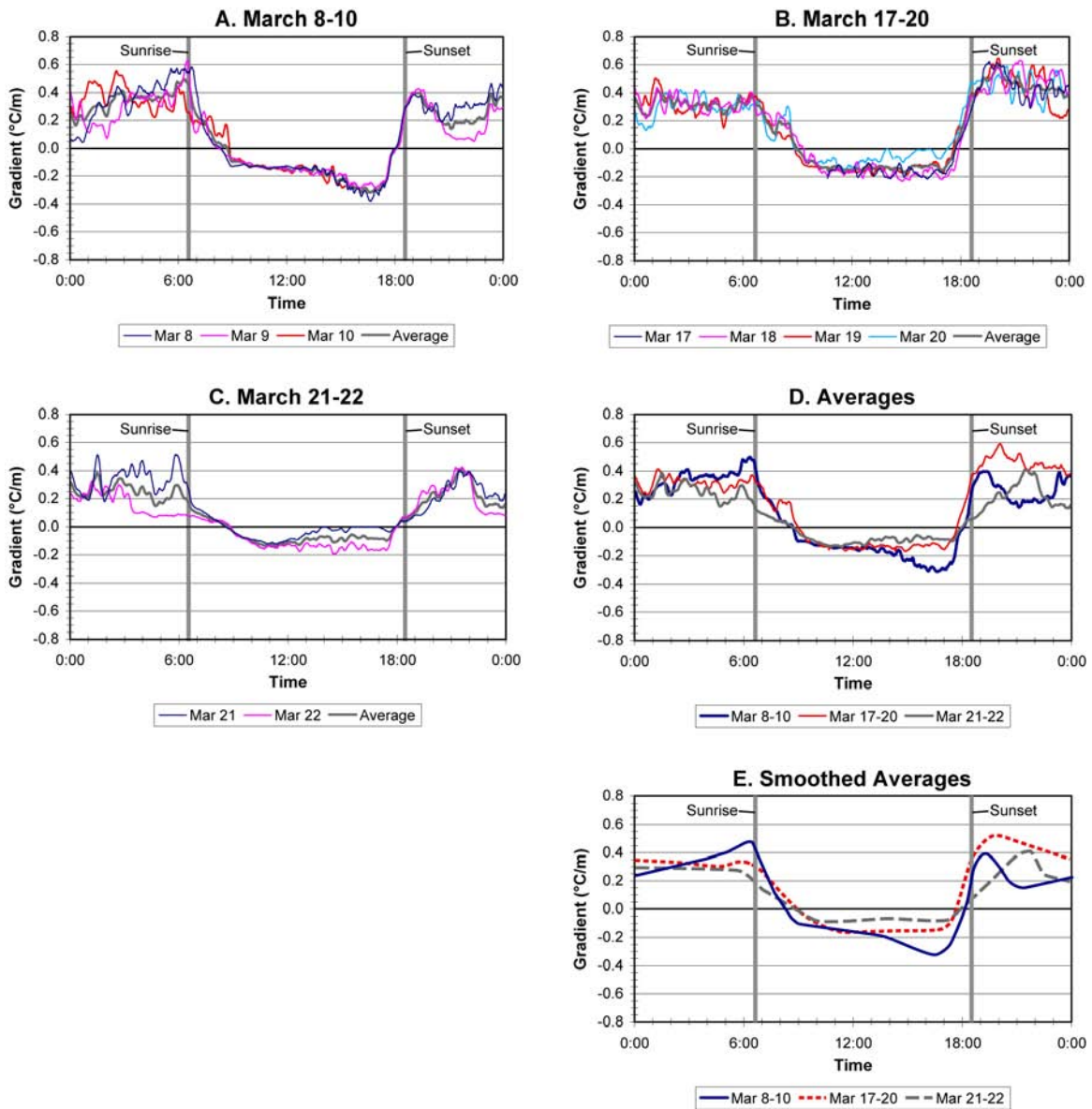


Figure 32. Temperature Gradients, March 2004 Measurements

Comparison Temperature Gradients, Week 1, March 2004

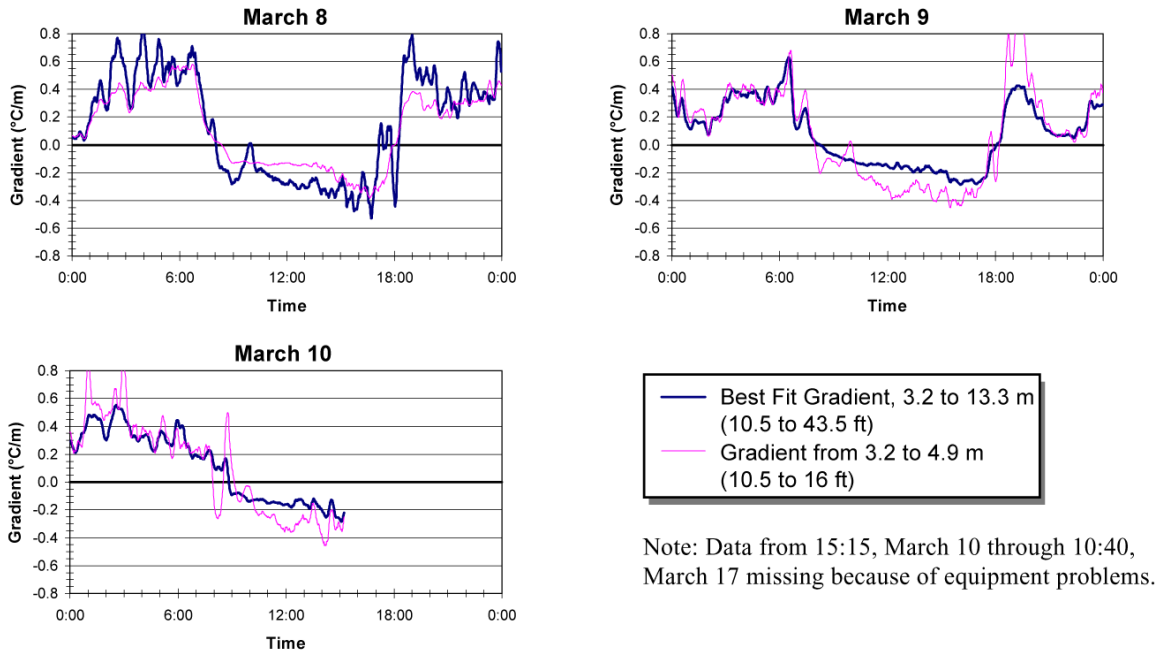


Figure 33. Two Methods of Measuring Ground Level Temperature Gradient, March 8-10, 2004

Comparison Temperature Gradients, Week 2, March 2004

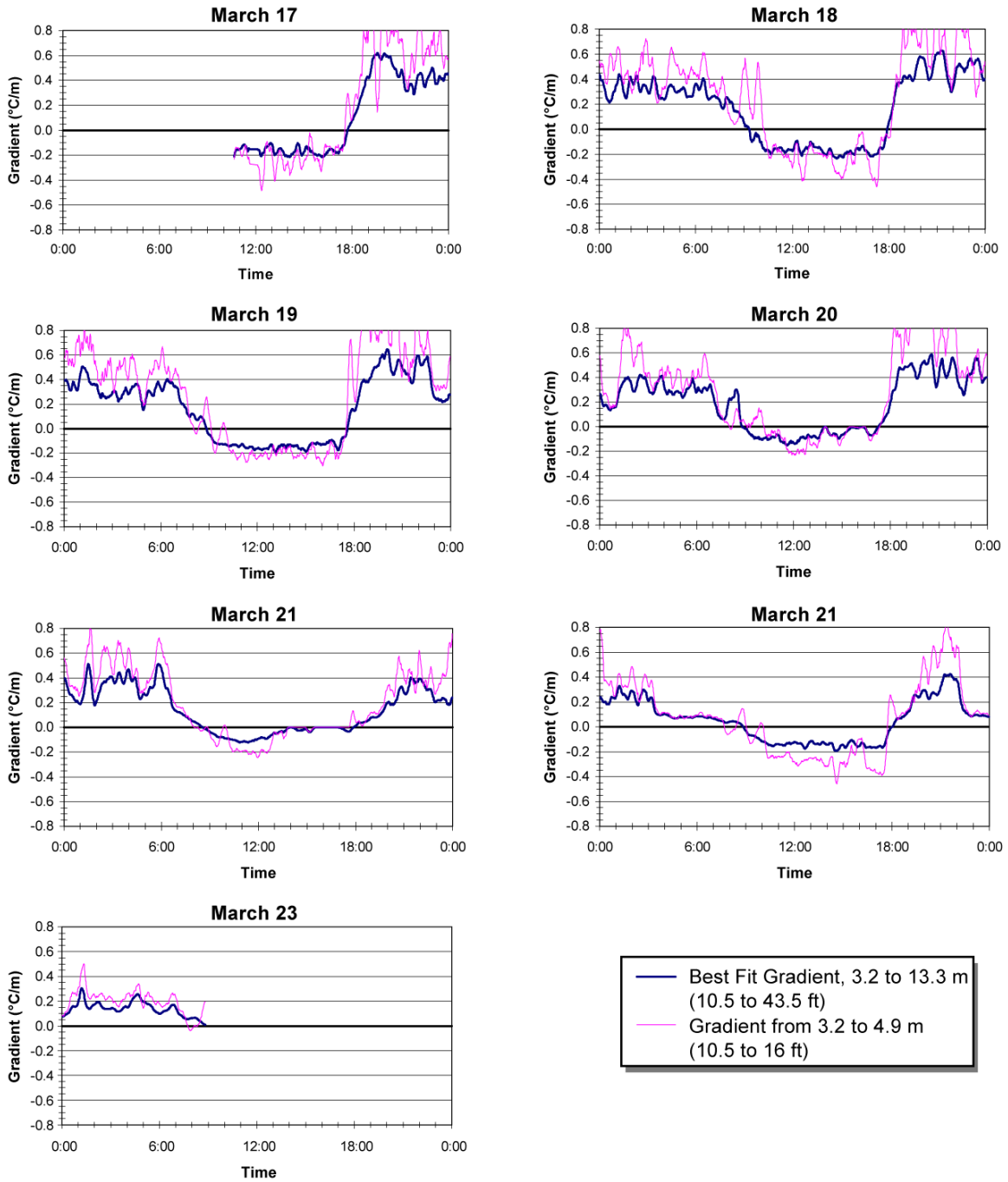


Figure 34. Two Methods of Measuring Ground Level Temperature Gradient, March 17-23, 2004

4.2.4 Normalized Noise Data

The primary factors that affect sound levels at locations 1/4 mile or more from a freeway are:

1. The strength of the freeway noise source. The noise source strength is dependent on the traffic volume, speed, and mix of vehicles. Because the truck volumes on the Pima Freeway are usually less than 1.5%, relatively little error is introduced by assuming 100% automobiles.
2. Geometric spreading of sound energy. As sound propagates away from a source, the sound intensity drops because the sound energy is spread over an ever increasing area.
3. Atmospheric absorption of sound energy. As discussed in Section 4.2.3, except in extreme cases, changes in temperature and relative humidity will change the A-weighted noise levels by only 1 to 2 dB.
4. Interaction of the sound waves with the ground. This includes both the impedance of the ground and the various obstructions along the propagation path. We have ignored any shielding effects of the houses and low walls that are along the propagation path from the freeway to the measurements sites in Scottsdale west of the Pima Freeway.
5. Refraction of sound caused by sound speed gradients.
6. Background noise. The background noise during the measurements in March and October 2004 included neighborhood activities, local traffic, aircraft over flights, lawn mowing, and plowing of the fields. During the March measurements before the quiet pavement was installed, the freeway noise was usually dominant during the early morning hours. However, during the mid-day periods when freeway noise was much lower due to the upward refraction, other noise sources were often dominant. In October after the ARFC had been installed and the A-weighted freeway noise had dropped about 10 dB, freeway noise was the dominant noise source only in the early morning hours. Other sources tended to dominate in the late night hours when traffic volumes were low and in the mid-day period when there was upward refraction.

Separating out the effects of refraction (item 5 above) from the other five factors is the principal goal of this study. To do this we have used TNM Version 2.5 to calculate the expected noise levels due to factors 1 through 4 and then compared the measurements and predictions to estimate the contributions of refraction effects and background noise. We cannot eliminate the effects of background noise, although we reduced the influence of background noise by deleting periods when background noise was clearly dominant. The deleted periods were sound level peaks caused by transient events such as aircraft over flights, local traffic, and lawn mowing or other landscaping activities.

Figure 35 shows the projected traffic noise levels under neutral atmospheric conditions. Because the Scottsdale site where the measurements were made is quite flat and the roadway is straight, accurate projections could be made using a fairly simple model. The projections assume a “flat world” and do not account for the acoustic shielding provided by the houses and property line walls between Sites 2 and 3 and the freeway. To further simplify the modeling, we did not vary the temperature and humidity and used the default conditions of 70°F, 50% RH for all calculations.

The graphs in Figure 35 show the predicted hourly Leq values for 3 days during the Phase 2 measurements in October 2004 and one 24-hour period during the Phase 1 measurements in March. Unfortunately we only had a few periods of complete traffic counts during the Phase 1 measurements. However, as is clear from Figure 35, the volumes and speeds were quite consistent and the predicted levels are generally within ± 1 dB. The largest variations occur in the afternoon commute period when congestion often causes average speeds to drop to 30 to 40 mph.

The “Combined Average” curves shown in Figure 35 have been used to normalize the average 15-minute Leq data in Figure 23 and Figure 24 (see pages 47 and 48) and to approximately separate out the sound propagation effects. The results are shown in Figure 36. What these graphs show is the measured sound levels relative to the TNM predicted levels. Sound levels greater than zero indicate the measured sound levels are greater than predicted by TNM and less than zero indicate measured levels are lower than predicted by TNM. Following are some observations and conclusions relative to the graphs in Figure 35:

- A-weighted sound levels at Site 1 were typically 2 to 3 dB higher than the predicted levels in March 2004 (Phase 1) and about 8 dB lower than the predicted levels in October 2004 (Phase 2). This is a clear demonstration that the ARFC reduced A-weighted noise source levels by approximately 10 dB. The comparison of sound levels before and after installing the ARFC is discussed in more detail in Section 4.4.
- The concrete roadway had transverse tinning during the March 2004 measurements, which will cause noise levels higher than the national average used in TNM. The results in Figure 35A, B, and C suggest that source levels during March 2004 were 2 to 3 dB higher than the national average. This also suggests that the ARFC reduced A-weighted noise levels to about 7 dB below the national average.
- The difference between the 2 weeks in March is quite interesting. During the first week (Figure 35B), the normalized sound levels at Sites 2 and 3 were similar except during the mid-day period. It is likely that background noise at Site 3 caused the normalized mid-day sound levels to be 2 to 3 dB higher than at Site 2. In the second week (Figure 35C), the normalized levels at Site 3 were consistently 3 to 5 dB higher than at Site 2. As for the first week, the mid-day difference can be attributed to the background noise at Site 3. However, in the late evening to early morning period, traffic noise was dominant. This means that the higher normalized sound levels at Site 3 are due to a propagation effect. We suspect that the wind patterns were such during the second week that there was consistent focusing at Site 3 but not at Site 2. The most likely cause of the focusing is the low-speed, east-to-west flow air jets that apparently form in this area at elevations greater than 20 m (66 ft).
- We would expect that the normalized levels for Site 1, which was only 30 m (100 ft) from the freeway, would be a straight line in Figure 36A through Figure 36C for the daytime period. The drop in the normalized levels at Site 1 during the afternoon commute period may be due to the stop-and-go traffic caused by congestion during this period.
- The normalized levels at Sites 2 and 3 for the October 2004 measurements (Figure 35D) were strongly influenced by background noise, particularly during the mid-day period when freeway noise was lowest.
- The normalized levels at Site 1 for the October 2004 measurements are a relatively straight line at about -8 dB from 4 AM to 9 PM (21:00) except for a small peak at 5 PM (17:00) that is probably related to the afternoon commute period congestion. The Site 1 normalized levels are higher during the late night to early morning period. This is during the period when traffic volumes are lowest.
- Assuming that the transverse tinning caused sound levels during the March 2004 measurements to be 3 dB higher than TNM, the data in Figure 35 indicates that, compared to neutral atmospheric conditions:
 1. Inversion conditions caused sound levels to be 5 to 8 dB higher.
 2. Lapse conditions caused sound levels to be 0 to 10 dB lower.

3. The sound level increase due to inversion conditions is fairly consistent from shortly after sunset until shortly after sunrise.
4. The sound level reduction due to lapse conditions tends to grow through the day until about one hour before sunset.

The sound level change during the transition from inversion to lapse conditions can be relatively gradual (1 to 2 dB per hour in week 1 of the March measurements) or very rapid (a 10 dB change in 1 hour in week 2 of the March measurements). This is probably related to how quickly the sun breaks up the inversion condition. Referring to the temperature gradients in Figure 32 (page 59), it is not obvious that the difference in the temperature gradients was sufficient for there to be such a large difference in the rate of transition from inversion to lapse conditions.

Sound Levels Predicted Using TNM (No Atmospheric Effects)

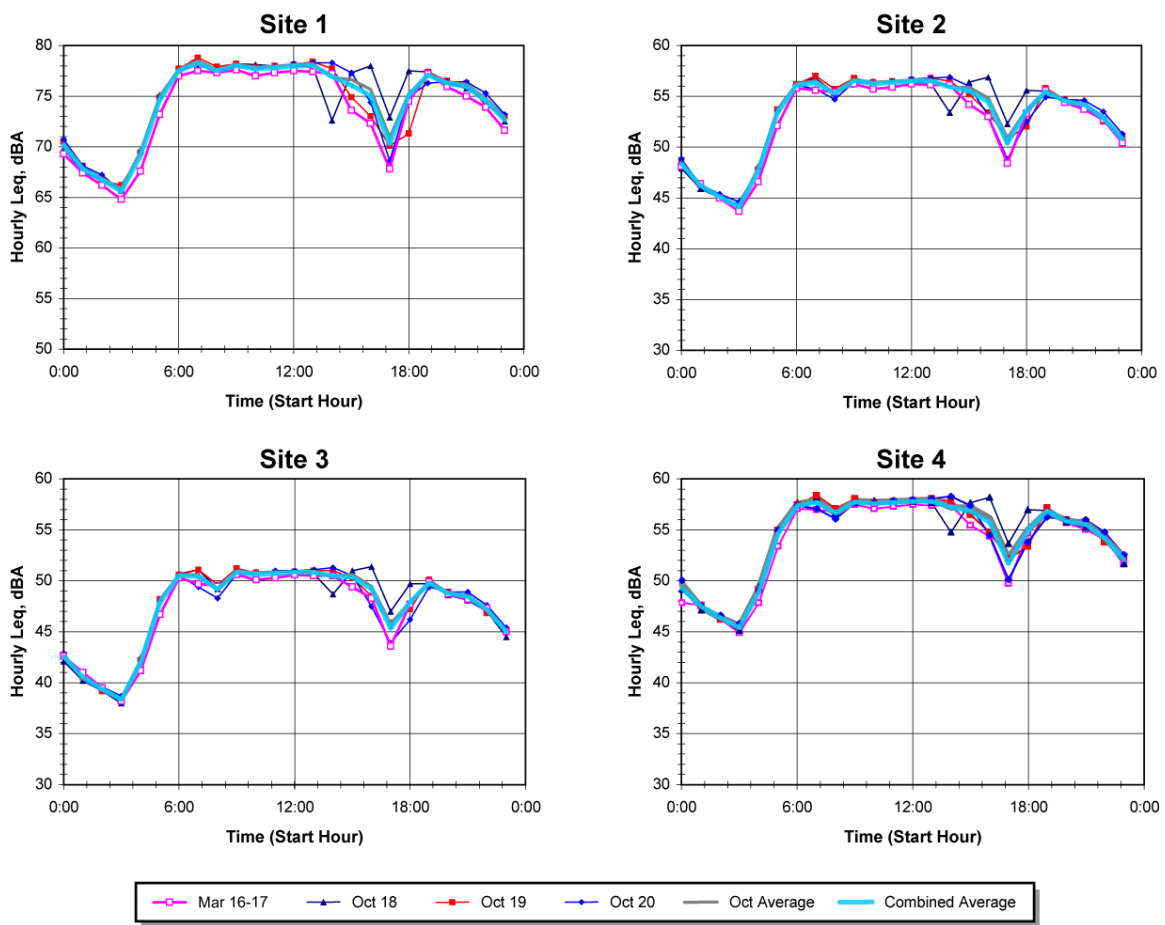


Figure 35. TNM Projections over a 24-Hour Period

TNM Normalized Sound Levels (15-minute Leq)

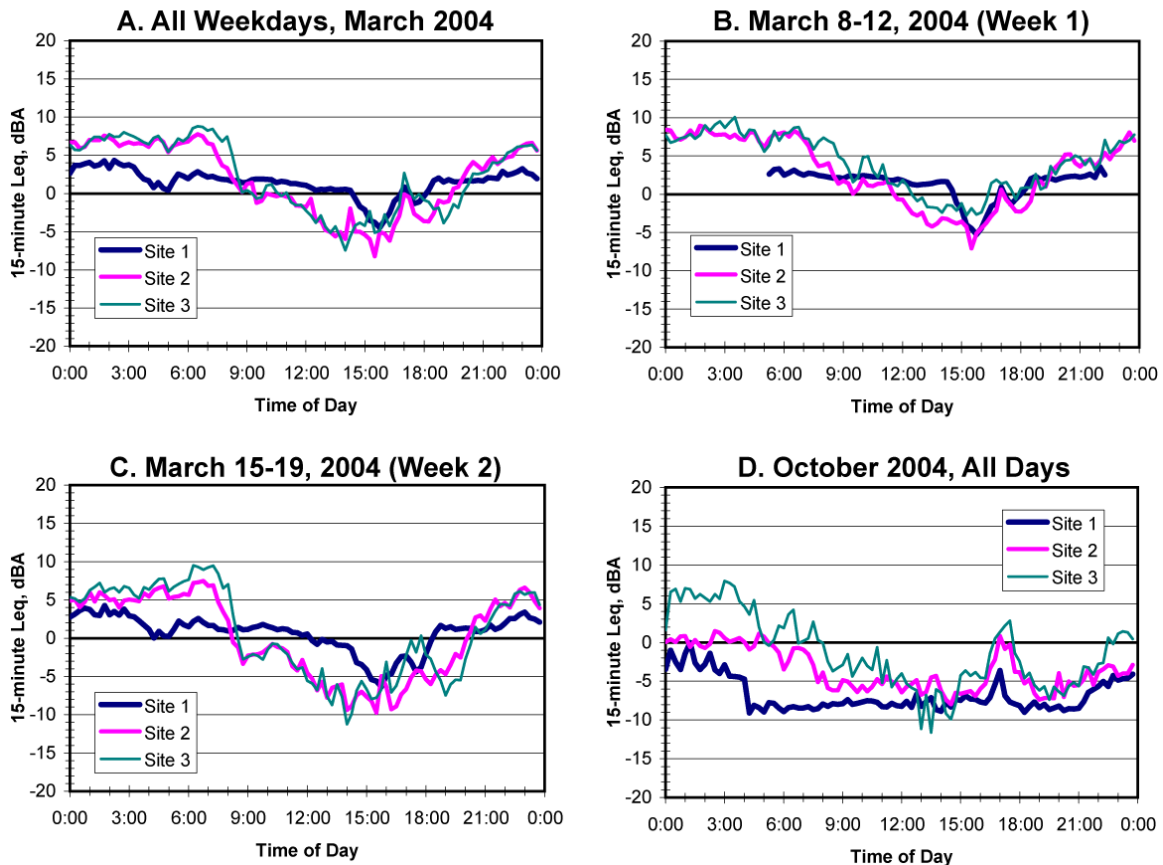


Figure 36. Average Sound Levels Normalized Using TNM Projections

4.3 SHORT TERM NOISE MEASUREMENT RESULTS

This section summarizes the short-term (3 hour) measurements performed on three mornings during the Phase 2 tests and looks in detail at one period of dramatic sound level change during Phase 1. The three Phase 2 short-term measurements were all performed between 6 AM and 9 AM. Inversion conditions existed at 6 AM and the transition from inversion to lapse conditions started at sunrise (around 6:30 AM). All three mornings were clear with scattered cloud cover with calm or very low wind speeds at ground level. The observers at each site noted any significant non-freeway noise sources, wind speed, and the apparent direction of the noise source.

One of the interesting observations is that the direction of the noise source would change dramatically over a period of several minutes. Although one would expect the sound to always seem to be coming directly from the freeway, over a 30-minute period the apparent sound source might move from north, to directly from the freeway, to south and then back to north. At no time during these measurements was there more than a light breeze at ground level. For the measurements on the west side of the freeway, we could see whether there was any wind at elevations up to 15 m (50 ft) by observing whether there was any movement in the palm fronds at the tops of the palm trees. At no time did we observe more than a slight ruffling of the palm fronds, indicating that the sound level fluctuations that we observed were due to wind currents at elevations greater than 15 m (50 ft).

TNM Normalized Sound Levels (15-minute Leq)

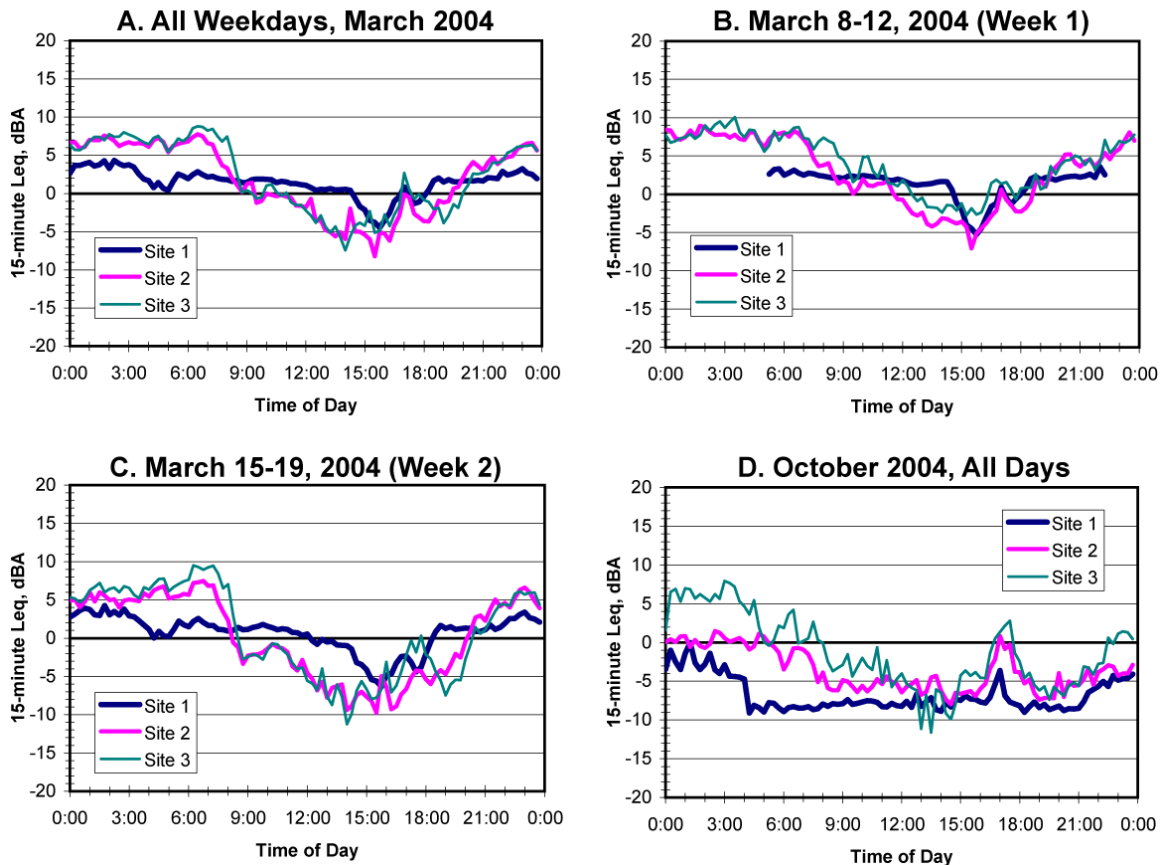


Figure 36. Average Sound Levels Normalized Using TNM Projections

4.3 SHORT TERM NOISE MEASUREMENT RESULTS

This section summarizes the short-term (3 hour) measurements performed on three mornings during the Phase 2 tests and looks in detail at one period of dramatic sound level change during Phase 1. The three Phase 2 short-term measurements were all performed between 6 AM and 9 AM. Inversion conditions existed at 6 AM and the transition from inversion to lapse conditions started at sunrise (around 6:30 AM). All three mornings were clear with scattered cloud cover with calm or very low wind speeds at ground level. The observers at each site noted any significant non-freeway noise sources, wind speed, and the apparent direction of the noise source.

One of the interesting observations is that the direction of the noise source would change dramatically over a period of several minutes. Although one would expect the sound to always seem to be coming directly from the freeway, over a 30-minute period the apparent sound source might move from north, to directly from the freeway, to south and then back to north. At no time during these measurements was there more than a light breeze at ground level. For the measurements on the west side of the freeway, we could see whether there was any wind at elevations up to 15 m (50 ft) by observing whether there was any movement in the palm fronds at the tops of the palm trees. At no time did we observe more than a slight ruffling of the palm fronds, indicating that the sound level fluctuations that we observed were due to wind currents at elevations greater than 15 m (50 ft).

As discussed in Section 3.2, the ADEQ data from 43rd Avenue shows that down-slope air flows in the Phoenix valley under inversion conditions cause 3 to 5 m/sec (7 to 11 mph) air jets at elevations of 40 to 100 m (130 to 330 ft). It is likely that the sound level fluctuations observed during the short-term measurements were caused by low-speed air jets as observed at 43rd Avenue. Perhaps the key conclusion from these tests is that the sound level fluctuations were apparently caused by wind currents at elevations greater than 15 m (50 ft). This means that to really understand how atmospheric conditions are affecting sound propagation at distances of 400 m (1/4 mile) or greater requires knowledge of the wind speeds and directions at elevations up to at least 60 m (200 ft). Furthermore, this indicates that when conditions are controlled by down-slope winds, wind speed, and direction data from a typical 10 m meteorological tower is not suitable for predicting refraction effects.

October 18, 2004

The first short-term sample is from October 18, 2004. The observed measurements at Sites 4 and 4B on tribal land east of the Pima Freeway are shown in Figure 37A. The simultaneous unobserved measurements at Sites 2 and 3 west of the freeway are shown in Figure 37B. Figure 37A and B are 1-minute Leqs and Figure 37C is the same data consolidated into 5-minute Leqs. Weather conditions were clear and calm with scattered high clouds drifting from southeast to northwest. There was never more than a light breeze at ground level. The breeze was going from east to west. There were a number of aircraft over flights starting at around 7:00 AM and several vehicles drove past the measurement sites. The noise from these events has been removed from the analysis.

The A-weighted sound levels at Sites 4 and 4B follow each other closely, with Site 4B typically being 1 to 2 dB lower than Site 4. Sites 2 and 3 on the west side of the freeway follow a different pattern. It is interesting that Sites 2 and 3 do not have nearly as much of a sound level drop after sunrise as was observed in March 2004 during the Phase 1 measurements.

Both the sound level and the apparent direction of the freeway noise at Sites 4 and 4B were constantly drifting throughout the measurements. During periods of higher noise, the sound would usually seem to be coming directly from the freeway. During periods of lower noise, the sound would appear to be coming from either the north or south. Given the nearly calm conditions at ground level, we assume that the wind currents responsible for the sound level fluctuations did not reach ground level.

Perhaps the most interesting feature of these measurements is the sound level dip centered on 8:00 AM. From 7:30 to 8:00 sound levels at both Sites 4 and 4B dropped by 10 dB. During the period when sound levels were a minimum, the sound seemed to be coming from somewhere south of the Indian School Road overpass. We could see smooth traffic flow on the freeway during this period, but it seemed as if the traffic was not making any noise. By 8:30 to 8:45, the freeway noise was back to normal.

Figure 38 shows the 5-minute average 1/3 octave band spectra at 7:30 and 8:00. The spectrum at 7:30 is 10 to 15 dB higher than the 8:00 spectrum over the frequency range of 400 to 4000 Hz. This indicates that the cause of the noise level changes was relatively frequency independent over this frequency range. One exception is the 5 dB dip centered on 1000 Hz. It is not clear why this occurred.

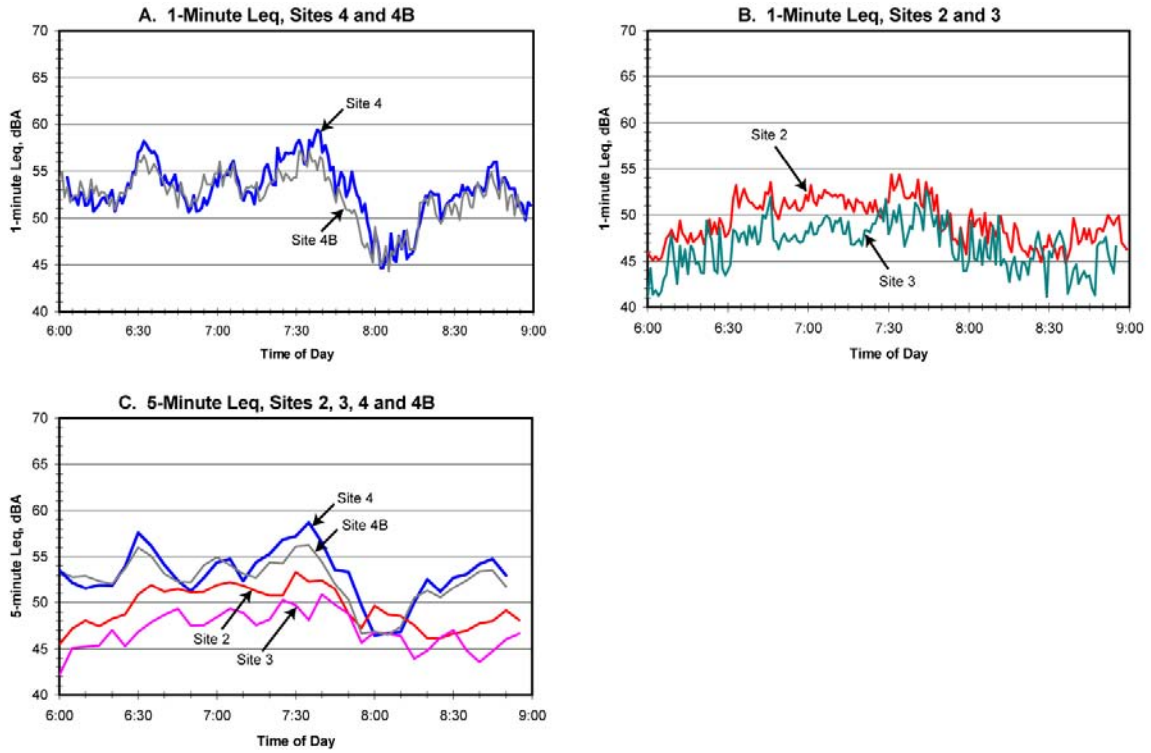


Figure 37. 1-Minute and 5-Minute Leqs, Monday October 18, 2004

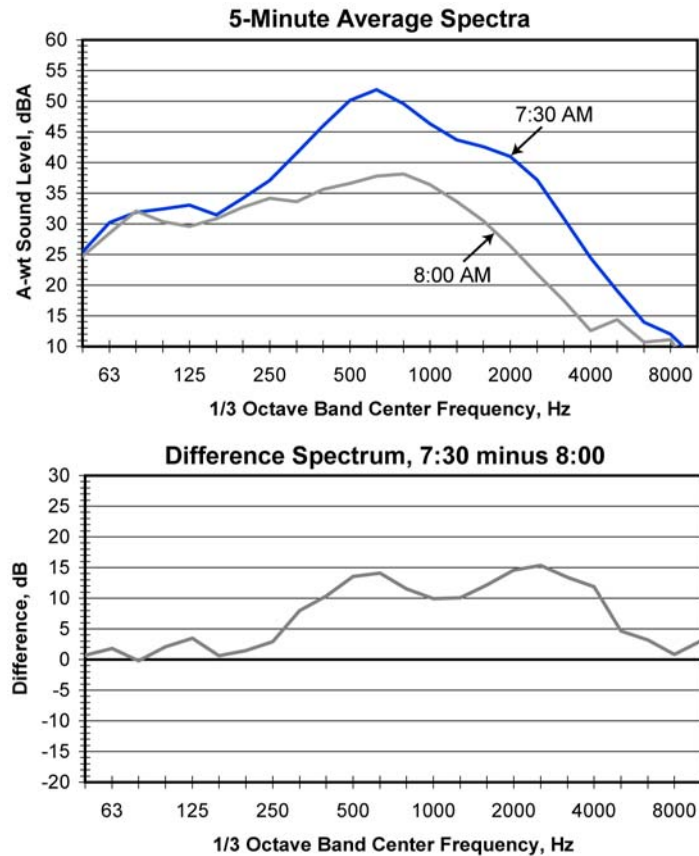


Figure 38. Change in 1/3 Octave Band Levels at Site 4B over 30-Minute Period on October 18, 2004

October 19, 2004

The results for the short term measurement on October 19, 2004 are shown in Figure 39. The results on this day were considerably less interesting than the measurements at Sites 4 and 4B the previous day. Sound levels at Sites 2, 2B, and 2C, which were all approximately the same distance from the Pima Freeway, follow each other closely and there is considerably less fluctuation than observed the previous day. There was about a 5 dB sound level drop from 7:15 to 7:30, which, based on the March 2004 measurements, is before sound levels start to drop as the solar heating breaks up the inversion conditions. The same drop occurred at Sites 2, 2B, and 2C at approximately the same time.

Weather conditions during the measurement were clear and calm with only a slight breeze in the tops of the palm trees. Conditions changed from clear with clouds on the western horizon at the start of the measurements to broken cloud cover towards the end of the measurements. The high altitude clouds were generally moving from east or southeast to west or northwest. There was about a 5 dB drop in the A-weighted sound levels between 7:00 and 7:30 AM, after which the sound levels were consistently around 52 dBA. Based on the March 2004 measurements, the inversion conditions do not dissipate until at least 1 hour after sunrise. Sunrise was at 6:36 AM on October 19. We suspect that the conditions on October 19, 2004 represented relatively weak inversion conditions, and this resulted in a smaller sound level fluctuation than observed during most of the March 2004 measurements.

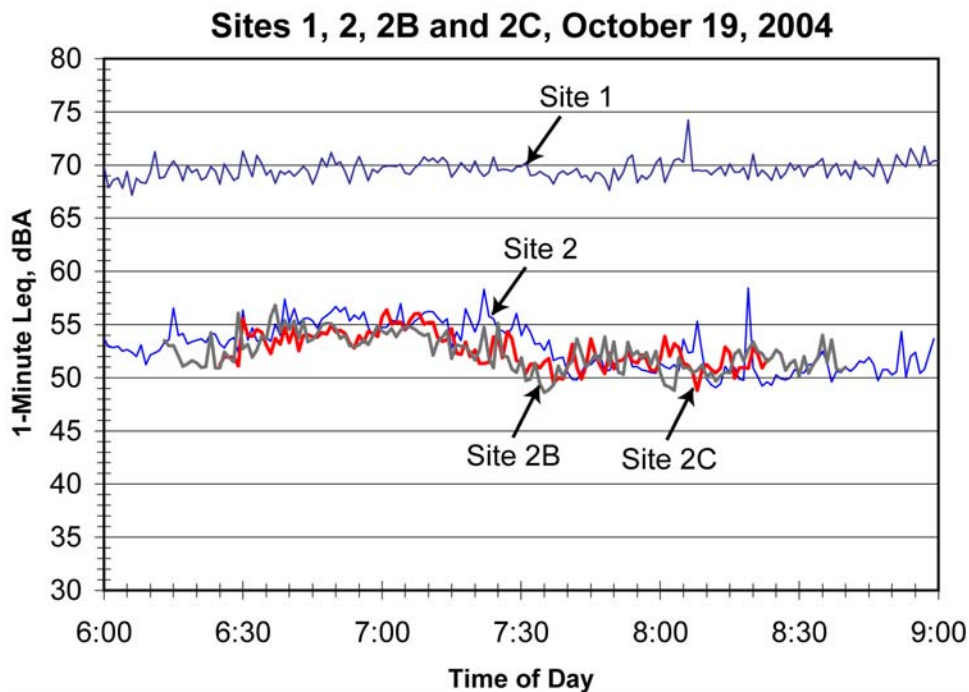


Figure 39. Short-Term Noise Measurement on October 19, 2004

October 23, 2004

Because of the storm front that passed through the Phoenix area mid-week during the October 2004 measurements, the only suitable day for the final short-term measurement was on Saturday. The measurement was approximately 24 hours after the effects of the storm had passed, and we suspect this was not sufficient time for the normal weather patterns to redevelop. The weather on

the morning of the measurement was scattered high clouds, calm (at ground level), and cool. For this measurement we had short-term measurements at Sites 2B, 2C, and 3B in addition to the three long-term measurements at Sites 1, 2, and 3. As seen in Figure 18 (page 37), Sites 2, 2B, and 2C are approximately the same distance from the freeway and Sites 3 and 3B are approximately the same distance from the freeway.

The measurement results are shown in Figure 40. The bottom two figures show the results for Site 2 and Site 3 on an expanded vertical scale. Note that peaks in the sound levels that were clearly from local noise sources were deleted prior to calculating the 5-minute Leq values. It is quite remarkable how closely the sound levels for the three Site 2 locations and the two Site 3 locations follow each other. The biggest difference in the A-weighted sound level for the three Site 2 locations is about 2 dB except at the very end of the measurement when the difference increases to 3 dB. Similarly for the two Site 3 locations, the sound levels track very closely until 8:15, after which Site 3 is consistently 2 decibels higher than Site 3B.

Other interesting observations from these measurements are:

- The Site 3 average is consistently 2 to 3 dB higher than Site 2 between about 7:30 to 8:00. As discussed elsewhere, based on normal geometric spreading, the levels at Site 3 would be approximately 4 dB lower than at Site 2.
- The approximately 5 dB sound level drop at Sites 2 and 3 between 7:00 and 8:30 coincides with sunrise and the expected dispersion of the inversion conditions. We believe that the sound level change is less dramatic than was observed in the March 2004 measurements because the inversion conditions were stronger in March.
- The Site 2 results all have a 3 to 4 dB peak at 7:15 and the Site 3 results all have a 2 to 3 dB dip at 7:10. From the observer notes it is clear that sound levels were dominated by highway noise and other sources, such as aircraft overflights, are not the cause. We expect that these represent short-term focusing and de-focusing effects, although they are small enough to have been caused by turbulence.

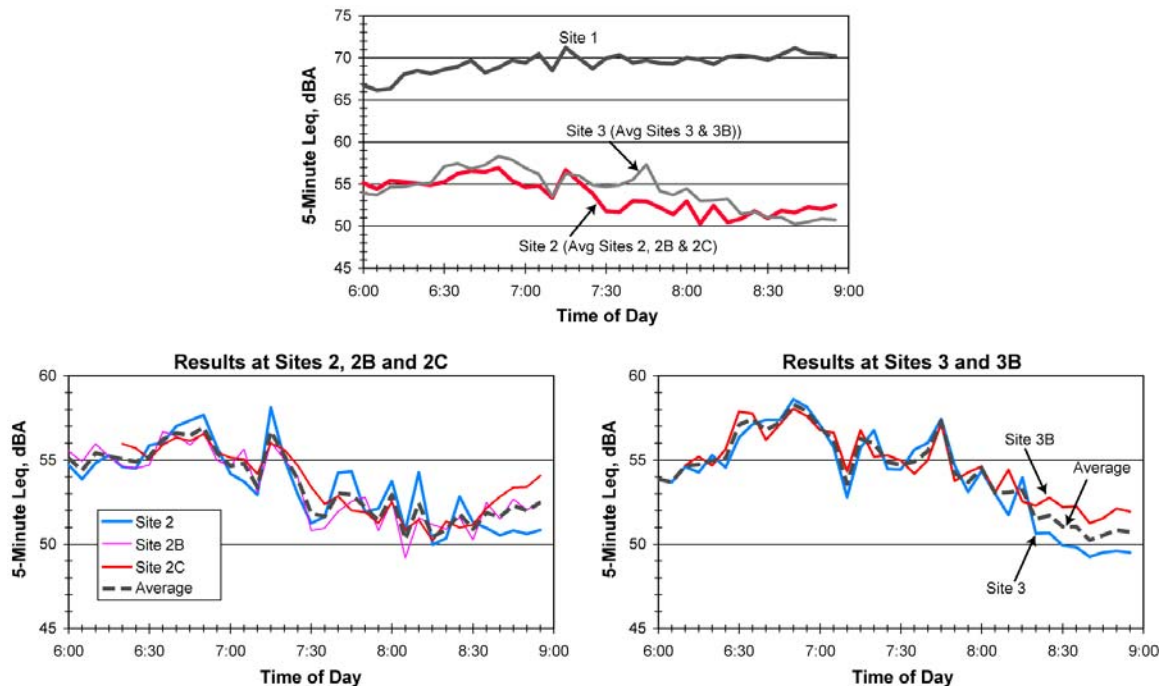


Figure 40. Short-Term Noise Measurement on October 23, 2004

March 18, 2004 5:30 to 9:30 A.M.

The morning transition on March 18, 2004 from inversion to neutral conditions is worth closer investigation because of several interesting events. The 1-minute Leq time history for this period is shown in Figure 41 and the spectrogram is shown in Figure 42. Referring to the spectrogram first, we observe that:

- The sound levels and the frequency content at Site 1 are very consistent throughout the 4 hour period.
- At Sites 2 and 3, the sound levels increase with some intermittent fluctuations from 5:30 to about 6:30, are relatively constant from 6:30 to 7:30, and then drop rapidly from 7:30 to 8:30.
- Site 4, which was about the same distance from the freeway as Site 2 but on the opposite side of the freeway, follows a very different pattern than Sites 2 and 3. The sound level starts out relatively low, peaks briefly at 6:20, has a second, broader peak at 7:45 to 7:50, and then stays higher than Sites 2 and 3 until 8:00.
- There are isolated peaks in the spectrograms that were probably caused by other noise sources. There are two examples at Site 4 between 7:45 and 8:00 and one at Site 3 at about 8:10. We suspect that the sound level peaks starting at 8:30 at Site 4 were caused by plowing of the fields.
- Site 2 and Site 3 have more high-frequency sound (3,000 Hz and higher) than at Site 4. The high frequency sound started just before 6:00 AM and was probably caused by birds. Site 4 was surrounded by plowed fields so there was little bird activity near the site.

How these different events affected the overall A-weighted sound levels is seen in Figure 41. Sound levels at Site 1 varied between 77 and 80 dBA while sound levels at the other three sites varied between 70 and 45 dBA. Two particularly interesting events are the peak at Site 4 at 6:20 and the sound level fluctuations at all three sites at 7:00.

The 6:20 AM peak at Site 4 starts with sound levels at 55 dBA at 6:10, increases to a maximum 1-minute Leq of 64.5 dBA at 6:20, and then steadily decreases back to 55 dBA at 6:30. By 6:45, sound levels are back up to 65 dBA.

The 7:00 fluctuation is interesting in that A-weighted sound levels increased by 2 to 4 dB at Site 2 while at the same time they were decreasing by a few dB at Sites 3 and 4. These are small enough fluctuation that they could have been the result of turbulence, although they could also reflect a small change in the wind conditions that broke up some of the apparent focusing at Site 3 and caused a small amount of focusing at Site 2. Given the relatively calm conditions at ground level, it is more likely that these fluctuations were caused by changes in the wind patterns.

Another interesting observation about the results in Figure 41 is how the sound levels at Site 3 are very similar to those at Site 2 until 7:00, there is then a 10 minute period that sound levels increase at Site 2 while they are decreasing at Site 3, followed by a period of about one hour where sound levels were higher at Site 3 than at Site 2. As noted earlier, based on geometry, sound levels at Site 3 should average 4 dB lower than at Site 2.

The measurements shown in Figure 41 and Figure 42 were not observed. There were no significant fluctuations in the wind speeds measured at Site 2, although from the observed measurements we know that the sound level variations were probably due to wind speed and direction changes at elevations higher than our 13.3 m (43.5 ft) tower at Site 2. We infer from

these results that relatively low velocity winds at elevations above 20 m can cause relatively large sound level fluctuations over periods of a few minutes.

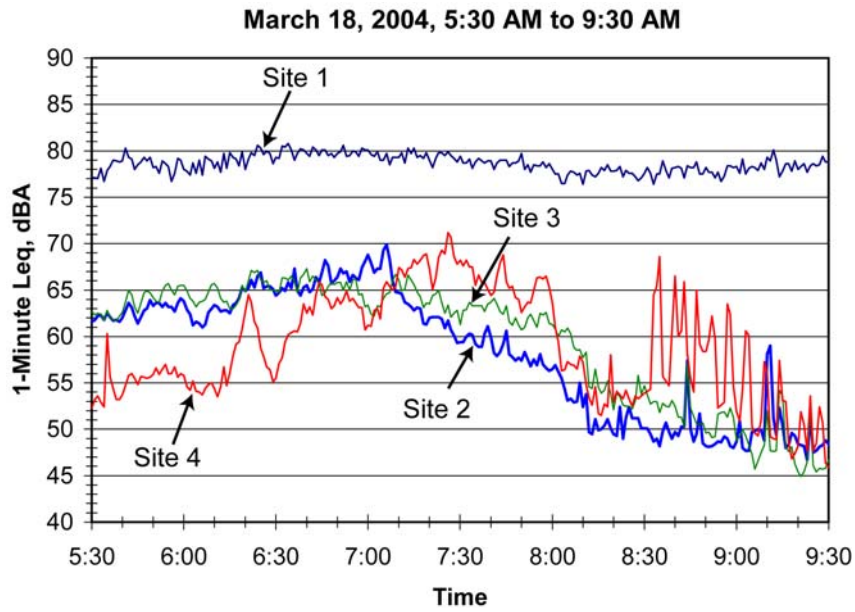


Figure 41. Time History, March 18, 2004, 5:30 to 9:30 AM

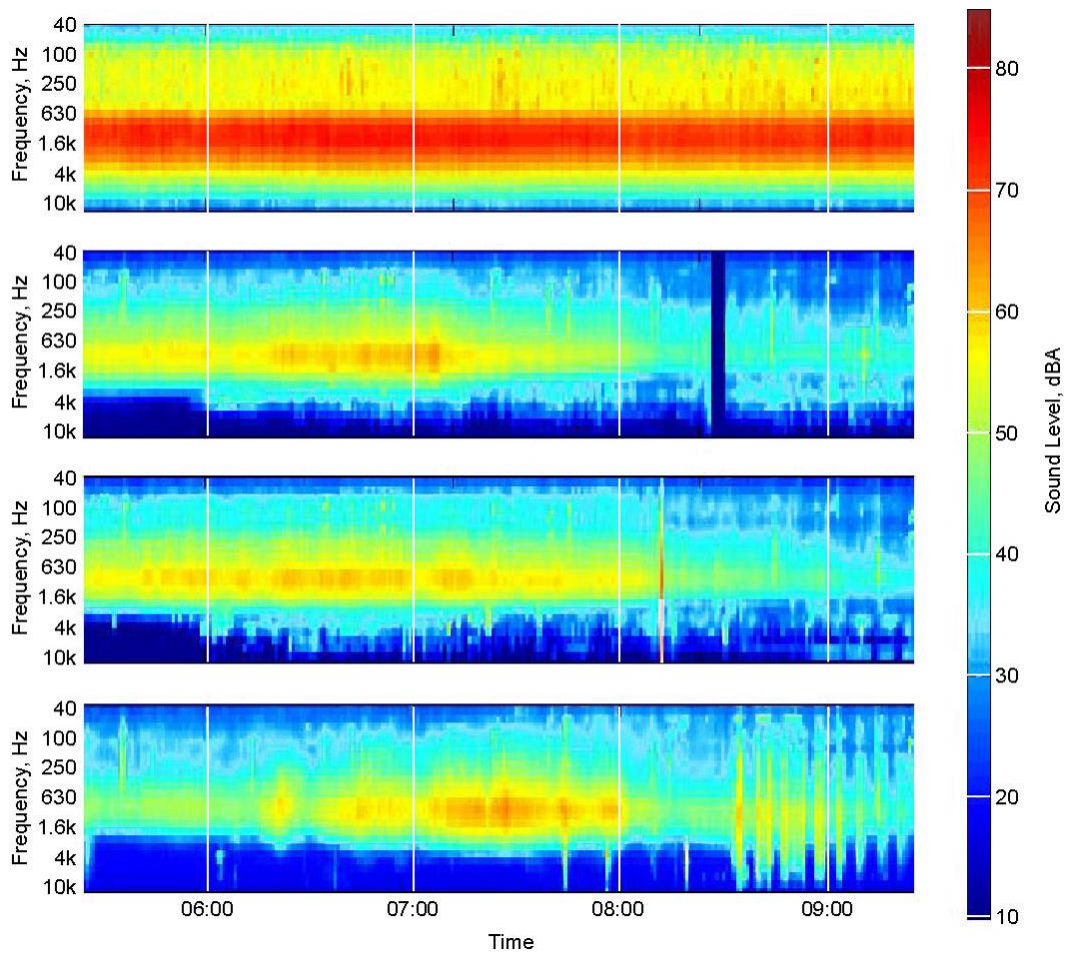


Figure 42. Spectrogram, March 18, 2004, 5:30 to 9:15 AM

4.4 ACOUSTIC BENEFITS OF ARFC INSTALLATION

The original test plan for this project was modified so that a second set of measurements would be performed after ARFC was installed on the Pima Freeway. The installation was completed in June 2004 and the second set of measurements was performed in October 2004. The sound level difference at all sites was dramatic. However, it is not straightforward to accurately quantify the sound level changes attributable to the ARFC at the distant sites because of the compounding effects of refraction.

Figure 43 shows the difference in average A-weighted sound levels using the curves from Figure 36 (page 65) and the overall averages are tabulated in Table 7 for the different periods of the day. Because there was a pronounced difference in the sound level patterns between week 1 and week 2 of the March measurements, we have shown the differences using all of the March data (Figure 43A), just the week 1 data (Figure 43B), and just the week 2 data (Figure 43C). Following are discussions of the results for each period:

- **Late night/early morning:** In this region, the A-weighted sound levels were consistently 5 to 6 dB lower at Site 1, 6 to 8 dB lower at Site 2, and 4 to 6 dB lower at Site 3. An issue could be the higher percentage of heavy trucks during this period, particularly in the early morning hours. The truck percentage averages 3 to 5% of total volume in the early morning compared to 1% or less for the rest of the day (see Table 6, page 51). Another issue is that the low volumes result in relatively low community sound levels, particularly for the October measurements after the ARFC had been installed. It is likely that the October results in this period were affected by background noise from local traffic and non-traffic sources.
- **Daytime traffic and inversion conditions:** This is the period when traffic is at the daytime levels and there is free-flowing traffic. The mid-day temperature lapse period from 8:15 AM to 8:15 PM has been excluded for Sites 2 and 3 because, under daytime lapse conditions in October, noise from the freeway traffic was often below the levels of the background noise. Reductions of A-weighted sound levels were consistently 9 to 10 dB at Site 1 and 8 to 9 dB at Site 2. As discussed elsewhere, there appears to have been focusing in the early morning hours at Site 3 during the second week of the March measurements. The focusing caused sound levels during this period to be 3 to 4 dBA higher than normal. Since this focusing did not appear to occur during the October measurements, we believe that using the week 2 March results for Site 3 will tend to overstate the benefits of the ARFC.
- **Afternoon congestion:** Sound levels are lower in this period because of the lower traffic speeds. Data is only shown for Site 1 because traffic noise in October was not sufficiently above the background noise at Sites 2 and 3. The average reduction of the A-weighted sound level at Site 1 was 3 to 5 dB during this period, probably a reflection of the low speeds reducing tire noise to the point where it was comparable with engine, exhaust, and other vehicle noise sources.

Representative 1/3 octave band spectra for the March and October 2004 measurements are shown in Figure 44A for Site 1 and Figure 44B for Site 2. From Figure 44A, it is clear that the ARFC resulted in a large drop in sound levels between 500 and 4,000 Hz.

The results at Site 2, which was just over 500 m from the freeway, are less clear because of the refraction effects. There is a large difference between the March and October measurements at 6 AM, but at 12 PM the results are much less dramatic. This is because highway noise at Site 2 in October was often lower than the background noise under mid-day lapse conditions.

Figure 44C and D show the difference between the March and October measurement results. As seen in Figure 44C, the 6 AM and 12 PM results are very similar for Site 1 (30 m from the

roadway). The differences at Site 2 are much higher at 6 AM than at 12 PM because during the mid-day period the freeway noise during the October measurements often was lower than the background noise.

The bottom plots (Figure 44E and F) show that the apparent effects of ARFC at Site 2 vary somewhat from the effects at Site 1. The ARFC appears to be more effective at low frequencies at Site 2 and more effective at high frequencies at Site 1. In both cases we suspect that the differences between Sites 1 and 2 are related to background noise effects and are not related to the ARFC.

The overall conclusion is that the noise reduction benefits of ARFC measured at sites close to a freeway appear to translate to equal benefits at more distant community areas. However, the benefits at more distant sites can be obscured by background noise, refraction, and the normal sound level fluctuations caused by turbulence and other factors.

Table 7. Comparison of Average Sound Levels Before and After ARFC Installation			
Period	Average Difference in A-wt Sound Levels, dB		
	Site 1	Site 2	Site 3
All Data			
Late night/early morning	6.4	7.6	5.4
Daytime traffic	9.5	8.4	9.2 ⁽¹⁾
Afternoon congestion	4.3	--	
Week 1 March Data			
Late night/early morning	5.5	8.1	4.7
Daytime traffic	9.4	8.7	7.9
Afternoon congestion	4.5	--	--
Week 2 March Data			
Late night/early morning	6.4	7.0	5.8
Daytime traffic	9.0	8.2	10.3 ⁽¹⁾
Afternoon congestion	2.7	--	--
Definitions (24-hour clock)			
Late night/early morning: 22:00 to 4:15			
Daytime traffic			
Site 1: 4:15 to 14:00 & 18:30 to 22:00			
Sites 2 & 3: 4:15 to 8:00 & 20:15 to 22:00 (daytime lapse period excluded)			
Afternoon congestion: 15:15 to 18:00			
Note:			
⁽¹⁾ Sound levels at Site 3 during week 2 of the March measurements appear to have been elevated by focusing that did not occur during the October measurements. Therefore, these Site 3 differences probably overstate the difference due to the ARFC.			

Sound Level Change After ARFC Installation

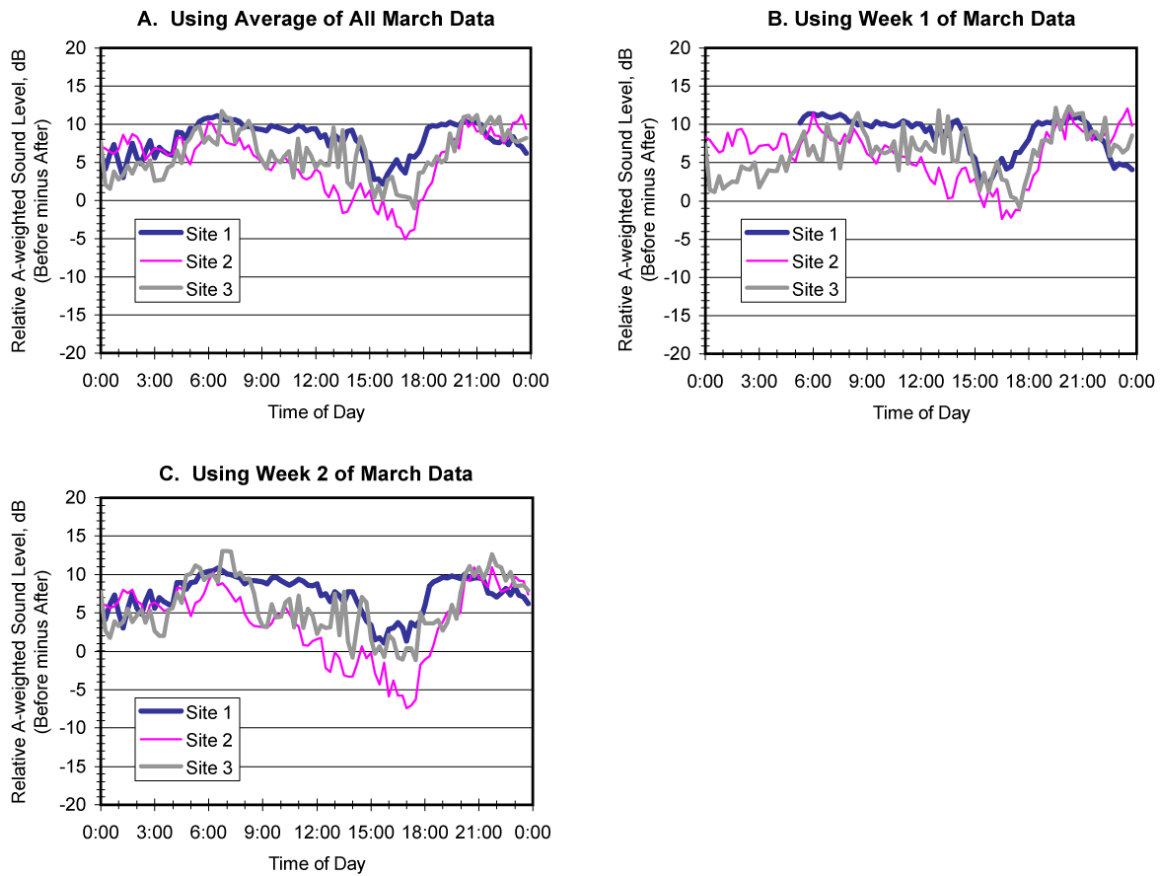


Figure 43. Comparison of Sound Levels Before and After Installation of ARFC
(Curves are differences of normalized 15-minute L_{eq} values in Figure 36, page 65.
A positive value indicates lower sound levels in October 2004.)

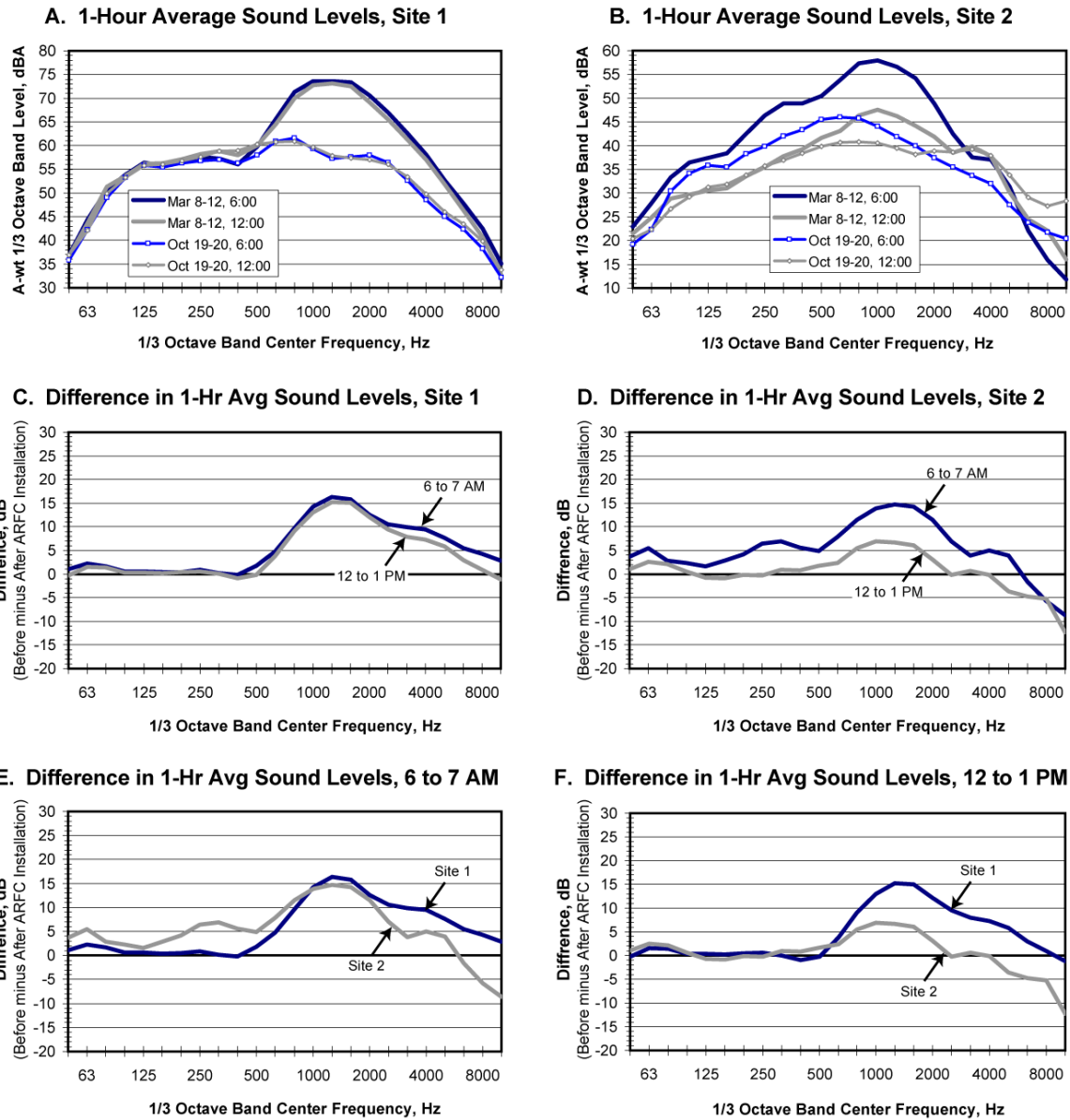


Figure 44. 1/3 Octave Band Spectra at Sites 1 and 2 Before and After Installation of ARFC

5. COMPUTER MODELING

5.1 OUTDOOR SOUND PROPAGATION

Understanding the propagation of sound over long distances remains a very challenging task because of the complexity of the environment.¹⁹ The main challenges lie in the inherent complexity of any realistic medium and that of any realistic ground surface. The complexity of the medium affects the governing wave equation, whereas the complexity of the ground impacts the associated boundary conditions.

Several factors contribute to the complexity of the acoustic medium. While these factors have been considered earlier, they are critical to computer modeling of sound propagation and are thus briefly reviewed here. Wind and temperature gradients are responsible for sound speed gradients and the subsequent refraction of sound, which can radically change the sound field. In the case of wind gradients, which are almost always present in ground-to-ground propagation due to the no slip condition imposed by the ground (e.g., wind speed is zero at the ground surface), the sound waves are turned toward the ground in the downwind direction and away from the ground in the upwind direction as shown schematically Figure 45.

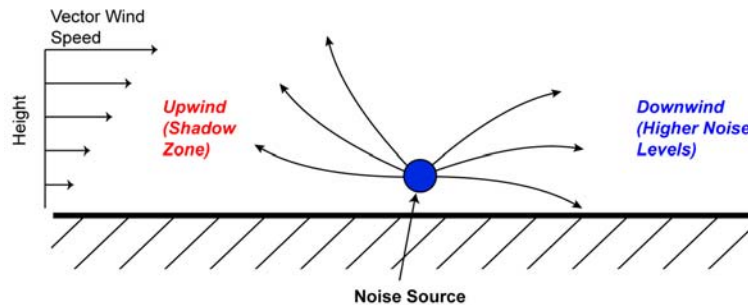


Figure 45. Influence of Wind Speed Gradients on Sound Propagation

Temperature changes above the ground also influence the propagation of sound waves. When temperature decreases with height as is common on sunny days, sound waves are bent upward. This is referred to as a temperature *lapse*. If the temperature increases with height, a temperature *inversion* condition, sound waves will be turned toward the ground. Inversion conditions are common during radiational cooling at night while the lapse conditions usually happen during ground heating after sunrise. As seen in the schematic in Figure 46, lapse conditions tend to create a sound shadow around the noise source while inversion conditions tend to increase sound levels.

Fluctuations caused by atmospheric turbulence also act to introduce random processes which lead to the scattering of sound within the medium.

Similarly, several factors contribute to the complexity of the ground effects. The ground may be of finite impedance which greatly complicates the reflection of spherically spreading sound waves. The ground impedance variation from point to point may be gradual, as with vegetation, or discontinuous, such as an asphalt road next to a grass field. Another aspect of the ground effects are large scale irregularities in the topography of the terrain which cause diffraction, scattering, and complex acoustic shadow regions. Sufficiently large topography, such as a mountain range, can influence the local meteorological conditions such as through the formation of inversion zones or prevailing winds, which will in turn affect acoustic propagation. As discussed elsewhere, the cyclical temperature gradients caused by ground heating in the day and radiational cooling at night, in combination with the low-velocity winds caused by the mountain ranges, are probably the primary cause of relatively high noise levels near Phoenix valley freeways during spring and fall months.

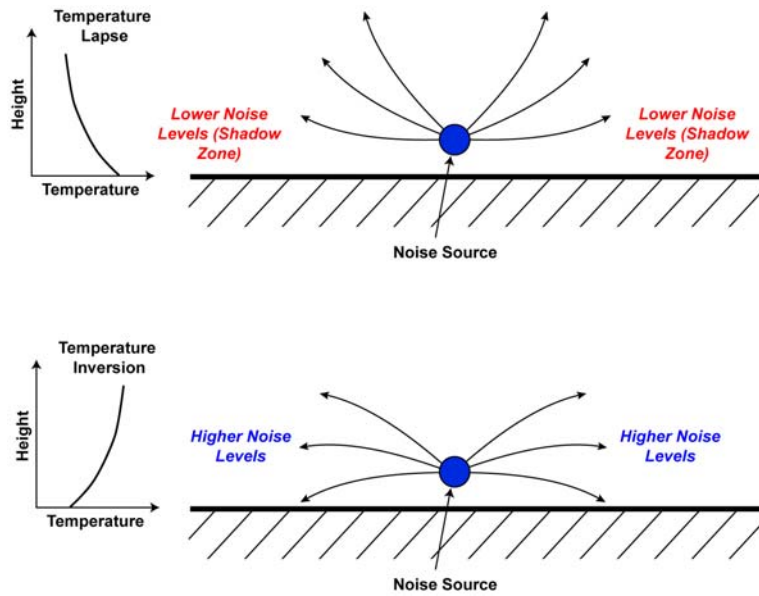


Figure 46. Influence of Temperature Gradients on Sound Propagation

In view of the complexity of long range sound propagation in the atmosphere, numerical techniques are the most appropriate tool for efficient predictions in a realistic environment. One such numerical technique is the PE method.^{9,13} While other methods are available (e.g., see introductory discussion in Section 2.2.3, page 23), PE methods incorporate the most physically based methods. This precision comes at the expense of computational speed, but advances in computer power in the last two decades have transformed this previously significant obstacle into a minor issue. The PE model is a marching solution that begins at the source and sequentially solves the governing wave equation, step by step, to the receiver position. As such it would be capable of being “perturbed” along its route to account for modifications such as the presence of a barrier.

5.2 METEOROLOGICAL MODELING

The accuracy of the PE method depends in large part on the accuracy of the input meteorological conditions. Discussions with staff of the ADEQ indicated that while copious amounts of meteorological data and analysis have been collected and conducted in the Phoenix area, the majority of it was for heights of 200 m and higher in pursuit of macroscopic meteorological phenomena. A general rule of thumb in acoustic work is that metrological conditions up to approximately 10 to 20% of the desired propagation range are needed for proper analysis. For the range of approximately 1 km for the problem at hand, this indicated metrological data below 200 m was desired. Furthermore, while historical data can be useful in analyzing general trends, acoustic propagation is linked with instantaneous metrological conditions and as such, a meteorological station capable of measuring wind and temperature was set up in conjunction with the noise monitoring equipment.

For the temperature analysis, (and the adiabatic lapse rate) one can use the modeling of Stull²² and use the ground level temperature gradient to approximate the overall temperature profile up to the inversion height. The parameters for the Stull model are shown in the sketch below. For these parameters:

$$T(z) = T_S + \left[1 - \left(1 - \frac{z}{H} \right)^\alpha \right] \times \Delta T$$

at $z = 0$, $T(z) = T_S$

at $z = H$, $T(z) = T_S + \Delta T = T_H$

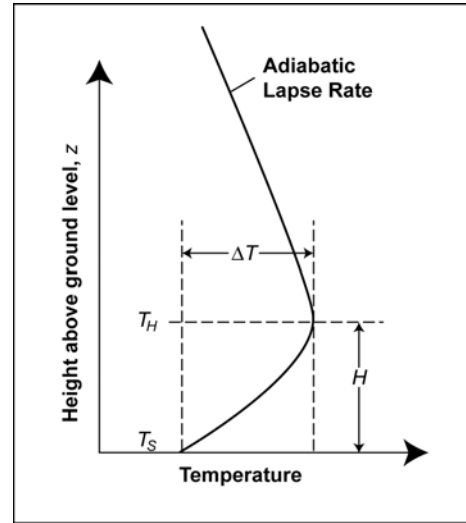
The value for α is greater than 2 and less than 3.
We assumed $\alpha = 2.5$.

This gives:

$$\frac{dT}{dz} = -\Delta T \times \alpha \times \left(1 - \frac{z}{H} \right)^{\alpha-1} \times \left(\frac{-1}{H} \right)$$

and, at $z = 0$,

$$\frac{dT}{dz} = \frac{\Delta T \alpha}{H}$$

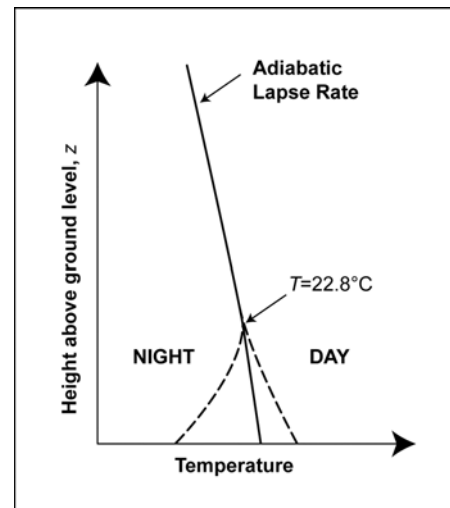


Basically the height of H and ΔT are linked and we can use dT/dz (which we have from the measurements) and assume one to get the other.

As a first cut, we assumed that T_H went to a max of 22.8°C (73°F) as this is the temperature where the temperature gradient goes to zero at approximately 9:15 AM and should be an indicator of the upper air temperature before higher level cooling kicks in. A sketch of the swing of near ground level temperatures as a function of time of day is shown in the sketch to the right.

Thus the measured temperature gradient near ground level was used along with some reasonable assumptions to get a sound speed profile as an input to the PE model.

While wind speed measurements were acquired as part of the field exercise, they only extended to an elevation 13 m (43.5 ft) and did not indicate any significant wind effects. Although we are confident that many of the sound level fluctuations that we observed were due to wind effects, apparently the effects were at elevations greater than 13 m.



Sketch of near ground level temperatures

Discussions with the ADEQ staff indicated that there is a “typical, time averaged” wind profile caused by daytime heating of air. This forces air up into the mountains and drainage flow during the evening through early morning period which has air moving down into the valley. This drainage flow is, on average, east to west in the Scottsdale area where we performed the noise measurements.

As part of the ongoing ADEQ studies of meteorology in the Phoenix valley, a study of wind speeds on 43rd Avenue was conducted in January 2003. A snapshot of wind speeds below 200 m at 6 AM was used as part of this exercise. The use of wind speeds from a different location and time is not an ideal solution. However, using the 43rd Avenue data and the temperature profile discussed above in the PE model allows testing the sensitivity of the refracted sound field to

realistic wind profiles. As discussed later in Section 5.3, the modeling demonstrates that the temperature gradients are sufficient to describe the overall diurnal sound level trends while the wind speeds act to provide local spatial and temporal variations about these mean levels.

In addition to the meteorology inputs, the PE model requires assumptions about source and receiver locations, ground type, and spreading losses. The assumptions used are summarized below:

- **Source Height:** The noise source height was assumed to be 0.2 m (8 in). This represents a balance between tire noise close to ground level and engine noise which is approximately 1 m above the ground. This tends to ignore truck stack emission noise, which is at a higher source height. Because heavy truck volumes are generally around 1% of the total traffic volume except between 3 and 5 AM, we do not believe that neglecting truck exhaust noise introduces significant error.
- **Receiver Locations:** The receiver locations for the model analysis were set from 0 m to 1.5 km from the roadway, which encompasses the area of primary interest.
- **Receiver Height:** Receiver height was set at 1.5 m to represent a typical human ear height.
- **Ground Type:** The ground along the propagation path was assumed to be fairly hard (5000 cgs Rayls) since a significant fraction of the propagation path on the Scottsdale side of the Pima Freeway is pavement or hard soil.
- **Spreading Loss:** Because the PE model is two dimensional, it is necessary to independently model the sound energy dissipation as it propagates away from the source and expands into an increasing volume. On one extreme, a point type source would exhibit losses of $20 \times \log(\text{distance})$ or 6 dB for every doubling of distance from the source. However, an infinitely long noise source, which is a good approximation of a long straight highway, should exhibit losses of $10 \times \log(\text{distance})$. From investigating the low frequency octave bands (63 Hz, 125 Hz), which should be relatively unaffected by ground or air absorption, under what we assumed were close to neutral conditions (9:15 AM), we found spreading losses close to $15 \times \log(\text{distance})$, halfway between the two extremes. Physically, this might represent certain elements not present in our modeling efforts, such as turbulent scattering, and the elevated portions of the highways (overpasses), which would mimic point-like sources with a bigger than normal contribution than other highway segments. Thus, as a compromise, we used $15 \times \log(\text{distance})$ to account for typical geometrical spreading.

5.3 MODELING RESULTS

The PE model was run for the meteorological and geometrical inputs discussed above. While the experimental data was collected over a 2 week period in March, the modeling efforts focused on March 18 and 19, as these days seemed fairly representative of the phenomena under investigation and additional measurements from handheld observes were available for portions of the data. The time frames of 6 AM, 7:15 AM, 8:15 AM, 9:15 AM, and 3:00 PM (15:00) were chosen to capture the periods of increased sound levels (6:00 AM and 7:15 AM), the transition period (8:15 AM), the neutral period (9:15 AM), and afternoon period of decreased levels (3 PM).

The A-weighted sound level at the measurement locations is dominated by sound energy concentrated around 1 kHz. However, many of the meteorology phenomena under investigation are frequency dependant so the PE model was run for octave bands from 63 Hz to 1 kHz to provide a full picture of the influence of meteorology effects. The model accounts for air absorption, which is temperature and humidity dependant, and ground absorption.

The model was run for four cases:

- **Neutral:** The entire propagation space consisted of a neutral atmosphere with constant temperature and relative humidity based upon ground values.
- **Temperature Only:** A temperature profile based on measured temperature values at Site 2 using the models discussed in Section 5.2.
- **Temp Downwind:** The temperature profile with a representative vector wind speed from the 43rd Avenue ADEQ measurements added. This model run assumes wind speed from east to west and is intended to describe conditions at the Scottsdale measurement sites west of the highway.
- **Temp Upwind:** The same as “Temp Downwind” with the wind direction reversed. This case should indicate what is occurring on the east side of the highway.

For the downwind case, the effects of temperature and wind on the noise should tend to reinforce each other since the sound waves are refracted downward in both cases. In the upwind case, the temperature and wind effects are battling each other and more volatility is expected with one sometimes canceling the other out and other times one or the other being dominant.

Sample outputs of the individual PE runs are shown below. The output of the PE program is the Excess Attenuation (EA) or sound level relative to what would be expected above and beyond normal spreading losses.

Temperature Only, 1000 Hz

Figure 47 indicates that for the temperature-only case at 1000 Hz, there is a significant amount of downward refraction causing an increase in sound levels above the spreading loss for neutral conditions. Beyond 300 m (1000 ft), the levels at 1.5 m (5 ft) above ground level are approximately 5 to 15 dB greater than the neutral case.

The PE output indicates some structure in the elevated levels. This structure represents constructive and destructive interference between various waves after multiple bounces off the ground. The effects of the constructive and destructive interference are similar to the patterns of surface waves one sees when a pebble is dropped into a pond near an edge or near some debris. In real world conditions, the structure in the results is smoothed out by factors including: scattering from turbulence in the atmosphere, scattering from house to house reflections in the neighborhood, the different propagation path lengths and variation in meteorological conditions for sound coming from different parts of the highway, and the interaction of different frequencies. In addition, averaging over time, even over periods as short as 1 minute, will tend to smooth out the structure in the propagation curves.

It should also be pointed out that the PE used is a marching solution to the wave equation and as such it marches sound waves away from the source in the propagation direction. The dark blue region above the source location (near 0,0) is an artifact of the program and does not indicate that there is no sound above the highway; it is simply a region where the model is not valid.

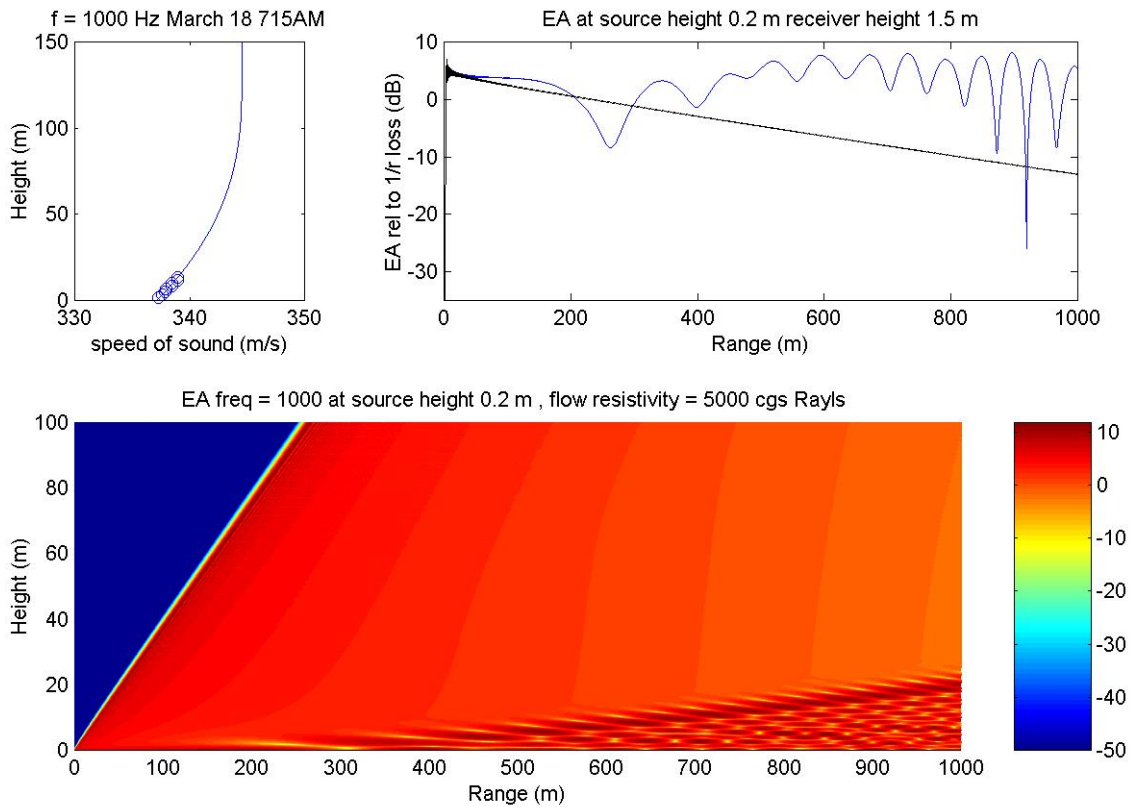


Figure 47. Sample PE Output, Temperature Effects Only, 1000 Hz

Upper left: Assumed sound speed profile. Circles are sound speed based on measured temperature and the solid line is the sound speed based on the temperature scaling laws.

Upper right: PE output at the receiver height of 1.5 m (5 ft). Blue line is PE output while the black line is the “Neutral” case for comparison.

Bottom: Full PE output indicating relative sound levels (red higher, blues lower).

Temp Downwind, 1000 Hz

Figure 48 shows the output for the same case as Figure 47 with the addition of the wind profile. The addition of the moderate wind at 1 to 2 m/s (2.2 to 4.5 mph) does not qualitatively change the results as the sound levels beyond 300 m are still increased by 5 to 15 dB. What the wind does do is to cause local sound level increases and decreases that are different than those for the temperature-only case. This change in the structure is due to the convection of sound by the wind as evidenced in the sound “jets” in the PE output below 50 m (which coincides with the bulge in the wind speed profile).

Again the output in Figure 48 represents propagation of one frequency, 1000 Hz, from one section of the highway. There would be considerable smoothing of the structure in the curves due to factors such as scattering and variations in the meteorological conditions. However, both the logged data and local observers indicate that superimposed over the generally increased levels there are significant local sound level fluctuations of several dB. It is proposed that the daily temperature inversion due to radiational ground cooling at night is responsible for the majority of the increase in sound levels and that wind effects are responsible for local variations and additional focusing and defocusing of the sound.

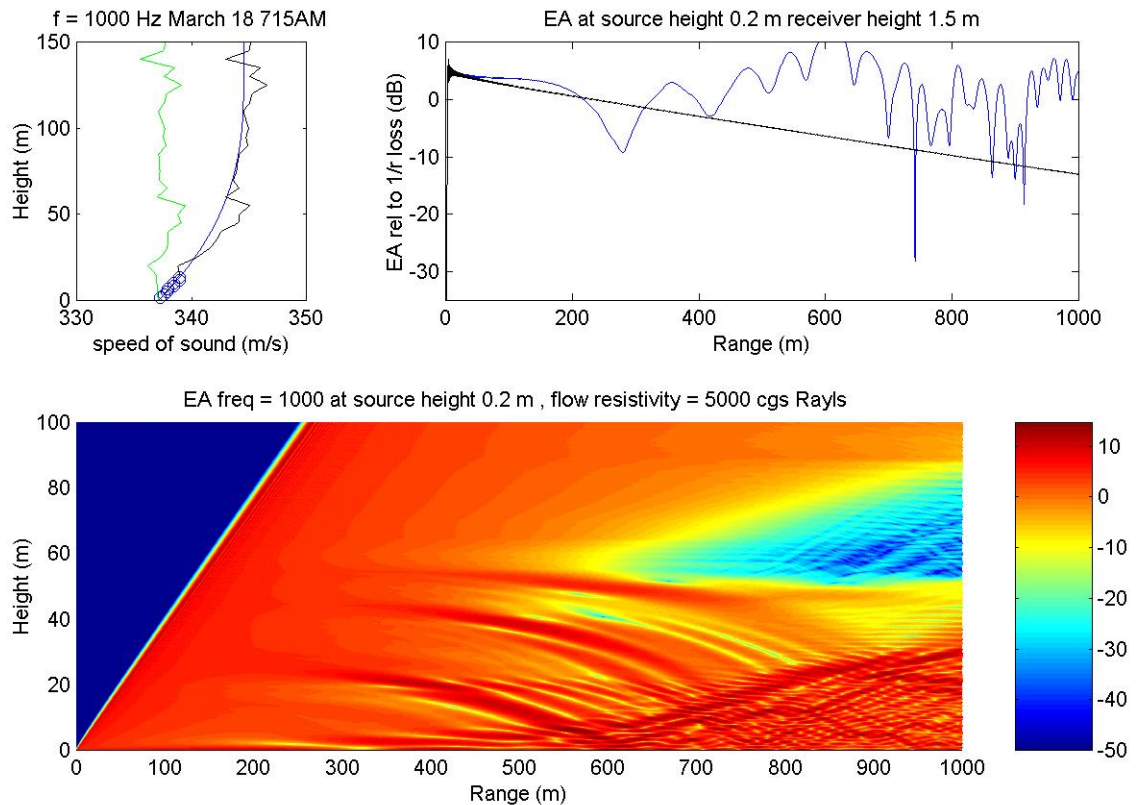


Figure 48. Sample PE Output, Temp and Downwind Condition, 1000 Hz

Upper left: Assumed sound speed profile. Circles are sound speed based on measured temperature and the solid blue line is the sound speed based on the temperature scaling laws. The light green line is the wind speed profile by itself (shifted to fit on scale) and the black line is the combined sound speed profile.

Upper right: PE output at a receiver height of 1.5 m (5 ft). Blue line is PE output while the black line is the “Neutral” case for comparison.

Bottom: Full PE output indicating relative sound levels (red higher, blues lower).

Wind Only, Downwind, 1000 Hz

Figure 49 shows the output at 9:15 AM when the temperature gradient was zero. This case should represent a neutral case or wind dominated case. There are no significant differences from the neutral case until a range of about 800 m and the strongest effects occur beyond 1 km. It is counterintuitive that before the 1 km focusing occurs, the downwind case results in lower sound levels. One would expect downwind conditions to force downward refraction and increased levels. From a close look at the wind speed profile in Figure 49, one observes that there is a slight backflow of wind from the ground up to a height of approximately 15 m. This backflow provides a slight bit of upward refraction before the downward refraction from the wind at 50 m takes over. Such shear flows or counter direction flows are common in the real world and greatly complicate predicting absolute sound levels under realistic conditions.

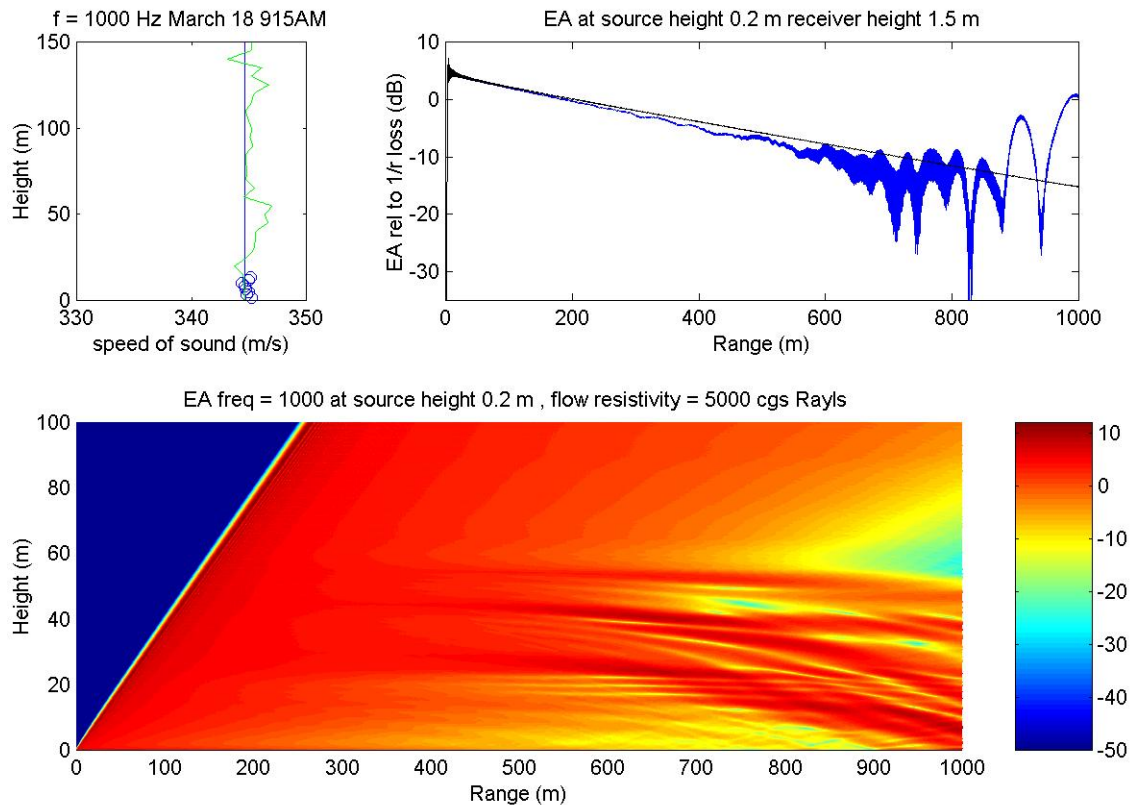


Figure 49. Sample PE Output, Wind Only, Upwind Condition, 1000 Hz
 Upper left: Assumed sound speed profile. Circles are sound speed based on measured temperature at 9:15 AM. The light green line is sound speed profile incorporating the wind speed profile.
 Upper right: PE output at a receiver height of 1.5 m. Blue line is PE output while the black line is the “Neutral” case for comparison.
 Bottom: Full PE output indicating relative sound levels (red higher, blues lower).

Modeling Conclusions

The example PE runs discussed above were combined across frequencies from 63 Hz to 1,000 Hz for each of the five time frames and four meteorological conditions to produce predicted overall levels to compare against measured data. The measured octave band sound levels at Site 1 (near roadway) were used to predict the sound levels at Sites 2-4 and at some additional sites where handheld measurements were performed. The spreading loss from Site 1 to the other sites was estimated using the relationship $15 \times \log(\text{distance})$, which, as discussed above, is a compromise between spherical losses from a point source and cylindrical losses from an infinite line source. This adjusted level was then added to the PE outputs. The PE model accounts for ground and atmospheric absorption losses as well as losses or gains due to atmospheric refraction. The sound levels in each octave band were then combined to predict overall levels.

The results of this exercise for 7:15 AM are summarized in Table 8 and the results for 9:15 AM are summarized in Table 9. The data from Table 8 and Table 9 are shown graphically in Figure 50 and Figure 51. The model outputs are from the Temperature Only case. There is reasonably good agreement between the measurements and the model with the exception of Site 4 at 7:15 AM. The morning sound levels at Site 4 are somewhat volatile. We believe this is

because the temperature effects and wind affects tend to compete so that when the wind changes there can be a substantial change in sound level. The Site 4 Upwind results are also shown in the tables and the figures. The upwind results are closer to the measured levels and we suspect that if the actual wind profile were available, the agreement would be substantially better.

Table 8. Measured and Predicted Octave Band Levels for 7:15 AM March 18 (Results from Temperature Only PE Model)								
Frequency Range	Sound Levels, dBA (A-weighting included in octave band levels)							
	Site 1	Site 2		Site 3		Site 4		
	Meas.	Meas.	PE Model	Meas.	PE Model	Meas.	PE Model	PE Model (Upwind)
Octave Band Levels								
63 Hz	51.8	34.9	41.7	38.5	41.5	36.5	41.3	41.9
125 Hz	60.2	46.1	52.3	43.9	44.8	44.7	52.1	53.1
250 Hz	62.6	47.9	49.7	49.5	46.8	51.7	53.6	53.5
500 Hz	65.0	53.4	51.2	56.9	45.9	59.9	48.7	52.1
1 kHz	76.5	59.8	60.3	61.8	57.2	66.6	59.1	63.5
Overall								
63-1000 Hz⁽¹⁾	77.1	61.8	61.7	63.2	58.2	67.6	61.1	64.5
Full Range⁽²⁾	79.5	63.2		63.9		68.6		
Notes:								
⁽¹⁾ The PE calculation was for the frequency range of 63 to 1000 Hz. Shown are the measured and predicted levels over this frequency range.								
⁽²⁾ Measured A-weighted sound level over full frequency range.								

Table 9. Measured and Predicted Octave Band Levels for 9:15 AM March 18 (Results from Temperature-Only PE Model)							
Frequency Range	Sound Levels, dBA (A-weighting included in octave band levels)						
	Site 1	Site 2		Site 3		Site 4	
	Meas.	Meas.	PE Model	Meas.	PE Model	Meas.	PE Model
Octave Band Levels							
63 Hz	52.0	29.4	33.0	30.9	30.0	35.9	33.8
125 Hz	59.2	37.1	40.3	38.6	37.4	40.7	41.4
250 Hz	62.3	37.6	43.0	38.2	39.8	40.9	44.0
500 Hz	65.3	41.8	44.2	43.5	40.2	43.7	45.5
1 kHz	75.5	45.2	46.6	44.1	38.7	47.1	50.0
Overall							
63-1000 Hz ⁽¹⁾	76.2	47.8	50.2	48.0	45.3	50.1	51.9
Full Range ⁽²⁾	78.5	49.1		48.7		51.0	
Notes:							
⁽¹⁾ The PE calculation was for the frequency range of 63 to 1000 Hz. Shown are the measured and predicted levels over this frequency range.							
⁽²⁾ Measured A-weighted sound level over full frequency range.							

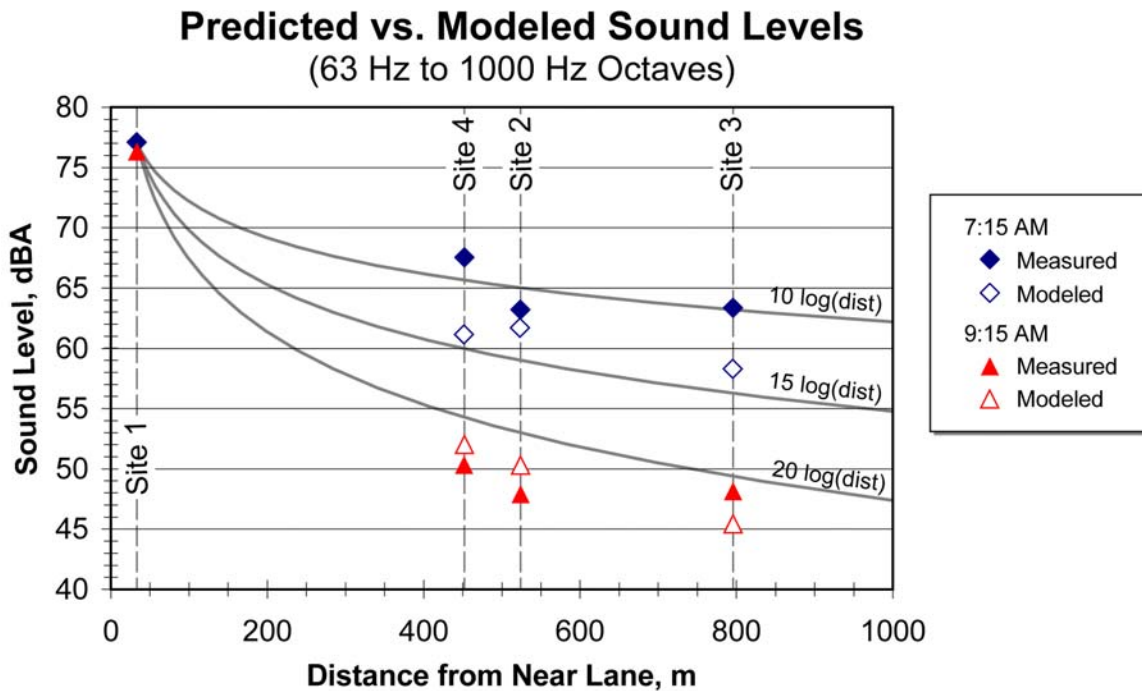


Figure 50. Measured vs. Predicted Levels, March 18, 7:15 and 9:15 AM

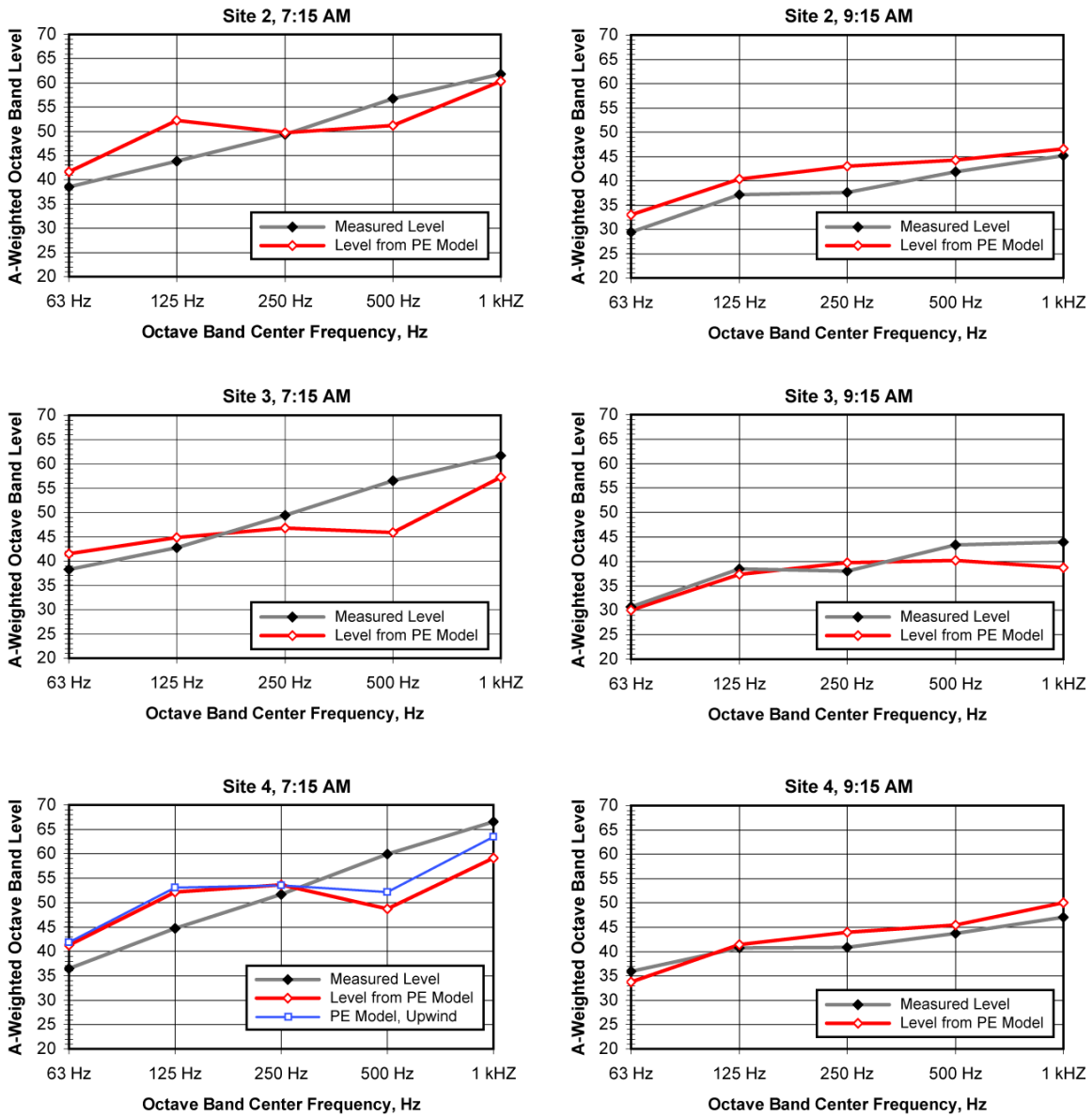


Figure 51. Measured and Predicted Octave Band Levels, March 18, 7:15 and 9:15 AM

Detailed results of the PE models are shown in Appendix C (Figure 96 through Figure 105). These figures indicate that there is a persistent increase in the sound levels in the early morning (6:00 AM, 7:15 AM) of approximately 10 to 15 dB in both the data and the model predictions. The model predicts fluctuations of 5 dB or so. The model predicts levels from an instantaneous snapshot of meteorological conditions. In the real world, fluctuations will be spatial (due to interference patterns) and temporal due to wind fluctuations. The key point is that the fluctuations shown in the figures in Appendix C show sound level fluctuations of the same magnitude as observed in the field measurements lending credence to the conclusion that the sound level patterns observed in the measurements were primarily caused by refraction.

Note for instance the varying sound levels observed using a handheld meter on 86th Street at 6:00 AM and 7:15 AM on the March 18. These locations were at the same range from the highway as Sites 2 and 3, but at different locations. They exhibit different levels which might be due to either local effects such as the proximity to an individual house, or due to meteorological

variations. Also at 6 AM, these data points were approximately 5 dB above the levels predicted by temperature alone as was the level at Site 2. However, the temperature + wind profile indicates a peak at the right level at a range halfway between these two measurement sites. Certainly a slightly different wind profile than the one assumed could have produced a local peak at either or both of these locations.

It should be noted that the Site 4 data, which is east of the Pima Freeway, shows some marked variability with a dramatic swing between 6:00 AM and 7:15 AM on March 18. Given that the dominant early morning wind flow is east to west, west of the highway the wind and temperature effects are cumulative and east of the highway they are in competition. A large portion of the measured data indicated that while levels east of the highway are indeed elevated with respect to neutral conditions, they are not as consistently elevated as those west of the highway. This would suggest a temperature inversion that is intermittently cancelled by a wind effect. If the wind gusted sufficiently, it might neutralize the downward effects of the temperature and result in the lower sound level as observed at 6 AM.

The wind profile utilized has a slight backflow near the ground which the PE model indicates is capable of creating a sharp localized increase in sound near the highway as seen at 7:15 in the model and data. Without accurate and instantaneous wind speed measurements it is not feasible to predict absolute real time or site specific levels. However, by choosing reasonable profiles, the data presented here indicates that mean levels and typical fluctuations about the mean levels can be predicted.

The 8:15 AM period is during the transition from temperature inversion and neutral temperature effects. On the both March 18 and 19, sound levels at 8:15 AM were lower than at 6:00 AM and 7:15 AM levels and were approaching the levels predicted with no meteorological effects.

The temperature data indicates that there should be minimal temperature effects around 9:15 AM as a zero, or near zero, temperature gradient is present. On the March 18, the 9:15 data coincides with the predictions for no meteorological effects. On the March 19, the 9:15 data is elevated compared to the no meteorological prediction. At this time frame, the wind effects, which are unknown, were likely to be dominant. The prediction by the PE model of a 10 dB increase at 1 km (0.6 mi) for our assumed profile suggests that a slightly different wind profile could easily generate the increase above neutral conditions seen in the March 19 data.

The PE model at 3 PM indicates that a massive amount of upward refraction should result in A-weighted freeway noise being up to 20 dB lower than under neutral conditions. Even during the March 2004 measurements before the quiet pavement had been installed, the levels of freeway noise at the community measurement sites was much lower than in the early morning period although not 20 dB below the neutral condition levels. This is because turbulent scattering, which is not part of the PE model, scatters some sound into the shadow region so that it is not possible to get as strong a shadow effect as suggested by the PE model. Also, under mid-day lapse conditions, the background noise was closer to the levels of the freeway noise making it difficult to observe sound levels 20 dB below the neutral conditions.

5.4 LINE SOURCE MODEL

One of the limitations of the PE code used here is that it is two dimensional, which means that it cannot accurately represent a line source in a three dimensional space. We have used the two dimensional PE code to approximate a partial line source by:

1. Dividing the roadway into 20 segments, each 15 m in length. This is illustrated in Figure 52.

2. Performing a PE calculation for each roadway segment using the receiver distances of r_1 , r_2 , r_3 , etc. as shown in Figure 52.
3. Using the PE result for each segment to approximate the Transmission Loss between source and receiver. Each segment is assumed to generate the same sound power.
4. Logarithmically combining the levels for the 20 segments to obtain a total level at the receiver.

Since the actual source level at the road itself is unknown, the values of the octave band noise levels at Site 1 were used as a baseline and adjusted uniformly until the predicted level at Site 1 matched the measured level at site one. That is, the model provides a relative description of the propagation from Site 1 to Sites 2, 3, and 4. This approach removes the need for heuristic arguments about whether the geometric spreading loss should have been 10, 15, or 20 times log distance and simply estimates the individual level contributions that should be combined to determine the level in the field.

The results of this process are shown in Figure 53. As expected, there is substantially less fluctuation than with the point source model. The overall conclusions are that the partial line source model:

- Reasonably predicts the field measurements and supports the previous observations regarding the influence of meteorology on increases in noise levels.
- Predicts that downward refraction on March 18 and 19 was sufficient to increase morning A-weighted sound levels at distances of 500 m (1,600 ft) by 9 dB.
- Indicates that downward refraction effects were greatest at distances greater than 200 m (660 ft) from the roadway. Sound levels are predicted to increase by about +1 at distances of 40 to 100 m (130 to 330 ft) and +2 at distances of 100 to 200 m (330 to 660 ft).
- Predicts that upward refraction during the mid-day period caused sound level to monotonically decrease compared to the neutral atmospheric condition. The predicted levels are -3 dB at 100 m (330 ft), -5 dB at 200 m (660 ft), and -12 dB at 500 m (1,600 ft). However, we believe these are greater than will actually occur because scattering and other effects moderate the upward refraction effects.

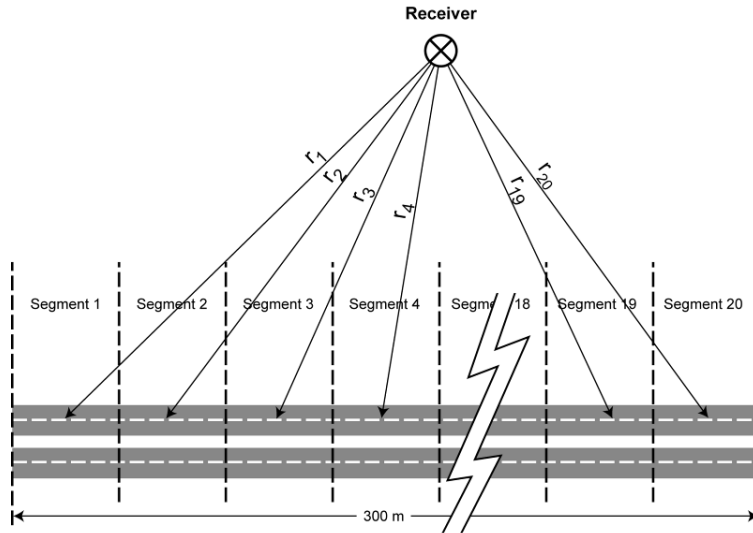


Figure 52. Partial Line Source Model Constructed from 2-D PE Model

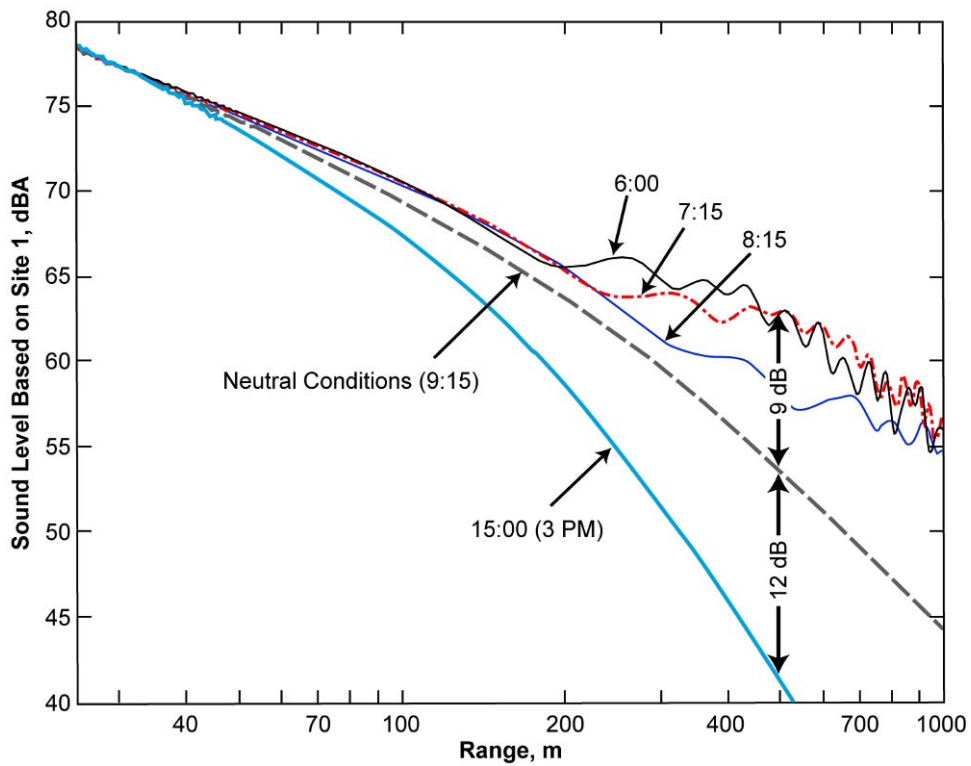


Figure 53. Results of Partial Line Source Model, March 18, 2004 Conditions

6. CONCLUSIONS

This study has involved a detailed review of the literature relevant to sound propagation in general and atmospheric effects on sound propagation in specific, detailed noise and meteorological measurements east and west of the Pima Freeway between Indian School Road on the south and Chaparral Road on the north, and use of the Parabolic Equations numerical procedure to study how variations in the atmospheric conditions affect sound propagation. Additional aspects of the study that were not part of the original scope were a pilot study of basic acoustic models to predict how different pavement parameters are likely to affect noise generation and community noise measurements before and after installation of an asphalt rubber friction course on the Pima Freeway intended to reduce community noise levels.

This section presents a concise summary of the conclusions that we have drawn from the efforts of this study along with some suggestions of fruitful areas for additional research efforts.

6.1 ATMOSPHERIC EFFECTS ON SOUND PROPAGATION

The overall conclusions of the study on how atmospheric conditions affect long distance sound propagation in the Phoenix valley are:

1. The nighttime inversion conditions that are common from October through March result in increases in A-weighted sound levels of 5 to 8 dB at distances greater than 400 m (1/4 mi) from freeways. Similar effects probably occur in the warm weather months as well.
2. The computer modeling indicates that refraction effects are relatively modest, on the order of 2 to 4 dB, out to distances of 200 m (650 ft) from the noise source. After 200 m, there is a relatively rapid onset of refraction effects and at distances greater than 300 m (1000 ft) the refraction effects are often on the order of 10 dB. This is an important conclusion since most highway noise analyses focus on noise sensitive land uses a few hundred feet from the highway, distances at which refraction effects are relatively modest. Additional measurements to verify that the accuracy of the PE model on this topic would be a valuable topic for future studies.
3. Daytime lapse conditions often result in A-weighted sound levels that are 5 to 10 dB lower than would be the case under neutral atmospheric conditions. Based on the results of the PE models, the reduction due to lapse conditions steadily increases with distance from the roadway. The computer model we used indicates that lapse conditions can reduce A-weighted sound levels by more than 20 dB at distances greater than 1 km (0.6 mile). This model does not include effects of turbulence, which should not cause significant errors when there is sound enhancement due to downward refraction, but may result in a significant overstatement of the noise reduction due to upward refraction. We believe that the maximum noise reduction relative to neutral atmospheric conditions is more likely to be in the range of 5 to 10 dB.
4. The nighttime down-slope drainage flows off the mountain ranges surrounding the Phoenix valley cause localized focusing and de-focusing of sound levels. These effects can exhibit consistent patterns over several days or can be isolated events occurring over a period of minutes. Focusing/de-focusing effects on the order of -10 to +4 dB were observed during the measurements. The PE computer model, which proved to be a valuable tool for investigating refraction effects, could be used to investigate specific focusing effects if it were possible to obtain instantaneous wind speed and direction profiles up to elevations of 200 to 300 feet.
5. The down-slope flows apparently generated air jets at elevations greater than about 20 m (65 ft). The air jets do not cause ground level air flows, which means that variations in the air jets that are unobservable at ground level can cause significant changes in the sound levels.

Means for estimating the locations and speeds of air flows are something that should be considered for any future study of atmospheric effects on sound propagation. There are some sophisticated systems using sonar and lasers to measure wind and temperature as a function of elevation (e.g., SODAR, Lidar). Less sophisticated approaches would include tethered balloons and smoke streams. Simply observing the dispersion of a smoke stream can provide information on wind speed and direction as a function of elevation.

6. Sound level variations under inversion conditions appear to be greatest at locations that are upwind relative to the down-slope flows.
7. Community sound levels are driven by a combination of the fluctuations in traffic volumes and speeds plus the many propagation effects, especially refraction effects. At distances greater than 200 to 300 m from the roadway, refraction effects will tend to increase noise levels by 5 to 10 dB from about 1 hour before sunset to 2 hours after sunrise. During the mid-day period, sound levels will tend to decrease by 0 to 10 dB due to upward refraction. During the summer, sunrise occurs as early as 5:30 AM and inversion conditions breakup before traffic reaches mid-day volumes. This means that the sound level increases due to inversion conditions would be less noticeable.
8. Any location where there is a consistent pattern of inversion conditions at night and lapse conditions during the daytime is likely to experience relatively high levels of traffic noise from the time the sun starts to set until a couple of hours after sunrise. This means that many cities in the southwest, such as Las Vegas, Albuquerque, Los Angeles, Fresno, and Sacramento, are likely to have regions near freeways where inversion conditions cause relatively high noise levels on a fairly consistent basis.
9. The potential for inversion or lapse conditions is an important issue to be aware of when making noise measurements at any location except within about 200 m (650 ft) from the noise source. At distances greater than this, the sound level change from lapse to inversion conditions could be as much as 20 dB.
10. The measurement data from the meteorological tower indicates that simple two-position temperature measurements can be sufficient to show whether an inversion or lapse condition exists and may be sufficient to indicate the strength of the condition. This is an area where further research would provide valuable guidance on procedures for measuring temperature gradients. It seems reasonable that temperature gradient measurements will need to be a standard feature of community noise measurements any time that the major noise source is more than 200 m from the measurement position.

6.2 PAVEMENT PARAMETERS AFFECTING NOISE

The pavement parameter study was a pilot study to see how much information on the manner that important pavement parameters affect noise generation could be gleaned from models derived from acoustic principals and previously published literature. The overall conclusion is that the quietest pavements will be very smooth in the macro and mega texture ranges, be highly porous with about 25% voids, have a thickness of 1 inch or more, be self-cleaning so the porosity does not change, have a non-stick surface that minimizes stick-snap, and have a friction characteristic that minimizes stick-slip. Following is a more detailed summary of our observations and conclusions:

- **Propagation over an elastic/porous surface:** The modeling shows a substantial potential benefit from enhanced acoustical absorption properties for porous pavements. The modeling only looked at propagation over a porous pavement. Based on the modeling, we conclude the following:

1. **Thickness:** Increasing porous layer thickness will reduce the peak absorption frequency and broaden the range of effectiveness.
 2. **Resistivity:** Increasing flow resistance will tend to broaden the range of effectiveness. With low flow resistance, the propagation loss will have strong peaks. As the resistivity increases, the peaks flatten out.
 3. **Porosity (% Voids):** Increasing the percent voids will tend to increase the absorption.
 4. **Tortuosity:** The tortuosity (void shape factor) mainly affects the peak frequency of the absorption coefficient.
 5. **Multiple Layers:** A couple of cases were run to test the effect of having multiple porous layers. For the test cases, the extra layer provided only small benefits compared to a single layer of the same thickness as the two layers.
- **Radiation from pavement:** The modeling indicates that sound radiation from the pavement is probably small compared to the radiation from the tire casing.
 - **Pavement stiffness:** There is no indication that pavement stiffness affects radiated sound levels.
 - **Pavement texture:** The modeling tends to support the empirical observations that macro texture on the order of 3/4" and greater will affect sound levels. Averaging over the contact patch area tends to diminish the effects of small wavelength texture at least in terms of harmonic forces driving the tire.
 - **Air pumping:** We only took a quick look at modeling of air pumping noise. Intuitively, we expect an increase in porosity to reduce noise by increasing the effective cavity size, at least when tire and pavement pores line up. However, the available modeling indicates that an increase in porosity could increase the effective number of cavities and the effective cavity volume displacement, both of which would be expected to increase noise levels. Based on the available data, we believe that the net effect of increasing porosity will be reduced noise from air pumping.

6.3 MEASURED EFFECTS OF ARFC PAVEMENT

The noise measurements before and after resurfacing the Pima Freeway with ARFC showed that A-weighted sound levels were consistently reduced by 8 to 10 dB both at the close-in and community measurement sites. The effects were almost entirely at frequencies of 500 Hz and higher. Before the ARFC, the sound level spectrum was dominated by sound in the 630 to 3000 Hz 1/3 octave bands. The spectrum was much more evenly balanced after the ARFC. The reduced sound levels were very evident at all of the measurement sites and a number of residents commented to us how pleased they were with the lower community sound levels. The more balanced spectrum also improved the sound "quality" and reduced the annoyance characteristic of the noise. This improved sound quality was evident at the freeway shoulder. The improved sound quality was less evident at the community sites because, with the reduced sound levels, the traffic noise often was no longer the dominant noise source.

APPENDIX A. PHOTOGRAPHS OF NOISE MEASUREMENT SITES



Figure 54. Site 1 Looking East Toward Freeway



Figure 55. Site 1 Looking Northeast



Figure 56. Meteorological Tower at Site 2 (8701 W. Highland Ave.), Looking Southwest



Figure 57. Site 2 (8701 E. Highland Avenue) Looking West



Figure 58. Short-Term Measurement in Front of Site 2 (8701 E. Highland Avenue) Looking East



Figure 59. Site 3 (8547 E. Highland Avenue) Looking East Toward Pima Freeway



Figure 60. Site 3 (8547 E. Highland Avenue) Looking Southwest



Figure 61. Short-Term Measurement in Front of Site 3 Looking East



Figure 62. Site 4 (Tribal land off 92nd Street), Looking West Toward Pima Freeway



Figure 63. Site 4, Looking Southwest Toward Indian School Road Overpass

APPENDIX B. NOISE MEASUREMENT RESULTS

B.1 ONE-MINUTE LEQ VALUES

1-Minute Leqs, March 8-14, 2004

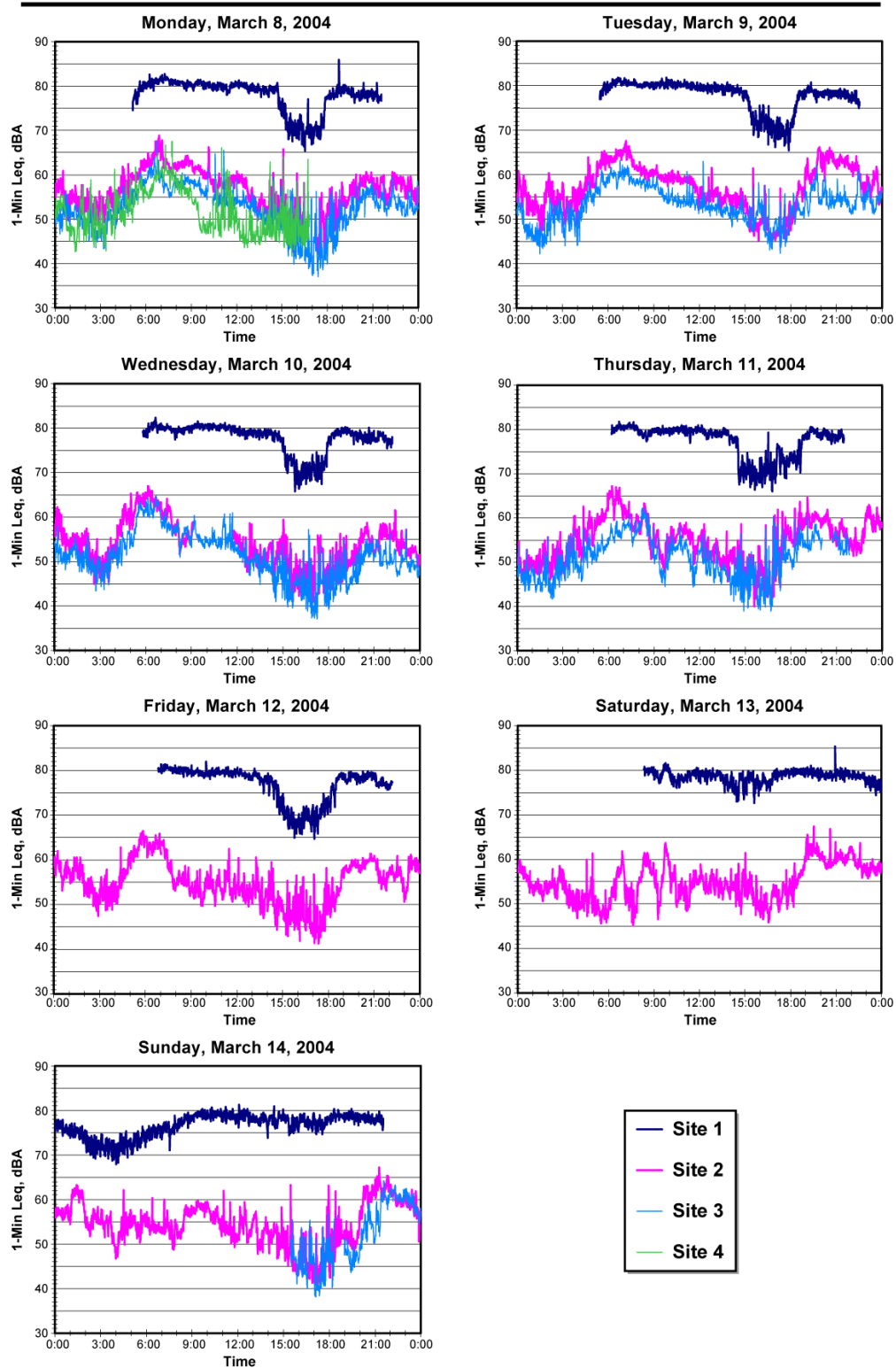


Figure 64. One-Minute Leq Data, March 8-14, 2004

1-Minute Leq, March 15-22, 2004

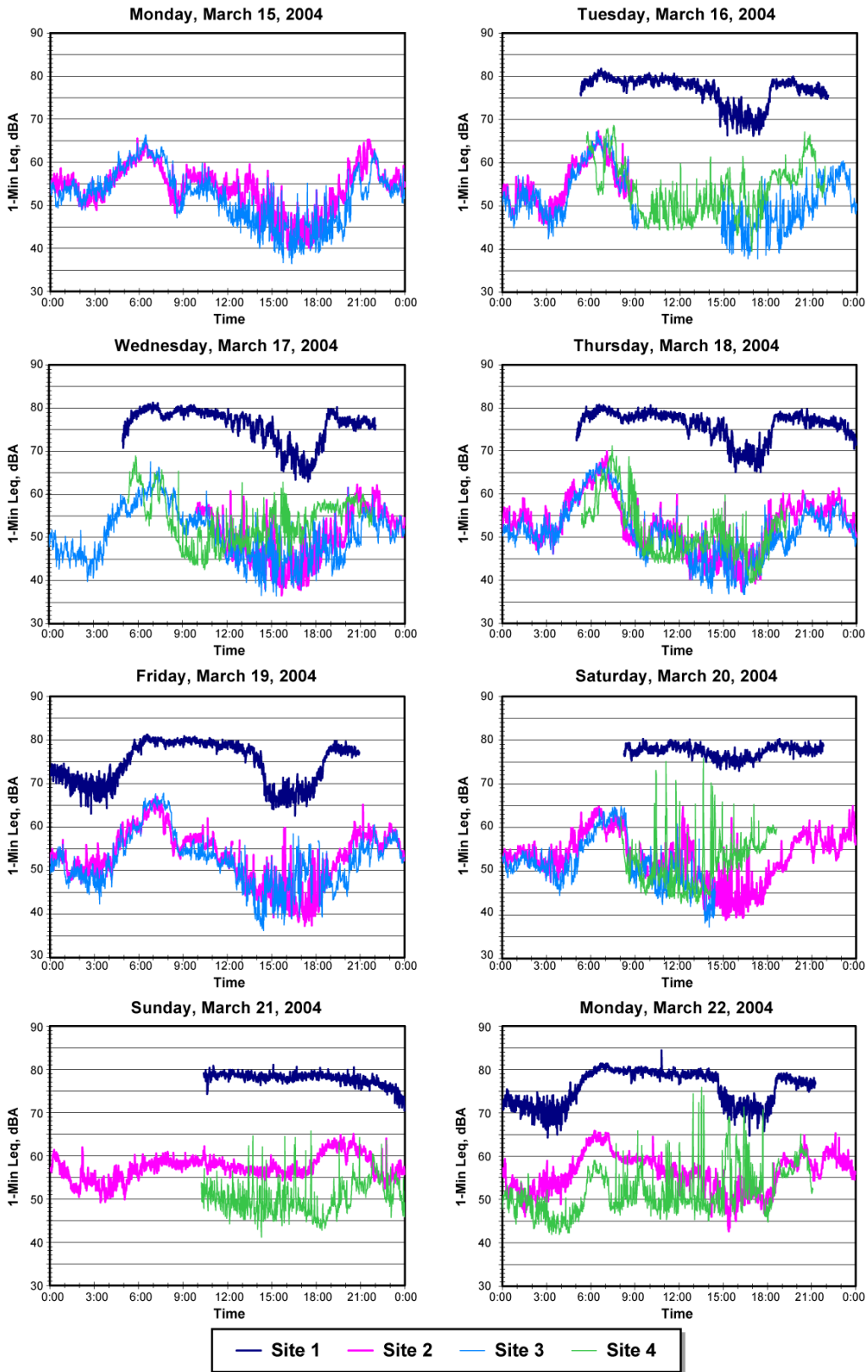


Figure 65. One-Minute Leq Data, March 15-22, 2004

1-Minute Leqs, October 17-23, 2004

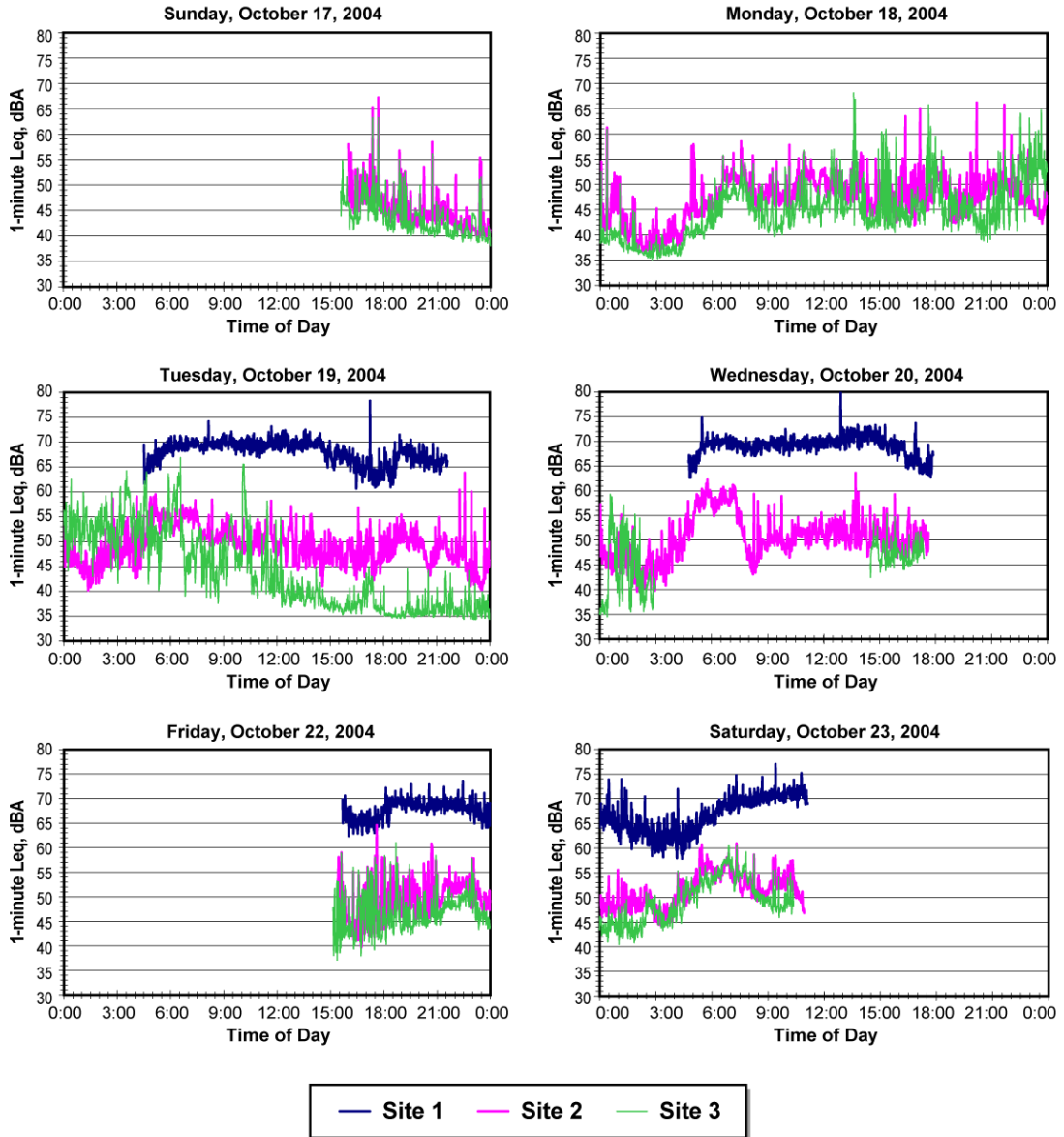


Figure 66. One-Minute Leq Data, October 17-23, 2004

B.2 15-MINUTE LEQ VALUES

15-Minute Leqs, March 8-14, 2004

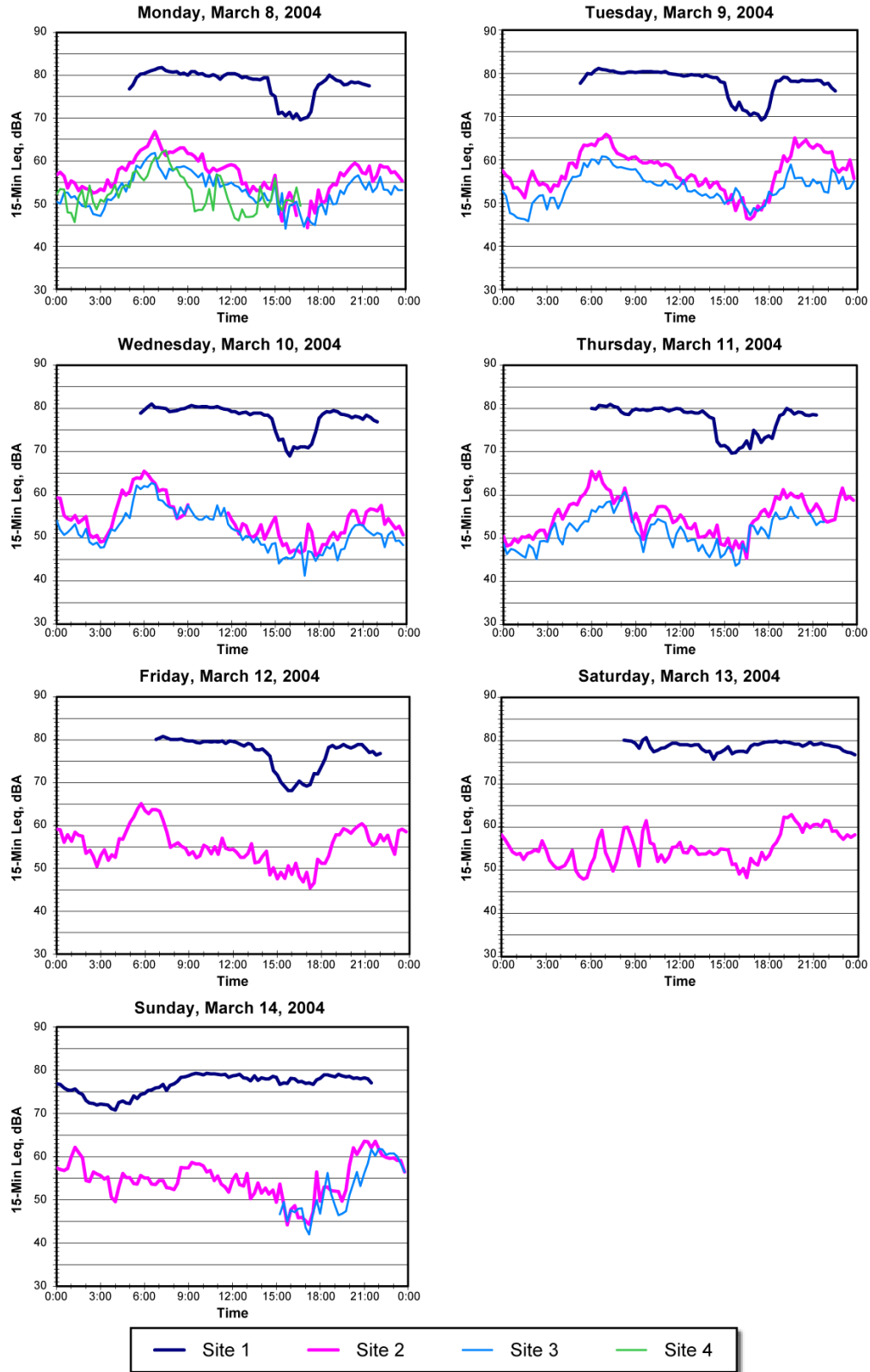


Figure 67. 15-Minute Leq Data, March 8-14, 2004

15-Minute Leqs, March 15-22, 2004

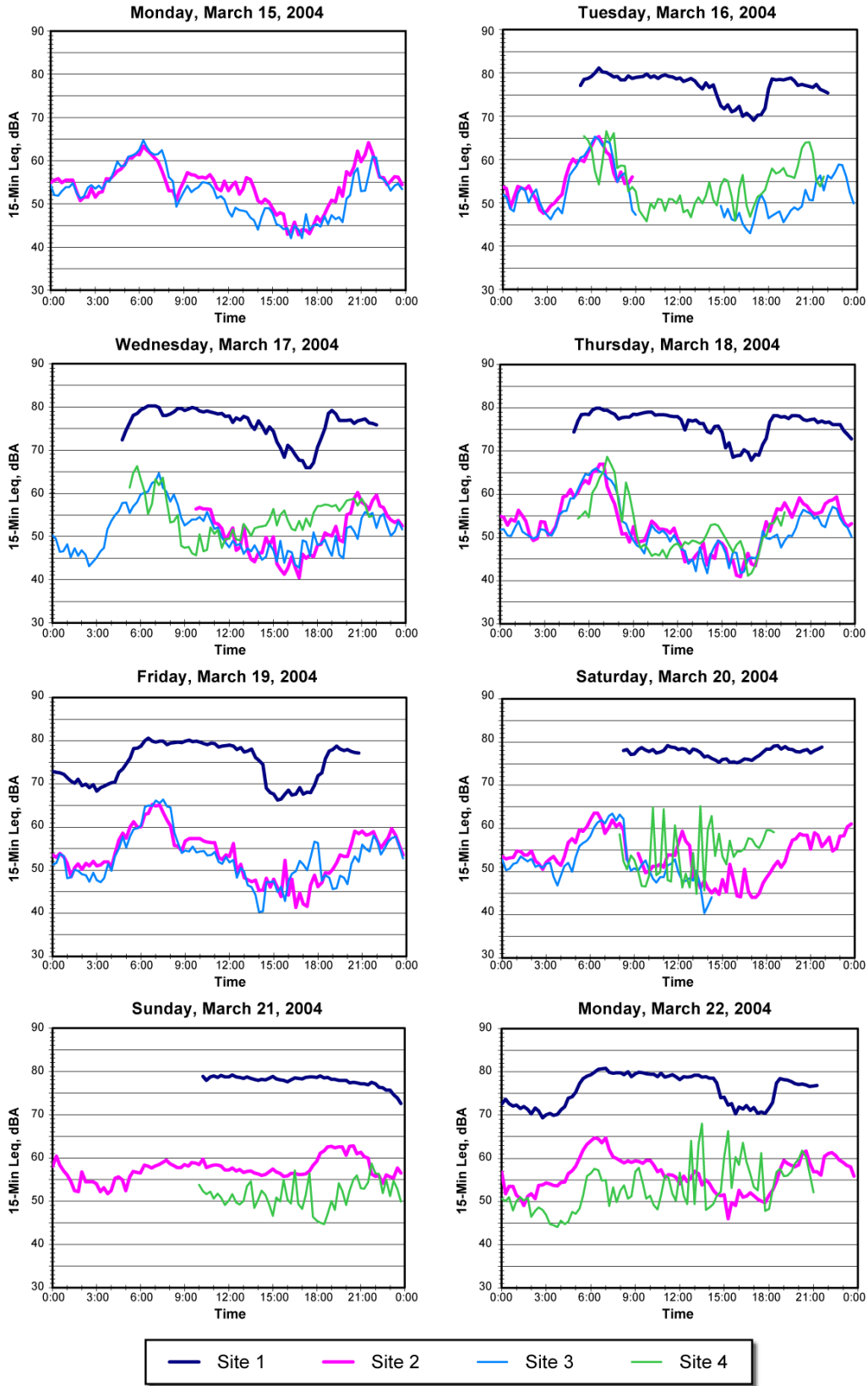


Figure 68. 15-Minute Leq Data, March 15-22, 2004

15-Minute Leq, October 17-23, 2004

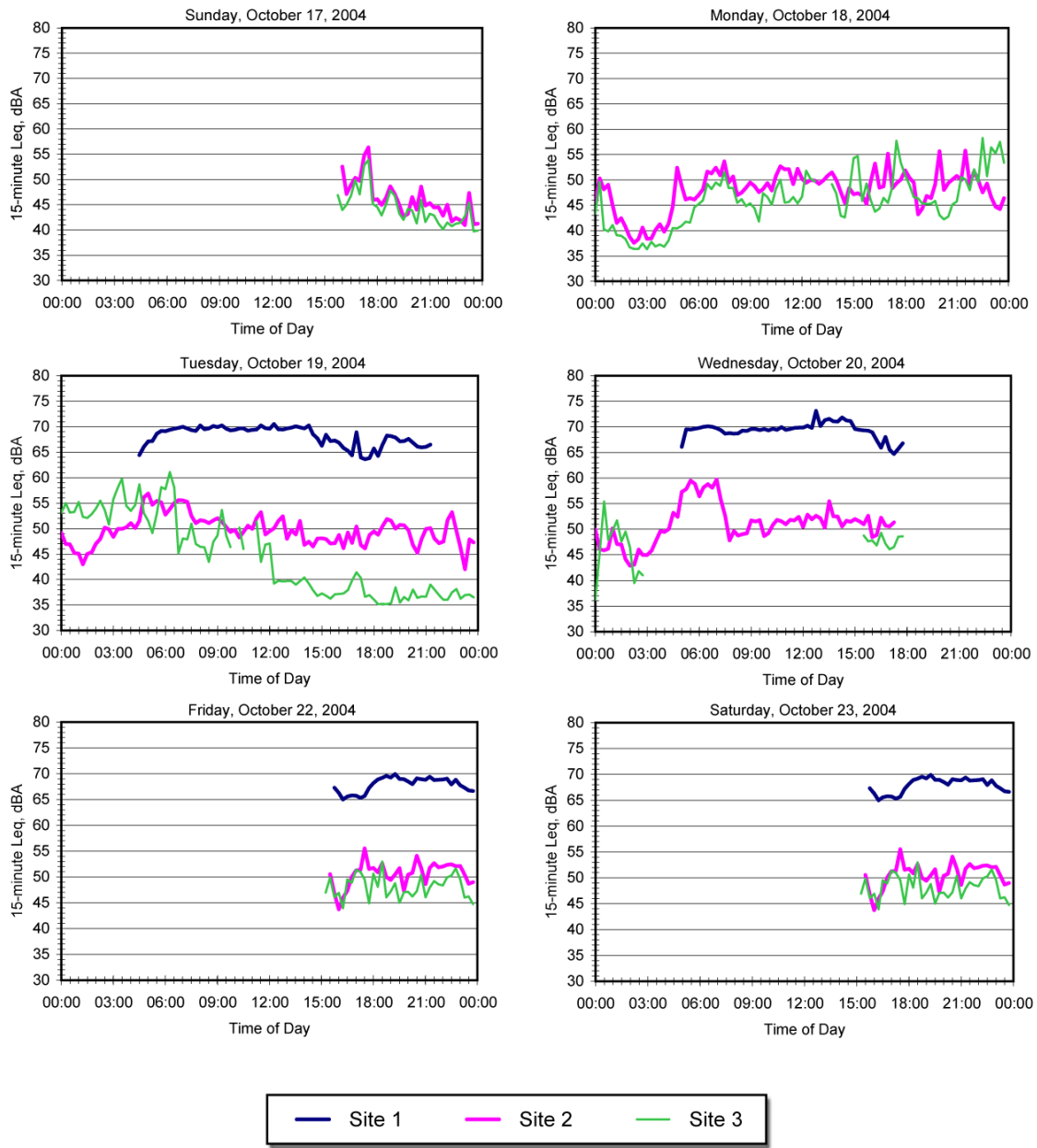


Figure 69. 15-Minute Leq Data, October 17-23, 2004

B.3 1/3 OCTAVE BAND SPECTRA, 6 AM TO 12 PM

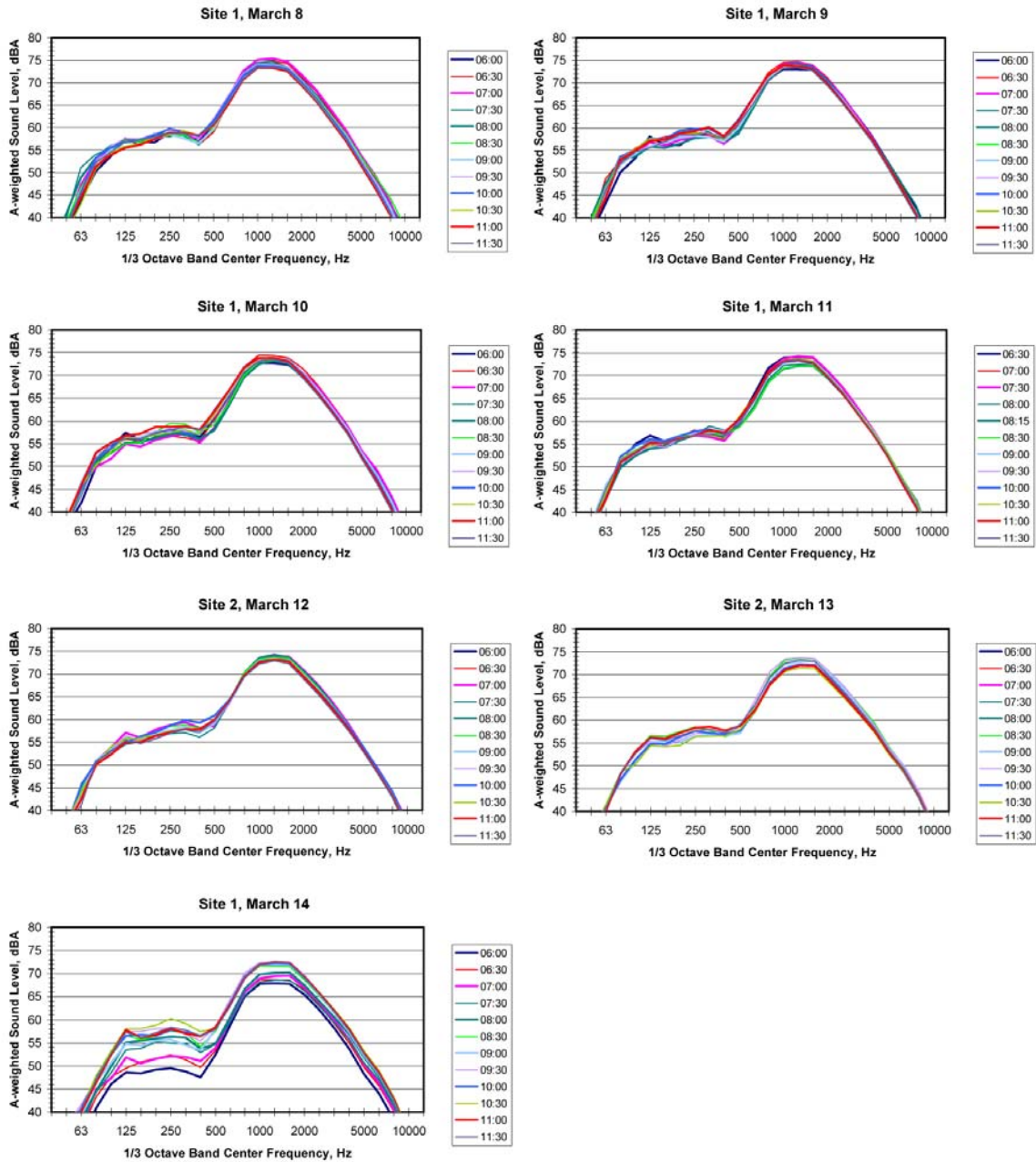


Figure 70. 1/3 Octave Band Spectra, Site 1, March 8-14, 2004

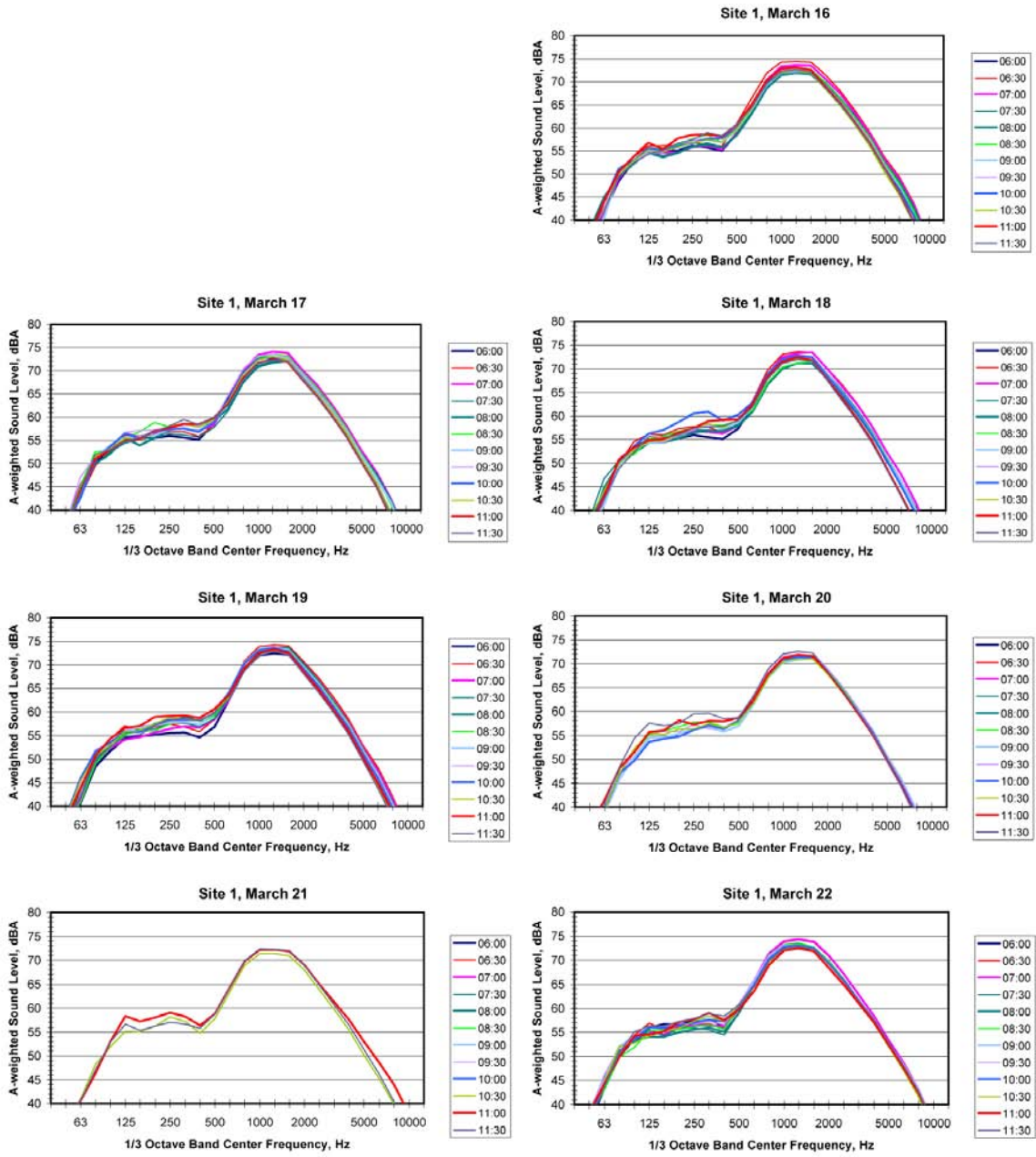


Figure 71. 1/3 Octave Band Spectra, Site 1, March 16-22, 2004

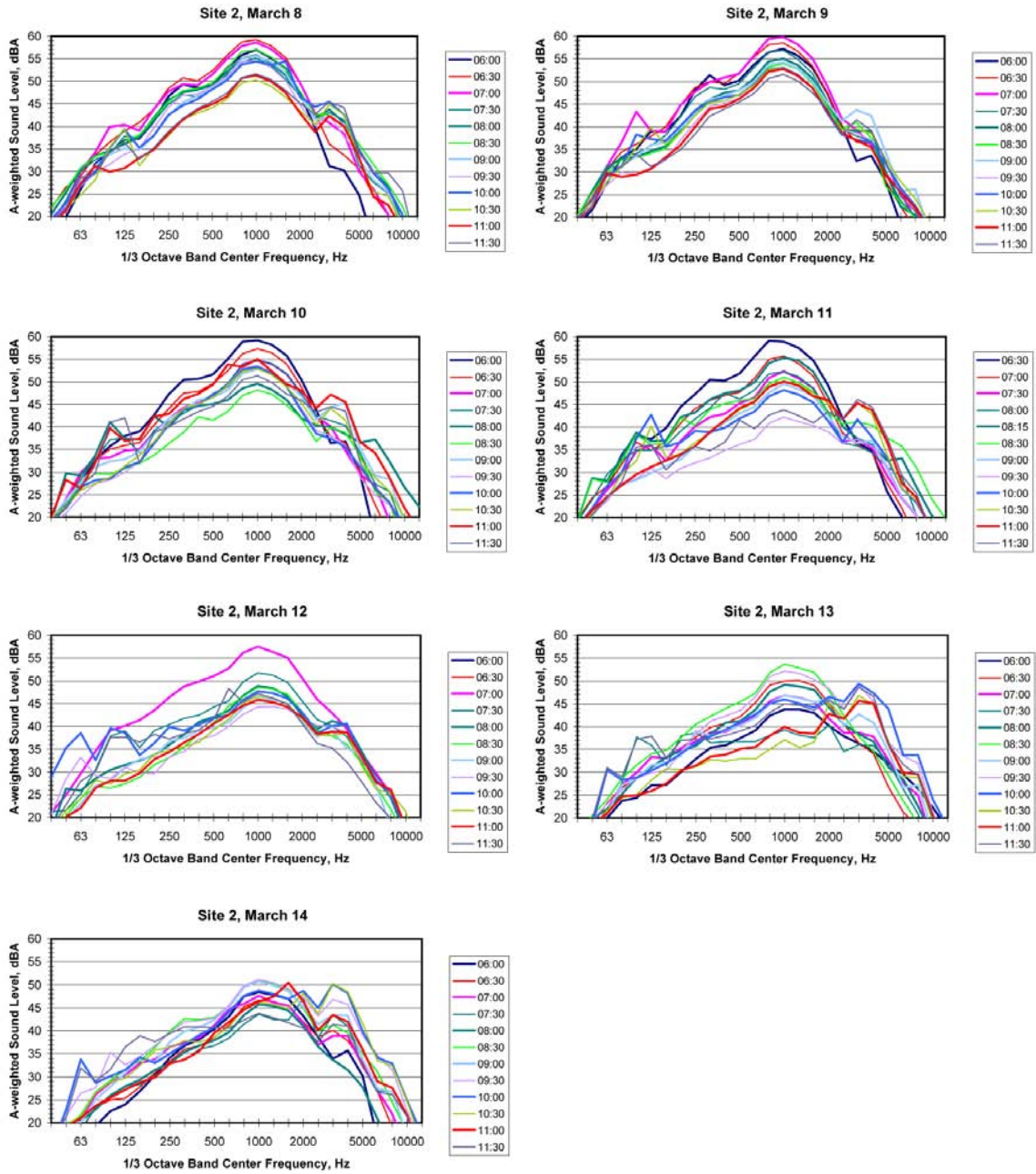


Figure 72. 1/3 Octave Band Spectra, Site 2, March 8-14, 2004

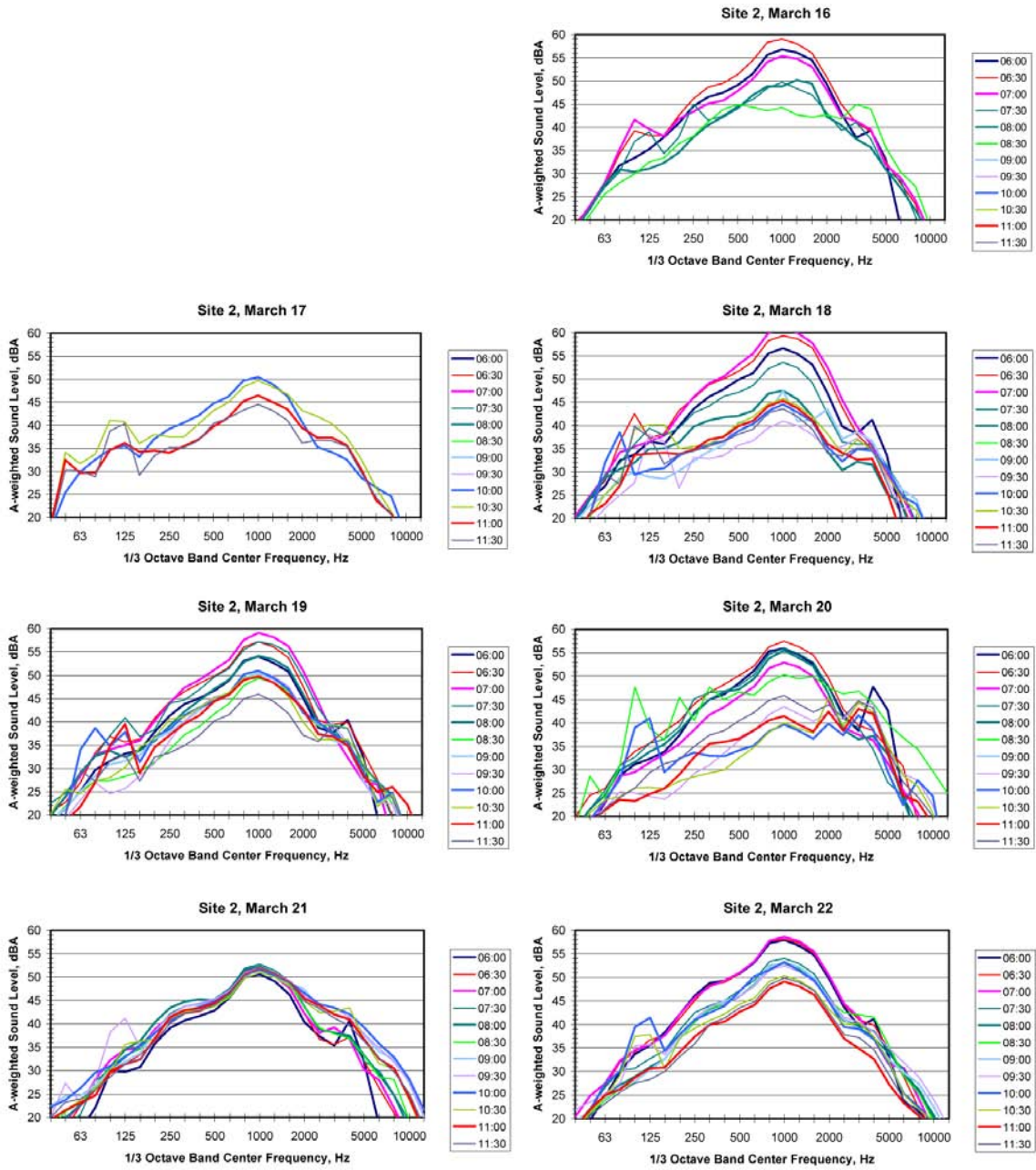


Figure 73. 1/3 Octave Band Spectra, Site 2, March 16-22, 2004

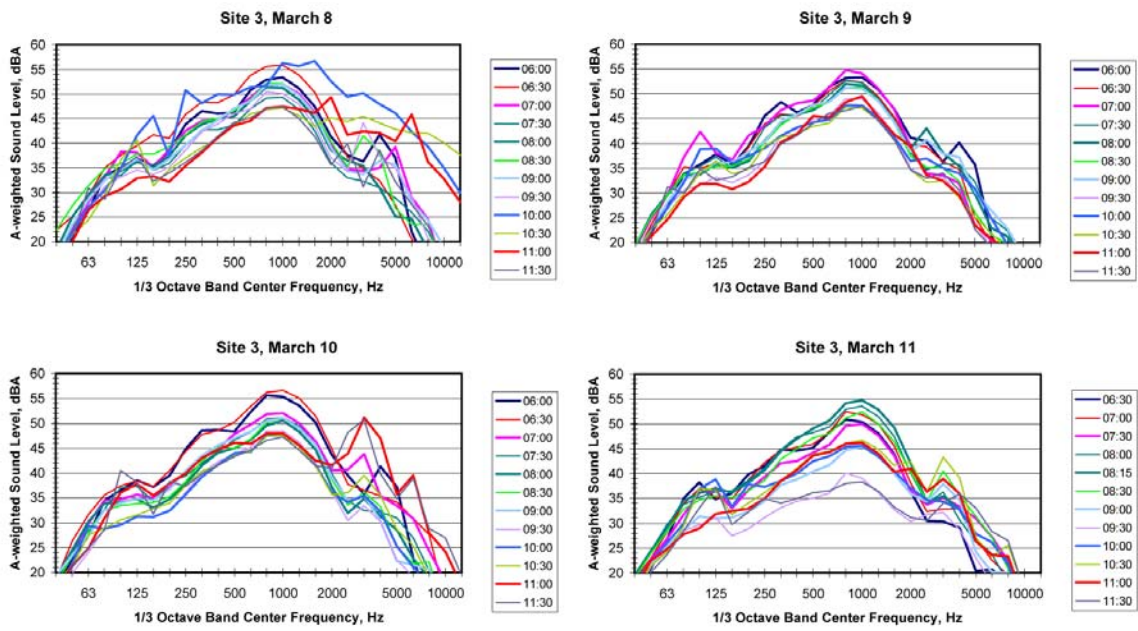


Figure 74. 1/3 Octave Band Spectra, Site 3, March 8-11, 2004

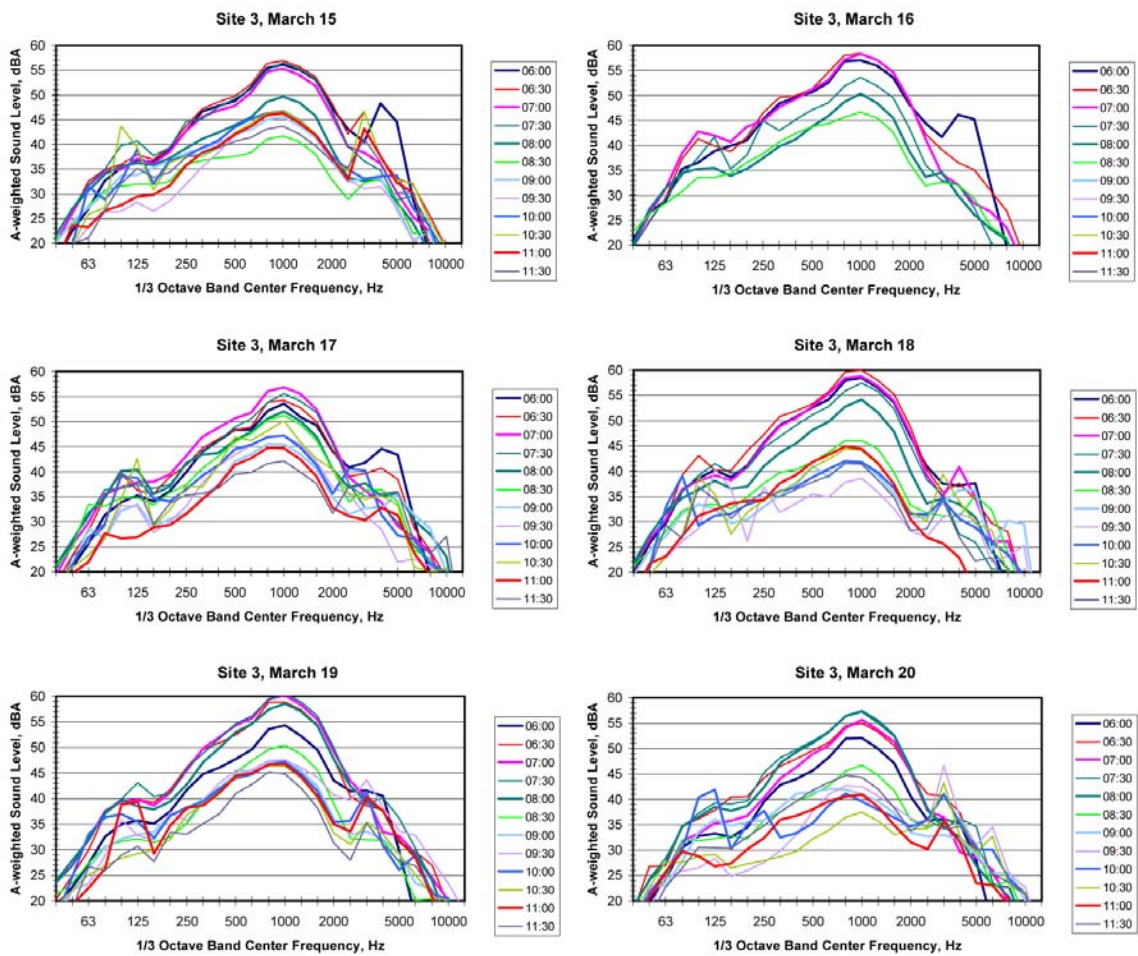


Figure 75. 1/3 Octave Band Spectra, Site 3, March 15-20, 2004

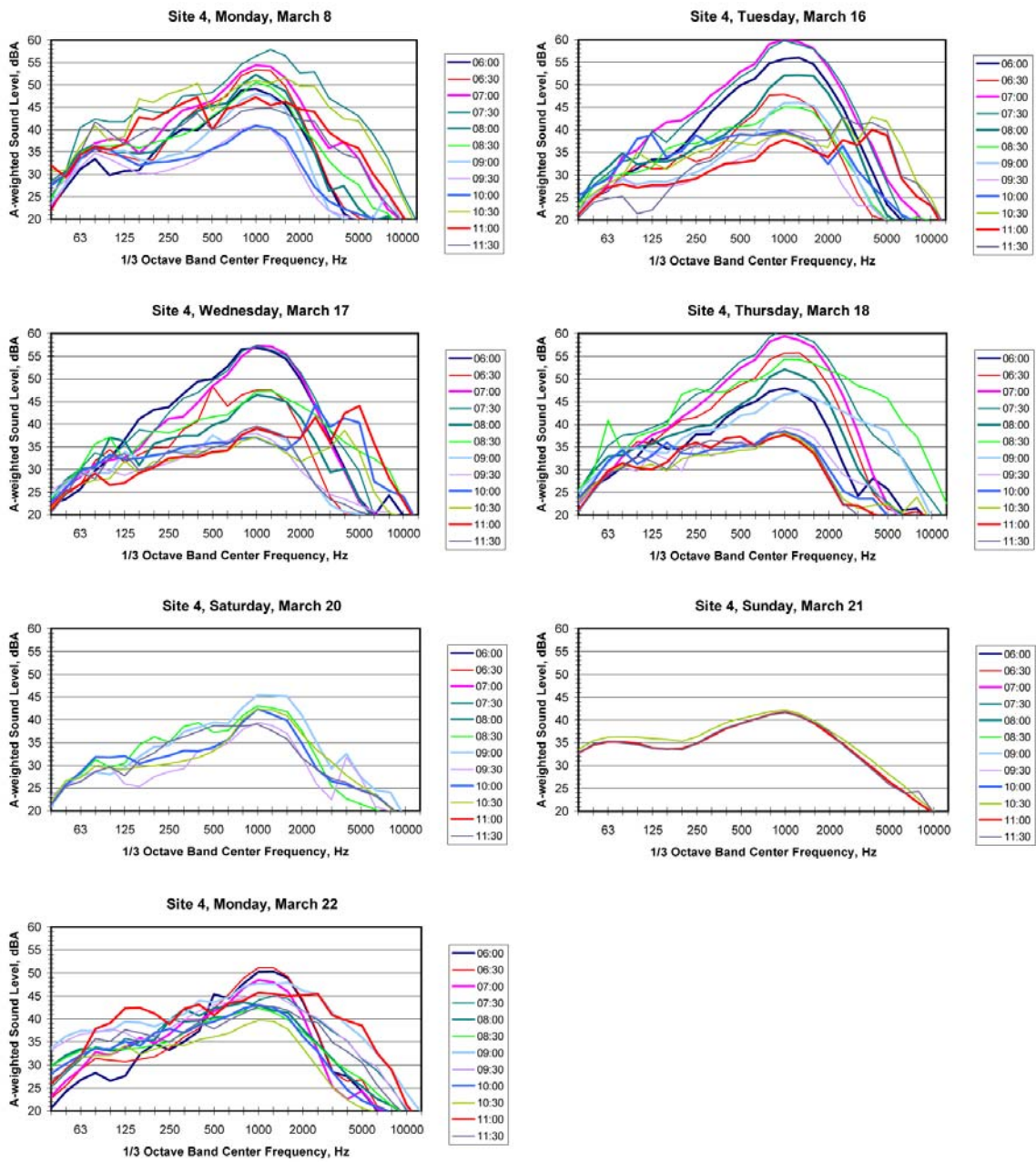


Figure 76. 1/3 Octave Band Spectra (15-min Leq), Site 4, March 2004

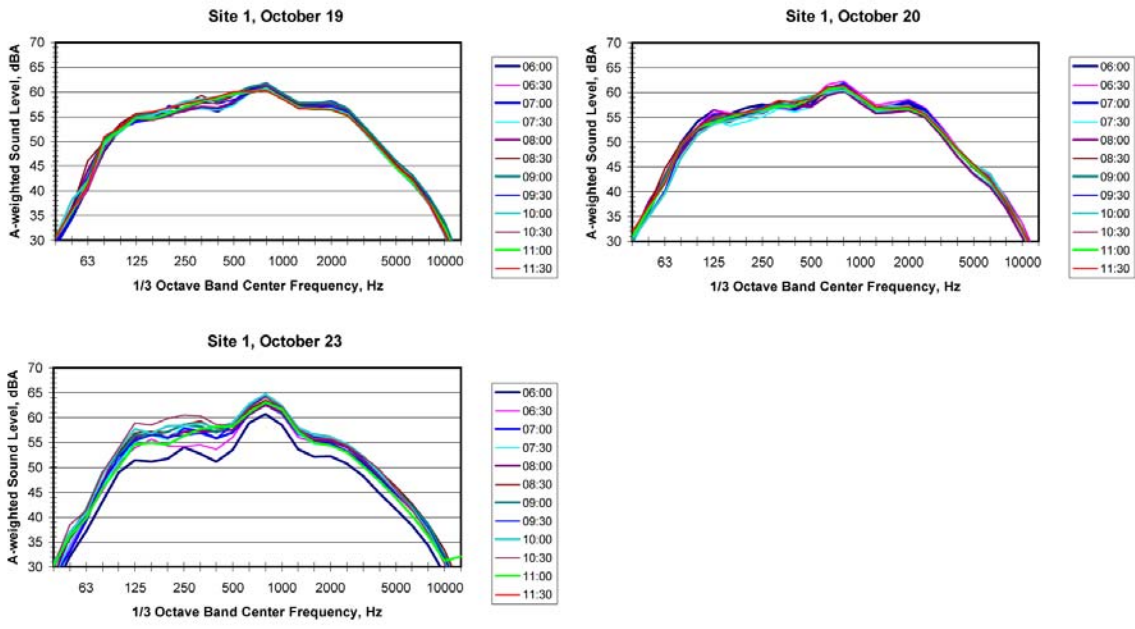


Figure 77. 1/3 Octave Band Spectra (15-min Leq), Site 1, October 2004

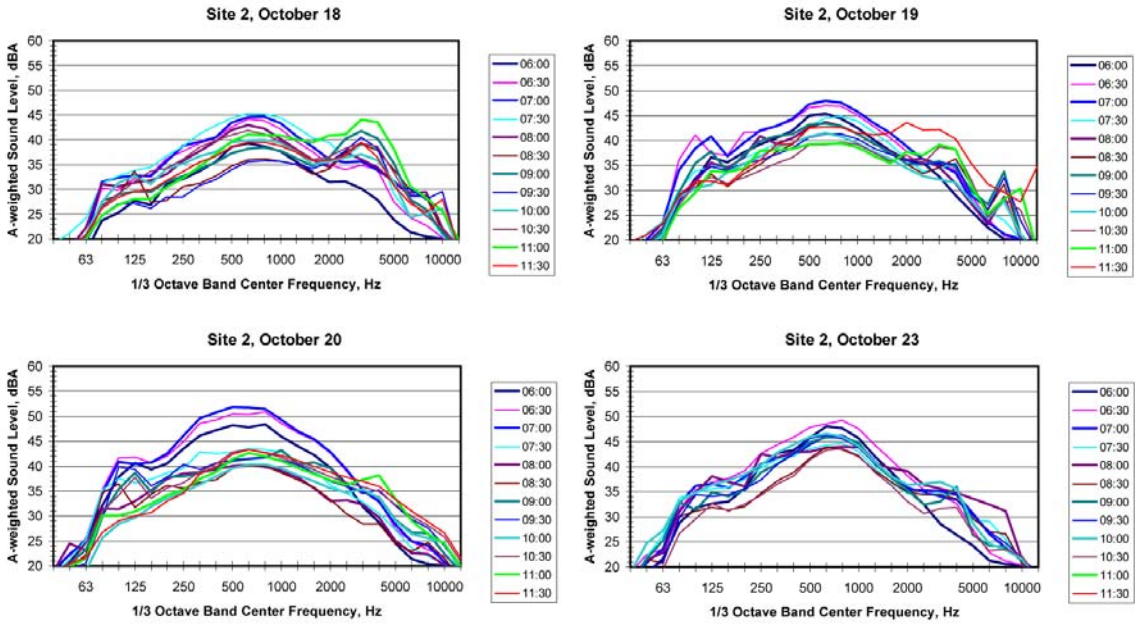


Figure 78. 1/3 Octave Band Spectra (15-min Leq), Site 2, October 2004

B.4 SPECTROGRAMS, WEEKDAYS, 5 AM TO 11 AM

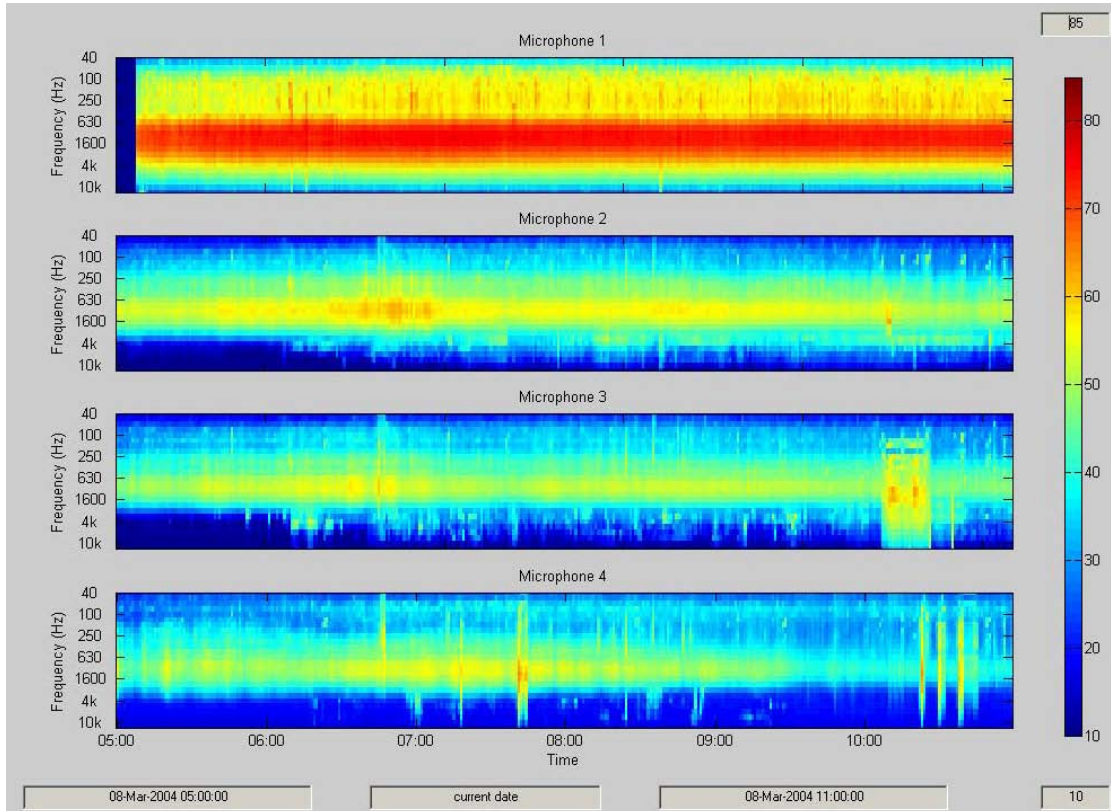


Figure 79. Spectrogram, Monday, March 8, 2004

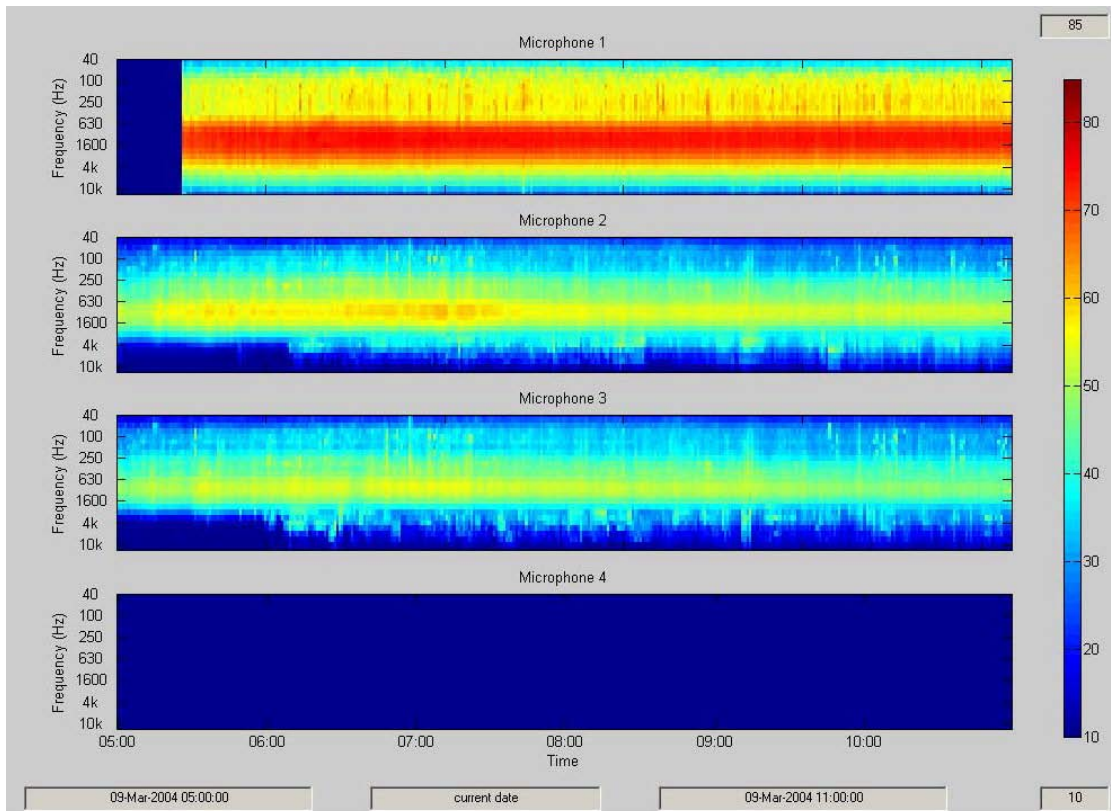


Figure 80. Spectrogram, Tuesday, March 9, 2004

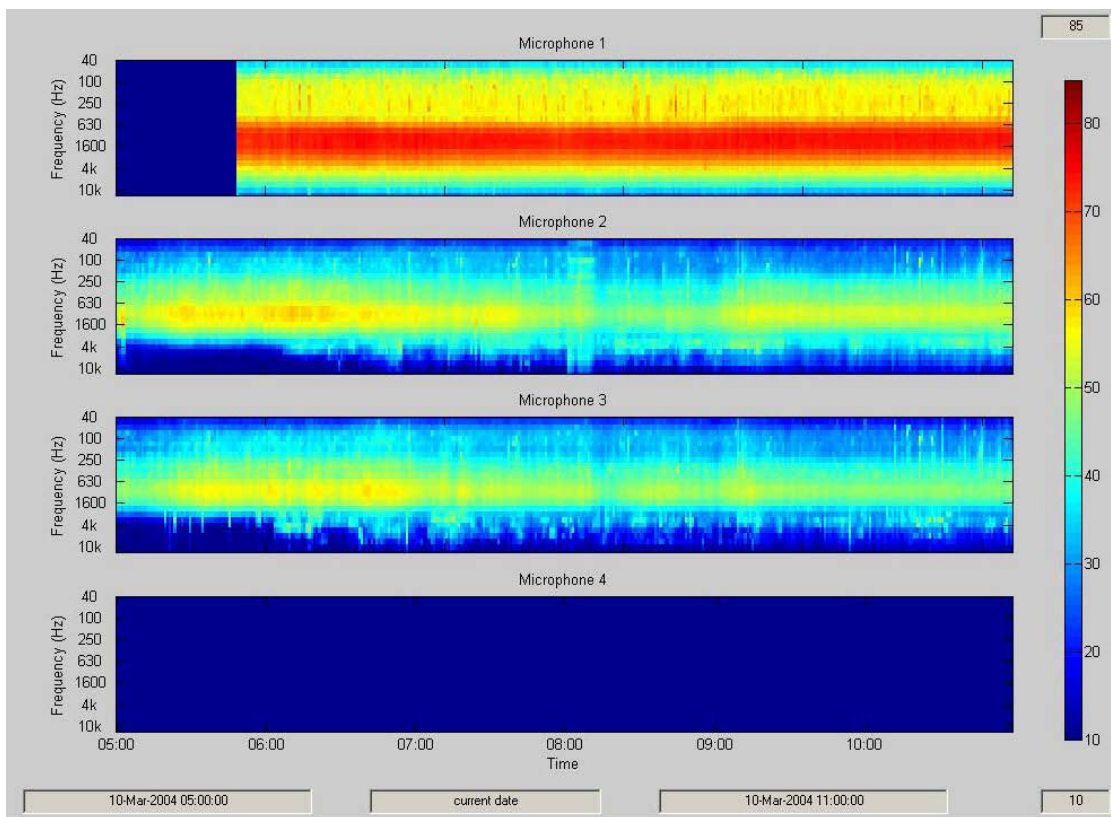


Figure 81. Spectrogram, Wednesday, March 10, 2004

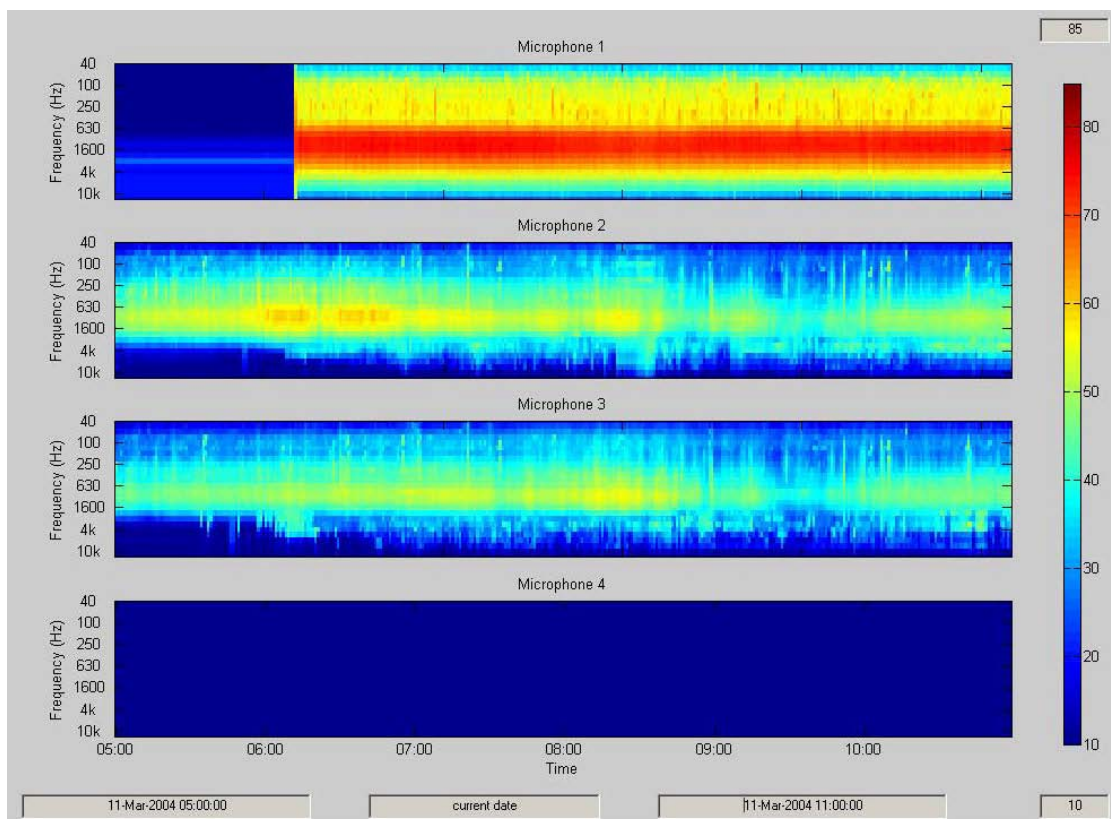


Figure 82. Spectrogram, Thursday, March 11, 2004

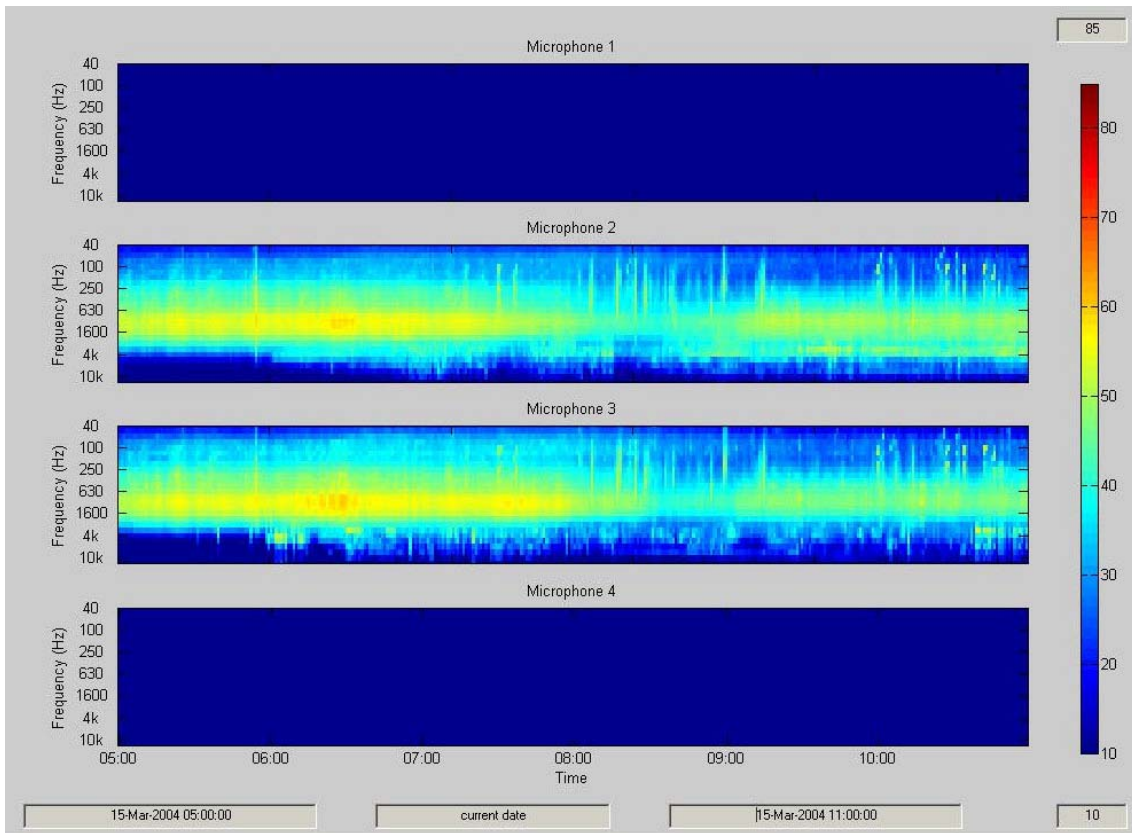


Figure 83. Spectrogram, Monday, March 15, 2004

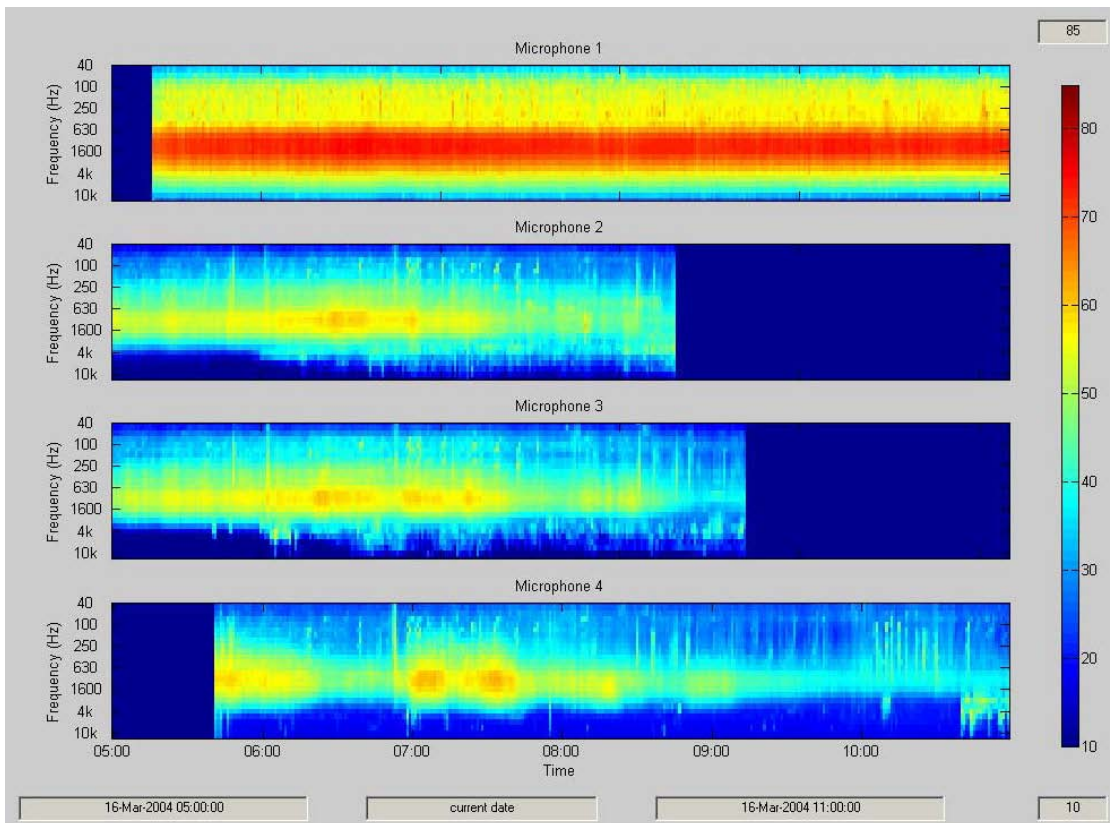


Figure 84. Spectrogram, Tuesday, March 16, 2004

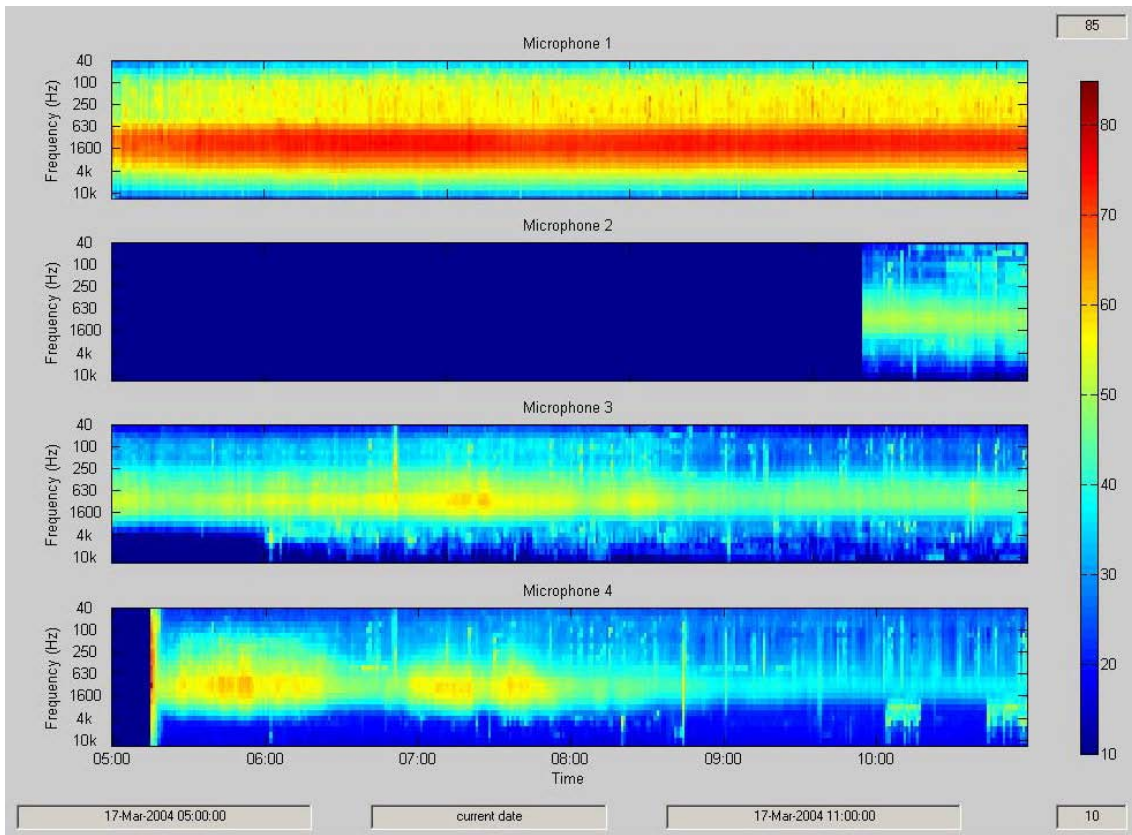


Figure 85. Spectrogram, Wednesday, March 17, 2004

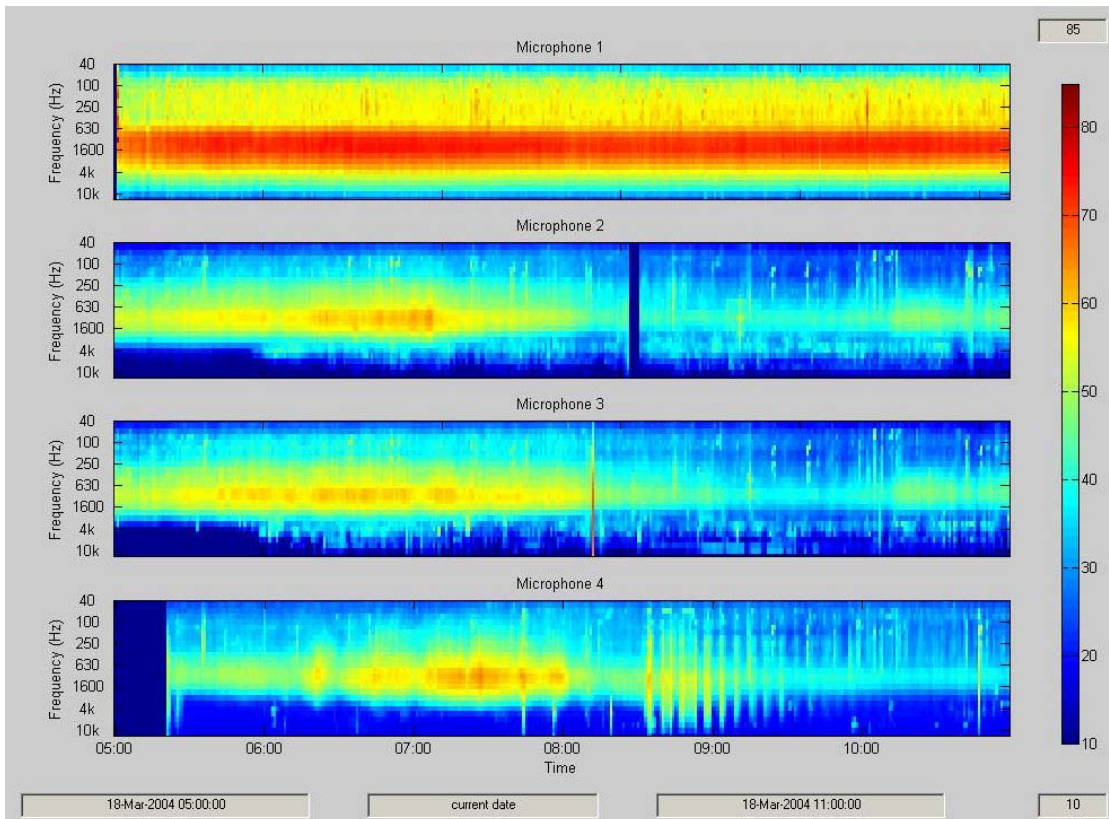


Figure 86. Spectrogram, Thursday, March 18, 2004

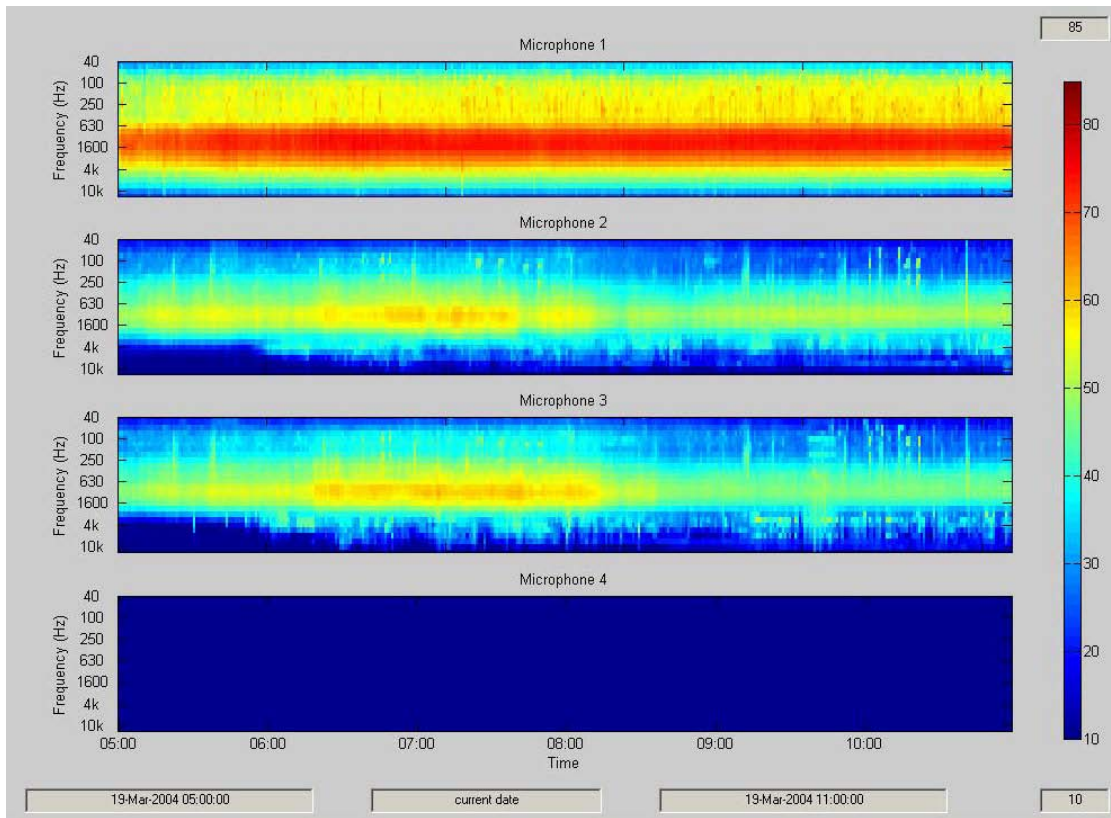


Figure 87. Spectrogram, Friday, March 19, 2004

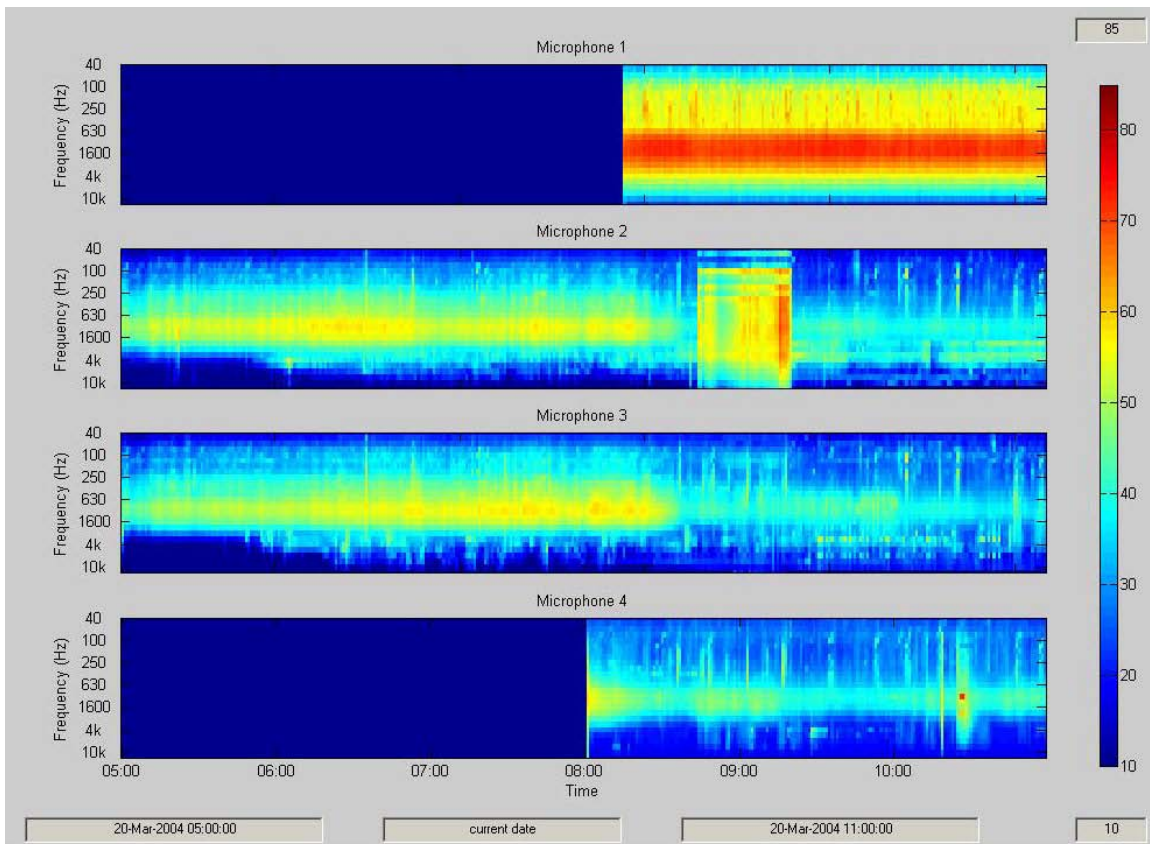


Figure 88. Spectrogram, Saturday, March 20, 2004

B.5 METEOROLOGICAL DATA

Temperature, Dew Point and Humidity, Week 1 of March 2004 Measurements

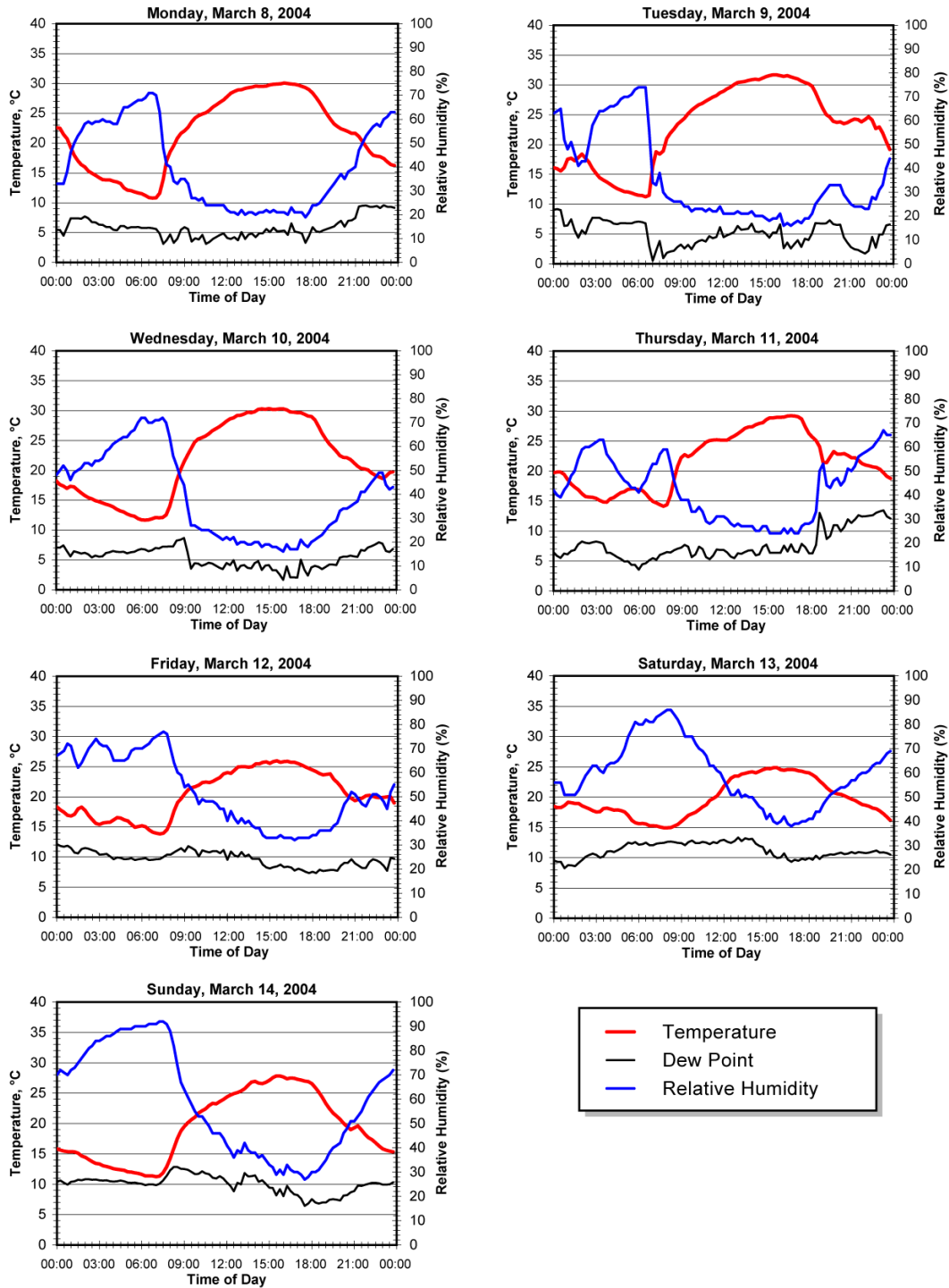


Figure 89. Temperature and Humidity, Site 3, March 8-14, 2004

Temperature, Dew Point and Humidity, Week 2 of March 2004 Measurements

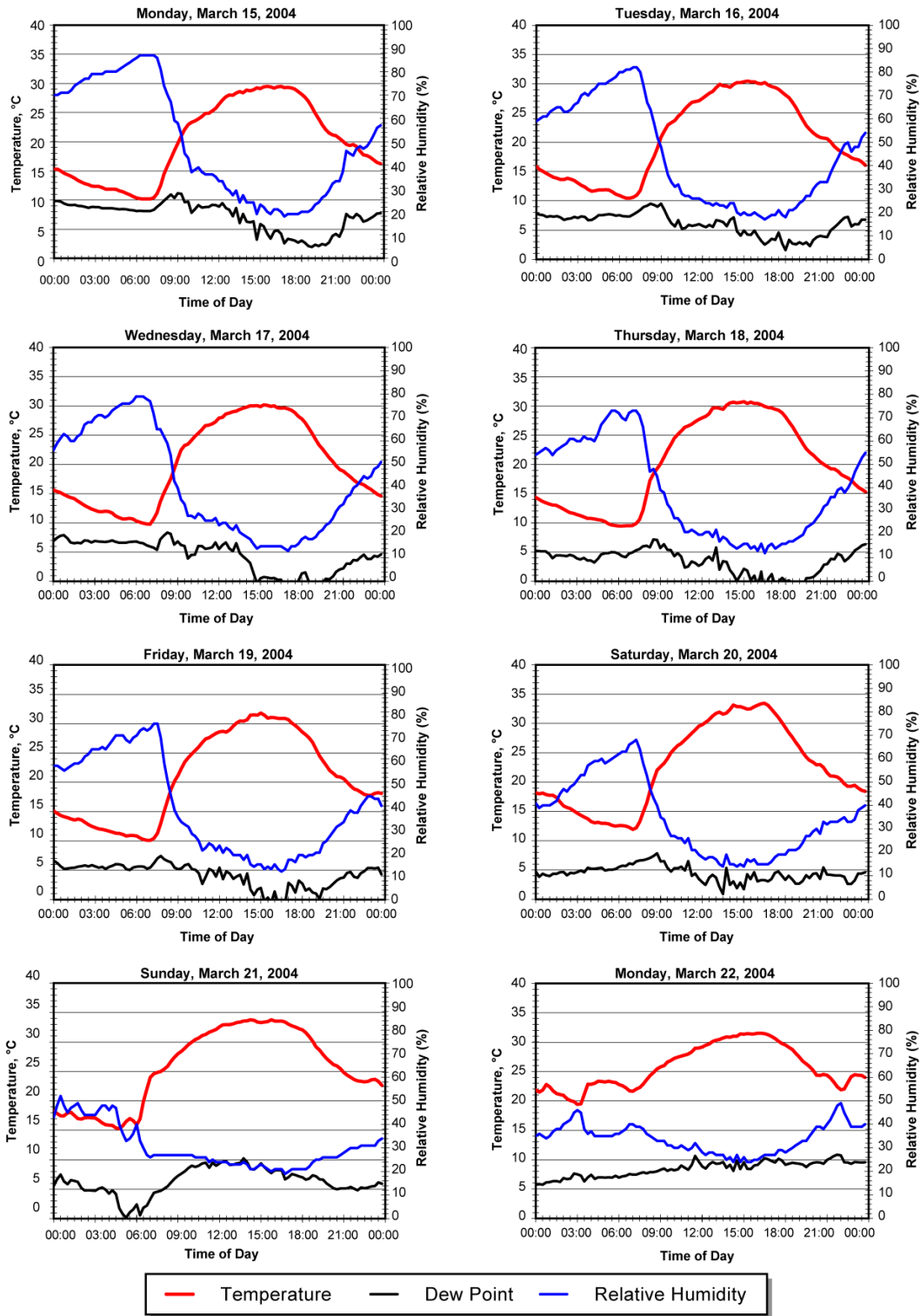


Figure 90. Temperature and Humidity, Site 3, March 15-22, 2004

Temperature, Dew Point and Humidity, October 2004 Measurements

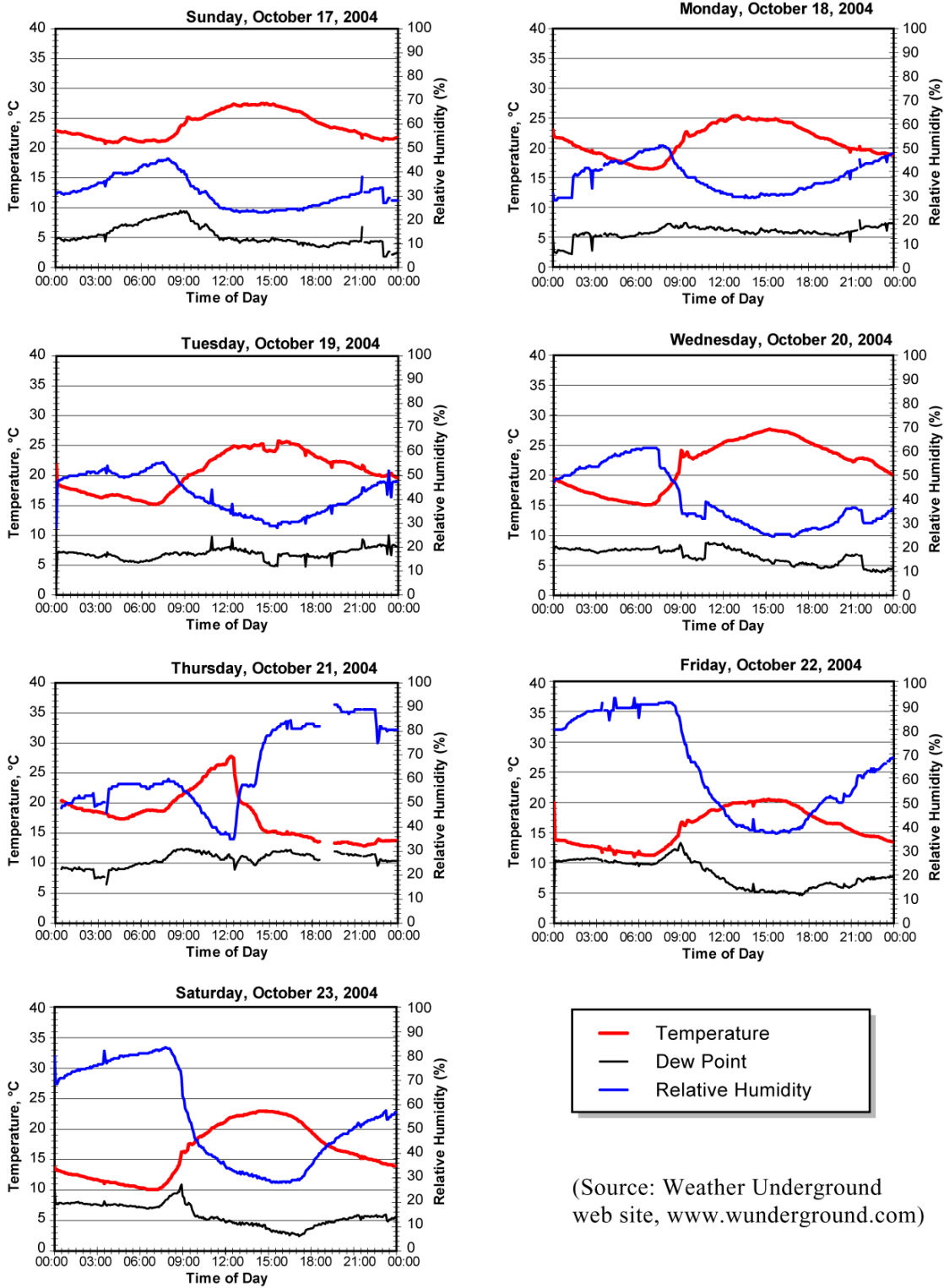


Figure 91. Temperature and Humidity, October 17-23, 2004

Wind Speed and Direction, Site 2, March 17-23, 2004
(45 ft Above Ground Level)

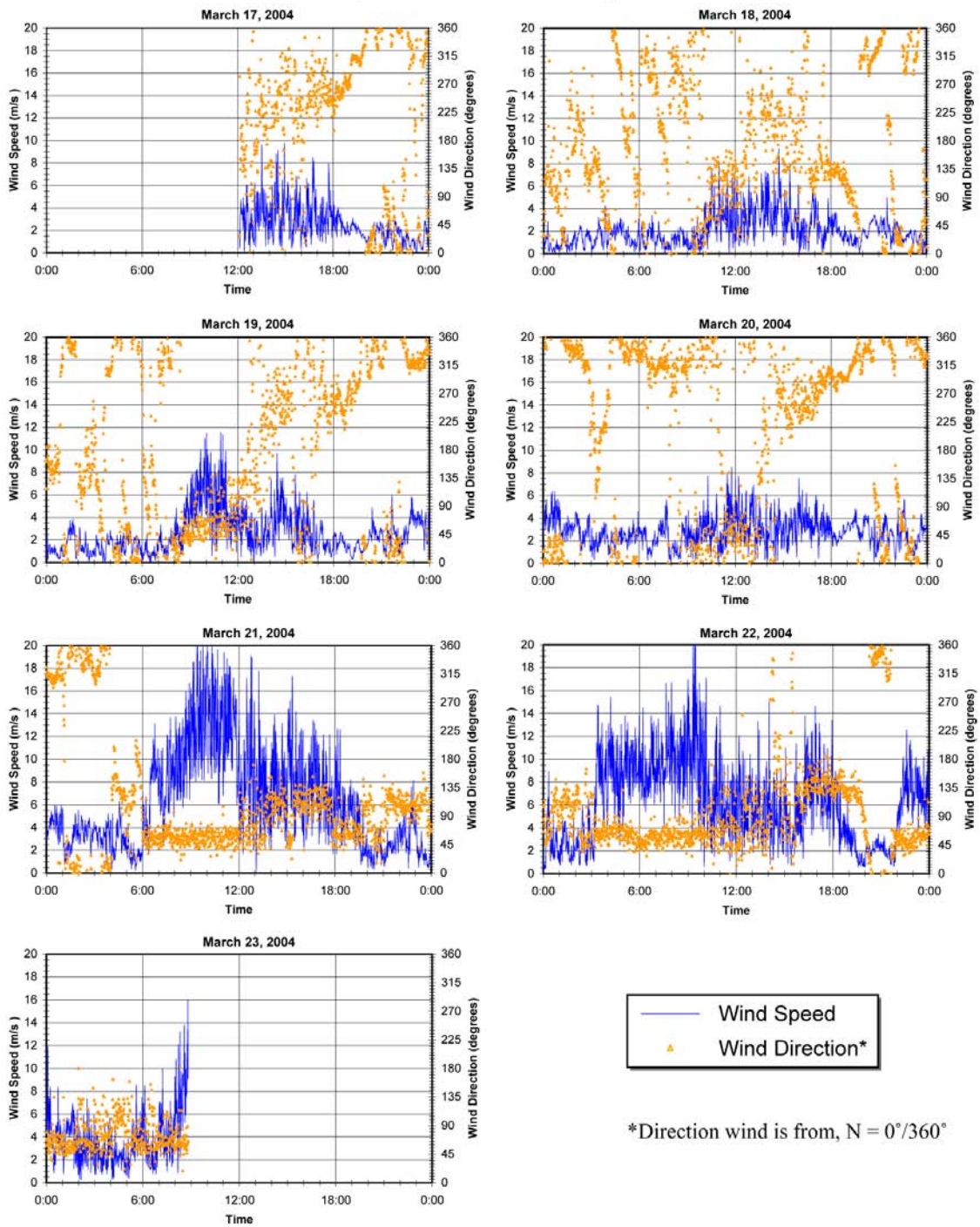
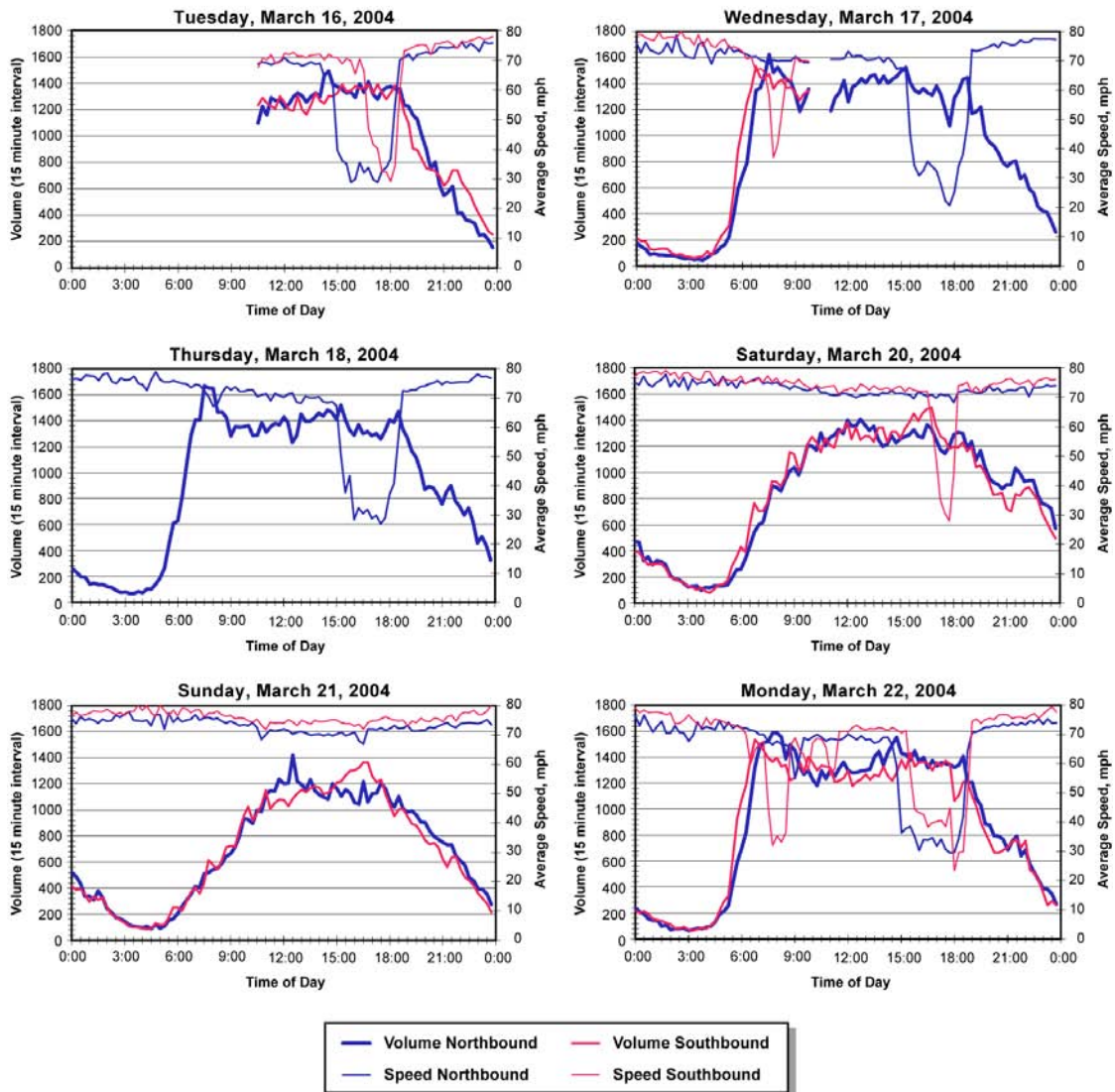


Figure 92. Wind Speed at 43.5 ft, Site 2, March 17-23, 2004

B.6 TRAFFIC COUNTS

Total Traffic Counts and Average Speed (15-Minute Intervals) March 16-22, 2004

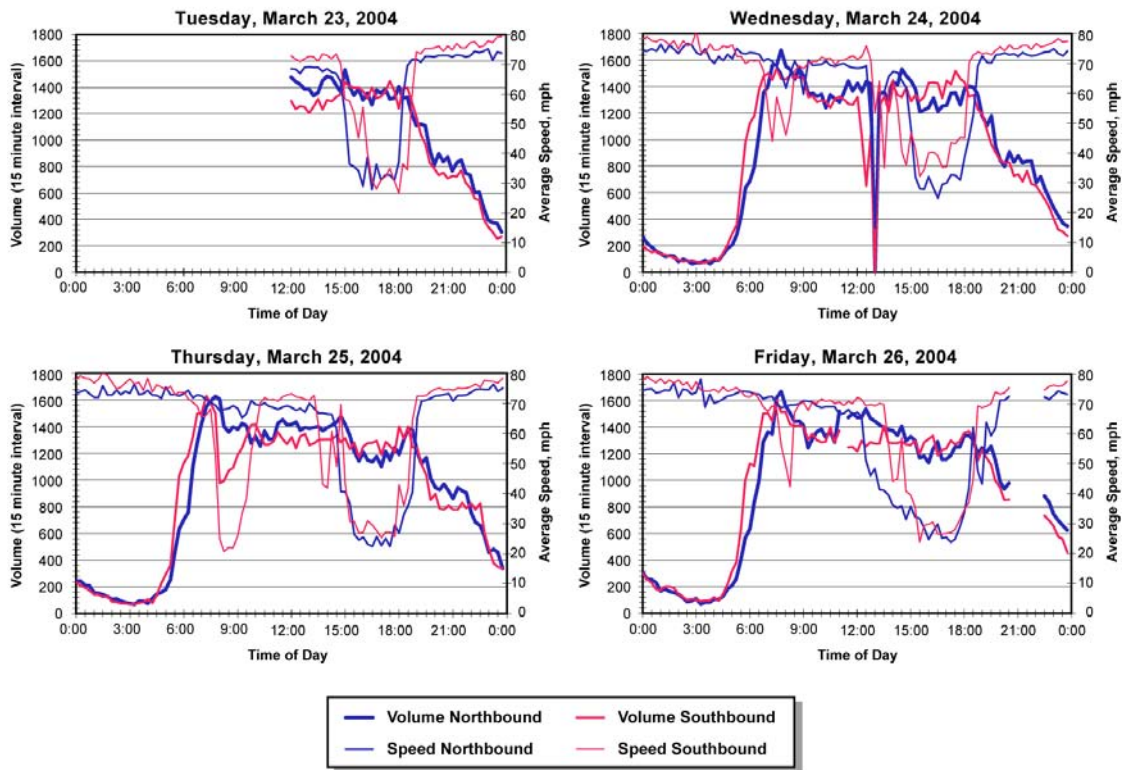


Note: No traffic counts available for March 19.
Source: Traffic Research & Analysis, Inc.

Figure 93. Summary of Traffic Counts, March 16-22, 2004

Total Traffic Counts and Average Speed (15-Minute Intervals) March 23-26, 2004

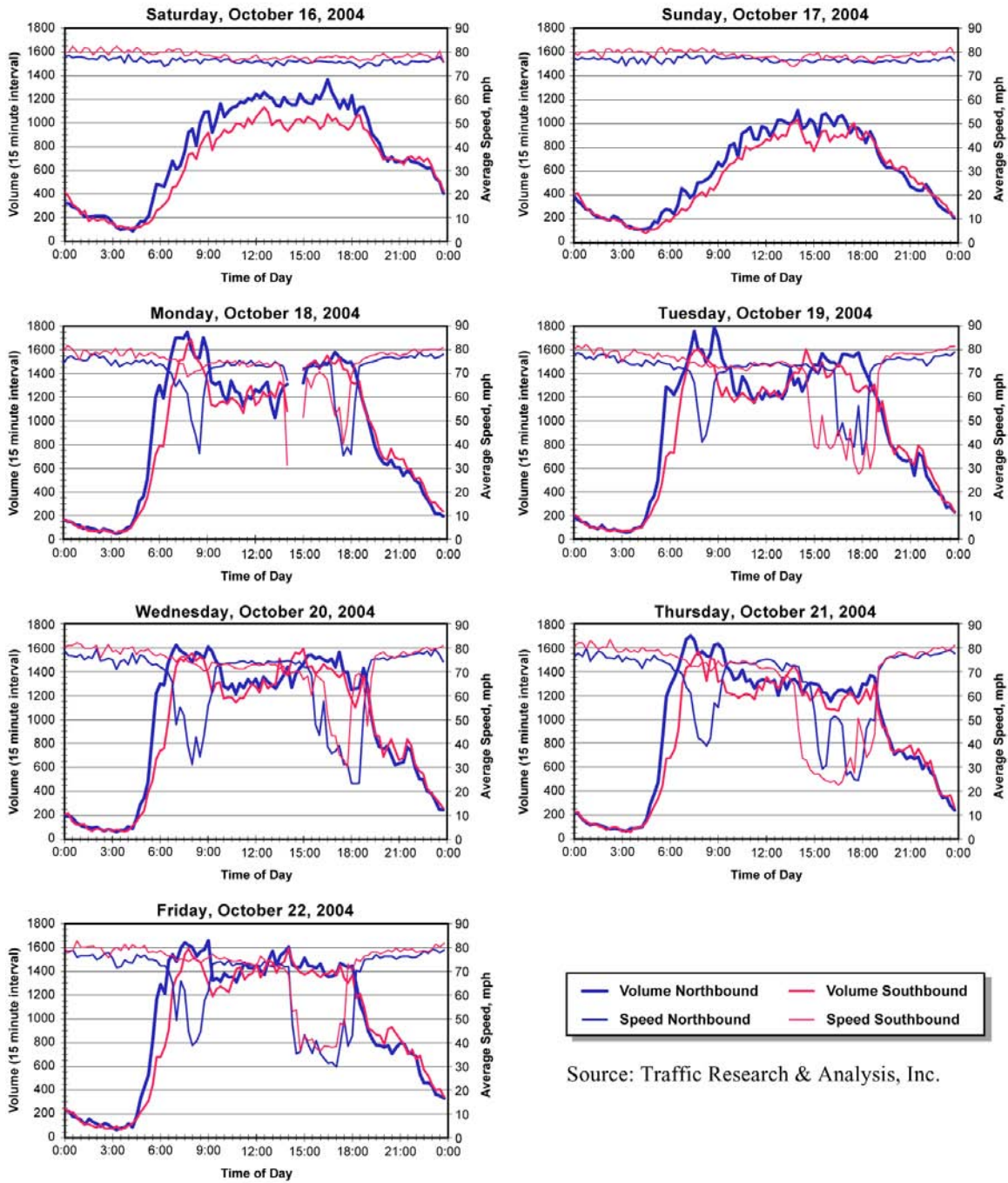
(Traffic counts after noise measurements were completed on March 22, 2004)



Source: Traffic Research & Analysis, Inc.

Figure 94. Summary of Traffic Counts, March 23-26, 2004

Total Traffic Counts and Average Speed (15-Minute Intervals) October 16-22, 2004



— Volume Northbound — Volume Southbound
— Speed Northbound — Speed Southbound

Source: Traffic Research & Analysis, Inc.

Figure 95. Summary of Traffic Counts, October 16-22, 2004

APPENDIX C. DETAILED RESULTS OF PE MODELS

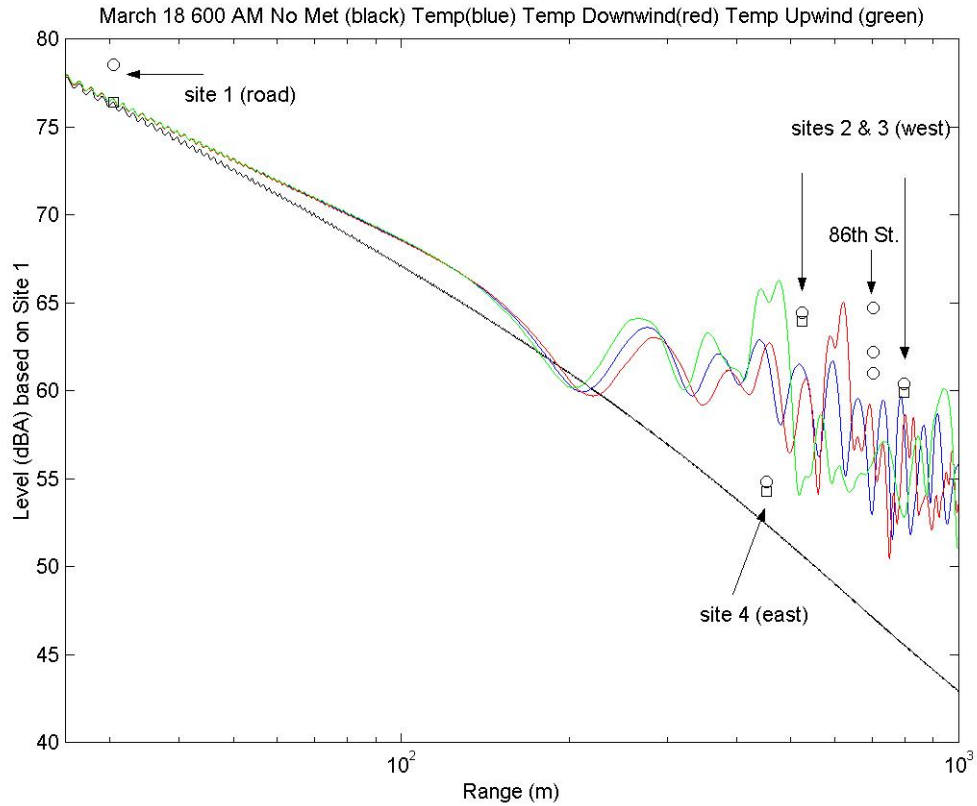


Figure 96. PE Model Output, March 18, 6:00 AM

Black line: Neutral meteorology conditions

Blue line: Temperature only

Red line: Temp Downwind (wind speed added to temperature effects)

Green line: Temp Upwind (wind speed subtracted from temperature effects)

Circles: Overall measured A-weighted sound levels

Squares: A-weighted sound levels including only 63 Hz to 1000 Hz octave bands

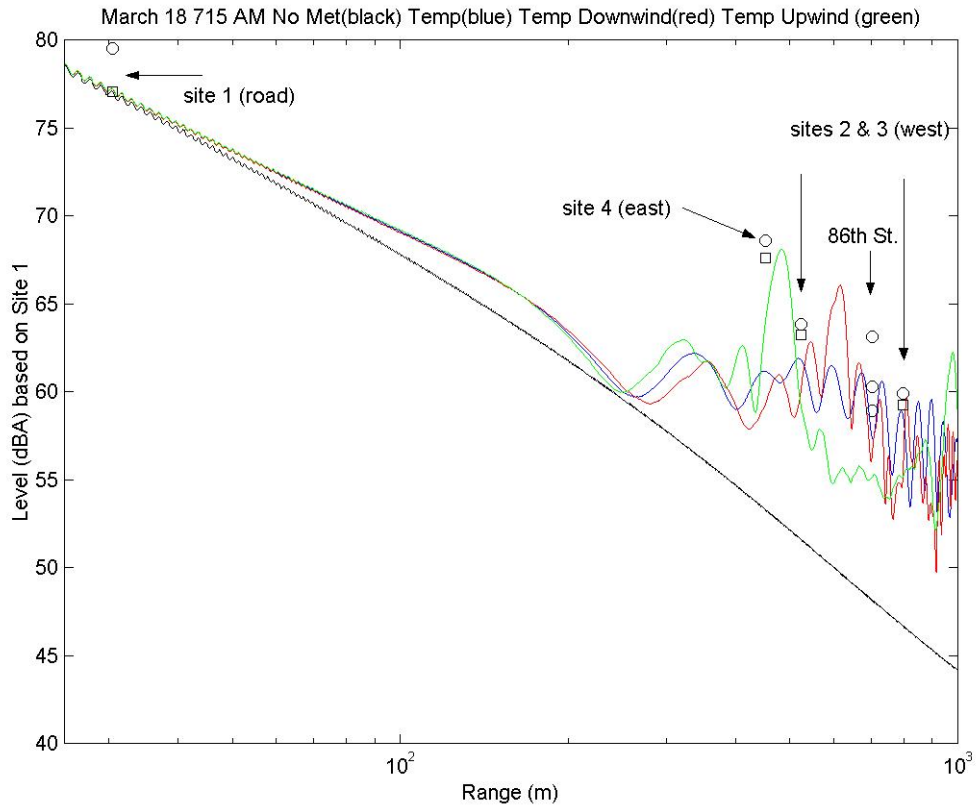


Figure 97. PE Model Output, March 18, 7:15 AM

Black line: Neutral meteorology conditions

Blue line: Temperature only

Red line: Temp Downwind (wind speed added to temperature effects)

Green line: Temp Upwind (wind speed subtracted from temperature effects)

Circles: Overall measured A-weighted sound levels

Squares: A-weighted sound levels including only 63 Hz to 1000 Hz octave bands

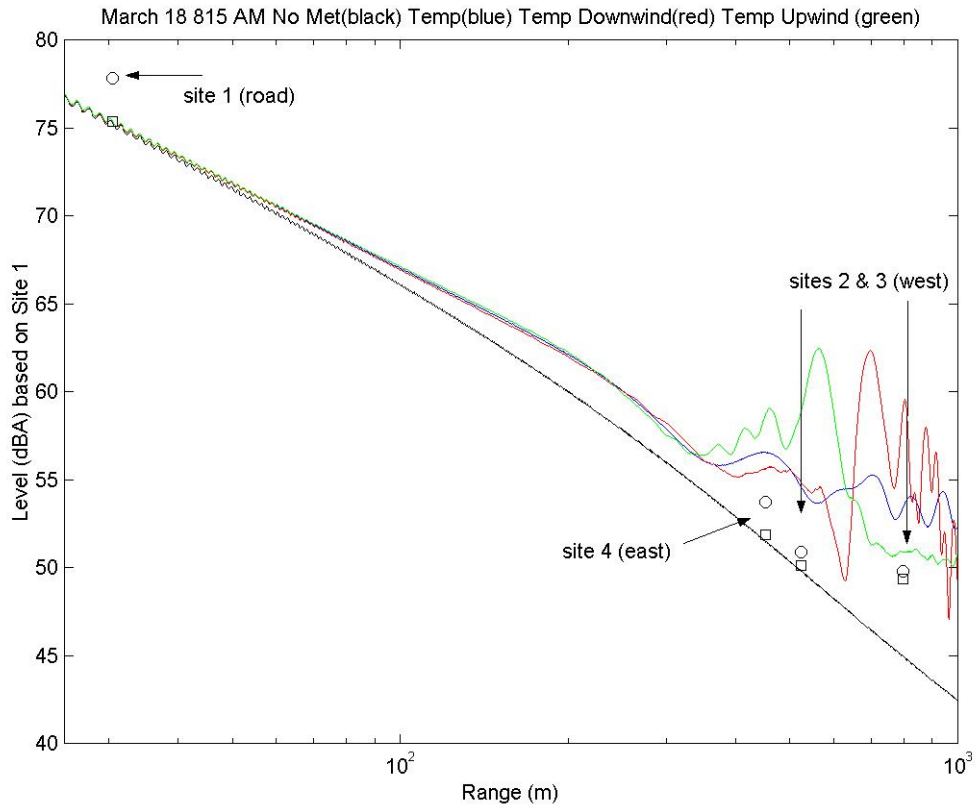


Figure 98. PE Model Output, March 18, 8:15 AM

Black line: Neutral meteorology conditions

Blue line: Temperature only

Red line: Temp Downwind (wind speed added to temperature effects)

Green line: Temp Upwind (wind speed subtracted from temperature effects)

Circles: Overall measured A-weighted sound levels

Squares: A-weighted sound levels including only 63 Hz to 1000 Hz octave bands

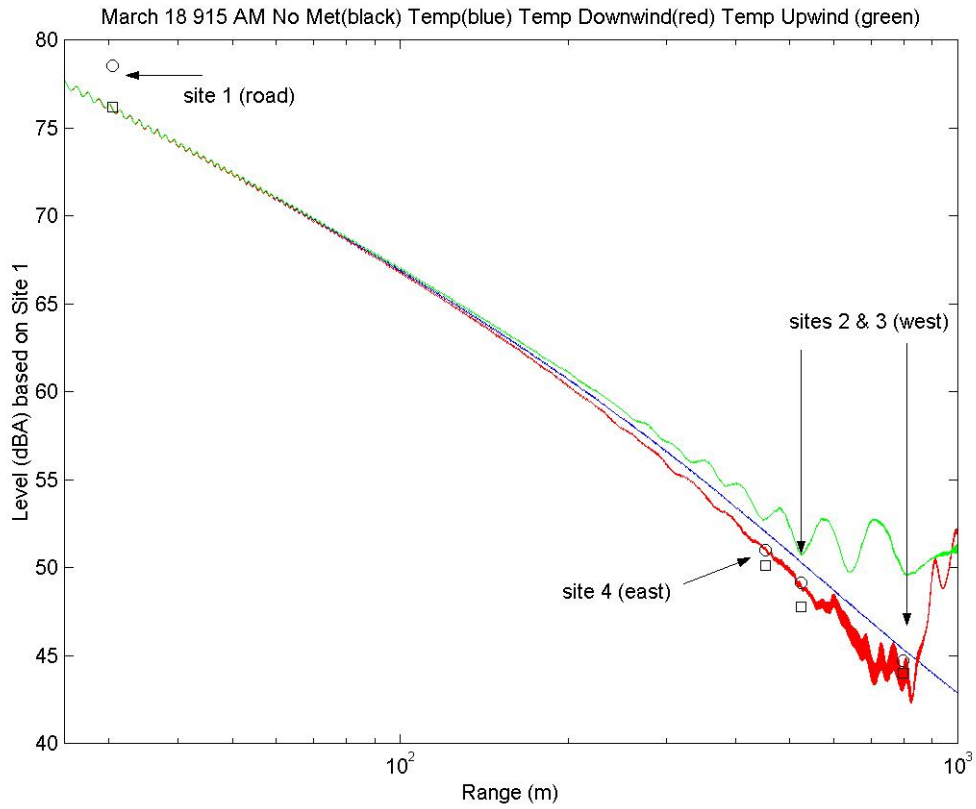


Figure 99. PE Model Output, March 18, 9:15 AM

Black line: Neutral meteorology conditions

Blue line: Temperature only

Red line: Temp Downwind (wind speed added to temperature effects)

Green line: Temp Upwind (wind speed subtracted from temperature effects)

Circles: Overall measured A-weighted sound levels

Squares: A-weighted sound levels including only 63 Hz to 1000 Hz octave bands

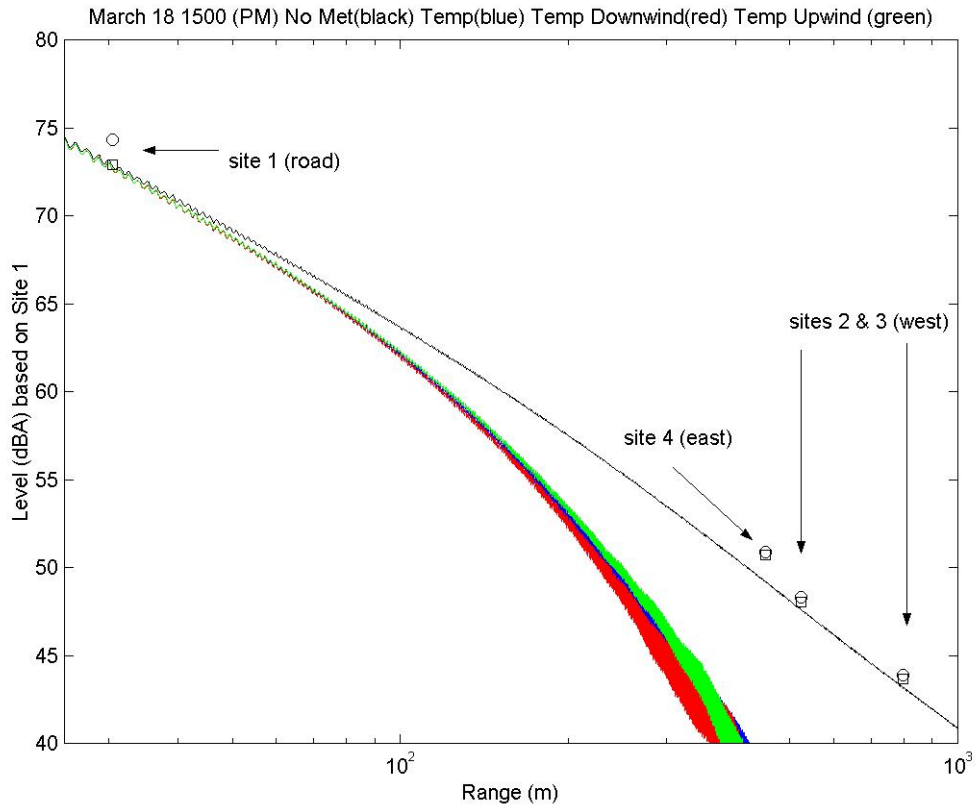


Figure 100. PE Model Output, March 18, 3:00 PM

Black line: Neutral meteorology conditions

Blue line: Temperature only

Red line: Temp Downwind (wind speed added to temperature effects)

Green line: Temp Upwind (wind speed subtracted from temperature effects)

Circles: Overall measured A-weighted sound levels

Squares: A-weighted sound levels including only 63 Hz to 1000 Hz octave bands

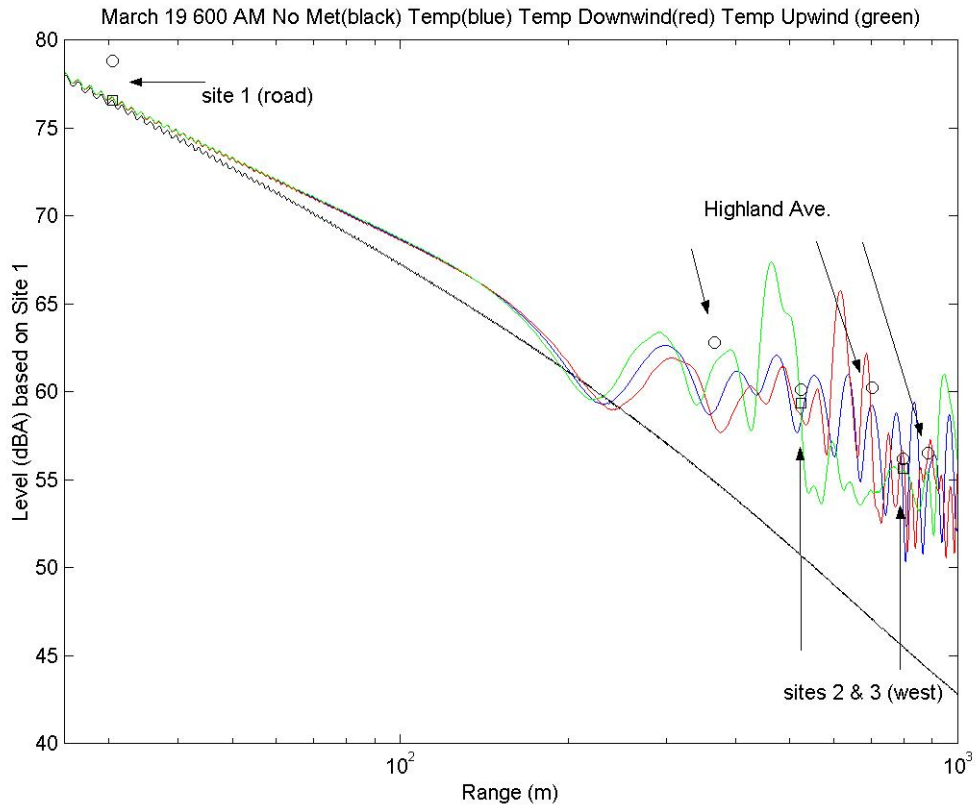


Figure 101. PE Model Output, March 19, 6:00 AM

- Black line: Neutral meteorology conditions
- Blue line: Temperature only
- Red line: Temp Downwind (wind speed added to temperature effects)
- Green line: Temp Upwind (wind speed subtracted from temperature effects)
- Circles: Overall measured A-weighted sound levels
- Squares: A-weighted sound levels including only 63 Hz to 1000 Hz octave bands

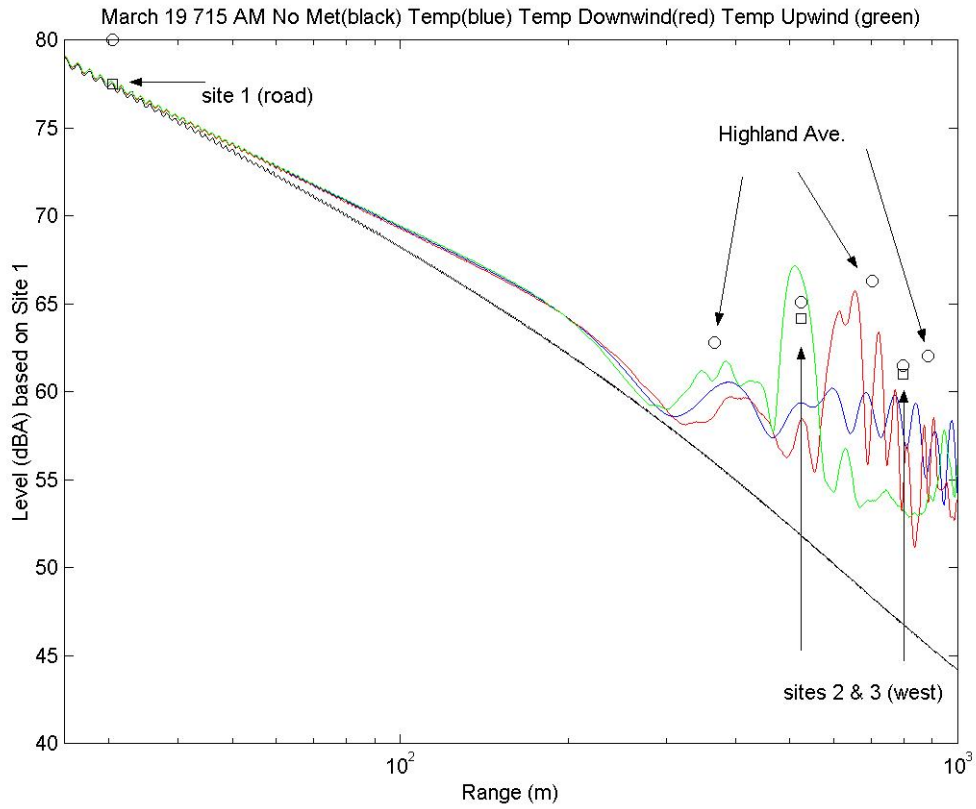


Figure 102. PE Model Output, March 19, 7:15 AM

- Black line: Neutral meteorology conditions
- Blue line: Temperature only
- Red line: Temp Downwind (wind speed added to temperature effects)
- Green line: Temp Upwind (wind speed subtracted from temperature effects)
- Circles: Overall measured A-weighted sound levels
- Squares: A-weighted sound levels including only 63 Hz to 1000 Hz octave bands

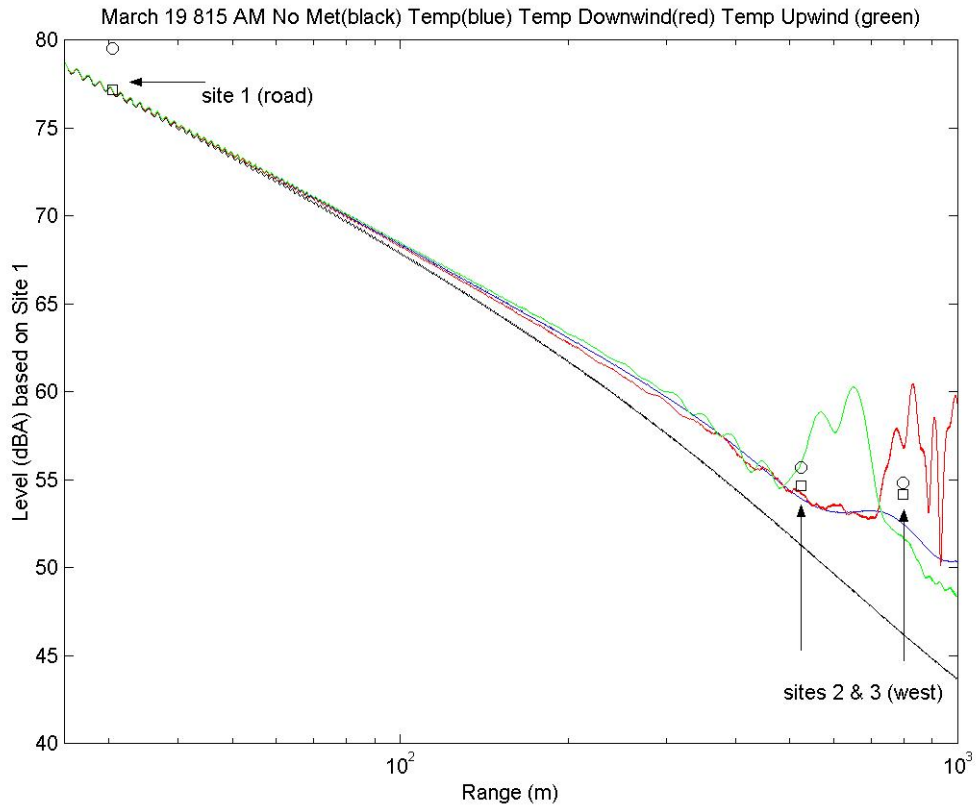


Figure 103. PE Model Output, March 19, 8:15 AM

Black line: Neutral meteorology conditions

Blue line: Temperature only

Red line: Temp Downwind (wind speed added to temperature effects)

Green line: Temp Upwind (wind speed subtracted from temperature effects)

Circles: Overall measured A-weighted sound levels

Squares: A-weighted sound levels including only 63 Hz to 1000 Hz octave bands

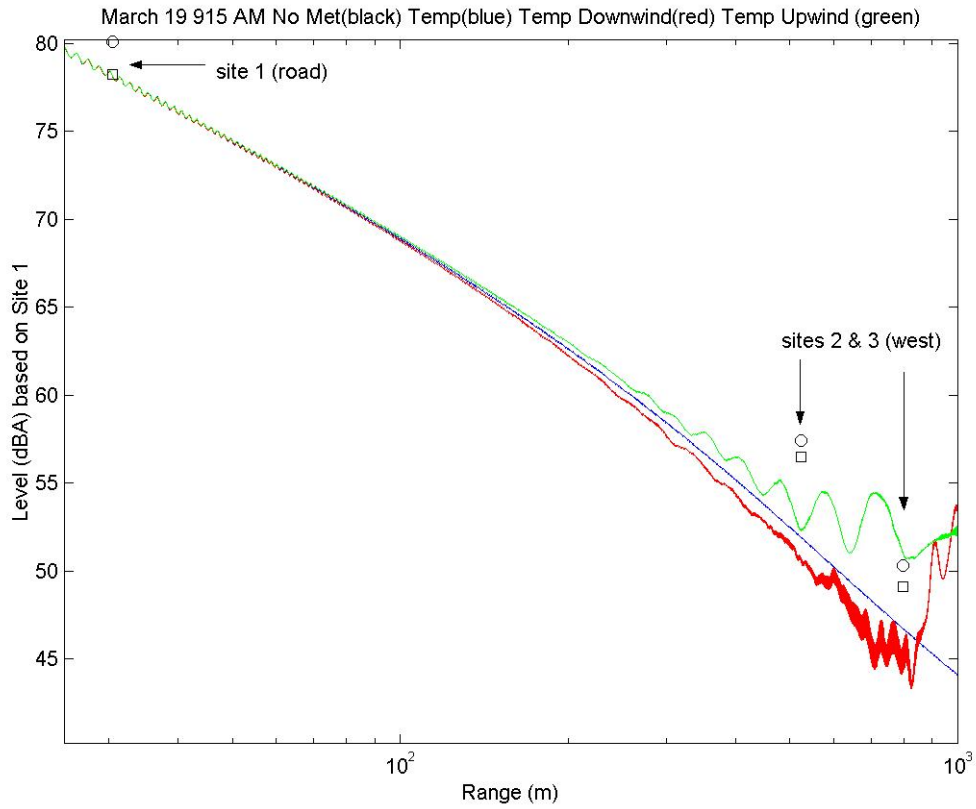


Figure 104. PE Model Output, March 19, 9:15 AM

Black line: Neutral meteorology conditions

Blue line: Temperature only

Red line: Temp Downwind (wind speed added to temperature effects)

Green line: Temp Upwind (wind speed subtracted from temperature effects)

Circles: Overall measured A-weighted sound levels

Squares: A-weighted sound levels including only 63 Hz to 1000 Hz octave bands

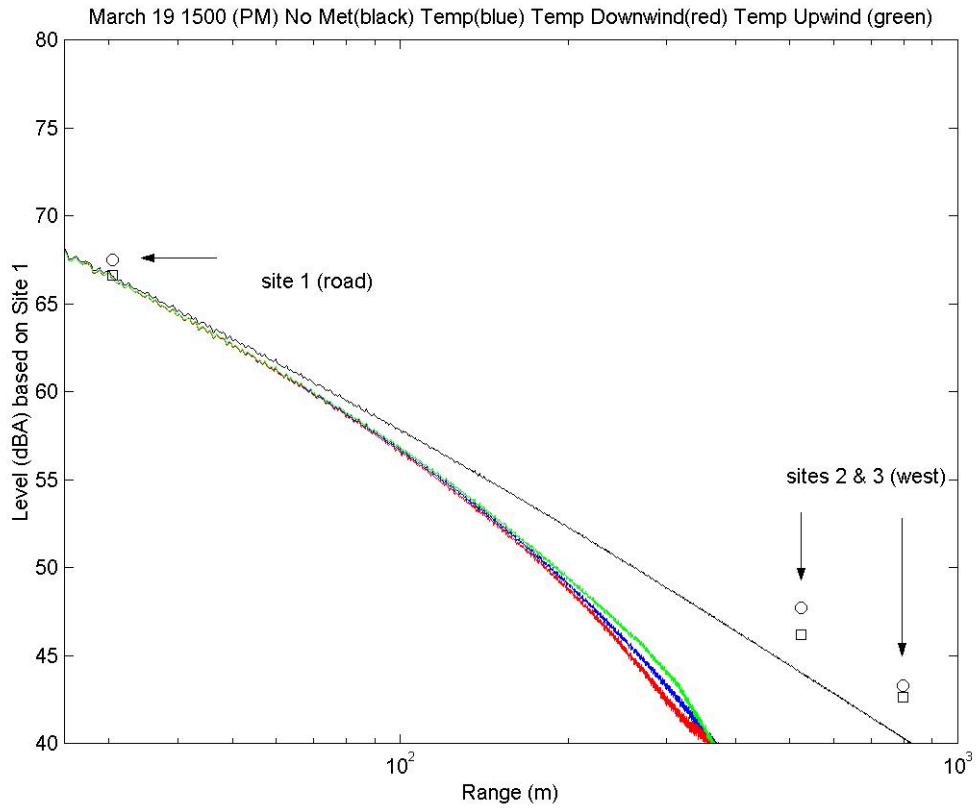


Figure 105. PE Model Output, March 18, 3:00 PM

Black line: Neutral meteorology conditions

Blue line: Temperature only

Red line: Temp Downwind (wind speed added to temperature effects)

Green line: Temp Upwind (wind speed subtracted from temperature effects)

Circles: Overall measured A-weighted sound levels

Squares: A-weighted sound levels including only 63 Hz to 1000 Hz octave bands

APPENDIX D. TIRE NOISE PARAMETRIC STUDIES

Following is the text from two memorandums that were prepared on the pilot study to determine whether relatively simple mathematical models of tire/pavement noise that are based on fundamental acoustical principles can predict how different pavement parameters affect levels of tire/pavement noise. The ultimate goal was to have tools that provide insights about how variations in different pavement parameters will affect noise and can be applied to developing pavements that are optimized for low noise levels. The first memorandum provides an overview of the tire noise issue and the second memorandum presents the results of the pilot study.

D.1 OVERVIEW OF TIRE NOISE STUDY

The following material is from the memorandum “Overview of Tire Noise” submitted by Hugh Saurenman to the Technical Advisory Committee on Jun 16, 2004.

Introduction

Attached is a technical memorandum from Dr. Joel Garrelick of Applied Physical Sciences, Inc. summarizing his investigations into parametric models of tire/pavement noise. Although there have been numerous studies of the noise generation properties of different types of pavements, we are not aware of any tools that can be used in the design of an optimized “quiet” pavement. This is largely due to the number of different mechanisms by which a pneumatic tire rolling on pavement generates noise, each of which can be affected independently by different pavement parameters. In fact, sometimes there are counterbalancing effects. For example, long wavelength texture (roughness) may tend to increase noise while short wavelength texture tends to reduce noise.

Our goal on this task was to determine whether relatively simple mathematical models of tire/pavement noise that are based on fundamental acoustical principles can predict how these parameters affect levels of tire/pavement noise. The ultimate goal is to have tools that provide insights about how variations in different pavement parameters will affect noise and can be applied to developing pavements that are optimized for low noise levels.

The mathematics of the modeling are described in Dr. Garrelick’s memo. The purpose of this memo is to provide an introduction to the mechanisms of tire/pavement noise that will give a clearer context for the study results and to summarize the results of Dr. Garrelick’s pilot study.

Noise Generating Mechanisms

Before summarizing the results of Dr. Garrelick’s study, it is important to have some understanding of the mechanisms of tire/pavement noise. The generating mechanisms thought to be most important are summarized in Table 10 and discussed below. This discussion is largely based on the information in Chapter 11 or Ulf Sandberg’s book on tire/pavement noise.

The primary noise generating mechanisms are:

- **Roadway Roughness:** First are the forces generated at the tire/pavement contact patch caused by irregularities in the pavement surface. Excitation is at the wavelength of the surface irregularity and the frequency of excitation depends on the vehicle speed:

$$f = \text{speed}/\lambda$$

where f = frequency in Hz, λ = wavelength in inches, and speed = vehicle speed in inches per second.

For example, at 60 mph we expect the following relationship between roughness wavelength and frequency:

<u>Wavelength</u>	<u>Frequency</u>
21"	50 Hz
11"	100 Hz
2"	500 Hz
1.1"	1,000 Hz
0.5"	2,000 Hz
0.2"	5,000 Hz
0.11"	10,000 Hz

The values above illustrate that roughness at wavelengths of about 0.1 to 20 inches affect noise radiation for this mechanism. Because other mechanisms are more important at frequencies of 1000 Hz and higher, it is actually wavelengths of about 1/2 inch and greater that are important. Having a smoother road surface at these wavelengths will reduce noise levels at frequencies below 1000 Hz.

Table 10. Noise Generating Mechanisms			
Noise Generating Mechanism	Freq Range	Relevant Pavement Parameters	Effect on Noise
Tire casing excitation at roadway roughness frequency	<1000 Hz	Surface smoothness, aggregate size	Increase
Tread block impact	800-1250 Hz	Texture	Increase
Air pumping	>1000 Hz	Roughness Porosity	Decrease Decrease
Stick-slip (friction)		Microtexture	Increase
Stick-snap (adhesion)		Texture	Decrease
Horn effects (amplification)		Texture/Porosity	Decrease
Absorption (source strength and propagation)		Porosity ⁽¹⁾ Coatings	Increase Decrease?
Closed cavity effects with tire tread or pits in pavement surface (resonator, pipe modes)		Unconnected pits in pavement surface	Increase
Notes:			
(1) Porosity parameters that affect sound levels include percent voids, size of voids, thickness of porous layer, flow resistance, and void shape factor (tortuosity).			

- **Tread Block Impact:** This mechanism is important in the mid-frequency range of about 800 to 1250 Hz. Noise is caused by tread blocks hitting the roadway at the leading edge of the tire plus a sort of inverse impact as tread blocks leave the roadway surface at the trailing edge. Presumably a smoother road surface will reduce the impact forces and the noise radiation, although the relationship is not all that clear.
- **Air Pumping:** Air trapped in the interstices of the road surface and the tire tread is pumped in and out as the tire rolls along the surface. This is particularly important if the tire tread or the road surface has unconnected interstices so there is no air pressure relief. Short wavelength roadway texture on the order of 1/2 inch or less and porosity reduces the air

pressure buildup and will tend to reduce air pumping noise, although there may be counterbalancing effects such as increasing tread block impacts.

- **Stick-Slip:** Slip-stick is caused by the friction between the tire and the roadway. The mechanism is much the same as the noise caused when running your palm over a smooth surface. Things that increase friction, such as micro-texture with size similar to single grains of sand, will tend to increase slip-stick.
- **Adhesion:** Adhesion between the tire surface and the roadway will generate noise as the adhesive bonds are broken. Although it is possible that this mechanism contributes to overall noise levels, tests that have been done to date do not seem to show this as an important noise source. Increasing micro-texture should reduce the bonding and the noise generated by this mechanism. Sandberg (Ref. 1) refers to this mechanism as stick-snap.
- **Horn Effects:** This is not really a noise generating mechanism; rather it is a mechanism by which sound levels are amplified. At the leading and trailing edges of the tire, the angle between the tire and the road surface acts like a small horn increasing the radiation efficiency of the vibrating tire. Acoustically absorptive (porous) pavements and possibly increasing texture at wavelengths of 1/2 inch or smaller may reduce the efficiency of the horn effect.
- **Absorption:** Increased absorption is one of the key effects of a porous pavement. This is not really a noise generating mechanism, but is included since it can have a strong effect on sound levels. Pavements that are acoustically absorptive will reduce the effective source strength by reducing the reverberant buildup in the under-vehicle area and will result in attenuation as the sound propagates across the pavement. Also, as discussed above, absorptive pavements may reduce the horn effect.
- **Closed Cavities:** This is a special case where either the tire tread or the pavement has closed cavities (open at the top, closed on the sides and bottom). The air pumped in and out of the closed cavities can substantially increase noise levels. This is not really applicable to either current tires or modern, well-constructed roads.

Pavement Parameters

In Table 11 we show which mechanisms are affected by key pavement parameters. To some degree this is repeating the information in Table 10. The pavement parameters and their effects are:

- **Texture:** By texture we are referring to all unevenness in the pavement surface. The texture at wavelengths of about 0.4 to 20 inches affects the basic excitation of the tire casing and the radiation of noise below about 1000 Hz. In this range, increased texture will increase noise levels. The next level is 0.02 to 0.4 inches. This texture range affects air pumping; the greater the texture, the lower the noise from air pumping. Very small wavelength texture will affect adhesion and friction; it is not clear whether this has more than a small to moderate effect on noise levels. Sandburg (Ref. 1) indicates that there may be noise generating mechanisms related to longer wavelength unevenness, although it is not clear what the mechanism would be or what frequency ranges would be affected.
- **Tining:** Tining of concrete pavements to reduce hydroplaning in wet conditions can cause significant sound level increases. This is particularly true when the tining is transverse. Longitudinal tining is thought to have only a small effect on sound levels.

Table 11. Effect of Pavement Parameters on Tire/Pavement Noise		
Parameter	Mechanism	Degree
Pavement Texture		
0.4 to 20 inches	Tire excitation	Strong
0.02 to 0.4 inches	Air pumping	Strong
Micro	Friction/adhesion	Moderate
Unevenness (>20 in.)	Not clear	
Tining		
Transverse	In phase excitation	Strong
Longitudinal	No special mechanism	Weak
Irregular	Similar to texture	Moderate
Porosity Parameters		
% voids (porosity)	Air pumping Absorption	High High
void size	Absorption Air pumping?	Moderate Moderate
layer thickness	Air pumping Absorption	Moderate Moderate
airflow resistance	Air pumping Absorption	Moderate Moderate
shape factor (tortuosity)	Absorption	Moderate
Stiffness and Binders	Tread block impact Other?	Not clear Not clear
Friction	Stick-slip	Moderate
Adhesion	Stick-snap	Moderate

- Porosity:** It is well understood that porous pavements tend to be quieter than non-porous pavements. This is apparently because porous pavements are more acoustically absorptive than non-porous pavements and because the porosity reduces the effects of air pumping. Important porosity parameters include the percent voids (generally speaking, the higher the better), the size of the voids (smaller is better), the layer thickness (affects the peak frequency), the resistivity (affects peak frequency and range of effectiveness), and the shape factor (affects peak frequency and range of effectiveness).
- Stiffness and Binder Additives:** Given the widespread conventional wisdom that adding crumb rubber to the asphalt binder is a key factor in making a quiet pavement, we are hesitant to say too much here. However, it is not clear how adding rubber to the binder would change any properties that affect noise levels unless the rubber affects the texture or the porosity. The added resilience of rubberized pavements compared to standard pavements is not sufficient to affect the excitation of the tire. The pavement stiffness is still effectively infinite compared to the stiffness of a pneumatic tire.
- Friction:** Reducing friction will reduce stick-slip noise. A relatively recent development on rail systems is use of “positive” friction material on the rail head to reduce stick-slip noise. Generally the coefficient of friction will drop as soon as friction forces are exceeded and two

surfaces start to move relative to each other. With positive friction materials, the friction forces continue to increase even after there is slippage between the two surfaces.

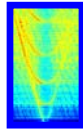
- **Adhesion:** A final property of pavements that can affect noise generation is adhesion. The greater the adhesion forces between tires and the roadway surface, the higher the level of stick-snap noise will be. Increasing microtexture will reduce adhesion as well as introducing artificial materials between the tire and the roadway (e.g., dirt or talcum powder and spray-on material as were used in some tests).

Summary of Conclusions from Structural-Acoustic Modeling

The overall conclusion is that the quietest pavements will be very smooth in the macro and mega texture ranges, be highly porous with about 25% voids, have a thickness of 1 inch or more, be self-cleaning so the porosity does not change, have a non-stick surface that minimizes stick-snap, and have a friction characteristic that minimizes stick-slip. Following is a more detailed summary of our observations and conclusions:

- **Propagation over an Elastic/Porous Surface:** The modeling shows a substantial potential benefit from enhanced acoustical absorption properties for porous pavements. The modeling only looked at propagation over a porous pavement. Based on the modeling, we conclude that:
 1. **Thickness:** Increasing porous layer thickness will reduce the peak absorption frequency and broaden the range of effectiveness.
 2. **Resistivity:** Increasing flow resistance will tend to broaden the range of effectiveness. With low flow resistance, the propagation loss will have strong peaks. As the resistivity increases, the peaks flatten out.
 3. **Porosity (% Voids):** Increasing the percent voids will tend to increase the absorption.
 4. **Tortuosity:** The tortuosity (void shape factor) mainly affects the peak frequency of the absorption coefficient.
 5. **Multiple Layers:** A couple of cases were run to test the effect of having multiple porous layers. For the test cases, the extra layer provided only small benefits compared to a single layer of the same thickness as the two layers.
- **Radiation from Pavement:** The modeling indicates that sound radiation from the pavement is probably small compared to the radiation from the tire casing.
- **Pavement Stiffness:** There is no indication that pavement stiffness affects radiated sound levels.
- **Pavement Texture:** The modeling tends to support the empirical observations that macro texture on the order of 3/4" and greater will affect sound levels. Averaging over the contact patch area tends to diminish the effects of small wavelength texture at least in terms of harmonic forces driving the tire.
- **Air Pumping:** We only took a quick look at modeling of air pumping noise. Intuitively, we expect an increase in porosity to reduce noise by increasing the effective cavity size, at least when tire and pavement pores line up. However, the available modeling indicates that an increase in porosity could increase the effective number of cavities and the effective cavity volume displacement, both of which would be expected to increase noise levels. Based on the available data, we believe that the net effect of increasing porosity will be reduced noise from air pumping.

D.2 TIRE NOISE RAMIFICATIONS OF PAVEMENT CHARACTERISTICS



Applied Physical Sciences Corp.

2 State Street, Suite 300

New London, CT 06320

Phone: (860) 440-3253, Fax: (860) 440-3075

TO: Hugh Saurenman, ATS Consulting, LLC

FROM: Joel Garrelick

SUBJECT: TIRE NOISE RAMIFICATIONS OF PAVEMENT CHARACTERISTICS

DATE: 10 May 2004

TECH MEMO: ATC-3038.1

I. INTRODUCTION AND SUMMARY

This report is intended to enhance the Arizona Department of Transportation's (ADOT) ability to evaluate trade-offs between noise and other pavement design criteria by assessing the gross design characteristics of pavements that likely influence tire noise over a broad range of traffic and environmental conditions. Specifically, the pavement characteristics that may be significant contributors to tire noise, as indicated by current research, are identified and evaluated using first principle structural-acoustic predictive models. Our focus is that portion of the overall vehicle noise spectrum typically attributed to "tire noise" (frequencies in the vicinity of 1 kHz).

Although the current state of the art precludes definitive findings, the conclusions presented below provide a preliminary rationale for assessing the acoustic performance of alternate pavements based on their gross features, namely, texture, stiffness, and porosity. These features and their relative significance are summarized below:

- **Pavement Texture – micro-texture: minor significance, macro/mega texture: moderate significance.** The length scales of pavement texture (e.g. micro texture, macro texture, and mega texture) are correlated with the characteristic wavelengths of a vibrating tire. Micro-texture on the order of single grains of sand, can affect the friction and the adhesion between the tire and the road surface. With more micro texture, friction increases and adhesion decreases which results in increased stick-slip noise and decreased stick-snap noise. The overall result is a minor effect on noise. However, this is not necessarily the case for the longer wavelength portion of the spectrum, say texture the order of 10 mm or higher, covering the upper end of the macro- and the mega-texture range. These length scales are the order of the characteristic wavelengths of the vibrating tire. Assuming contact is maintained

between tire and pavement, lowering the spectral levels of texture may be moderately beneficial. This moderation is a consequence of the increase in the amplitude of the individual tire impacts tending to be cancelled by the decrease in the number of impacts over the tire-pavement contact area. Note that there is a counterbalancing effect with increased texture at wavelengths in the 1 to 10 mm range. Texture at these wavelengths will tend to reduce air-pumping noise.

- **Relative Pavement Stiffness: minor significance.** The stiffness of all candidate pavements is much greater than that of a tire. Therefore, as related to the tire, all pavements act as rigid surfaces in terms of source mechanisms. This feature applies to rubber-modified bituminous binders whose introduction may have an acoustic influence (only) to the extent that they modify pavement porosity.
- **Pavement Porosity: major significance.** Pavement porosity has a major influence on tire noise. This is a consequence of absorptive influence on the source strength of noise generating mechanisms, and more generally on the near grazing propagation of the noise along the pavement. For a typically thin porous layer, the acoustic performance is frequency dependent, with peak performance near the natural frequency of the “tortuous” air path through the thickness. Peak noise reductions of about 5 dB have both been measured and predicted based on porosity. The four primary design parameters that affect the acoustical performance of a porous pavement are the layer thickness, porosity (percent voids), flow resistivity through the pores, and the tortuosity. The term “tortuosity” refers to the path through the pores and is also referred to as “structural” factor or “shape” factor. The thickness and tortuosity are crucial in centering the peak performance frequency (e.g., typically around 1 kHz for passenger vehicles), whereas porosity and flow resistivity are key in determining the absorption coefficient. Test procedures are available for these pore parameters, either in situ or with core samples.
- **Other Factors.** Other pavement factors that may affect tire noise that are not addressed in this report as they are outside the scope of our analysis include: adhesion between the tire and the pavement, tining of concrete pavements, air pumping as air is squeezed out of tire tread gaps, and resonating tread blocks caused by roadway impacts.

II. DISCUSSION OF RESEARCH TO-DATE

The relevant research into tire noise is quite extensive, extending over thirty years and involving an international group of investigators. However, definitive findings of the role of pavement design characteristics remain somewhat elusive, a consequence of the complexity of the overall tire noise problem. A recent and comprehensive review of general tire noise research can be found in Ref. 1*, *Tyre/Road Noise Reference Book* by Sandberg and Ejsmont. In this reference, the role of pavement design is summarized (reproduced below as Table 1) and candidly described

* References for Garrelick memo are listed separately on page 163.

as “Road surface characteristics known or believed to affect tyre/road noise emissions.” Our discussion focuses on surface texture, stiffness (or impedance), and porosity.

Table 1. Parameters with a potential influence on tire/road noise
(reproduced from Table 11.1 of Ref .1)

No.	Parameter	Degree of Influence
1	Macrotexture	Very High
2	Megatexture	High
3	Microtexture	Low-moderate
4	Unevenness	Minor
5	Porosity	Very High
6	Thickness of Layer	High, for porous surfaces
7	Adhesion (normal)	Low/moderate
8	Friction (tangent)	See microtexture
9	Stiffness	Uncertain, moderate

Texture

Three categories of texture are often distinguished according to wavelengths as follows:

<u>Category</u>	<u>Wavelengths</u>	<u>Peak Amplitude</u>
Microtexture	< 0.5 mm <0.02 inches	0.01 to 0.5 mm 0.0004 to 0.02 inches
Macrotexture (wavelengths on order of tread elements)	0.5 to 50 mm 0.02 to 2 inches	0.1 to 20 mm 0.004 to 0.8 inches
Megatexture (wavelengths on order of tire-pavement contact patch)	50 to 500 mm 2 to 20 inches	0.1 to 50 mm 0.004 to 2 inches

The correlation of tire noise to texture is ambiguous. For example, a compendium of 23 measurements using ISO compatible metrics, Mean Depth Profile (MDP) for texture and Close Proximity Index (CPXI) for noise level, show a strong correlation for only very rough surfaces (reproduced/modified from Ref. 2 in Fig. 1). Oriented texture achieved through tining or grooving, also affects noise levels. Transverse orientation tends to increase noise levels while longitudinal striations can be beneficial.

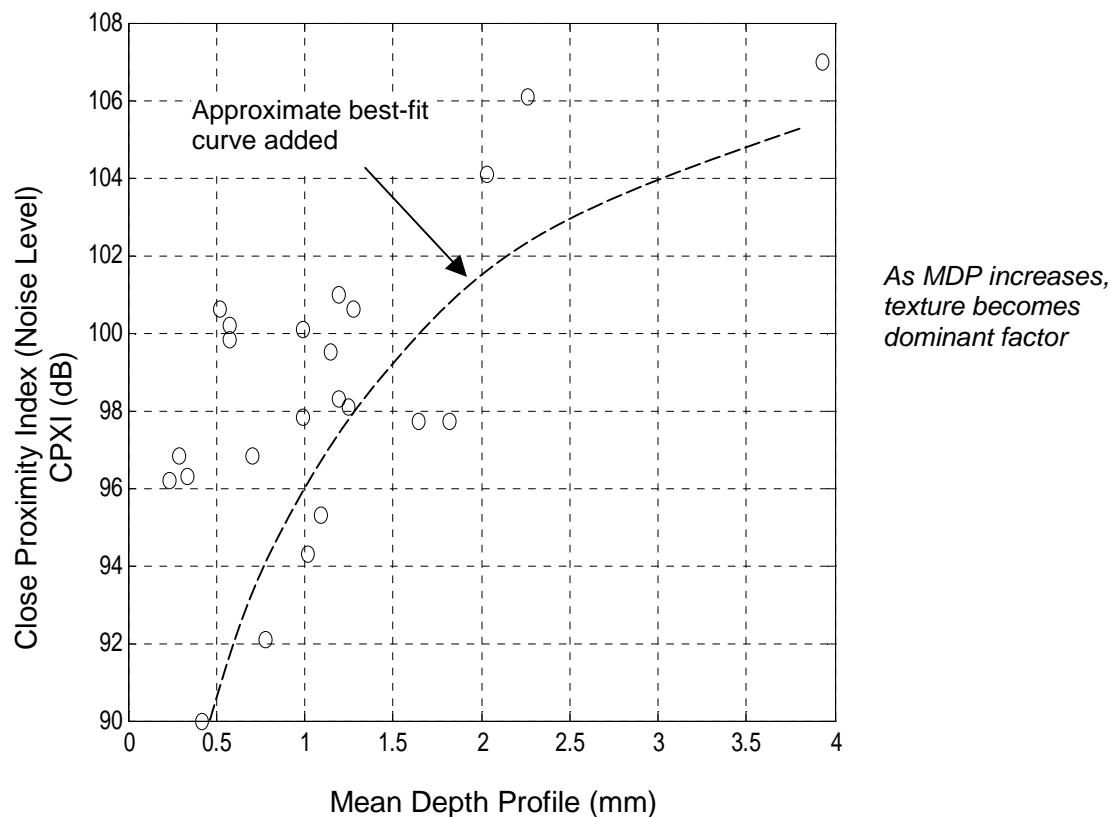


Fig. 1. Tire/road noise level versus road texture for 23 various surfaces (reproduced/modified from Fig. 6 of Ref. 2.)

Stiffness

We next consider the effective hardness, or stiffness of the surface (i.e. its reactive impedance). Typical pavements consist of stones, sand, filler and binder, in various proportions. Variations in stiffness are commonly attributed to variations in the binder material(s). For example, bitumen or “asphalt” binders are relatively flexible in relation to portland cement binders. To enhance the mechanical performance of the binder, fibers, plastic, and rubber have also been added. Certain measurement projects, perhaps unpublished, and involving pavements with alternate binders, viz. with rubber additives, apparently suggest a substantial influence on noise. However, as noted in Ref 1, “...where a direct comparison has been possible between the binder effects, no influence on noise has been demonstrated.” For example, Sandberg and Ejsmont report that they conducted controlled tests on “...surfaces with and without 8% of rubber powder added to the binder and found no significant noise difference.” They also note similar studies for binders with and without added fibers and for cement and bitumen binders. (On the other hand, a “plastic” binder is reported to have yielded a 1 dB relative reduction.) Thus, the acoustical benefits attributed to differences in binders and in turn “stiffness”, are more likely associated with related pavement characteristics that also varied during testing, e.g. porosity.

Porosity

The potential benefits of porous pavements are twofold, (1) a reduction in the source strength of tire-pavement noise mechanisms and (2) an enhanced propagation loss across the pavement at grazing angles. Noise data for porous pavements generally encompass both effects, and are complicated by the propagation loss being strongly dependent on overall roadway-receiver geometry. Nevertheless, measurements indicate that: “A new porous pavement can produce a 3-5 dB reduction, or more, in A-weighted sound level with respect to nonporous pavements.” [Ref 3] Data showing measured reductions along with the relative contributions of the source and propagation effects are reproduced here from Ref. 1, in Fig. 2. These results are believed to be typical (see Section III), with a broad peak in performance at a frequency depending principally on the porosity and layer thickness. Finally, it should be noted that the overall acoustic benefits of porosity may also be affected, positively or negatively, by the extent to which porosity influences surface texture.

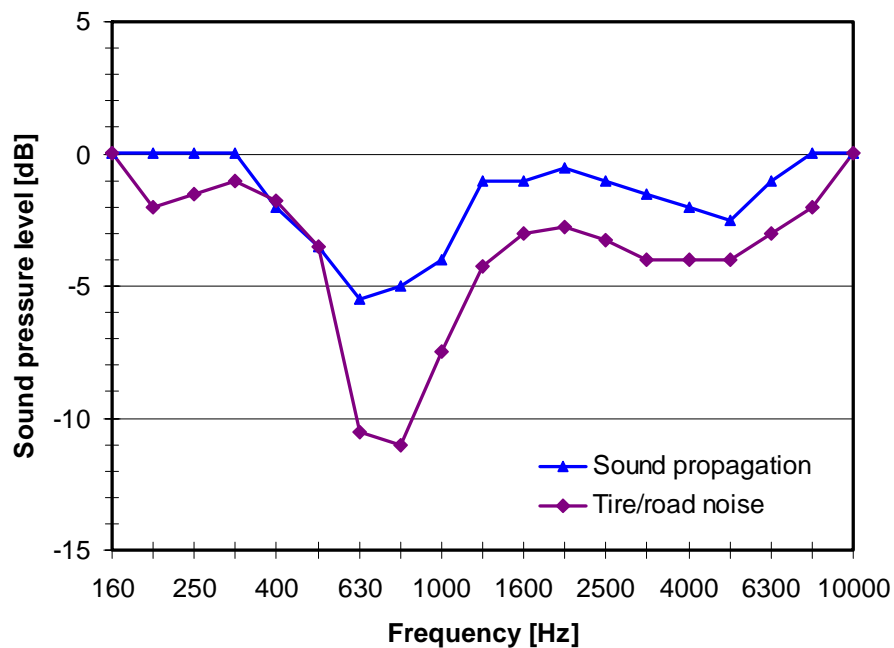


Fig. 2. Measured reductions in tire/road noise with porous versus dense asphalt pavements. Also shown is the reduction component attributable to propagation.
Data averaged over three tire types.
[Reproduced from Ref. 1, Fig. 11.34]

III. STRUCTURAL-ACOUSTIC MODEL INSIGHTS

The effects of roadway pavement design on both the intensity of tire noise sources and the propagation efficiency of such sources are addressed separately in the following sections.

A. Acoustic Propagation over an Elastic/Porous Surface

The issue of propagation efficiency is addressed in this section by considering the idealized mathematical model of noise from a compact (point) acoustic source propagating over a planar boundary (Fig. 3). The boundary is characterized by its normal impedance and may be wave bearing, contain pores, and of finite thickness.

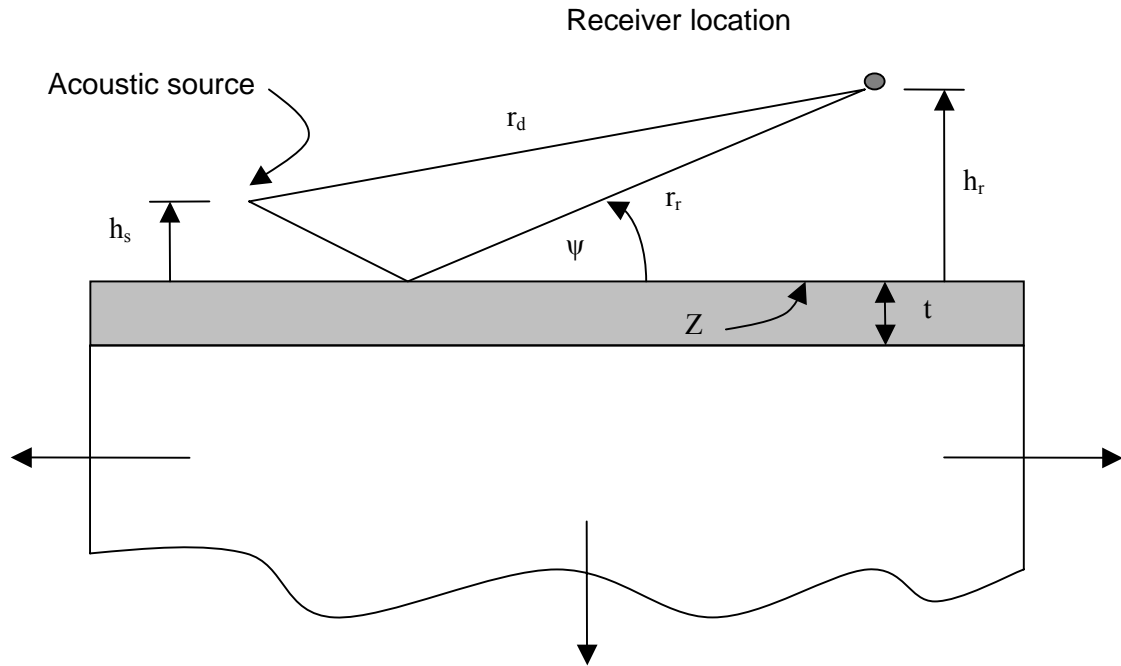


Fig. 3. Idealized geometry for a compact acoustic source propagating over an elastic/porous half space

Refs 3, 4 give the harmonic pressure propagated by a unit source over a locally reacting half space with impedance Z as:

$$p(r, \psi) = \frac{\exp(ikr_d)}{r_d} + \frac{\exp(ikr_r)}{r_r} [(1 - R_p)F + R_p] \quad (\text{A1})$$

where r_d and r_r are the direct and reflected ray path lengths, $k = \omega/c$ is the acoustic wavenumber with $\omega = 2\pi f$ circular frequency, c sound speed, ψ is the incident angle on the ground of the specular ray reaching the receiver, the reflection coefficient

$$R_p = (1 - \rho c / Z \sin \psi) / (1 + \rho c / Z \sin \psi) \quad (\text{A2})$$

and

$$F = 1 + 2iw^{1/2} \exp(-w) \int_{-iw^{1/2}}^{\infty} \exp(-u^2) du \quad (A3)$$

with

$$w = ikr_r [\sin \psi + \rho c / Z]^2 / 2 \quad (A4)$$

In the limiting case of $r_r \rightarrow \infty$, $F \rightarrow 0$, and in the limit of $Z \rightarrow \infty$, $F \rightarrow 1$.

With an acoustic wave bearing ground medium, Eqs. A1-A4 still holds but now:

$$Z \rightarrow Z / \chi \quad (A5)$$

with

$$\chi = [1 - (k / k_g)^2 \cos^2 \psi]^{1/2}$$

where the ground wavenumber $k_g = \omega / c_g$ with c_g the effective ground sound speed.

With a finite thickness surface stratum of thickness t ,

$$Z = Z_c \frac{[Z_{term} / (Z_c / \chi)] - i \tan(kt)}{1 - [Z_{term} / (Z_c / \chi)] \tan(kt)} \quad (A6)$$

where Z_c is the characteristic impedance of the layer (the product of effective sound speed and mass density), and Z_{term} its termination impedance. Wenzel [Ref. 5] expresses Eq. A1 more insightfully as

$$p(r, \psi) = \frac{\exp(ikr_d)}{r_d} + \frac{\exp(ikr_r)}{r_r} - \frac{\exp(ikr)}{r} \left[2 + \frac{ik}{\gamma^2 r} (2 - 2\gamma h + (\gamma h)^2 + O(r^{-2})) \right. \\ \left. + \varepsilon i 2\pi \gamma \exp(-\gamma h) H_0^{(1)}[\sqrt{k^2 + \gamma^2} r] \right] \quad (A7a)$$

or

$$p(r, \psi) = \frac{\exp(ikr_d)}{r_d} + \frac{\exp(ikr_r)}{r_r} - \frac{\exp(ikr)}{r} \left[2 - \frac{i}{\bar{Y}^2 k r} (2 - 2i\bar{Y}kh - (\bar{Y}kh)^2 + O(r^{-2})) \right. \\ \left. - \varepsilon 2\pi k \bar{Y} \exp(-ikh\bar{Y}) H_0^{(1)}[kr\sqrt{1 - \bar{Y}^2}] \right] \quad (A7b)$$

provided that

$$kh(h/r) \ll 1, \quad (A8a)$$

and

$$|\gamma| (r/k)^{1/2} \gg 1 \quad (\text{A8b})$$

where $h = h_s + h_r$, $r \cong (r_d + r_r) / 2$, and $\gamma = ik\bar{Y} = ik(Z / \rho c) \equiv \alpha + i\beta$. (It follows that $\bar{Y} \equiv \beta/k - i\alpha/k$ and the inequality in Eq. A8b may be expressed equivalently as $|\bar{Y}| (kr)^{1/2} \gg 1$)

For source and receiver on the ground, $r \cong r_d \cong r_r$, the first two terms are cancelled by the leading term of the expansion and Eq. A7a becomes

$$p(r, \psi) = \exp(ikr) \left[\frac{ik}{(\gamma r)^2} [2 - 2\gamma h + (\gamma h)^2] + \varepsilon i 2\pi\gamma \exp(-\gamma h) H_0^{(1)}[\sqrt{k^2 + \gamma^2} r] \right] \quad (\text{A9})$$

The first term is a “ground” wave and it attenuates as r^{-2} . The second term is a “surface” wave that decreases with height as $\exp(-\gamma h)$, and with distance as $r^{-1/2}$. It exists ($\varepsilon = 1$) provided that

$$\beta \geq 0 \quad (\text{A10a})$$

and

$$0 \leq \alpha \leq \beta / \sqrt{1 + (\beta/k)^2} \quad (\text{A10b})$$

or equivalently $\text{Re}\{k\bar{Y}\} \geq 0$ and $0 \leq -\text{Im}\{\bar{Y}\} \leq \text{Re}\{\bar{Y}\} / \sqrt{1 + [\text{Re}\{\bar{Y}\}]^2}$. Otherwise $\varepsilon = 0$.

Eqs. A10 ensure that the phase velocity of the surface wave in the far field is subsonic, since $\text{Re}\{\sqrt{k^2 + \gamma^2}\} > k \rightarrow k^2(\alpha^2 - \beta^2) + \alpha^2\beta^2 > 0$. Also, since $\beta - i\alpha = k\rho c Y$, this requires a passive, stiffness-like, boundary.

To accommodate the above analysis to a porous boundary, one utilizes a relatively simple phenomenological model that characterizes a porous medium as a dissipative compressive fluid [Ref. 3]. The effective complex density and bulk modulus are given by

$$\rho_g = \rho_0 q^2 (1 + i f_\mu / f) \quad (\text{A11})$$

and

$$K_g = \gamma P_0 \left[1 + \frac{\gamma - 1}{1 - i f / f_\theta} \right]^{1/2} \quad (\text{A12})$$

where the viscous term $f_\mu = \Omega R_s / 2\pi\rho_0 q^2$ and the thermal term $f_\theta = R_s / 2\pi\rho_0 N_{pr}$.

In these equations P_0 is ambient atmospheric pressure, γ is the specific heat ratio, N_{pr} is the Prandtl number, R_s is the flow resistivity of the porous structure, Ω is the porosity of the air-filled (connected) pores, and q^2 is the tortuosity (structural factor).

The associated complex wave-number and characteristic impedance are

$$k_g = k_0 q F_\mu^{1/2} \left[\gamma - \frac{\gamma - 1}{F_\theta} \right]^{1/2} \quad (\text{A13})$$

and

$$Z = (\rho_0 c q / \Omega) F_\mu^{1/2} \left[\gamma - \frac{\gamma - 1}{F_\theta} \right]^{-1/2} \quad (\text{A14})$$

with $F_\mu = 1 + i f_\mu / f$.

With the above model, and for a given layer thickness t , three input parameters are required, R_s , Ω , and q^2 . In Ref. 3 the flow resistivity was computed from (ISO 9053) measurements of the flow resistance on a sample of area S and thickness l , i.e. $R_s = RS/l$. Values of Ω , the porosity of the air-filled (connected) pores, were measured using gamma ray dosimetry. (Although such data include obstructed as well as connected pores, it is argued that with aggregate greater than 10 mm the former is less than 5% by volume.) Finally, values of the tortuosity, q^2 , were obtained indirectly from curve fitting absorption measurements on a sample, in a free-field or pulse tube, especially the frequency position of the resonant peak. (Two other parameters suggested by a micro-structural model, thermal pore and material viscosity “shape factors” were found to be of minor significance. [Ref. 6])

An example is presented in Ref. 3 for a sample with a resonant peak at 1 kHz, $t = 4\text{cm}$, $q^2 = 2.5$, $\Omega = 15\%$, and $R_s = 15,000 \text{Ns/m}^4$. This is reproduced here as Fig. 4. An absorption coefficient of almost unity is obtained within a bandwidth of roughly 400 Hz centered around 1.2 kHz.

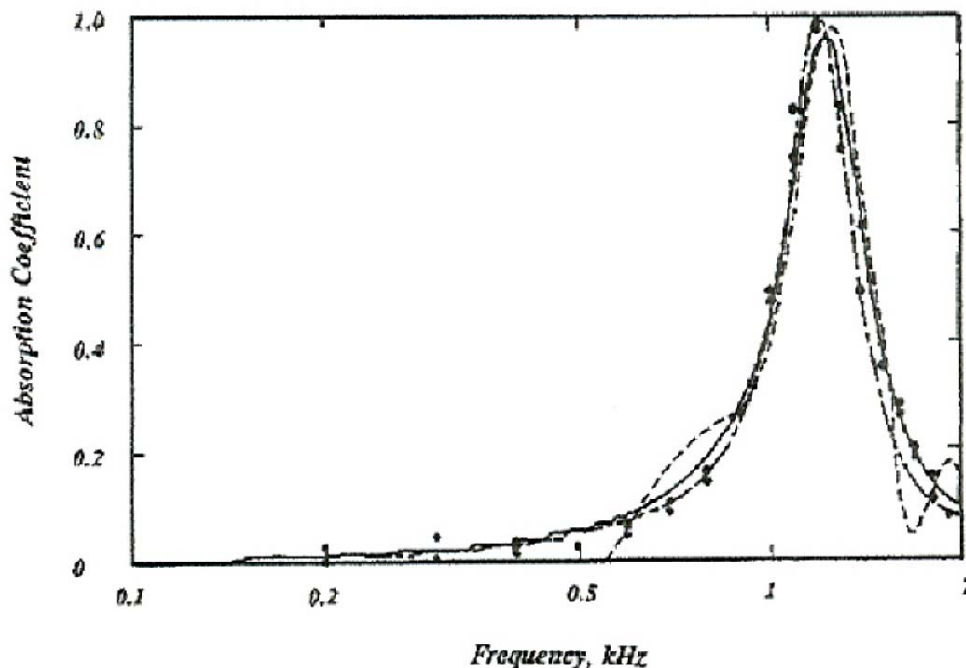


Fig. 4. Absorption coefficient results obtained by different approaches for a 10 cm diameter and 4 cm thick porous pavement sample:

- standing wave tube measurements
- theoretical prediction using phenomenological model,
- theoretical prediction using a micro-structural model

[Reproduced from Fig. 2 of Ref. 3]

Additional model calculations have been performed for this report in order to explore the relationship between acoustic performance and source-receiver geometry and pavement design characteristics. For this purpose, predictions will be presented in terms of the excess reduction in noise level relative to that with a perfectly rigid surface. The basic porosity design is as above, with $t = 4$ cm, $q^2 = 2.5$, $\Omega = 15\%$, and $R_s = 15,000$ Ns/m⁴.

First to illustrate the issue of geometry, two source heights above the pavement are considered, $h_s = 0$ and 0.2 m. The receiver height is kept constant at $h_r = 2$ m, (with reciprocity dictating that h_s and h_r are interchangeable). Results are presented in Fig. 5. The four curves in each panel refer to differing horizontal stand-off distances of the receiver, viz. 2 m, 5 m, 10 m and 20 m. The exact level of performance clearly varies with source-receiver geometry, although the fundamental performance, i.e. that in the vicinity of the fundamental thickness natural frequency of the porous layer, is reasonably robust.

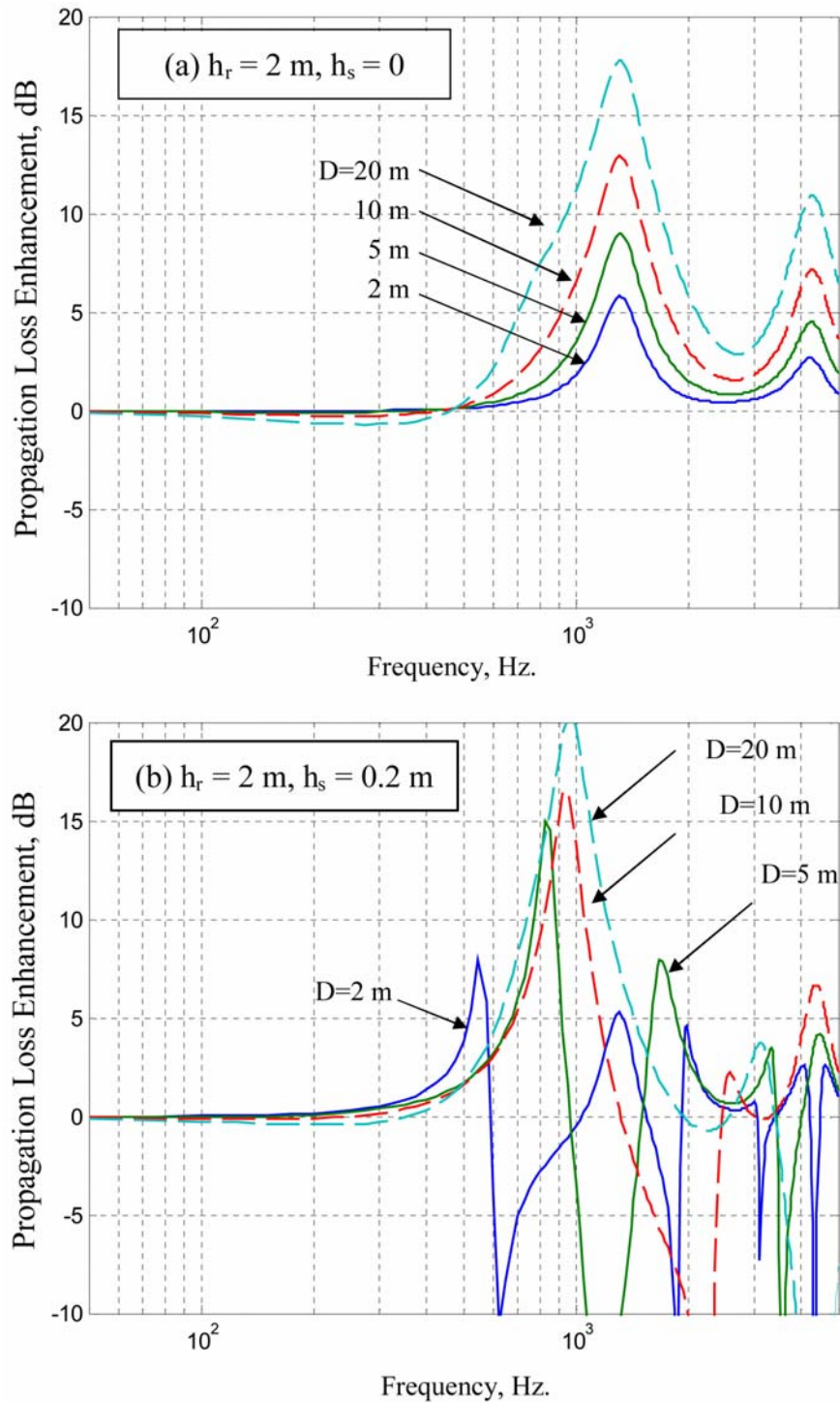


Fig. 5. Calculated propagation loss enhancement of porous pavement design relative to an effectively rigid surface: Influence of source height and receiver stand-off distance

With the source positioned off the surface (lower panel in Fig. 5), and especially at the higher frequencies, interference between the direct and reflected paths is prominent. (For perspective, the height (h_s) measures $\frac{1}{2}$ acoustic wavelength in air at about 850 Hz.)

The influence of varying the thickness of the porous layer is shown in Fig. 6. Thickening the layer has the effect of lowering the center frequency of peak performance and the value of peak performance, at the same time increasing performance bandwidth. This is the case up to the asymptotic limit of a semi-infinite layer.

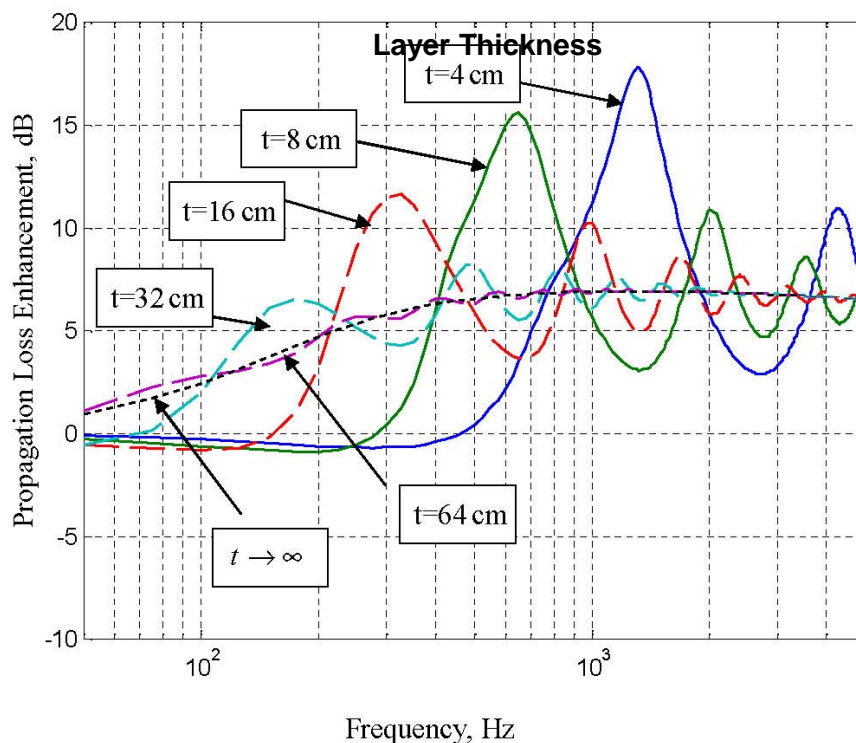


Fig. 6. Calculated propagation loss enhancement of porous pavement design relative to an effectively rigid surface: Influence of layer thickness ($D=20$ m, $h_s=0$, $h_r=2$ m)

In Figs. 7, 8, and 9 we show the effects of changing the resistivity, percent porosity, and tortuosity, respectively. Increases in resistivity lower and broaden peak performance while porosity tends to increase and broaden performance, although it is noted that the analysis is applicable only to moderate values of Ω . An increase in tortuosity lowers the frequency of peak performance much like an increase in layer thickness.

Finally, our discussion to this point has been limited to the acoustic performance of a single porous layer, that is, a layer whose properties are constant across its thickness. We now explore performance with multi-layers, specifically a two-tiered surface. The analysis follows the general format presented earlier, but here with Eq. A.6 cascaded in the fashion of a transmission line. To illustrate, we return to a basic layer with total thickness $t = 4$ cm and porosity $\Omega = 15\%$, but now also consider two-tier configurations with each tier 2 cm thick. The tortuosity and resistivity of each layer have values of $q^2=1$ or $q^2=4$ and $R_s = 15,000$ Ns/m⁴ or $R_s = 3*15,000$ Ns/m⁴. As with the single layer, the second, or bottom, layer is terminated with an effective rigid boundary.

Results are compared in Figs. 10. It is observed that for the (albeit limited) variations considered, there is no apparent performance gain over the uniform layer when the total thickness is kept constant.

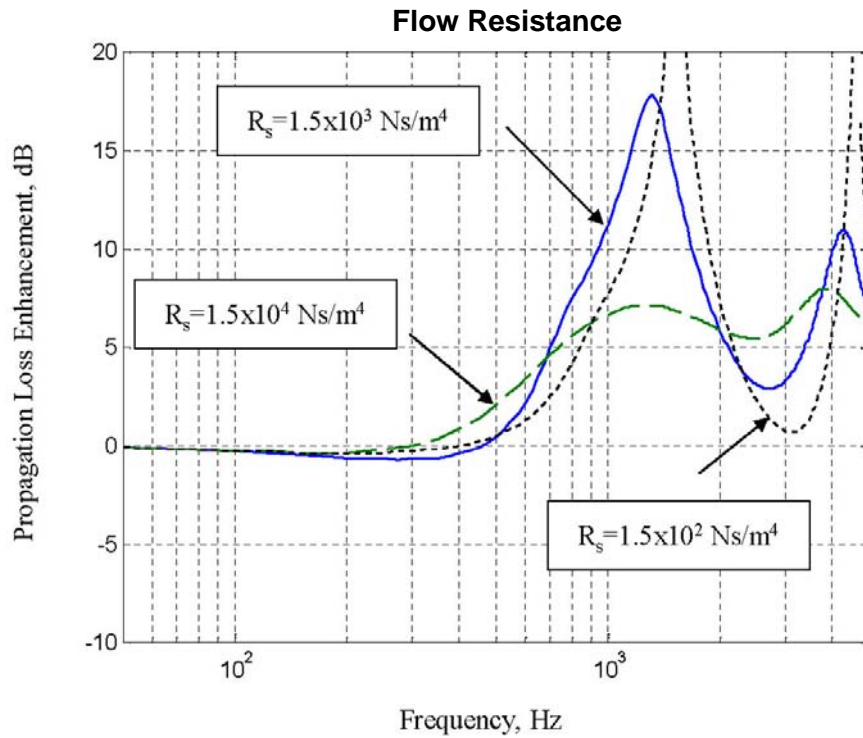


Fig. 7. Calculated propagation loss enhancement of porous pavement design relative to an effectively rigid surface: Influence of flow resistance ($D=20 \text{ m}$, $h_s=0$, $h_r=2 \text{ m}$)

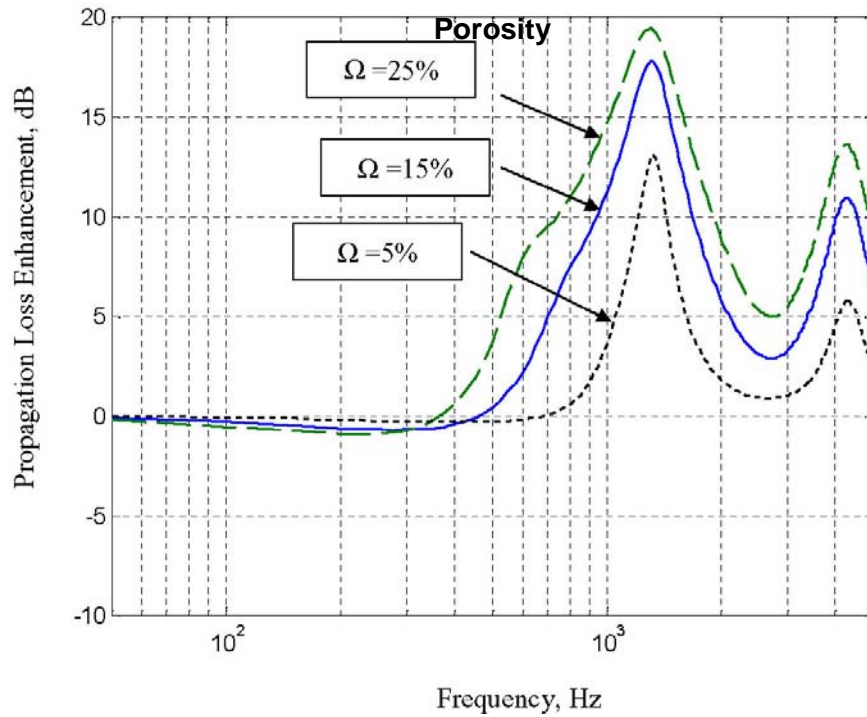


Fig. 8. Calculated propagation loss enhancement of porous pavement design relative to an effectively rigid surface: Influence of porosity ($D=20$ m, $h_s=0$, $h_r=2$ m)

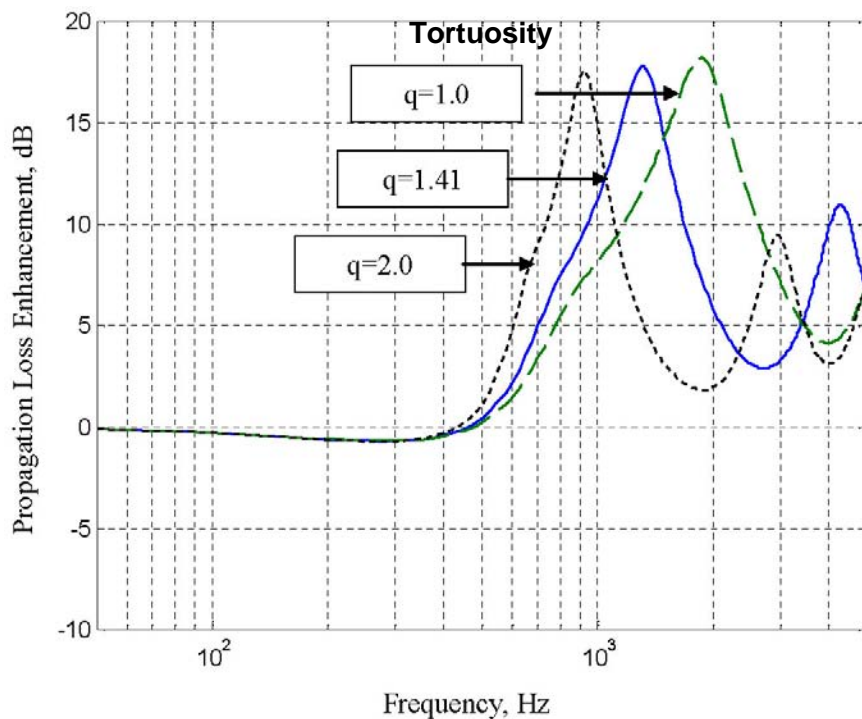


Fig. 9. Calculated propagation loss enhancement of porous pavement design relative to an effectively rigid surface: Influence of tortuosity ($D=20$ m, $h_s=0$, $h_r=2$ m)

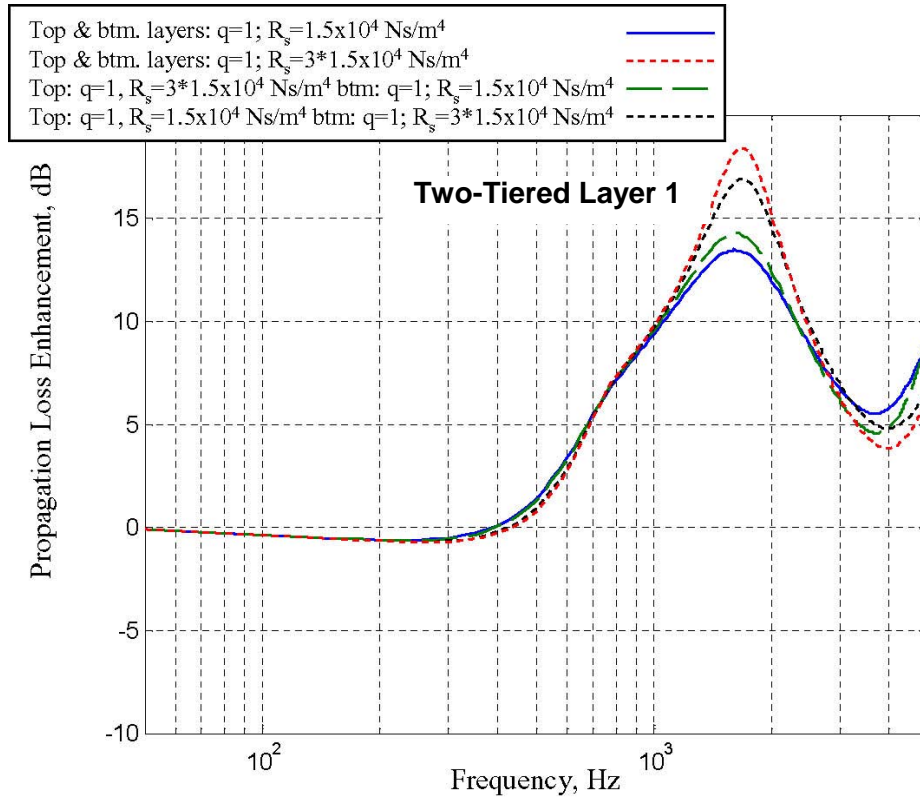


Fig. 10a. Calculated propagation loss enhancement of porous pavement design relative to an effectively rigid surface: Influence of two tiered layer ($D=20 \text{ m}$, $h_s=0$, $h_f=2 \text{ m}$)

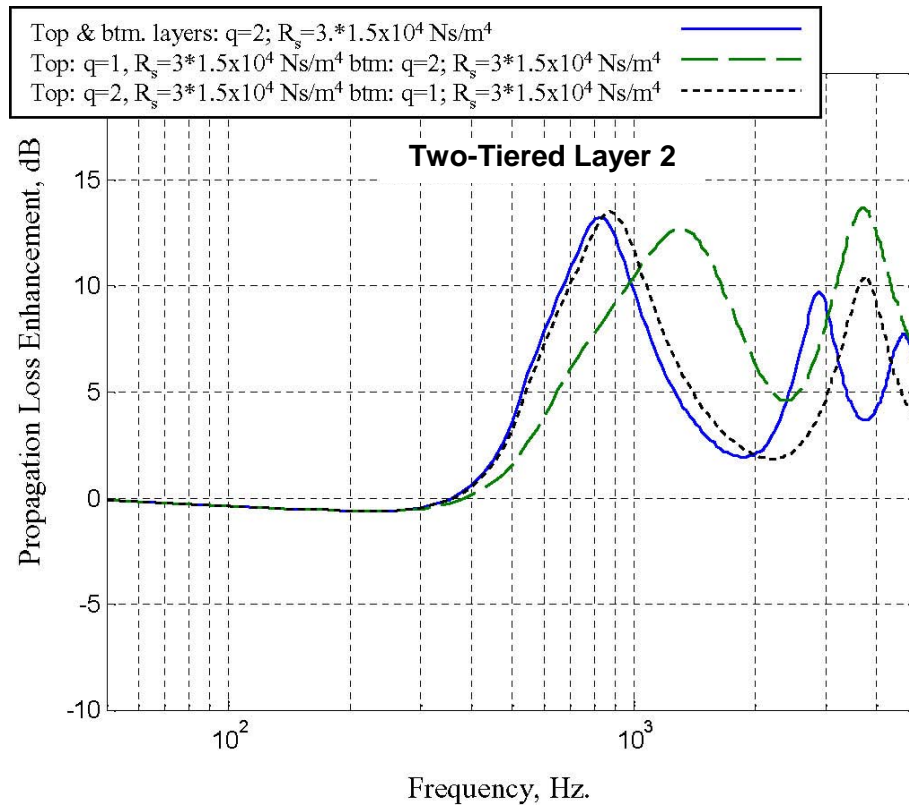


Fig. 10b. Calculated propagation loss enhancement of porous pavement design relative to an effectively rigid surface: Influence of two-tiered layer ($D=20 \text{ m}$, $h_s=0$, $h_f=2 \text{ m}$)

B. Radiation from Tire-Pavement Vibrations

In this section, we consider the influence of roadway pavement on the source strength of certain tire noise mechanisms, rather than on their propagation characteristics. Our focus is radiation from interface force-induced vibrations, both tire and pavement. Ignoring the effects of surface porosity and finite layer thickness, we consider the idealized model of radiation from the vibrations of a viscoelastic, planar, half space driven by a compact harmonic force [Fig. 11]. The noise field may be expressed in terms of the (Fourier) wavenumber transformed normal response of the surface. [Ref 7]

$$|p_{rad}(R, \theta; \omega)| R / F = \frac{(2\pi)^{-2} (c_{air} / c_{shr})^4 (\omega / c_{air}) \sqrt{\sin^2 \theta - (c_{air} / c_{dil})^2}}{[2 \sin^2 \theta - (c_{air} / c_{shr})^2]^2 - 4 \sqrt{\sin^2 \theta - (c_{air} / c_{dil})^2} \sqrt{\sin^2 \theta - (c_{air} / c_{shr})^2}} \quad (B1)$$

where θ is elevation angle, R range, the ratio p_{rad}/F is the radiated pressure normalized to the applied force (F), c_{air} is the sound speed in air, c_{dil} and c_{shr} the dilatational and shear speeds in the pavement, and ρ_{air} is air density.

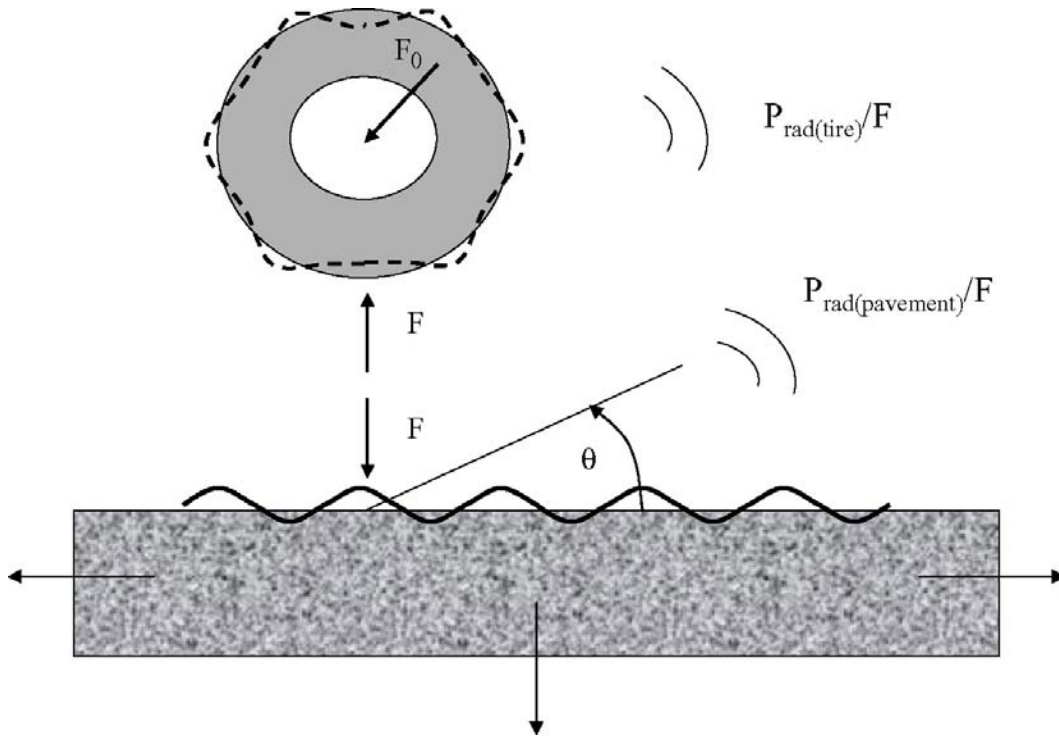


Fig. 11. Radiation from tire-pavement vibrations in response to interaction forces

At grazing, $\sin^2 \theta \rightarrow 1$, and Eq. B1 reduces to

$$|p_{rad}(R, \theta; \omega)| R / F = \frac{(2\pi)^{-2} (c_{air} / c_{shr})^4 (\omega / c_{air}) \sqrt{1 - (c_{air} / c_{dil})^2}}{[2 - (c_{air} / c_{shr})^2]^2 - 4 \sqrt{1 - (c_{air} / c_{dil})^2} \sqrt{1 - (c_{air} / c_{shr})^2}} \quad (B2)$$

with the shear and dilatational speeds given by

$$c_{shr} = \sqrt{\frac{G}{\rho}} \quad \text{and} \quad c_{dil} = c_{shr} \sqrt{\frac{4 - E / G}{3 - E / G}} > c_{shr}.$$

Viscous effects are taken into account by allowing for complex wave speeds, viz.,

$c_{shr} \rightarrow c_{shr} (1 - i\eta_{shr})^{1/2}$ and $c_{dil} \rightarrow c_{dil} (1 - i\eta_{dil})^{1/2}$ with η_{shr} and η_{dil} effective loss factors. For acoustically “slow” pavements (c_{air} / c_{dil}), (c_{air} / c_{shr}) $\gg 1$, and at grazing, Eq. B2 becomes

$$|p_{rad}(R, \theta = \pi / 2; \omega)| R / F \cong (\omega / c_{dil}) / (2\pi)^2 \quad (B3)$$

For acoustically “fast” pavements, which will typically be the case, (c_{air} / c_{dil}), (c_{air} / c_{shr}) $\ll 1$ and again at grazing, we have

$$|p_{pvnnt}(R, \theta = \pi / 2; \omega)| R / F \cong [(\omega / c_{dil}) / (2\pi)^2] (c_{air} / c_{shr})^2 / 4 \quad (B4)$$

For a crude evaluation of the corresponding radiation from this interaction force driving the tire casing (a detailed analysis is quite complex and well beyond the present scope [Ref. 8]), we express the admittance at the natural frequency of a hypothesized natural vibration mode of the tire as

$$|v_{tire} / F|_{\omega=\omega_{res}} = \frac{1}{\omega_{res} (mS)_{tire} \eta} \quad (B5)$$

and the associated radiation as

$$\begin{aligned} |p_{tire}(R, \theta; \omega_{res})| R / F &= (\rho_{air} \omega_{res} / 2\pi) (vS)_{tire} / F \\ &= (\rho_{air} / m_{tire}) / 2\pi\eta \end{aligned} \quad (B6)$$

where m_{tire} is the effective tire mass per unit surface area, S_{tire} is the effective surface area of the tire casing, η the effective dissipation (loss) factor of the resonant tire mode, and v_{tire} is the average resonant casing velocity at the natural frequency $\omega_{res} = 2\pi f_{res}$.

From Eqs. B5 and B6

$$\left| \frac{p_{pvmnt}(R; \omega_{res.})}{p_{tire}(R; \omega_{res.})} \right| = (\omega_{res.} t_{tire} / c_{dil})(c_{air} / c_{shr})^2 \eta (\rho_{tire} / \rho_{air}) / 8\pi \quad (B7)$$

Taking the casing thickness to be small in terms of the dilatational wavelength, we estimate $\omega_{res.} t_{tire} / c_{dil} = O(10^{-1})$. Also, for typical rubbers, $(c_{air} / c_{shr})^2 = O(10^{-2})$ and $\rho_{tire} / \rho_{air} = O(10^3)$. Thus, the order of magnitude of Eq. B7 becomes

$$\left| \frac{p_{pvmnt}(R; \omega_{res.})}{p_{tire}(R; \omega_{res.})} \right| = O(10^{-1})\eta \ll 1$$

In other words, we conclude that radiation from pavement vibrations driven by tire-pavement interaction forces is insignificant relative to that radiated by (resonant) tire-casing vibrations.

C. Pavement Stiffness

We now address an issue concerning the parametric dependence of the interaction force magnitude itself. While the detailed dynamics of the tire-pavement interaction are clearly beyond the scope of this report [Ref. 8, 9], a number of generic conclusions are suggested from the consideration of highly idealized, elementary models and insights.

First, consider the relative magnitude of the harmonic interaction force(s) between the tire and pavement. It is assumed that the “ultimate source” mechanically drives the tire elsewhere, e.g. through the tire hub, and that the tire and pavement remain in contact over a specified and compact contact area. It follows that the interaction forces on the tire are equal (and opposite) to those on the pavement, and may be expressed as

$$\vec{F}_{Interface} = \frac{V_0 \vec{Z}_{Tire} \vec{Z}_{Pavement}}{\vec{Z}_{Tire} + \vec{Z}_{Pavement}} = \frac{V_0 \vec{Z}_{Tire}}{1 + \vec{Z}_{Tire} / \vec{Z}_{Pavement}} \quad (C1)$$

where V_0 represents the actual drive source strength (taken to be pavement invariant) and Z_{tire} and $Z_{pavement}$ denote the interface drive impedances of the tire and pavement, respectively, with the arrow over-score indicating a direction vector. Under the premise that typically, along any given direction, the impedance of the pavement greatly exceeds that of the tire, Eq. C1 reduces to

$$\vec{F}_{interface} \cong V_0 \vec{Z}_{tire} \quad (C2)$$

In other words, the magnitude(s) of the interface drive force(s) are invariant to pavement characteristics, viz., its normal impedance or “stiffness”. This is consistent with the above mentioned findings from Ref.1 indicating that pavement stiffness has not been shown to affect sound levels.

D. Pavement Texture

Next, we consider the potential influence of pavement texture, or roughness, as a source of tire vibration and in turn, noise. Here, it is again supposed that the pavement is essentially rigid relative to the flexible tire and contact is maintained. (The influences of air turbulence and pumping mechanisms are also ignored.) Consequently, the pavement profile is impressed onto the tire over a specified contact area, generating harmonic forces that drive the tire. Representing the pavement texture as a packed grid of intruding hemispheres of radius a , assuming that each such hemisphere generates an uncorrelated force on the tire proportional to the indentation, i.e. radius, and that the tire surface is smooth, the overall rms force becomes

$$F_{texture}^2 = [K_t a]^2 [S/(2a)^2] = K_t^2 S/4 \quad (D1)$$

where S is the contact area, and K_t the effective dynamic stiffness of the tire. The first term in brackets is the magnitude of the individual forces, and the second is the number of such forces. Note that Eq. D1 actually turns out to be invariant to a , the characteristic roughness scale, at least under the assumption of a smooth, e.g. worn, tire. This is consistent with Sandberg's rejection of the "myth" that "the coarser the texture, the higher the noise emission becomes" [Ref. 2]. Also, since Eq. D1 indicates a 6 dB per doubling of contact width, and in turn area, it is also consistent with the comment in Ref. 2 that "the width of the tire is a very influential factor" and, roughly, the observation that a regression analysis of data is linear with a logarithmic width scale and a change from 155 mm to 195 mm tires would mean almost 2 dBA of noise increase (viz $10 \times \log(195/155) \cong 1 \text{ dB}$).

Pursuing the issue further, tire casing vibrations are dominated by length scales associated with compressional, shear, and flexural wavelengths in the sidewall and perhaps the acoustic wavelength of the enclosed air volume [Refs. 8, 9]. Of these, only flexure is dispersive, at least to first order, and it provides the shortest wavelength at frequencies of interest.

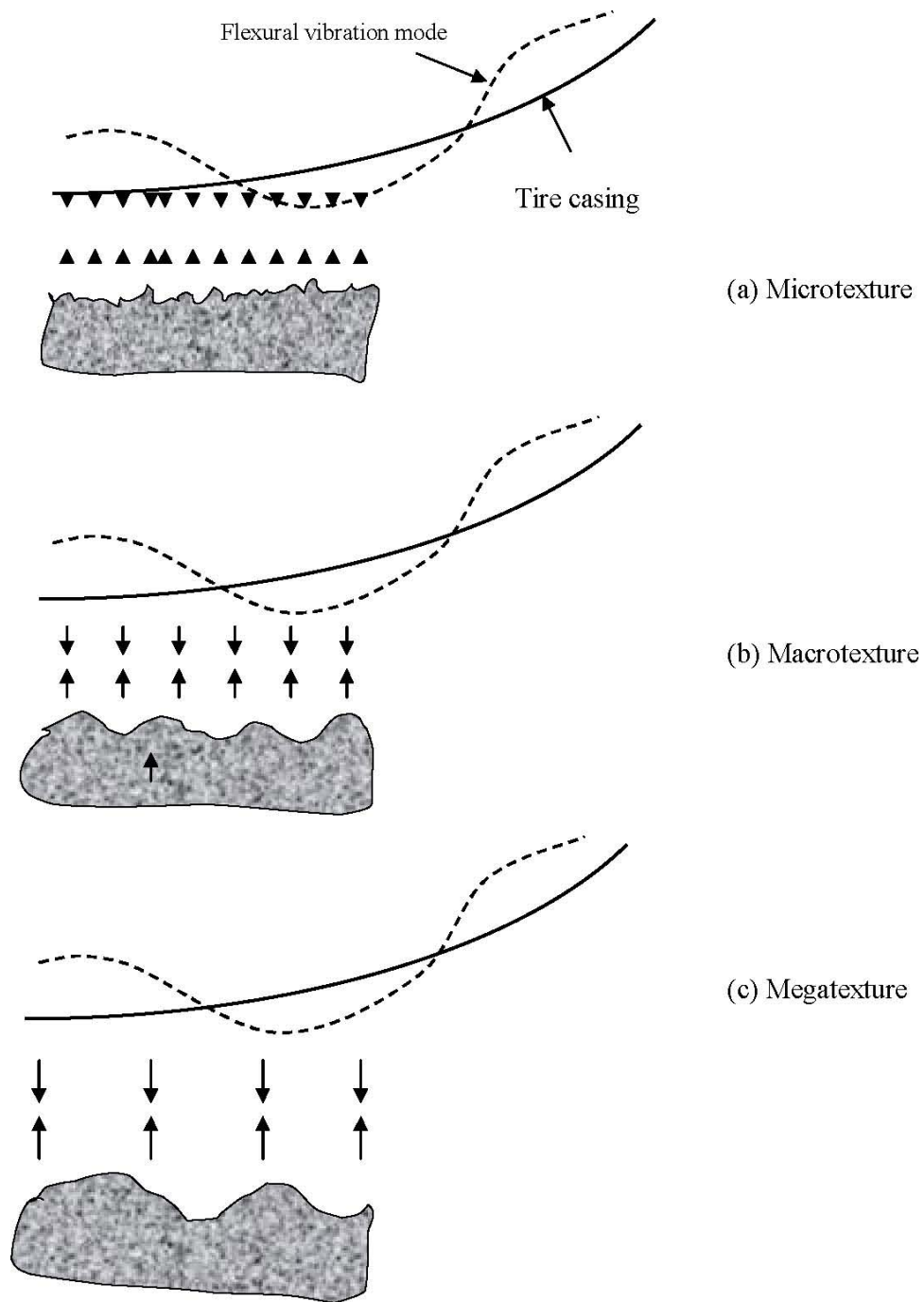


Fig. 12. Illustration of texture length scales relative to (flexural) wavelength in tire casing

To illustrate, taking $G = 4.9 \times 10^8 \text{ N/m}^2$, and $\rho \cong 1.2 \times 10^3 \text{ kg/m}^3$, we have $c_{shr} \cong 200 \text{ m/s}$ and $\lambda_{shr} (m) \cong 0.2 / f (kHz)$ with $E \cong 3G$, $c_{comp} \cong 340 \text{ m/s}$ and $\lambda_{comp} (m) \cong 0.34 / f (kHz)$.

Using the simplest Euler bending model, the wavelength of flexural waves is

$\lambda_{flex} \cong (2\pi / 12^{1/4}) \sqrt{c_{tire} t_{tire} / \omega}$ where c_{tire} is the effective plate speed in the tire sidewall, and t_{tire} is the sidewall thickness. Thus, letting $t \cong 8 \times 10^{-3} \text{ m}$, $c_{flex} \cong 7 \times 10^{-2} \sqrt{f (kHz)} \text{ m/s}$ and

$\lambda_{flex}(m) \cong 7 \times 10^{-2} / \sqrt{f(kHz)}$ or about 70 mm at 1 kHz. Since $c_{air} \cong 340 m/s$, we have flexural waves with phase velocities that are highly subsonic at frequencies of interest (e.g. around 1 kHz), and shear and compressional (membrane) waves that are transonic/supersonic. It is also observed that with frequencies on the order of 1 kHz, the tire-pavement contact area is typically small when measured in terms of (squared) compressional wavelengths, somewhat less so in terms of shear wavelengths, but large with respect to flexural wavelengths. Regardless, each wave type will tend to average over, and thus diminish the relative influence of texture length scales less than say 25% of their characteristic wavelength, e.g. at 1 kHz about 85 mm for compression and 18 mm for flexure. In other words, if a factor at all, one should expect the larger (macro) texture scales to be the more efficient drivers of tire vibrations. This holds for transversely oriented, as well as random, texture. With this simplified view, longitudinally oriented texture, via tining or grooving, is benign. On the other hand, transverse striations, with characteristic spatial scales of macro- or mega-texture, will be more problematic than comparable random texture, being coherent across the tire width.

The situation is more complex for tires that are not deemed smooth, i.e. those with pronounced tread. Here the scale of the tread block likely provides an upper limit on the scales driving the tire vibrations and thus, texture of all scales may be considerably less important. It is noted that Sandberg [Ref 1, Sect 11.5] suggests that tread block impact may dominate the overall tire noise levels in the vicinity of a cut-off frequency $f_c \cong 1 kHz$, with lower frequency levels increasing with pavement texture wavelengths in the range of 10 to 500 mm (0.4 to 20 inches) and with higher frequency levels decreasing with pavement texture wavelengths in the range of 0.5 to 10 mm (0.02 to 0.4 inches). The latter is related to the influence of texture on air displacement mechanisms.

E. Air Pumping

As the tire interacts with the pavement surface and compresses under load, it forces air in and out of pockets in both the tire tread and the road surface. This air pumping potentially affects tire noise and, although well beyond the present scope, is briefly considered below.

The pressure radiated from air pumping in and out of tread interstices may be expressed in the form [Ref. 10]

$$\langle |p|^2 \rangle = Const[(m\delta f_\delta w)V^2 / RS]^2 \quad (E1)$$

where δ is cavity depth, w is cavity width, S the circumferential cavity spacing, V vehicle speed, f_δ the fractional change in cavity volume, m the number of cavities per tire width, and R range. Pavement porosity may have the effect of increasing the radiated pressure levels either by reducing S and in turn increasing the frequency, $\omega = 2\pi V/S$, or, at a constant frequency, by increasing the effective cavity volume displacement, $m\delta f_\delta w$. On the other hand, should the pavement and tread pores line-up, noise levels may be lowered, e.g. by a reduction in f_δ .

TIRE NOISE REFERENCES (Garrelick memo)

1. Ulf Sandberg and Jerzy A. Ejsont, *Tyre/Road Noise Reference Book*, Informex, Sweden, 2002.
2. Ulf Sandberg, "Tyre/road Noise-Myths and Realities," Proceedings 2001 International Congress and Exhibition on Noise Control Engineering, The Hague, August 27-30, 2001.
3. M. C. Berengier, et al., "Porous road pavements: Acoustical characterization and propagation effects," *J. Acoust. Soc. Am.*, 101(1), 1997, 155-162.
4. T. F. W. Embleton, et al., "Outdoor sound propagation over ground of finite impedance," *J. Acoust. Soc. Am.*, 59(2), 267-222, 1976 [Eq. A4 has been corrected. In Embleton et al. (1992), in contrast to Berengier (1997) and Daigle (1979), r_r is printed as r_d].
5. A. R. Wenzel, "Propagation of waves along an impedance boundary," *J. Acoust. Soc. Am.*, 55, 956-963, 1974.
6. Yvan Champoux and Michael Stinson, "On acoustical models for sound propagation in rigid frame porous materials and the influence of shape factors," *J. Acoust. Soc. Am.*, 92(2) 1120-1131, 1992.
7. For example, X. M. Tang, et al., "Radiation patterns of compressional and shear transducers at the surface of an elastic half-space," *J. Acoust. Soc. Am.*, 95(1), January 1994.
8. William Leasure Jr. and Erich Bender, "Tire-road interaction noise," *J. Acoust. Soc., Am.*, 58, 1, July 1975, 39-50.
9. Richard F. Keltie, "Analytical model of the truck tire vibration sound mechanism," *J. Acoust. Soc. Am.*, 71(2), 359-366, 1982. Also, Modeling Tire Noise Treadband Vibration, Yong-Joe Kim and J. Stuart Bolton, *Internoise 2001*, August 27-30 2001, The Hague, Netherlands.
10. Richard Hayden, "Roadside noise from the interaction of a rolling tire with the road surface (A)," *J. Acoust. Soc. Am.*, 49, 113, April, 1971

REFERENCES

1. American National Standards Institute, "Method for the Calculation of the Absorption of Sound by the Atmosphere," ANSI S1.26 (1995). See, also: International Standards Organization for Standards, "Acoustics-Attenuation of sound during propagation outdoors, Part I: Method of Atmospheric Absorption." ISO 9613-1, (1993) and Part 2: General method of calculation" ISO 9613-2, (1994).
2. Attenborough, K, et al., "Benchmark Cases for Outdoor Sound Propagation Models," J. Acoust. Soc. Am. 97 (1), 173-191 (1995).
3. Bronsdon, R.L., and Forschner, H. "A Propagation Model Based on Gaussian Beams that Account for Wind and Temperature Inversions," J. Noise Control Eng, 47(5) Sept.-Oct (1999).
4. Brown, E.H. and Clifford, S.F., "On the Attenuation of Sound by Turbulence," J. Acoust. Soc. Am. Vol. 60, pp. 788-794, 1976.
5. Daigle, G.A., Piercy, J. E. and Embleton, T.F.W., "Line-of-Sight Propagation through Atmospheric Turbulence near the Ground," J. Acoust. Soc. Am., 74, 1505-1513, 1983.
6. Fernando, H.J.S, Lee, S.M., Anderson, J., Princevac, M., Pardyjak, E., Grossman-Clark, S. "Urban Fluid Mechanics: Air Circulation and Contaminant Dispersion in Cities," *Environmental Fluid Mechanics*, pp 107-164, Kluwer Academic Publishers, 2001.
7. Gabillet, Y, Schroeder, H., Daige, G.A. and Esperancea, A.L., "Application of the Gaussian Beam Approach to Sound Propagation in the Atmosphere: Theory and Experiments," J. Acoust. Soc. Am. 93(6), 3105-3116 (1993).
8. Galindo, M. and Havelock, D. I., "Temporal Coherence of a Sound Field in the Turbulent Atmosphere near the Ground," Proceedings, 7th Long Range Sound Propagation Symposium, Ecole Centrale de Lyon, Ecully Lyon, France, 24-26 July 1996.
9. Gilbert, K.E. and White, M.J., "Application of the parabolic equation to sound propagation in a refracting atmosphere," J. Acoust. Soc. Am, 85(2), pp. 630-637 (1989).
10. Gilbert, K, and Di, "A Fast Green's Function Method for One-Way Sound Propagation in the Atmosphere," J. Acoust. Soc. Am, 94, 1343-1352 (1993).
11. Hunt, F. V., *Origins in Acoustics*, Yale University Press, New Haven, CT (1978).
12. Kurze U. and Beranek, L.L., "Sound Propagation Outdoors," Chap. 7, *Noise and Vibration Control*, Beranek, L.L. (ed), McGraw-Hill Book Co., New York, 1971.
13. Lee, D and Papadakis, J.S., "Numerical solutions of the parabolic wave equation: an ordinary differential approach," J. Acoust. Soc. Am, 68(5), pp. 1482-1488 (1980).
14. Lee, W., Bong, N., Richards, W.F. and Rasset, R., "Impedance Formulation of the Fast Field Program for Acoustic Wave Propagation in the Atmosphere," J. Acoust. Soc. Am., 79(3), 628-634 (1986).
15. Li, Y.L. and White, M. J, "A Note on Using the Fast Field Program," J. Acoust. Soc. Am., 95(6), pp. 3100-3102 (1994).
16. Li, Y.L., "Exact Analytical Expressions of Green's Functions for Wave Propagation in Certain Types of Range-Dependent Inhomogeneous Media." J. Acoust. Soc. Am. 96, 484-490 (1994).
17. Lyon, R.H., "Role of Multiple Reflections and Reverberation in Urban Noise Propagation," J. Acoust. Soc. Am. Vol. 55, pp. 493-503, (1974).

18. Pierce, A.D., *Acoustics, an Introduction to Its Physical Principles and Applications*, McGraw-Hill Book Co., New York (1981).
19. Piercy, J.E., Embleton, T.F.W., and Sutherland, L.C., "Review of Sound Propagation in the Atmosphere," *J. Acoust. Soc. Am.* Vol. 61, pp. 1403-1418, (1977).
20. Rudnick, I., "Propagation of Sound in the Open Air," Chap. 3, *Handbook of Noise Control*, Harris, C.M. (ed), McGraw-Hill Book Co., New York, (1957).
21. Salomons, E.M., *Computational Atmospheric Acoustics*, Kluwer Academic Publishers, Boston, (2001).
22. Stull, R.B., *Meteorology for Scientists and Engineers, 2nd Edition*, Brooks/Cole. A Division of Thompson Learning, 2000.
23. Sutherland, L.C. (ed), "Sonic and Vibration Environments for Ground Facilities, A Design Manual," Wyle Laboratories Report WR-68-2, 1968.
24. Sutherland, L.C. and Daigle, G.A., "Atmospheric Sound Propagation," Chap. 32, *Encyclopedia of Acoustics*, M.J. Crocker, (ed), Wyle Interscience, New York, (1997).
25. Tedrick, R.N. and Polly, R.C., "A Preliminary Investigation of the Measured Atmospheric Propagation Effects upon Sound Propagation," NASA MTP-Test 63-6, May 1963.